

Evidence of Climate-Driven Increases in Salmon River Water Temperatures

J. Eli Asarian
Riverbend Sciences

Lyra Cressey and Bonnie Bennett
Salmon River Restoration Council

LeRoy Cyr
Six Rivers National Forest
Lower Trinity, Orleans and Ukonom
Ranger District

Jon Grunbaum
Klamath National Forest
Happy Camp Oak Knoll
Ranger District

Toz Soto
Karuk Tribe
Department of Natural Resources

November 2019



Riverbend
Sciences



Evidence of Climate-Driven Increases in Salmon River Water Temperatures

J. Eli Asarian

Riverbend Sciences

Eureka, CA

Lyra Cressey and Bonnie Bennett

Salmon River Restoration Council

Sawyers Bar, CA

Jon Grunbaum

Klamath National Forest, Happy Camp Oak Knoll Ranger District

Happy Camp, CA

LeRoy Cyr

Six River National Forest, Lower Trinity, Orleans and Ukonom Ranger District

Orleans, CA

Toz Soto

Karuk Tribe, Department of Natural Resources

Orleans, CA

Prepared for:

Salmon River Restoration Council

Sawyers Bar, CA

November 2019

Suggested citation:

Asarian, J.E., L. Cressey, B. Bennett, J. Grunbaum, L. Cyr, T. Soto. 2019. Evidence of Climate-Driven Increases in Salmon River Water Temperatures. Prepared for the Salmon River Restoration Council by Riverbend Sciences with assistance from the Salmon River Restoration Council, Klamath National Forest, Six Rivers National Forest, and Karuk Tribe Department of Natural Resources. 53 p. + appendices.

Photo credits for cover page:

Salmon River at Blue Hole (Eli Asarian, August 18, 2017)

EXECUTIVE SUMMARY

Key Points

- Water temperatures in the Salmon River and its tributaries are warming due to climate-driven increases in air temperatures and decreases in snowpack and river flow.
- During the period 1995-2017, mean August water temperatures warmed at a rate of 0.39 °C (standard error: 0.06 °C) per decade and mean daily maximum August water temperatures warmed at a rate of 0.21 °C (standard error: 0.07 °C) per decade.
- Our statistical models predict that the magnitude of water temperatures increases due to future climate change will vary by reach. Creeks are predicted to warm less than rivers. Under current conditions, the South Fork Salmon River currently has disproportionately (for its large size) cool summer water temperatures due to high elevation headwaters with late-melting snowpack. Once climate change reduces summer snowpack, the South Fork will no longer be especially cool but will instead become more similar to the future North Fork.
- We predict that water temperatures will warm by 1.7–3.3 °C (magnitude varies by stream reach) by the end of the 21st century (2070-2099) if global greenhouse gas emissions are not reduced substantially. Reduced emissions would limit these increases and help maintain cool water temperatures.

Background

The Salmon River is located in Siskiyou County, California, USA. High summer water temperatures are a primary factor limiting production of culturally and economically important salmon and steelhead, including spring-run Chinook salmon. In the mid-1990s, the Salmon River Restoration Council (SRRC) and its partners the Klamath National Forest (KNF), Six Rivers National Forest (SRNF), and Karuk Tribe initiated a long-term collaborative effort to monitor summer water temperatures in the Salmon River and its tributaries using continuous probes. This report presents the first comprehensive analysis of the dataset.

The goals of this study were to 1) acquire, compile, and quality check all available continuous stream temperature data collected within the Salmon River watershed since 1990, 2) describe the spatial patterns in stream temperatures, 3) quantify interannual (i.e., between years) variation within individual sites and attempt to quantitatively attribute that variation to environmental factors (e.g., streamflow and air temperature), 4) test whether time series trends are present within individual sites and all sites collectively, 5) qualitatively attempt to explain the causes of time series trends, 6) predict how climate change will affect water temperatures. The results will be used to refine monitoring plans and to inform development of projects to restore aquatic habitat and watersheds.

Data Compilation and Preparation for Analysis

The compiled stream temperature dataset spans 1965 to 2017, with a total of 104 sites and 951 unique site-year combinations. Data were relatively sparse prior to 1995. Data sources included SRRC, KNF, SRNF, Karuk Tribe, U.S. Geological Survey (USGS), U.S. Fish and Wildlife Service, and Humboldt State University. After an intensive screening process that corrected errors and inconsistencies, and identified overlap between the data sources, we calculated seasonal summary statistics for each site and year. These metrics included Maximum Daily Maximum Temperature (MDMT), Maximum Weekly Maximum Temperature (MWMT), and Maximum Weekly Average Temperature (MWAT), mean August temperature, and mean daily maximum August temperature.

To prepare for statistical modeling, all sites were assigned to reaches in a Geographic Information System (GIS) stream network modified from the National Stream Internet (NSI) project. Each NSI reach includes GIS variables which are useful predictors of stream temperature. In addition to the NSI variables, we calculated new predictor variables: April 1 snowpack (from the Variable Infiltration Capacity [VIC] hydrologic model), mean August tributary flow (from measurements and statistical models), and topographic and vegetative shade (from satellites and a shade model).

Seasonal Patterns in Stream Temperature

Stream temperatures in the Salmon River typically peak in late July or early August. On average, July is slightly warmer than August. There is considerable year-to-year and site-to-site variation in the date that peak temperatures occur. To maintain consistency with previous regional modeling efforts, we focus most of our analyses on August stream temperatures.

Causes of Interannual Patterns in Stream Temperature

Years with the warmest stream temperatures included 1977, 1992, 1994, 2001, 2009, and 2013–2015. These years generally coincided with low flows and high air temperatures. Conversely, 1999 had among the lowest stream temperatures, with high flows, and cool air temperatures. Other years with cool temperatures included 1993 (high flows and low air temperatures), 2008 (moderate flow and air temperatures, but widespread fires which started in late June), and 2010 (moderate snowpack and high flow) and 2011 (deep snowpack and high flow).

We used linear mixed-effects models to explore how August stream temperatures at each of 30 long-term monitoring sites responded to interannual variation in air temperature and streamflow. Flow sensitivity was lowest in small streams (i.e., high flows did not have a large effect on stream temperatures) and greatest in the South Fork Salmon River (i.e., high flows resulted in very cool temperatures).

Long-Term Trends

Our analyses of long-term trends for the period 1995–2017 showed that the stream temperatures in the Salmon River and its tributaries are warming due to climate-driven increases in air temperatures and decreases in snowpack and river flow. Analyzing all sites together, mean August stream temperatures warmed at a rate of 0.39 °C per decade (i.e., 0.9 °C over the 22-year period) and mean daily maximum August stream temperatures warmed at a rate of 0.21 °C per decade (i.e., 0.5 °C over the 22-year period). At individual sites, increasing trends were much more common than decreasing trends. The sites with the largest temperature increases (>1.0°C/decade) were all located on the South Fork Salmon River. Other sites with evidence of ($p < 0.05$) increases in at least one temperature metric included Black Bear Creek, East Fork South Fork Salmon River, mainstem Salmon River downstream of Nordheimer, Knownothing Creek, Methodist Creek, Plummer Creek, and Taylor Creek. The only two sites with evidence of decreases in at least one stream temperature metric were North Russian Creek and North Fork Salmon River at Mule Bridge.

We used linear mixed-effects models to statistically account for the influence of climate (streamflow, air temperature, snowpack, and smoke) on August stream temperature, yielding “climate-adjusted stream temperature” which we then used to evaluate if other factors (e.g., riparian vegetation, channel morphology, etc.) besides climate are contributing to long-term trends. In contrast to the stream temperature trends (mentioned in the previous paragraph) that

were mostly warming or flat, the climate-adjusted stream temperature trends were cooling or flat, indicating the warming stream temperatures are due largely to climate (e.g., rising air temperature, declining streamflow, and declining snowpack). Seven sites had evidence of ($p < 0.05$) decreasing trends in climate-adjusted stream temperature, meaning that in recent years temperatures at these sites have been cooler than would be expected based on climate conditions alone. These include two sites on the North Fork Salmon River as well as a single site each on North Russian Creek, South Russian Creek, Salmon River, Wooley Creek, and Nordheimer Creek. The reasons for these decreases are unclear, but we speculate it may be due to recovery of riparian vegetation and channel conditions from past flood events (e.g., January 1, 1997). The overall slopes (i.e., analyzing all sites together) for climate-adjusted temperatures were slightly negative (-0.09 °C/decade [standard error: 0.06 °C, $p < 0.001$] for mean August temperature and -0.14 °C/decade [standard error: 0.06 °C, $p < 0.001$] for mean daily maximum August temperature). The South Fork Salmon River had no trends in climate-adjusted stream temperature, suggesting that the steep increasing trends in stream temperatures during the 1995–2017 period are due to climate.

Spatial Stream-Network Models

We used a spatial stream-network (SSN) model to estimate mean daily maximum August stream temperatures for each 1-kilometer stream reach within the study area (Figure ES-1). The SSN model combines observed temperature data, GIS data about landscape attributes, interannual variation in climate (i.e., air temperature, streamflow, snowpack, and wildfire smoke), and the spatial relationships between sites (i.e., the nearest sites having the strongest influence, and tributary relationships are taken into account). The model was adapted from NorWeST, a U.S. Forest Service project that modeled stream temperatures throughout the Western U.S.

The root mean squared prediction error (RMSPE) for final spatial model was 0.62 °C, indicating excellent model performance. Large drainage areas and high air temperatures were associated with warm stream temperatures (i.e., model coefficients are positive) while high gaged flow, high elevation, high levels of wildfire smoke, deep snowpack, ample shade, and high average water yield were associated with cool stream temperatures (i.e., model coefficients are negative). The air temperature coefficient was 0.44 °C/°C, meaning that stream temperature increased by 0.44 °C for each 1 °C increase in August air temperature.

Climate Change Scenarios

We then used the SSN model to predict stream temperatures in the late 21st century (2070–2099) under two climate change scenarios. The first is a “business-as-usual” high emissions scenario Representative Concentration Pathway (RCP) 8.5 in which air temperatures increase by 4.4 °C, August streamflow declines by 46%, and April 1 snowpack is reduced by an average of 63%. The second is RCP 4.5 in which concerted efforts are made to reduce global greenhouse gas emissions, resulting in air temperature increases of 2.4 °C, August streamflow declines of 31%, and April 1 snowpack is reduced by an average of 83%. Our spatial models predict that in the 2070–2099 period, mean daily maximum August stream temperatures will be warmer than the 1990–2017 baseline by 0.9 – 2.0 °C under RCP4.5 or 1.7 – 3.2 °C under RCP8.5, depending on the reach (Figure ES-1). Increases are predicted to be greatest in the South Fork Salmon River, with lesser increases in the North Fork and mainstem Salmon River. The smallest predicted increases are in small headwater tributaries around the Salmon River watershed. Climate change will also likely affect stream temperatures through additional mechanisms that are not included in our

spatial statistical models, such as increased wildfire activity, changes to forests, and increased flood severity.

Despite a remote location and mountainous terrain that protects the Salmon River from the same degree of human impacts as other rivers in California, the river is vulnerable to climate change because most of its mountains have relatively moderate elevations which will transition from snow to rain as the climate warms, reducing summer flows and increasing summer stream temperatures.

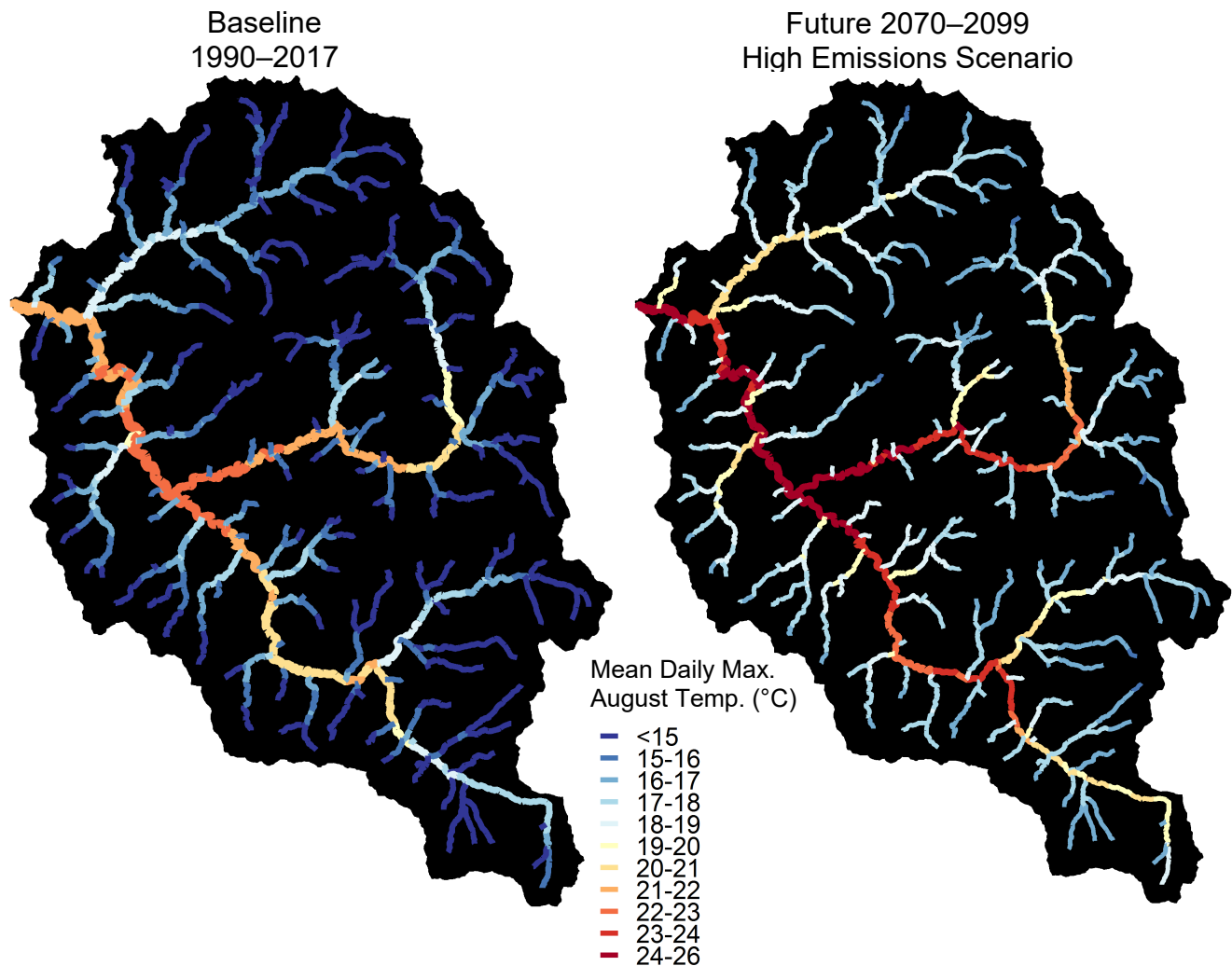


Figure ES-1. Modeled mean daily maximum August water temperature for streams in the Salmon River watershed for the period of observed data (left panel, 1990–2017) and predictions for end of the 21st century under a climate change scenario with high greenhouse gas emissions (right panel, 2070–2099). Predictions are outputs from a spatial stream-network model which uses observed temperature data and GIS predictor variables as inputs.

TABLE OF CONTENTS

Executive Summary	i
Table of Contents	v
List of Electronic Appendices.....	vi
List of Figures.....	vii
List of Tables.....	viii
1 Introduction.....	1
1.1 Description of Study Area.....	1
1.2 Previous Assessments of Salmon River Stream Temperatures.....	1
1.3 Study Goals.....	2
2 Methods	4
2.1 Overview of Data Sources and Methods.....	4
2.2 Stream Temperature Data Sources Acquired and Compiled.....	4
2.2.1 Salmon River Restoration Council.....	7
2.2.2 US Forest Service, Natural Resource Information System Aquatic Surveys.....	7
2.2.3 US Forest Service, Six Rivers National Forest.....	7
2.2.4 Karuk Tribe Department of Natural Resources.....	7
2.2.5 U.S Fish and Wildlife Service.....	8
2.2.6 Yurok Tribe Fisheries Program.....	8
2.2.7 Humboldt State University's Forest Science Project.....	8
2.2.8 USGS Geological Survey.....	8
2.2.9 Additional Datasets Not Acquired or Compiled.....	8
2.3 Quality Control and Cleaning of Stream Temperature Data.....	9
2.4 Assigning Stream Temperature Monitoring Sites to Stream Network GIS.....	9
2.5 Identifying Overlapping Data and Standardizing Site Locations.....	10
2.6 Calculation of Daily and Seasonal Summaries.....	10
2.6.1 Daily Summary Statistics.....	10
2.6.2 Initial Calculation of Seasonal and Monthly Summary Statistics.....	10
2.6.3 Refining Seasonal Statistics According to Data Completeness.....	12
2.7 Watershed Delineation.....	12
2.8 Environmental Data Used in Stream Temperature Models.....	13
2.8.1 Elevation.....	13
2.8.2 Drainage Area.....	13
2.8.3 Distance from Headwaters.....	13
2.8.4 Effective Shade (Topographic and Vegetative).....	13
2.8.5 Canopy.....	14
2.8.6 Slope.....	14
2.8.7 Mainstem Salmon Streamflow.....	14
2.8.8 Tributary Streamflow.....	14
2.8.9 April 1 Snowpack.....	16
2.8.10 Air Temperature Time Series and Mean Annual Precipitation.....	17
2.8.11 Wildfire Smoke (aerosol optical thickness, AOT).....	18
2.9 Other Environmental Data Used to Interpret Results.....	18
2.9.1 Wildfire Extent and Severity.....	18
2.9.2 Solar Radiation.....	18
2.10 Linear Mixed Effects Models to Account for Site-Specific Variation in Sensitivity of Stream Temperature to Interannual Climate Variability.....	19
2.11 Long-Term Trends in Stream Temperature and Climate-Adjusted Stream Temperature.....	19
2.12 Spatial Stream-Network Modeling.....	20
2.13 Climate Change Predictions.....	21
2.13.1 Summary.....	21
2.13.2 Representative Concentration Pathways.....	22
2.13.3 Air Temperature.....	22
2.13.4 April 1 Snowpack.....	23
2.13.5 Streamflow.....	25
3 Results and Discussion.....	27
3.1 Overall Seasonal Patterns in Stream Temperature and Relationships Between Temperature Metrics.....	27
3.2 Annual Time Series of Basinwide Summaries of Stream Temperature, Climate, and Wildfire.....	30

3.3	Linear Mixed Effects Models to Account for Site-Specific Variation in Sensitivity of Stream Temperature to Interannual Climate Variability	34
3.4	Long-Term Trends in Stream Temperature and Climate-Adjusted Stream Temperature	35
3.5	Spatial Stream-Network Model Calibration and Performance	39
3.6	Climate Change Predictions	41
3.7	Management Implications	44
4	Acknowledgments	45
5	References Cited	45
	Appendix A: Table of Tributary Streamflow	A1
	Appendix B: Effective Shade Model	B1
	Appendix C: Comparison of Snow Datasets	C1
	Appendix D: Additional Details on Linear-Mixed Effects Models	D1
	Appendix E: Additional Details on Spatial Stream-Network Models.....	E1
	Appendix F: Annual Time Series of Climate, Fire, and Stream Temperature at Long-Term Monitoring Sites.....	F1

LIST OF ELECTRONIC APPENDICES

ELECTRONIC APPENDIX: MS Access database of stream temperature data with tables for: a) 15-120 minute measurements, b) daily summaries, c) annual summaries, d) site locations.

LIST OF FIGURES

Figure 1. Map of Salmon River watershed. Figure copied from NCRWQCB (2005).....	3
Figure 2. Flow chart with overview of data sources and major data analysis steps used in stream temperature analyses including climate change predictions. For simplicity and clarity, some steps and details are omitted.....	5
Figure 3. Map showing locations of mainstem and tributary stream temperature monitoring stations in the Salmon River watershed. Symbol color denotes the number of years of available data at site.....	6
Figure 4. Daily time series of daily maximum, daily mean, daily minimum, 7-day average of daily maximum, and 7-day average of daily mean water temperatures at an example site-year (mouth of South Fork Salmon River in 2016). Maximum daily maximum temperature (MDMT), maximum weekly maximum temperature (MWMT), maximum weekly average temperature (MWAT) are the highest annual values for daily maximum, 7-day average of daily mean, and 7-day average of daily maximum, respectively. Mean daily maximum August temperature (Aug_meanMx), and mean August temperature (Aug_mean) are also shown.....	12
Figure 5. Map of mean August streamflow per unit watershed area for 1-km prediction reaches in the Salmon River watershed, estimated using statistical models fit with discrete measurements at 23 long-term monitoring stations and continuous data from one USGS gage.....	15
Figure 6. Average snow water equivalent (SWE) for April 1, May 1, and June 1 for the years 2003–2019 from the SNOW Data Assimilation System (SNODAS) model. Spatial resolution is 1 km. Maps were created with Google Climate Engine.	17
Figure 7. Average April 1 snow water equivalent (SWE) for 1971–2000 from the Xiao et al. (2016) Variable Infiltration Capacity (VIC) model. Spatial resolution is 6 km.	17
Figure 8. Modeled summer (June, July, and August) air temperature at Forks of Salmon for the historical period (1950–2005) and predictions for 2006 to 2099 under moderate (RCP 4.5) and high (RCP 8.5) greenhouse gas emissions scenarios from an ensemble of 20 general circulation models (GCMs).....	23
Figure 9. Modeled average April 1 snowpack for 1971–2000 (Xiao et al. 2016) and 2070–2099 under RCP8.5 (Xiao et al. 2016 adjusted by predicted percent declines from Mote et al. 2014).....	24
Figure 10. Monthly median streamflow for three Sierra Nevada rivers predicted by the Soil and Water Assessment Tool (SWAT) hydrologic model under moderate (B1) and high (A2) greenhouse gas emissions scenarios from 16 general circulation models (GCMs). Figure created using data from Ficklin et al. (2012).	26
Figure 11. Seven-day moving averages of daily maximum temperature (7DADM) for every site and every year in the Salmon River watershed.....	27
Figure 12. Date each year 1969–1979 and 1990–2017 upon which MWMT temperature occurred at sites in the Salmon River watershed.	28
Figure 13. Comparison of mean July stream temperatures with (A) mean June stream temperatures, and (B) mean August stream temperatures, for each site-year in the 1990–2017 Salmon River watershed dataset.....	28
Figure 14. Correlation matrix comparing maximum weekly maximum temperature (MWMT), maximum weekly average temperature (MWAT), annual single maximum (MDMT), August mean (Aug_mean), and August mean temperatures (Aug_meanMx) for the entire Salmon River watershed dataset.....	29
Figure 15. Annual time series 1965–2017 of: A) percent of Salmon River watershed burned, B) mean monthly aerosol optical thickness (a proxy for wildfire smoke) estimated from satellites, C) April 1 snowpack for Salmon River watershed from VIC hydrologic model, D) mean monthly air temperature for Salmon River watershed (from PRISM model), E) mean monthly flow measured at USGS gage, F) watershed summaries of mean daily maximum monthly stream temperature measured, and G) watershed summaries of seasonal stream temperature metrics (MDMT, MWMT, and MWAT).....	31
Figure 16. Number of sites per year 1966–2017 in the Salmon River watershed with data available for A) mean daily maximum monthly stream temperature, and B) seasonal stream temperature metrics (MDMT, MWMT, and MWAT), which were used to calculate the adjusted averages shown in Figure 15 A/B.....	32
Figure 17. Map showing US Forest Service estimates of wildfire burn severity (percent canopy change) in the Salmon River watershed for years 1977–2017.....	32

Figure 18. Maps showing US Forest Service estimates of wildfire burn severity (percent canopy change) in the Salmon River watershed for each year 1977–2017 in which at least 20 km ² burned.....	33
Figure 19. Maps showing sensitivity of mean daily maximum August stream temperature to gaged streamflow (i.e., expected change in stream temperature per unit change in flow) at 27 long-term monitoring sites in the Salmon River watershed.	34
Figure 20. Boxplot of slopes (i.e., trend magnitudes) at 27 long-term sites in the Salmon River watershed for A) five stream temperature metrics [MDMT, MWMT, MWAT, mean daily maximum August temperature, and mean August temperature], and B) two climate-adjusted stream temperature metrics.	36
Figure 21. Site-specific results of statistical trend tests at 27 long-term sites in the Salmon River watershed for A) five stream temperature metrics [MDMT, MWMT, MWAT, mean daily maximum August temperature, and mean August temperature], and B) two climate-adjusted temperature metrics.....	37
Figure 22. Map of site-specific results of statistical trend tests at 27 long-term sites in the Salmon River watershed for A) five stream temperature metrics [MDMT, MWMT, MWAT, mean daily maximum August temperature, and mean August temperature], and B) two climate-adjusted temperature metrics.	38
Figure 23. Comparison of observed mean daily maximum August stream temperature and predictions from the final spatial model for sites in the Salmon River watershed.	40
Figure 24. Predicted mean daily maximum August temperature for streams in the Salmon River watershed for the period 1990-2017. Predictions are outputs from a spatial stream-network model which uses observed temperature data and GIS predictor variables as inputs.....	40
Figure 25. Comparisons of spatial stream-network model predictions for mean daily maximum stream temperatures, and increases above the 1990-2017 baseline, for streams in the Salmon River watershed predicted under moderate (RCP4.5) and high (RCP8.5) emissions future climate scenarios for 2070-2099.	42
Figure 26. Map comparing spatial stream-network model predictions for mean daily maximum stream temperatures for streams in the Salmon River watershed predicted under (A) moderate RCP4.5 and (B) high RCP8.5 emissions future climate scenarios for 2070-2099, and (C, D) increases between the baseline and future scenarios.	43
Figure C27. Comparison of annual time series of snow water equivalent at specific measured Snow Course sites (BFT, ETN, RRM, SWJ) and model predictions summarized across the whole Salmon River watershed (BCM and SNODAS), by month for 1977–2018.	C1

LIST OF TABLES

Table 1. Summary of stream temperature data compiled for use in this project.	4
Table 2. Air temperatures and August streamflow selected for use in spatial statistical stream temperature model climate change scenarios.....	22
Table 3. Comparison of modeled April 1 snowpack in the Salmon River watershed for historic and future climate periods, from multiple data sources.	24
Table 4. Climate change projections for mean August flow at three sites (Trinity River, Feather River, American River) predicted by the Variable Infiltration Capacity (VIC) model using the mean of 10 general circulation models (GCMs) as meteorological inputs. Data from the Integrated Scenarios of Climate, Hydrology, and Vegetation for the Northwest project (Mote et al. 2014).....	26
Table 5. Parameter estimates for the final spatial models used to predict mean August stream temperature in Salmon River watershed.	40
Table A6. Mean August streamflow estimated at 23 sites where streamflow was measured on at least 4 dates.	A1
Table D7. Comparison of linear mixed-effects models to predict mean August stream temperature and mean daily maximum August stream temperature for streams in the Salmon River watershed and surrounding areas.	D1
Table E8. Proportion of total variance explained by the covariates (predictor variables), spatial autocovariance, and random effects in the final spatial stream-network model for mean daily maximum August temperature.	E1
Table E9. Comparison of summary statistics for alternative spatial stream-network models to predict mean daily maximum August stream temperature for streams in the Salmon River watershed and surrounding areas.	E2

1 INTRODUCTION

1.1 DESCRIPTION OF STUDY AREA

The Salmon River is located in Siskiyou County, California, USA (Figure 1). The watershed is sparsely populated with only about 250 people residing within the 751 mi² watershed, 98.7% of which is managed by the U.S. Forest Service (Elder et al. 2002). Federal lands include the. The Salmon River was identified as a high priority Key Watershed in the Northwest Forest Plan. In addition to Marble Mountain, Trinity Alps, and the Russian Wilderness areas which comprise 45% of the watershed, 25% of the watershed is managed as Late-Successional Reserves. Elevations range from 500 feet to 9000 feet (Elder et al. 2002). Much of the watershed is steep, mountainous terrain. Precipitation ranges from less than 40 inches along the South Fork to over 80 inches in upper Wooley Creek (Elder et al. 2002). The Salmon River watershed is located within the Klamath Mountains physiographic province. Approximately 81% of the watershed is covered in conifer forest, with 9% in hardwood forests (Elder et al. 2002). Detailed history of the land use and watershed conditions in the Salmon River watershed can be found in Klamath National Forest watershed analyses and planning documents (KNF 1994a, 1994b, 1995a, 1995b, 1995c, 1996, 1997, 1999).

1.2 PREVIOUS ASSESSMENTS OF SALMON RIVER STREAM TEMPERATURES

Water temperatures have long been identified as a primary factor limiting production of salmon and steelhead within the study area and have been a priority for fisheries management and research (Kier Associates 1991, NRC 2004, NMFS 2014). The Salmon River watershed is listed as impaired under the Clean Water Act Section 303(d) for temperature, and the North Coast Regional Water Quality Control Board¹ has established a Total Maximum Daily Load (NCRWQCB 2005). Previous assessments of stream temperatures within the study area include the analysis of long-term trends (Bartholow 2005, Isaak et al. 2018), the Salmon River TMDL (NCRWQCB 2005), regression modeling to predict Klamath Basin stream temperatures based on meteorology and topography (Flint et al. 2008, Flint et al. 2012), Klamath National Forest annual monitoring reports for stream temperature (Laurie 2012) and stream shade (Laurie and Reichert 2011), riparian vegetation assessments (Alexander 1992, Cressey and Greenberg 2008), evaluation of the thermal refugia and salmonids' thermal tolerances (Strange 2010, 2011), analysis of mainstem river temperatures using thermal infrared imaging (Watershed Sciences 2010, Stillwater Sciences 2018), and the effects of wildfire smoke on stream temperatures (David et al. 2018).

In addition to the local analyses mentioned in the previous paragraph, there have been two major regional stream temperature compilations and analysis projects in northwest California which encompasses the Salmon River. The Humboldt State University (HSU) Forest Science Project (FSP) compiled data for 1990-1998 from a multitude of entities, including private timber companies, state and federal agencies, non-profit organizations, and consultants (Lewis et al. 2000). Lewis et al. (2000) then applied statistical models to these data to evaluate relationships between water temperature and variables including air temperature, distance from the Pacific Ocean, elevation, watershed area, and site-specific attributes (e.g., channel width, gradient, and canopy).

¹ http://www.waterboards.ca.gov/northcoast/water_issues/programs/tmdls/

The NorWeST² stream temperature model uses observed temperature data, Geographic Information Systems (GIS) data, and a spatial regression model to predict mean August temperature throughout the entire stream network (Chandler et al. 2016, Isaak et al. 2016, 2017). It was first applied in the Boise River Basin in Idaho (Isaak et al. 2010). In 2015, the U.S. Forest Service’s Rocky Mountain Research Laboratory (USFS RMRS) applied the NorWeST model to the North Coast of California including the Klamath Basin. NorWeST refers to this project area as the “Northern California Coastal Klamath processing unit”. After first calibrating the model and running a scenario for current conditions, they ran a variety of climate change scenarios. Model predictions³ and daily/annual summaries of measured water temperature data⁴ are available online (Chandler et al. 2016, Isaak et al. 2016). They compiled a large amount of stream temperature data for use as model inputs; however, the compilation focused on existing large regional compilations such as the U.S. Forest Service’s Natural Resource Information System Aquatic Surveys (NRIS AqS)⁵ and U.S. Geological Survey’s U.S. Geological Survey’s (USGS) National Water Information System (NWIS)⁶. In the Klamath Basin, this was supplemented by a database of mainstem Klamath River water temperature data from the U.S. Fish and Wildlife Service’s Arcata Office. Many existing temperature datasets within the region were not included, including data from SRRC and the Humboldt State University Forest Science Project 1990-1998 compilation. In the time since the 2015 NorWeST modeling began, several projects within the North Coast have compiled new stream temperature datasets. These projects included several Riverbend Sciences projects in the Salmon River (this report), Klamath Basin (in-progress), South Fork Trinity River (Asarian 2016), Yurok Ancestral Territory (Asarian 2017), and Eel River (Asarian et al. 2016). Given the availability of large new temperature datasets within the North Coast, as well as previous compilations which were not utilized such as the HSU FSP project mentioned in the previous paragraph, RMRL completed a re-run of the NorWeST model for the entire North Coast in April 2017 (Isaak et al. 2017). Long-term trends in stream temperatures within the NorWeST study area were assessed by Isaak et al. (2018).

1.3 STUDY GOALS

The goals of this study were to 1) acquire, compile, and quality check all available continuous stream temperature data within the Salmon River watershed, 2) describe the spatial patterns in stream temperatures, 3) quantify interannual (i.e., between years) variation within individual sites and attempt to quantitatively attribute that variation to environmental factors (e.g., streamflow and air temperature), 4) test whether time series trends are present within individual sites and all sites collectively, 5) qualitatively attempt to explain the causes of time series trends, 6) predict how climate change will affect water temperatures. The results of this analysis will be used to refine watershed monitoring plans and to inform development of future projects to restore aquatic habitat and watersheds.

² <http://www.fs.fed.us/rm/boise/AWAE/projects/NorWeST.html>

³ <http://www.fs.fed.us/rm/boise/AWAE/projects/NorWeST/ModeledStreamTemperatureScenarioMaps.shtml>

⁴ <http://www.fs.fed.us/rm/boise/AWAE/projects/NorWeST/StreamTemperatureDataSummaries.shtml>

⁵ <http://www.fs.fed.us/nrm/index.shtml>

⁶ <http://waterdata.usgs.gov/nwis>

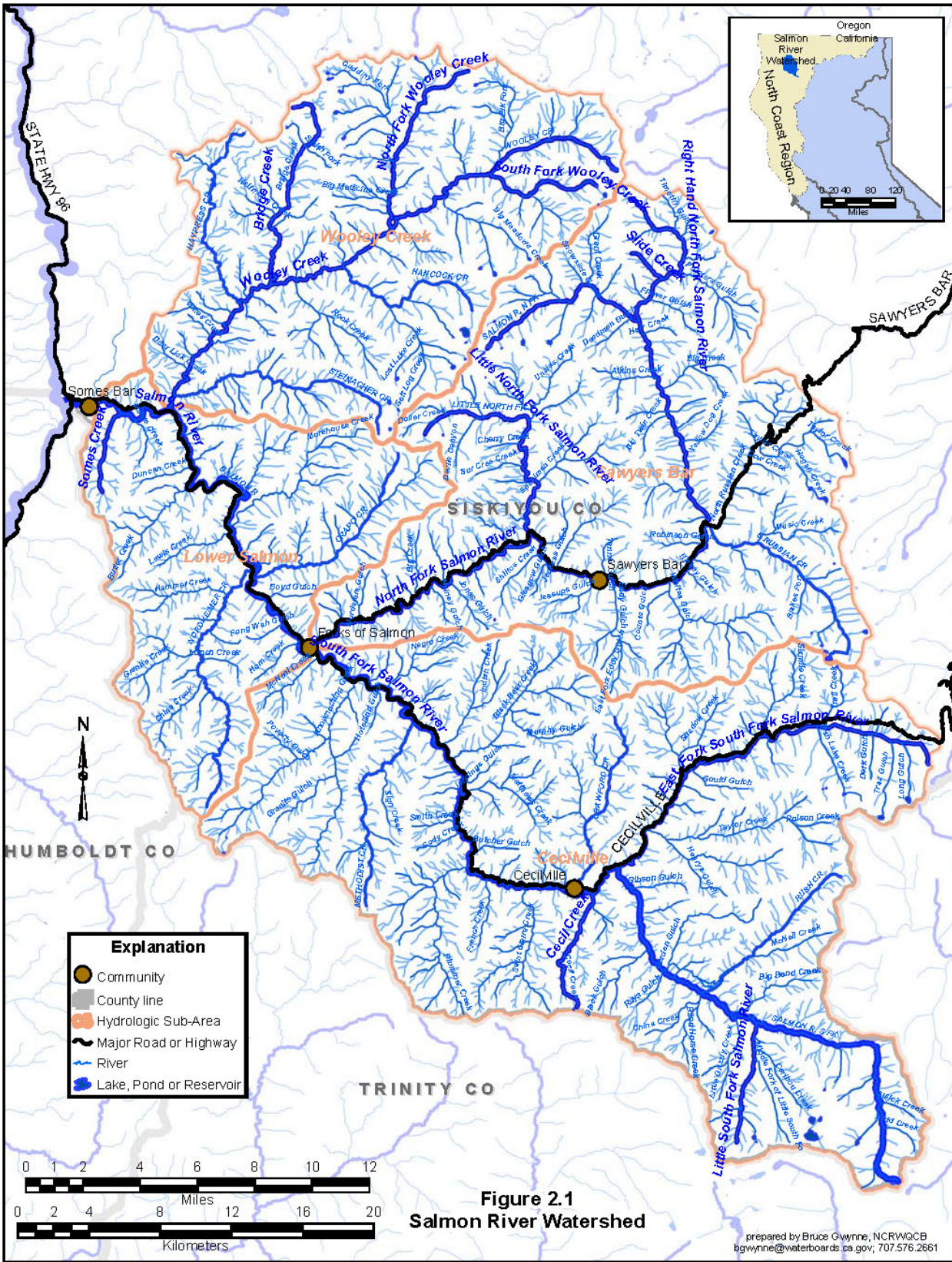


Figure 1. Map of Salmon River watershed. Figure copied from NCRWQCB (2005).

2 METHODS

2.1 OVERVIEW OF DATA SOURCES AND METHODS

Figure 2 provides a flow chart showing an overview of the data sources and major data analysis steps used in this project.

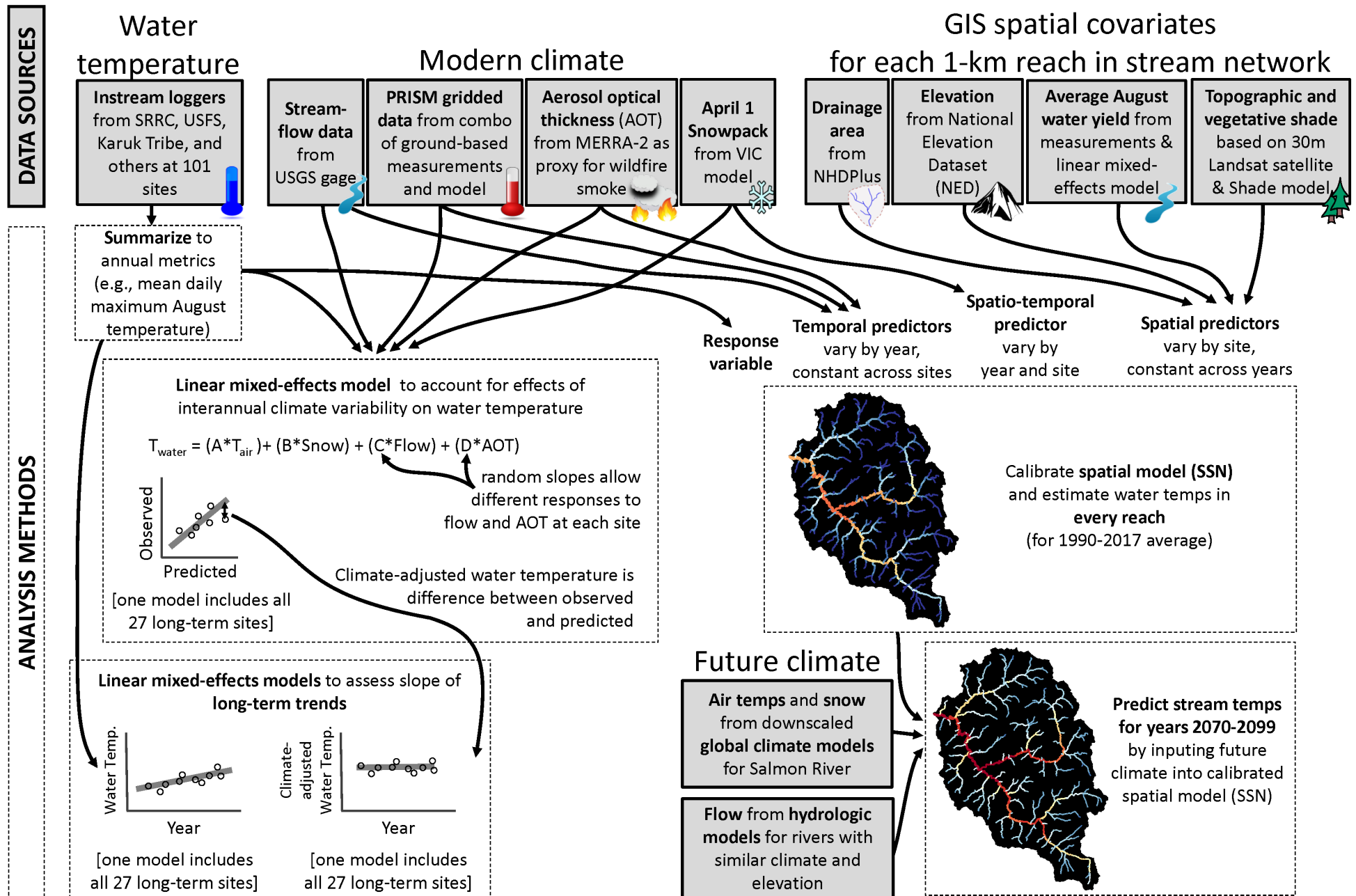
2.2 STREAM TEMPERATURE DATA SOURCES ACQUIRED AND COMPILED

Data for the years 1965 through 2017 were acquired from a multitude of sources (Table 1, Figure 3). Some probe deployments were included in multiple source compilations, resulting in up to three copies of the same data (i.e., overlap, see section 2.5). The overlap was retained in the master database, but was not used for analysis. Excluding the overlap, there were a total of 104 sites and 951 unique site-year combinations (Table 1). The number of years of data available at a site ranged from one to 23, except for the lower Salmon River at the USGS gage where there were 36 years.

Table 1. Summary of stream temperature data compiled for use in this project. Grey text in the *Overlap* column indicate portions of data sources that were excluded from analysis because they overlap (i.e., are duplicate copies of the same data) with other data sources or had data quality issues. Totals do not equal the sum of the individual rows because some sites and reaches are shared between datasets, and totals do not include the datasets flagged as overlap. Data sources are listed in descending order of number of site-years. *Sites before std.* is the original number of sites prior to standardization of adjacent comparable sites (see section 2.5).

Source entity full name	Source entity abbreviated	Overlap with other datasets?	First year	Last year	Site-years	Sites	Sites before std.
Salmon River Restoration Council	SRRC	No	1995	2017	449	85	92
		To be superseded by USFS_NRIS_AqS in future when NRIS is fixed	1999	2016	25	10	10
		Dup./Superseded by USFS_NRIS_AqS	1997	2016	259	44	45
U.S. Forest Service Natural Resource Information System Aquatic Surveys	USFS_NRIS_AqS	No	1990	2016	434	65	74
		Dup./Already in USFS_NRIS_AqS as another site	1997	2006	13	3	4*)
		Suspect data or coords, not used	1997	2016	33	19	19
Six Rivers National Forest	SRNF	No	2004	2017	34	4	4
		Dup./Superseded by USFS_NRIS_AqS	1997	2010	29	4	4
U.S Geological Survey, National Water Information System	USGS	No	1965	1979	15	1	1
Karuk Tribe Dept. of Natural Resources	KarukWQ	No	2005	2017	13	1	1
Humboldt State University's Forest Science Project	HSU_FSP	No	1998	1998	1	1	1
		Dup./Superseded by USFS_NRIS_AqS	1997	1998	2	1	1
U.S. Fish and Wildlife Service	USFWS	No	2002	2007	5	1	1
Yurok Tribe Fisheries Program	YTFF	Dup./Superseded by USFS_NRIS_AqS	2003	2003	1	1	1
TOTALS (EXCLUDES OVERLAP)			1965	2017	951	104	174

Figure 2. Flow chart with overview of data sources and major data analysis steps used in stream temperature analyses including climate change predictions. For simplicity and clarity, some steps and details are omitted.



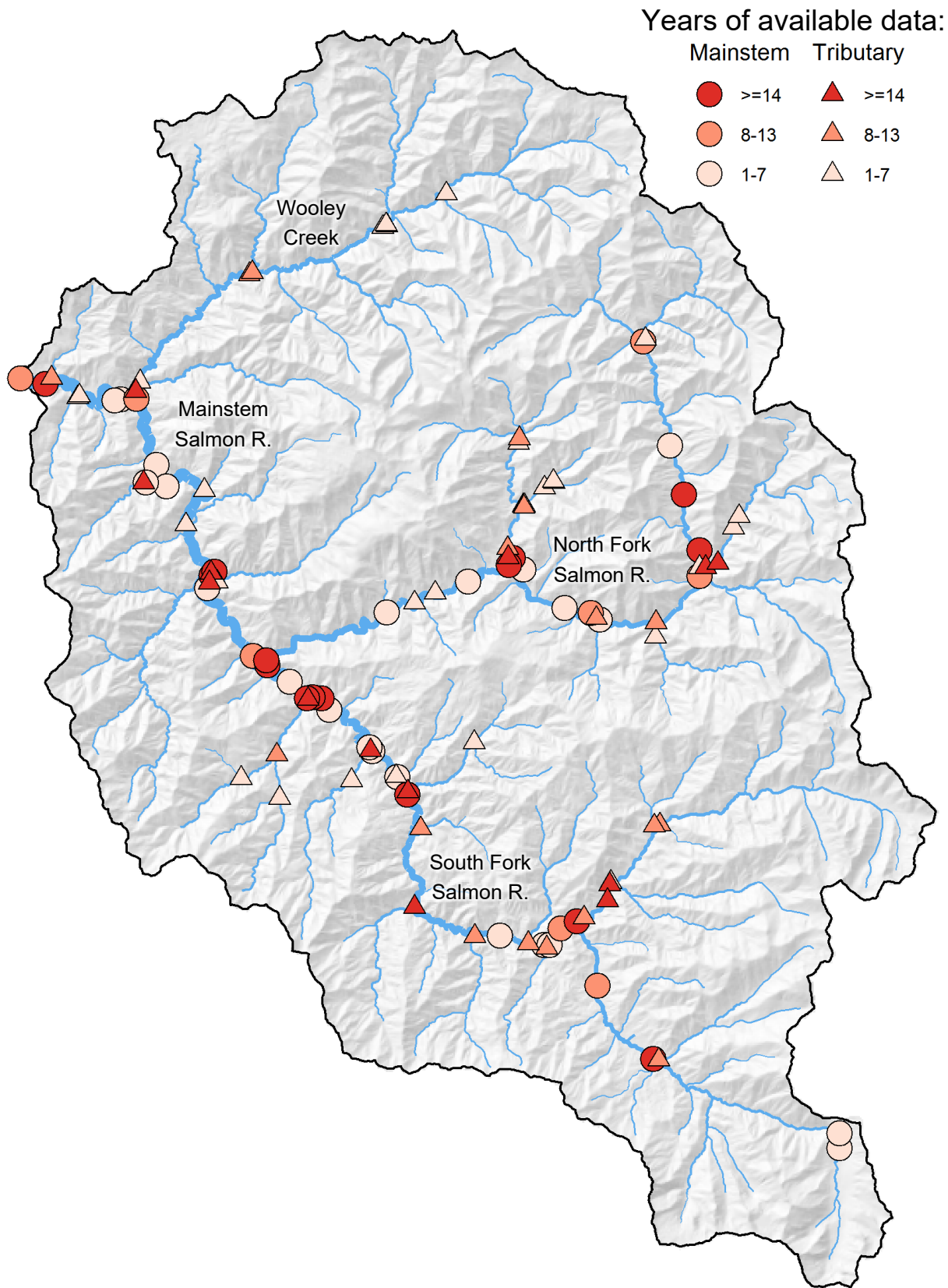


Figure 3. Map showing locations of mainstem and tributary stream temperature monitoring stations in the Salmon River watershed. Symbol color denotes the number of years of available data at site. Only sites with >14 years were used to assess long-term trends. Some symbols overlap and mask those beneath.

2.2.1 SALMON RIVER RESTORATION COUNCIL

The Salmon River Restoration Council (SRRC⁷) and its cooperators have been monitoring water quality in the Salmon River and its tributaries since 1992. The monitoring program is coordinated with the Klamath National Forest, Six Rivers National Forest, and the Karuk Tribe. SRRC's water quality monitoring program plays an important role in the scientific assessment of overall river health and is contributing to the action plan of the Clean Water Act's Total Maximum Daily Load (TMDL) for the Salmon River. The monitoring program establishes baseline water quality data, supports the Clean Water Act's TMDL process, correlates river temperatures with fish behavior, characterizes fisheries refugia conditions, identifies opportunities for habitat improvement, and assesses restoration effectiveness. This monitoring program focuses on stream temperatures and stream flow at a network on long-term sites, especially during the summer months when low flows and warm temperatures pose the greatest threat to the health of the fishery. The number of temperature sites monitored each year varies according to available resources (e.g., 47 were sites monitored in 2015). The temperature data for 1997-2002 were initially stored in the Klamath Resource Information System (KRIS⁸) database until 2003 when SRRC transitioned to a Microsoft Access database which now includes data for 1997-2015. Plans for managing temperature data for recent years are currently being developed.

2.2.2 US FOREST SERVICE, NATURAL RESOURCE INFORMATION SYSTEM AQUATIC SURVEYS

Most water temperature data collected by U.S. Forest Service (USFS) within the study area, including data collected by staff from the Klamath National Forest (KNF) and Six Rivers National Forest (SRNF), are input into the national Natural Resource Information System (NRIS) Aquatic Surveys (AqS) database. Hydrologist Callie McConnell of the USFS office in Corvallis, Oregon extracted all NRIS AqS temperature data within the study area in December 2016 and provided it for use in this project. NRIS AqS also includes most, but not all, stream temperature data collected by the Karuk Tribe's fisheries program, as well as most data collected by SRRC since 2010.

2.2.3 US FOREST SERVICE, SIX RIVERS NATIONAL FOREST

With the onset of continuous temperature sensor technology, the SRNF in partnership with the Forest Science Project at Humboldt State University initiated a stream temperature monitoring program in 1994. Some SRNF temperature data are included within the NRIS AqS database. However, USFS stream temperature data for the lower Salmon River that were not available in the NRIS AqS database for this assessment were obtained from LeRoy Cyr, Orleans Ranger District fish biologist for the years 2011-2017.

2.2.4 KARUK TRIBE DEPARTMENT OF NATURAL RESOURCES

The Karuk Tribe's water quality program monitors water temperature and other water quality parameters at the USGS streamflow gage near the mouth of the Salmon River. We downloaded these temperature data from the Karuk Tribe's online water quality portal⁹. The Karuk Tribe's fisheries program participates in collaborative monitoring of Salmon River water temperatures with the USFS and SRRC. The vast majority of these temperature data collected have been input into the NRIS AqS database, so we did not include any additional Karuk Tribe fisheries program

⁷ <http://srrc.org/publications/index.php>

⁸ http://www.krisweb.com/krisklamathtrinity/krisdb/webbuilder/sa_c20.htm

⁹ <http://waterquality.karuk.us:8080/>

data in our analyses. The Karuk Tribe fisheries program does have some additional data (primarily associated with special studies such as thermal refugia monitoring) that could be compiled at some point in the future.

2.2.5 U.S FISH AND WILDLIFE SERVICE

The U.S. Fish and Wildlife Service¹⁰ (USFWS) office in Arcata, California collects stream temperature data at a network of monitoring sites within the Klamath and Trinity River basins and maintains the data in a well-organized Microsoft Access database. Data were received from USFWS fisheries biologist Aaron David in February 2017. The database includes data for one site at the mouth of the Salmon River for portions of the years 2002 through 2007.

2.2.6 YUOK TRIBE FISHERIES PROGRAM

We obtained lower Salmon River stream temperature data from the Yurok Tribe Fisheries Program (YTFP¹¹) for the year 2003 from Yurok Tribe biologist Jamie Holt. These data already existed in NRIS AqS, so we did not use them.

2.2.7 HUMBOLDT STATE UNIVERSITY'S FOREST SCIENCE PROJECT

As noted above in section 1.2, Humboldt State University's (HSU) Forest Science Project (FSP) compiled data from the North Coast of California for 1990-1998 from a multitude of entities, including private timber companies, state and federal agencies, non-profit organizations, and consultants (Lewis et al. 2000). The FSP was later renamed the Institute for Forest and Watershed Management and is now dissolved. The data are extremely well organized and were rigorously reviewed during the Lewis et al. (2000) analysis, but one deficiency of the version of the publicly shared version of the database is that there is no way to ascertain which entity collected any particular piece of data, which inhibits transparency and made it difficult to determine potential overlap with other datasets.

2.2.8 USGS GEOLOGICAL SURVEY

We downloaded daily minimum and maximum stream temperature data from the U.S. Geological Survey's (USGS) National Water Information System (NWIS) for the gage near the mouth of the Salmon River (USGS 11522500 SALMON R A SOMES BAR CA) for the years 1965-1979.

2.2.9 ADDITIONAL DATASETS NOT ACQUIRED OR COMPILED

During the outreach and research over the course of this project, we became aware of some datasets that we were not able to compile due to time and budget constraints:

- A few unique (i.e., not overlapping with other datasets) temperature datasets are available in the Klamath Resource Information System (KRIS¹²), including these two daily summaries:
 - o 1989-1995 data¹³ compiled by the North Coast Regional Quality Control Board and originally collected by the Klamath National Forest, Six Rivers National Forest, the California Department of Fish and Game, and Pacific Power and Light Company. This compilation includes several site-years not included in the USFS NRIS AqS and

¹⁰ <http://www.fws.gov/arcata/fisheries/activities/waterQuality/klamathWQ.html>

¹¹ <http://www.yuroktribe.org/departments/fisheries/reportsandpublications.htm>

¹² http://www.krisweb.com/krisklamathtrinity/krisdb/webbuilder/selecttopic_temperature.htm

¹³ http://www.krisweb.com/krisklamathtrinity/krisdb/webbuilder/mk_cst27.htm

SRRC datasets: Negro Creek [trib to SF Salmon River] (6/12/1990-9/30/1990 and 6/27/1991-10/14/1991), NF Salmon River at Big Creek (7/10/1991-10/16/1991), NF Salmon River just upstream of Forks (7/1/1993-9/30/1993), Upper NF Salmon River (7/9/1991-10/15/1991), and Wooley Creek below Big Meadow (1/1/1992-8/27/1992).

- Mid-May to early July 1995 data¹⁴ collected by students at Forks of Salmon School, community volunteers, and SRRC staff at: Kanaka Cr, Salmon River above the junction with the Klamath River, Little NF Salmon River, NF Kerrick Creek, NF Salmon River at McBroom's property, North Fork Salmon River at Stud Hole, Olson Creek, SF Salmon River downstream of the East Fork, SF Salmon River upstream of the East Fork, and Taylor Creek
- Additional water temperature (as well as dissolved oxygen, pH, and specific conductivity) data were compiled by Tetra Tech (2004) in preparation for the Klamath River TMDL (NCRWQCB 2010). Our review of this compilation (it is available upon request from Riverbend Sciences), found that most of it overlaps with (and are now superseded by) other datasets such as SRRC and USFS NRIS AqS. One exception is Watercourse Engineering (2003) data for the year 2000 sponsored by the US Bureau of Reclamation and PacifiCorp which included a site at the mouth of the Salmon River which was deployed for a few additional months longer than the nearby USFS/SRRC site.

2.3 QUALITY CONTROL AND CLEANING OF STREAM TEMPERATURE DATA

Data collected with continuous probes, such as the temperature data that is the subject of this project, must be cleaned/trimmed to remove data corrupted when a probe malfunctions or is exposed to air during pre/post deployment or when a stream dries up. The condition of the datasets we received varied among data sources and year, so a fairly intensive screening and trimming process was initiated, informed by protocols from Dunham et al. (2005), Sowder and Steel (2012), and U.S. EPA (2014). All data values for the period when the stream appeared to be dry were removed but the data from the remainder of the probes' deployment when water was flowing in the respective stream reaches were retained. Additional details on the processes we used are provided in Asarian (2017).

A list of all specific issues identified in the review were sent back to original data providers to give them an opportunity to correct their datasets for future uses.

2.4 ASSIGNING STREAM TEMPERATURE MONITORING SITES TO STREAM NETWORK GIS

All stream temperature datasets had x-y spatial coordinates (e.g., UTM or latitude/longitude) when we acquired them (or if not then we requested and receive them later); however, assigning each site to a GIS stream network (rather than solely x-y coordinates) greatly increases the utility of the data. We selected the National Stream Internet (NSI) Hydrography Network¹⁵ as the GIS stream network due to its use in the NorWeST model. NSI network was created by the U.S. Forest Service's Rocky Mountain Research Lab by modifying the NHD-Plus¹⁶ Version 2 medium-resolution (1:100,000-scale) hydrography layer for all streams in the contiguous United States. NHD-plus contains a large database of descriptors for each reach (e.g., stream name,

¹⁴ http://www.krisweb.com/krisklamathtrinity/krisdb/webbuilder/sa_ct51.htm

¹⁵ http://www.fs.fed.us/rm/boise/AWAE/projects/NationalStreamInternet/NSI_network.html

¹⁶ http://www.horizon-systems.com/nhdplus/NHDPlusV2_home.php

watershed area, stream gradient, climate variables, and percent of various land-use types within the watershed) which are useful predictor variables in spatial analyses. Assigning the temperature monitoring points to NSI/NHD-plus stream reaches allowed the data to be easily integrated into NorWeST and other stream network models. Each stream temperature monitoring station was assigned to reaches in the National Stream Internet (NSI) Hydrography Network GIS using steps described in Asarian (2017). In addition, each station was assigned to a 1-km NorWeST prediction reach which is based on the same hydrography as the NSI but has shorter reaches and includes all NorWeST covariates (i.e., predictor variables).

2.5 IDENTIFYING OVERLAPPING DATA AND STANDARDIZING SITE LOCATIONS

As noted above in section 2.1, some deployments were included in multiple source compilations, resulting in up to three copies of the same data. Using a combination of automated and manual methods, we conducted a detailed review to identify and exclude these duplicate (i.e., overlapping) data. After seasonal summary statistics were calculated (see section 2.6), we grouped data by year and 1-km NorWeST reach ID and produced a spreadsheet listing all site-years. If a reach had multiple sites (either from the same source or different sources) within the same year, we compared the maximum weekly average temperature (MWMT) values and automatically flagged those that were within 0.02°C of each other because that indicated that the data were duplicate copies. We also manually reviewed site-years that had too short a duration to have seasonal summary statistics (see section 2.6.3 below) and manually flagged any that were deemed duplicate copies. Where overlap was identified, we flagged one copy of the data as overlap to be excluded from analysis, giving priority to largest and actively maintained source datasets¹⁷. The overlap was retained (and flagged) in the master compiled database, but was not used for analysis. This review process detected additional issues (misabeled sites and incorrect coordinates) in the source databases which were then corrected in the compiled versions.

2.6 CALCULATION OF DAILY AND SEASONAL SUMMARIES

2.6.1 DAILY SUMMARY STATISTICS

All compiled data were acquired at their original temporal resolution, which ranged from 15 to 120 minutes. On days when data completeness was at least 80% (e.g., if data's temporal resolution is 30 minutes, then at least 38 out of the maximum possible 48 measurements must be present), we calculated daily summary statistics included number of measurements, minimum, maximum, mean, and range. All metrics were calculated using R 3.5.1 (R Core Team 2018).

2.6.2 INITIAL CALCULATION OF SEASONAL AND MONTHLY SUMMARY STATISTICS

Key seasonal temperature metrics were selected based on a review of previous stream temperature analyses (Lewis et al. 2000, Welsh et al. 2001, Dunham et al. 2005, Isaak et al. 2010, McCullough 2010) and calculated for each site and year, including:

¹⁷ Order of priority: USFS_NRIS_AqS (highest), SRNF, SRRC, KarukWQ, USFWS, HSU_FSP, and YTFP (lowest). There were no overlap between USGS and other datasets.

- *Maximum Daily Maximum Temperature (MDMT)* – The highest instantaneous maximum temperature recorded during the summer (Figure 4).
- *Maximum Weekly Maximum Temperature (MWMT)* – The highest seven-day average of the daily average temperature. In simple terms, it is the average temperature during the warmest seven-day period of the year. Steps for calculation (Figure 4):
 - Step 1. Calculate maximum temperature for each day.
 - Step 2. Calculate 7-Day Average of the Daily Maximum (7DADM), which is calculated for each day as the average of the daily maximum temperature (Step 1) for the three prior days, the current day, and three following days.
 - Step 3. Select highest 7DADM (Step 2) value of the year.
- *Maximum Weekly Average Temperature (MWAT)* – The highest seven-day moving average of the daily maximum temperatures. In simple terms, it is the average daily maximum temperature during the warmest seven-day period of the year. Steps for calculation (Figure 4):
 - Step 1. Calculate mean temperature for each day.
 - Step 2. Calculate 7-Day Average of the Daily Average (7DADA), which is calculated for each day as the average of the daily mean temperature (Step 1) for the three prior days, the current day, and three 3 following.
 - Step 3. Select highest 7DADA (Step 2) value of the year.
- *Mean August temperature (Aug_mean)* – Metric used in the NorWeST model (Isaak et al. 2017) because August is often the warmest month in snowmelt-dominated streams. Metric only calculated when data available for 90% (28 of 31) of days.
- *Mean Daily Maximum August temperature (Aug_meanMx)* – The August average of the daily maximum temperatures. Metric only calculated when data available for 90% (28 of 31) of days.

The date of occurrence of MDMT, MWMT, and MWAT was also calculated. In cases where the same maximal value was reached on more than one date, the seasonal statistic date was assigned to the date on which a larger number of sites had the maximal value¹⁸.

Section 2.10 provides justification for which metrics we chose to focus our analyses on.

¹⁸ Potential alternatives would be to randomly choose one of the dates, or to assign the mean date, but in cases where long distances separate the occurrence of maximal values, then the mean date might be during a cool period. For example, if maximal values are reached on July 1 and July 30, then the mean date would be July 16.

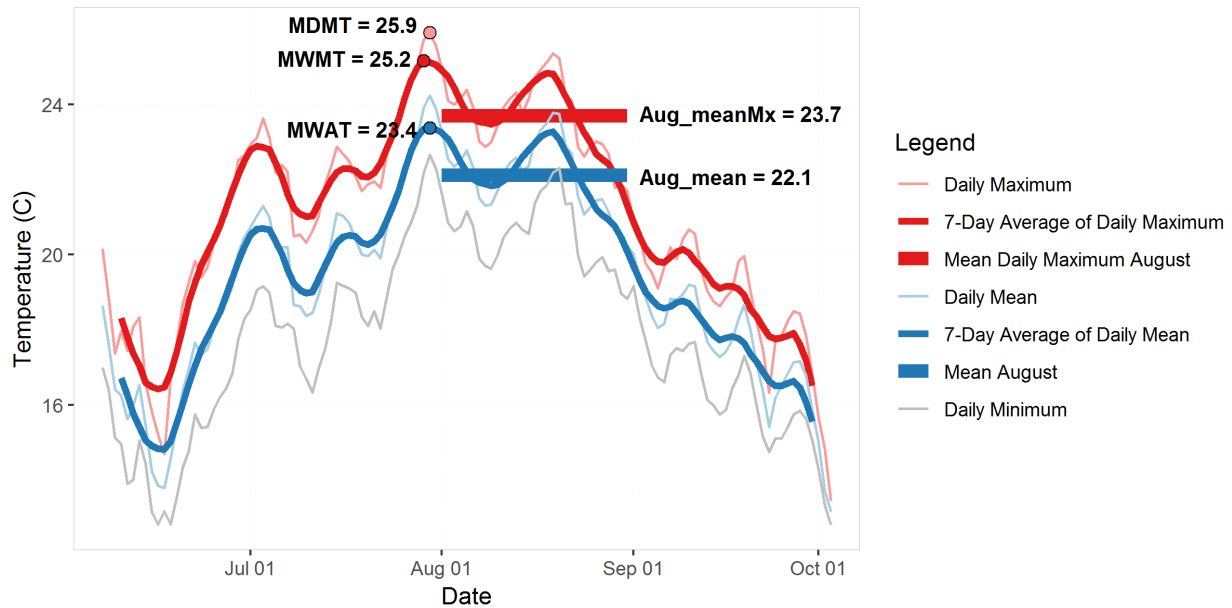


Figure 4. Daily time series of daily maximum, daily mean, daily minimum, 7-day average of daily maximum, and 7-day average of daily mean water temperatures at an example site-year (mouth of South Fork Salmon River in 2016). Maximum daily maximum temperature (MDMT), maximum weekly maximum temperature (MWMT), maximum weekly average temperature (MWAT) are the highest annual values for daily maximum, 7-day average of daily mean, and 7-day average of daily maximum, respectively. Mean daily maximum August temperature (Aug_meanMx), and mean August temperature (Aug_mean) are also shown.

2.6.3 REFINING SEASONAL STATISTICS ACCORDING TO DATA COMPLETENESS

Seasonal summary statistics are relatively simple to calculate when data are available for the entire warm season (i.e., June–Sept.); however, many available datasets only contained data for part of the summer season and thus had to be screened for comparability. Seasonal statistics may be biased low if they are calculated from only a short period and did not include the warmest days of the year. Conversely, excluding seasonal statistics when gaps occurred outside the warmest days would be an unnecessary loss of important information. As described in Section 2.6.2, seasonal statistics were initially calculated for all years and sites. Values were then either retained (i.e., kept) or excluded (i.e., deleted) based on data completeness.

Similar to Asarian (2017), we applied an automated multi-step procedure to screen data completeness. Since MWMT, MWAT, and MDMT almost always occur in July or August, seasonal statistics were retained¹⁹ for datasets which included all of July and August²⁰. For datasets that were missing some days in July or August, seasonal statistics were only automatically retained if the data were present at that site for each day on which that statistic occurred in at least two other sites²¹. This approach makes maximal use of available data while minimizing the chance that un-representative statistics were retained.

2.7 WATERSHED DELINEATION

¹⁹ Seasonal statistics were initially calculated for all years and sites. Values were then either retained (i.e., kept) or excluded (i.e. deleted) based on data completeness.

²⁰ Actually June 28 through September 2 because the 7-Day Average of the Daily Maximum (7DADM) and 7-Day Average of the Daily Average (7DADA) require data to be present for three days before and three days after.

²¹ We chose two sites as the threshold rather than one site because a single site might have unique characteristics or a data quality issue whereas two or more sites should indicate a more widespread pattern.

Using the NHDPlus Version 2 BasinDelineator tool²² in ArcGIS, we delineated a GIS polygon for the watershed contributing to each NHDPlus reach. These polygons allowed us to summarize a variety of GIS data, including climate, to the watershed level for use in stream temperature models.

2.8 ENVIRONMENTAL DATA USED IN STREAM TEMPERATURE MODELS

As described in the following sections, we used a variety of environmental and GIS data in our stream temperature analyses (Figure 2).

2.8.1 ELEVATION

We used the National Elevation Dataset (NED) and GIS to extract the elevation for each site of interest based on its spatial coordinates.

2.8.2 DRAINAGE AREA

Initial estimates of drainage area (i.e. contributing watershed areas) for each reach were obtained from NHDplus/NSI. In NHDplus, drainage area at the bottom of a reach is assigned to all sites within that reach. Reaches split at tributary confluences, so most reaches are only a few kilometers long and actual drainage area does not increase much from the top to the bottom of a reach; however, in headwater reaches, actual drainage area can increase several fold along the reach, so assigning the same drainage area to all sites within that reach would result in drainage areas that are too high in the upper part of the reach. To account for this, we developed a refined estimate of drainage area in R/SSN which uses linear interpolation to adjust the drainage area for each 1-km reach based on its position within the NHDplus reach. For example, if the drainage area at the bottom of an NHDplus reach is 20 km², the drainage area at the bottom of the adjacent upstream reach is 10 km², and the site of interest (i.e., center point of 1-km reach) is located one quarter of the way up from the bottom of the NHDplus reach, then the site is assigned a drainage area of 17.5 km².

2.8.3 DISTANCE FROM HEADWATERS

Using R and SSN, we developed a multi-step method²³ to calculate the distance from headwaters (i.e., further upstream point in the stream network) to each site of interest. In the SSN models, we used distance from headwaters as an alternative to drainage area to represent the natural tendency of streams to warm as water flows downstream from shaded headwaters to solar-exposed downstream reaches.

2.8.4 EFFECTIVE SHADE (TOPOGRAPHIC AND VEGETATIVE)

We used the Washington Department of Ecology's (WDOE) Shade spreadsheet tool to calculate effective shade (the combination of topographic and riparian shading) for each 1-km stream reach. The Shade tool was adapted from the Heat Source model (Boyd and Kasper 2003). Our shade methods and datasets are similar to Detenbeck (2017). Details are provided in Appendix B. Key inputs datasets used include:

- 30-meter resolution remote-sensed canopy height and canopy closure from the Landscape Ecology, Modeling, Mapping, and Analysis (LEMMA) Gradient Nearest Neighbor (GNN) dataset (Ohmann and Gregory 2002, Ohmann et al. 2014)

²² http://www.horizon-systems.com/nhdplus/NHDPlusV2_tools.php#NHDPlusV2%20BasinDelineator%20Tool

²³ Details are too intricate to describe here.

- Wetted width and bankfull width estimated by regressing watershed area with field measurements collected during the Salmon River TMDL (NCRWQCB 2005)
- Digital elevation model from the National Elevation Dataset (NED)

2.8.5 CANOPY

As an alternative to effective shade, in some (not the final) temperature models we experimented with using the average canopy data provided by NorWeST for each 1-km reach. These reach summaries were calculated in GIS by overlaying the canopy layer from the 2011 National Land Cover Database (NLCD) on the stream hydrography and calculating the average canopy value for each reach. The NLCD canopy values are a remote sensing product derived from Landsat satellite imagery (Homer et al. 2015). The models apply 2011 canopy conditions to all years; however, canopy has undoubtedly changed in some locations over the 1995–2017 period due to wildfires and subsequent forest re-growth. Wildfire is discussed in sections 2.9.1 and 3.2.

2.8.6 SLOPE

In some temperature models we experimented with using the average channel slope data provided by NHDplus/NSI for each reach.

2.8.7 MAINSTEM SALMON STREAMFLOW

The USGS operates streamflow gage 11522500 on the Salmon River near its mouth. We used these data to represent interannual variations in streamflow for all sites in the watershed.

2.8.8 TRIBUTARY STREAMFLOW

SRRC, the Karuk Tribe Department of Natural Resources, SRNF Orleans-Ukonom Ranger District, and KNF Happy Camp Ranger District have collaboratively monitored summer streamflows in Salmon River and Middle Klamath tributaries since 2001, with a few additional measurements in 1996, 1997, and 2000. At Salmon River tributary sites, flows were measured zero to six times per year using Marsh-McBirney (Orleans RD prior to 2001) or Swoffer (Orleans RD after 2001 and all others) flow meters. The total number of measurements per site in the 1996–2017 period ranged from one to 27.

There were not enough flow measurements to generate a continuous time series of flow for individual tributaries, so instead we used the flow measurements to produce spatial maps of typical August flows. We used the tributary flow measurements from 23 sites with at least four measurements to fit a linear mixed-effects model that estimates streamflow at each site based on flow at the USGS gage. The model includes random effects that allow each site to have its own intercept, and allow the relationship (i.e., slope) between a site and the USGS gage to vary between sites. Inserting the mean August streamflow value measured at the USGS gage (256 cfs, calculated lumping all years 1990-2017), we then applied the model to estimate long-term mean August streamflow at each of the 23 sites. We then input the 23 sites' flows into a spatial statistical model to estimate long-term mean August streamflow at every 1-km reach in the stream network²⁴ (see Section 2.10 for background information on this class of model). The final spatial statistical model uses only drainage area and the spatial correlations between sites (“exponential tail-up” covariance structure) as predictors.

²⁴ We recognized that it would have been ideal to use a single model rather than two models, but the spatial statistical models do not allow random slopes, only random intercepts. Random slopes were required because relationship between a site and the USGS gage varies considerably between sites.

Watershed area explains the greatest amount of variation in mean August flow, but some interesting spatial patterns are evident as well. For their drainage areas, Wooley Creek, Crapo Creek, Somes Creek, and the Little North Fork Salmon River have substantially higher flow than the other streams in the Salmon River watershed (Figure 5). A table of tributary flows and linear regression equations relating tributary flows to the flows at the USGS gage are provided in Appendix A. We experimented with additional models in an attempt to find variables (e.g., watershed precipitation and mean elevation) that could explain the spatial patterns in tributary flow but were unsuccessful, indicating that other factors may be important. These factors could include 1) The PRISM model indicates higher precipitation in the northwest portion of the Salmon River watershed which partially explains Wooley Creek, Crapo Creek, and the Little North Fork, but does not explain Somes Creek, 2) precipitation differences due to geographic orientation of slopes relative to prevailing direction of storm approach²⁵, 3) bedrock geology, 4) soil type and soil depth, including the presence of wet meadows Crapo Creek (Crapo Meadows), Haypress Meadows (Wooley Creek) and Hamilton Meadows (Little North Fork). The highest elevations in Wooley Creek, Crapo Creek, and the Little North Fork Salmon River watersheds all exceed 2000 m (6562 ft) which is much greater than the highest point in the Somes Creek watershed (Somes Mountain is 1617 m [5305 ft]).

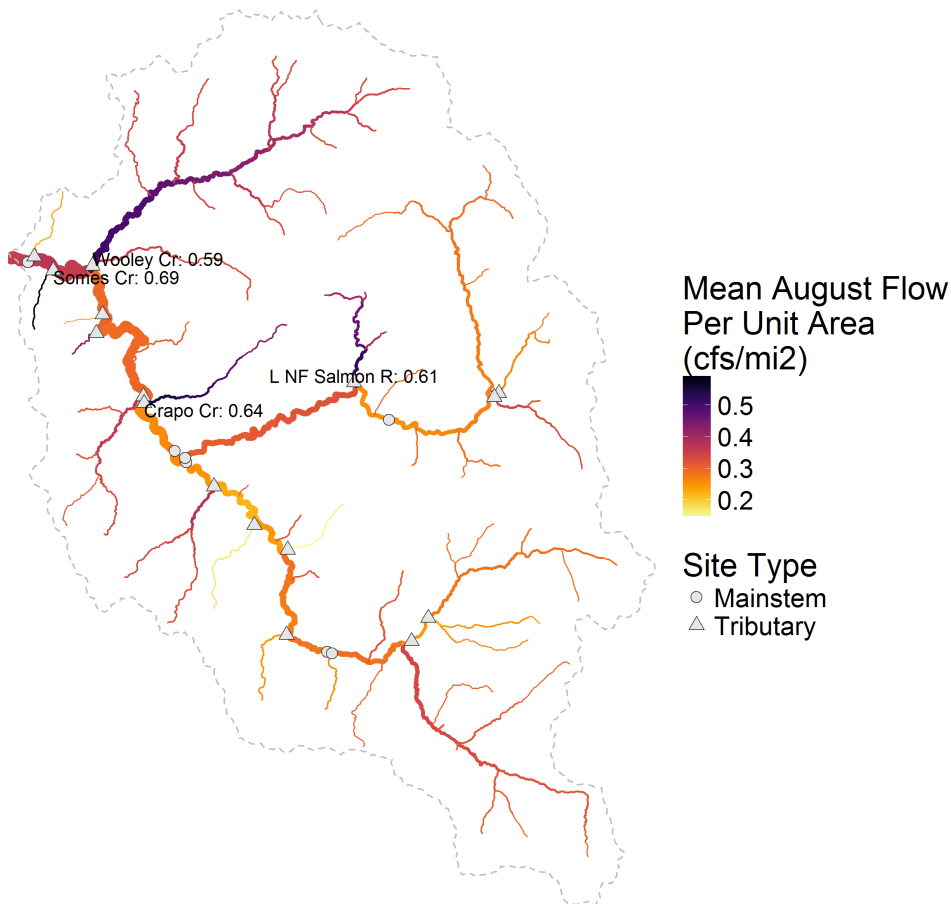


Figure 5. Map of mean August streamflow per unit watershed area for 1-km prediction reaches in the Salmon River watershed, estimated using statistical models fit with discrete measurements at 23 long-term monitoring stations and continuous data from one USGS gage. Only reaches with watershed areas greater than 10 square kilometers (or flow was measured) are shown. Line thickness denotes total streamflow (cfs) while line colors denote streamflow per unit area (cfs per square mile).

²⁵ The PRISM precipitation model attempts to include this factor but it is based on limited input data.

2.8.9 APRIL 1 SNOWPACK

Streams flowing from high elevation areas receive winter and spring snow which can result in spring and summer flows that are higher than in lower-elevation rain-dominated areas, providing a cooling influence on summer stream temperatures. There are a few long-term Snow Course monitoring stations within and adjacent to the Salmon River watershed which could be used as a general watershed-wide index of snowpack between years. However, we needed higher spatial resolution snowpack data for water temperature models to explain differences between sites and not just between years. We used annual time series of modeled April 1 (the typical annual peak) snow water equivalent in snowpack from the University of California Los Angeles Drought Monitoring System's implementation²⁶ (Xiao et al. 2016) of the Variable Infiltration Capacity (VIC) model (Liang et al. 1994). The model's spatial resolution is 1/16° (approximately 6 km) and is driven by gridded climate data similar to Livneh et al. (2013). To evaluate the modeled VIC snowpack data, we graphically compared it to data measured at long-term Snow Course sites (downloaded from the California Data Exchange Center, CDEC²⁷) and watershed averages from several other modeled snowpack datasets, including USGS BCM (Flint et al. 2013) and SNOW Data Assimilation System (SNODAS) from the National Oceanic and Atmospheric Administration's (NOAA) National Operational Hydrologic Remote Sensing Center (NOHRSC 2004) (Figure 6, Appendix C). BCM is a water and energy balance model similar to VIC but with higher resolution. SNODAS combines a model, ground-based snowpack measurements from Snow Courses, and satellite-based remote sensing. SNODAS has been independently validated with high-resolution LIDAR data (Hedrick et al. 2015, Bair et al. 2016). We generated SNODAS summaries for the Salmon River watershed using the Google Climate Engine²⁸. Although the absolute values are different (i.e., generally less snowpack in SNODAS than VIC and BCM), the interannual patterns between these modeled datasets in the Salmon River are generally similar (Appendix C). One exception is 2014 which had deep snowpack in BCM and sparse snowpack in all other modeled and measured datasets. Due to a combination of the 2014 BCM anomaly, available period of record (SNODAS does not start until 2003 and BCM is not yet available for 2017), availability of climate change scenarios, and ease of data accessibility, we used VIC for our modeling. Unfortunately, VIC appears to underestimate snowpack in the eastern rim of the Salmon River watershed, as well as the headwaters of Crapo Creek²⁹, considering the high elevation of those areas and deeper snowpack in SNODAS (Figure 6, Figure 7). Due to high elevations, snowpack lasts longer into the summer in the southeast corner of South Fork Salmon River than anywhere else in the Salmon River watershed (Figure 6).

²⁶ http://hydro.ucla.edu/SurfaceWaterGroup/forecast/monitor_pnw/index.shtml

²⁷ <https://cdec.water.ca.gov/>

²⁸ <http://climateengine.org/data-types/2018/1/5/noaa-snodas>

²⁹ This is likely due to the VIC model's spatial averaging of elevation within the 6-km pixel

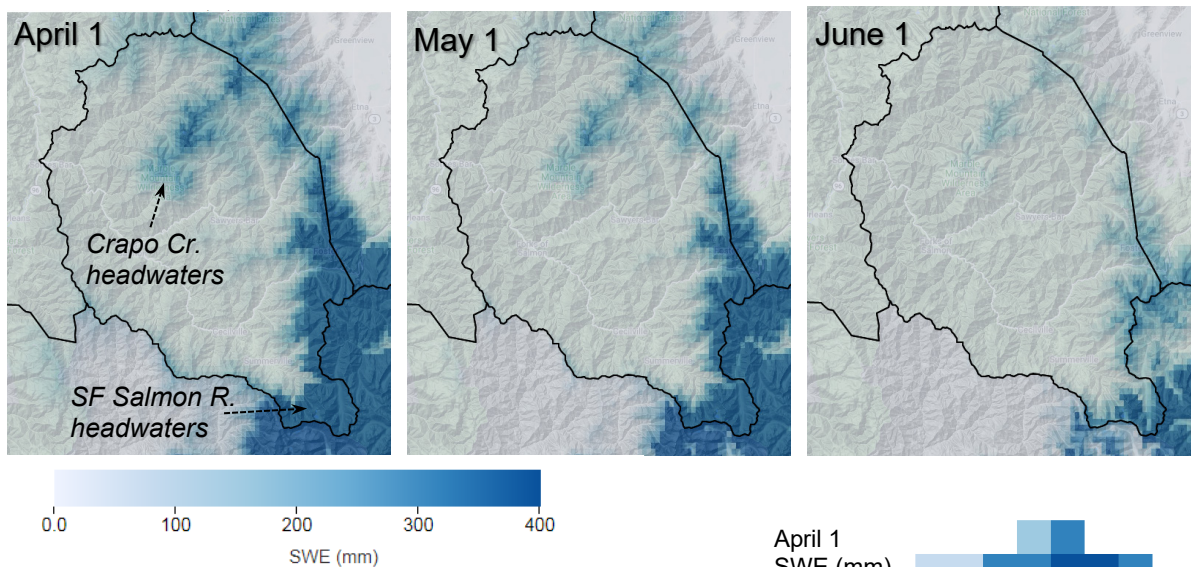


Figure 6. Average snow water equivalent (SWE) for April 1, May 1, and June 1 for the years 2003–2019 from the SNOw Data Assimilation System (SNODAS) model. Spatial resolution is 1 km. Maps were created with Google Climate Engine.

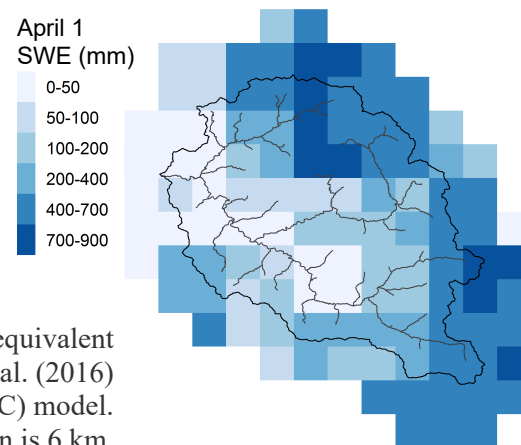


Figure 7. Average April 1 snow water equivalent (SWE) for 1971–2000 from the Xiao et al. (2016) Variable Infiltration Capacity (VIC) model. Spatial resolution is 6 km.

2.8.10 AIR TEMPERATURE TIME SERIES AND MEAN ANNUAL PRECIPITATION

PRISM³⁰ combines ground-based weather stations with GIS data and a statistical model to produce a spatially continuous 4-km grid of climate variables including air temperature and precipitation (Daly et al. 2008). After some initial exploratory analyses using the air temperature data for the specific 4-km pixels where our water temperature stations were located, we spatially averaged the air temperatures across the entire Salmon River watershed.

For mean annual precipitation (i.e., precipitation normals), we downloaded monthly 270-m resolution grids from the USGS Basin Characterization Model (BCM)³¹ (Flint et al. 2013) which was downscaled from PRISM. For each NHDplus reach, we then overlaid the delineated watershed polygon (Section 2.7) to extract a 1990–2017 monthly precipitation time series which we then summed to obtain annual totals and then averaged to obtain normals (long-term averages) for the 1990–2017 period. Precipitation was not utilized in the final water temperature models.

³⁰ <http://www.prism.oregonstate.edu>

³¹ https://ca.water.usgs.gov/projects/reg_hydro/basin-characterization-model.html

2.8.11 WILDFIRE SMOKE (AEROSOL OPTICAL THICKNESS, AOT)

We used aerosol optical thickness (AOT) as a proxy for wildfire smoke. AOT indicates the degree to which aerosols reduce transmission of light through the atmosphere by absorption or scattering. The most easily accessible long-term AOT data for the Salmon River are 1980–present remote sensed data from the Modern-Era Retrospective Analysis for Research and Applications, version 2 (MERRA-2) (Buchard et al. 2017, Randles et al 2017). For 2000 to present, these AOT data are based primarily on the MODerate resolution Imaging Spectroradiometer (MODIS) satellites. MERRA-2’s aerosol (and to a lesser extent, solar radiation) data prior to 2000 are substantially less reliable because the MODIS satellites had not yet been launched. Given the relatively coarse 50-km resolution of the MERRA-2 data, we downloaded³² the time series for a single point (Forks of Salmon) as representative the Salmon River watershed, rather than different coordinates for each site.

2.9 OTHER ENVIRONMENTAL DATA USED TO INTERPRET RESULTS

In addition to the environmental data described in Section 2.8 that was used in water temperature models, we analyzed additional data to provide watershed context for interpreting results.

2.9.1 WILDFIRE EXTENT AND SEVERITY

Wildfire is an important driver of forest dynamics, air temperatures, and water temperatures in the Salmon River (Elder et al. 2002, David et al. 2018). We downloaded GIS data of wildfire extent from CalFire for 1977–2016³³ and 2017³⁴ and severity for 1987–2016 from the U.S. Forest Service³⁵ Region 5. The burn severity data are based on remote sensing analysis of Landsat imagery before and after wildfires (Miller and Thode 2007; Miller and Quayle 2015; Miller et al. 2009, 2016). The burn severity data include several metrics but we used only the percent change in canopy cover. By overlaying the delineated watershed polygons (Section 2.7) in GIS and summarizing by year, we derived annual time series of the percent of each watershed burned (for total area as well as each burn severity category).

2.9.2 SOLAR RADIATION

Solar radiation is an important component of stream heat budgets, and thus has a large effect on water temperatures. Solar radiation follows a seasonal pattern with day length and the position of the sun, but is also affected by clouds and aerosols (i.e., smoke, dust, and sulfates). We used three remote sensed solar radiation datasets. The first is MERRA-2 (Buchard et al. 2017, Randles et al 2017) which accounts for aerosols, but has a coarse 50-km resolution so as with the MERRA-2 aerosol optical thickness we download data for a single location only. The National Solar Radiation Dataset (NSRDB) and the California Irrigation Management Information System (CIMIS) solar radiation datasets have higher spatial resolution, so we downloaded time series for individual sites using application program interfaces (APIs)³⁶ in R. CIMIS combines its network of ground-based weather stations and data from NOAA’s Geostationary Operational Environmental Satellite (GOES) to model solar radiation at 2 km spatial resolution (Hart et al.

³² using NASA’s Giovanni website: <https://giovanni.sci.gsfc.nasa.gov/giovanni>

³³ Version 16_1: http://frap.fire.ca.gov/data/frapgisdata-sw-fireperimeters_download

³⁴ <https://www.google.com/maps/d/u/0/viewer?mid=1TOEFA857tOVxtewW1DH6neG1Sm0&hl=en&ll=41.26392054233059%2C-122.3191750732422&z=9>

³⁵ <https://www.fs.usda.gov/detail/r5/landmanagement/gis/?cid=STELPRDB5327833>

³⁶ https://developer.nrel.gov/docs/solar/nsrdb/psm3_data_download/ and <http://et.water.ca.gov/>

2009). The CIMIS model does not explicitly represent aerosols, but remote sensing algorithms sometimes categorize dense smoke plumes as clouds. CIMIS data are available for 2004–2017. The NSRDB model combines cloud properties derived from GOES satellite imagery with aerosol data (from MERRA-2 and the MODIS satellites) into a Physical Solar Model which provides solar radiation at 4-km resolution (Sengupta et al. 2018). NSRDB data are available for 1998–2017.

2.10 LINEAR MIXED EFFECTS MODELS TO ACCOUNT FOR SITE-SPECIFIC VARIATION IN SENSITIVITY OF STREAM TEMPERATURE TO INTERANNUAL CLIMATE VARIABILITY

Air temperature sensitivity is the expected change in stream temperature per unit change in air temperature (Mayer 2012, Luce et al. 2014). Similarly, streamflow sensitivity is the expected change in stream temperature per unit change in streamflow (Luce et al. 2014). Spatial stream-network (SSN) models (sections 2.12 and 3.5) are our primary method for assessing air temperature sensitivity and streamflow sensitivity. However, the currently available R package to implement SSN models (SSN, Ver Hoef et al. 2014) does not include random slopes (e.g., site-specific variation in the streamflow sensitivity), so as an exploration of the spatial variation in climate sensitivity across our long-term monitoring sites, we constructed linear mixed-effects models for the 27 sites that had at least 14 years of August stream temperature data. In addition to flow and air temperature, we also included wildfire smoke (AOT) and April 1 snowpack. We tested several combinations of variables and model structures and then used AIC to inform selection of a final model. We assessed multicollinearity by calculating condition index according to Belsley et al. (1980) and avoided models with a condition number greater than 30. Models were fit using R 3.5.1 (R Core Team 2018) and the lme4 package version 1.1-19 (Bates et al. 2015).

All summer temperature metrics are highly correlated with each other (section 3.1), making it unnecessary to do every analysis on every metric. Due to time and budget constraints we limit our linear mixed effects models to two metrics: mean August temperature and mean daily maximum August temperature. As shown below in section 3.1, water temperatures in the Salmon River watershed typically peak in July or August. We focus our analyses on August to increase compatibility with previous regional stream temperature modeling efforts (Isaak et al. 2017, Asarian 2017). NorWeST (Isaak et al. 2017) models mean August temperature, but we chose mean daily maximum August temperature to target conditions that are more acutely stressful to aquatic organisms. We used monthly summaries for our linear mixed effects models and spatial stream-network models because the exact day that alternative temperature metrics such as MWAT, MWMT, and MDAT occur varies between years and sites, making it more difficult to construct models to predict those alternative metrics based on air temperature and streamflow. Complete time series for all metrics including months May–September are included in Appendix F.

2.11 LONG-TERM TRENDS IN STREAM TEMPERATURE AND CLIMATE-ADJUSTED STREAM TEMPERATURE

At 27 long-term monitoring sites (defined as having at least 14 years of temperature data), we used linear mixed-effects models and regression models to calculate slopes and evaluated the statistical significance of these trends. Two models were run for each temperature metric, one to provide an overall slope representing all sites and another to provide separate slopes for each individual site. The first was a linear mixed-effects model with a fixed effect of year and a random effect that allowed the intercept to vary by site. The year coefficient provides the single

linear slope representing the trend of all long-term sites. The second was a linear regression model with year as a fixed effect and an interaction of year and site. The year coefficient for each individual site provides a linear slope for each individual long-term site.

In addition to evaluating long-term trends in stream temperature as described in the preceding paragraph, we also evaluated long-term trends in climate-adjusted stream temperature, which we define as the underlying trend in stream temperature once the effects of interannual variation in climate (air temperature, streamflow, snowpack, and AOT [smoke]) are accounted for using statistical models (Figure 2). This process had three steps for each variable (mean August temperature and mean daily maximum August temperature). The first step was to develop linear mixed-effects models to account for climate (section 2.10 above). The second step was to calculate model residuals (observed value minus modeled value) for each data point. The final step was to run two linear mixed-effect models on the residuals. The first model provided an overall slope representing all sites and the second provided separate slopes for each individual site. The first model has only a fixed effect for year, which provides the single linear slope representing the trend of all long-term sites. The second model had only a random effect that allowed the year slope to vary by site. These random slopes for year for each individual site provided a linear slope for each individual long-term site, and we used the associated p-values³⁷ provided by the lmerTest package (Kuznetsova et al. 2017).

Prior to implementing the two-model process described in the previous paragraph, we experimented with using a single model that included year in the same model as air temperature, streamflow, snowpack, and AOT. However, this was problematic because year and air temperature were not independent because the lowest (1995 and 1999) and highest (2016 and 2017) air temperatures occurred at the edges of the 1995-2017 trend period we evaluated. Due to the correlation of year and air temperature, the year slopes in this single model method were lower than in the two-model method because year pulled some influence from air temperature.

2.12 SPATIAL STREAM-NETWORK MODELING

We used spatial stream-network models to produce estimates of mean daily maximum August stream temperatures for each 1-kilometer stream reach within the Salmon River watershed. Justification for choosing this metric is provided above in section 2.10. We ran the models in version 1.1.8 of the SSN package for R (Ver Hoef et al. 2014), adapting the R code used by RMRS for the NorWeST modeling of the Northern California/Coastal Klamath processing unit which encompasses the Salmon River watershed (Isaak et al. 2017). Prior to running the spatial models, we used version 2.04 of the STARS toolbox in ArcGIS to prepare the data for analysis (Peterson and Ver Hoef. 2014), following the procedures in Nagel et al. (2017). SSN and STARS were downloaded from the RMRS website³⁸.

The statistical theory behind SSN and STARS is quite complex with many intricate details, and there are many potential applications for the models, not just stream temperature. Isaak et al. (2014) provides an excellent introduction to the topic. The stream temperature model applied in this project combines observed temperature data, Geographic Information Systems (GIS) data about landscape attributes, interannual variation in climate, and a spatial stream-network model. In the following paragraphs, some key model concepts are briefly described for the lay person.

³⁷ We recognize that these P-values are unreliable due to uncertainty regarding the number of degrees of freedom; however, we choose to use them as an index of evidence given lack of other suitable methods.

³⁸ https://www.fs.fed.us/rm/boise/AWAE/projects/SSN_STARS/latest_releases.html

The model accounts for interannual differences in the observed stream temperature data that is used to calibrate the model. This is necessary because site stream temperatures vary from year to year. If one reach was monitored only in a hot year and another reach was monitored only in a cool year, then using those single years to represent temperatures in those reaches would produce a biased map unless those interannual differences were addressed. The model resolves this in two ways. The first is to include year-specific air temperatures, streamflow, and snowpack as predictor variables in the regression. The second is to include year as random effect, meaning that after estimating how interannual differences relate to flow and temperature, the model also accounts for remaining unexplained variation attributed to differences among years.

The model estimates temperatures for each 1-kilometer reach by blending several components. To estimate stream temperature, each observed data point (e.g., mean August temperature for a site and year) was regressed against the GIS predictor variables (e.g., drainage area, canopy, etc., as described in section 2.8), interannual variations in climate (air temperature, streamflow, and snowpack, as described in section 2.8), and observed stream temperatures at other sites (with the nearest sites having the strongest influence). After including variation due to regressed variables, sites closest to the prediction site have greater influence on predicted temperatures than do sites that are further away. The model takes into account tributary relationships. For example, if there are observed data on both forks upstream of a confluence, the predicted temperature downstream of the confluence will be highly influenced by the information from observed data points.

2.13 CLIMATE CHANGE PREDICTIONS

2.13.1 SUMMARY

To evaluate how Salmon River stream temperatures might change in the future as the climate warms, we used predictions from downscaled climate models and hydrologic models as inputs into our spatial statistical modeling of stream temperature. No single data source provided all inputs, so we combined information from multiple sources. The scenarios we chose (Table 2), should be considered plausible estimates for the sake of exploration, but users should recognize that the magnitudes are subject to a relatively high degree of uncertainty, particularly for streamflow. The rationale for these choices is described in sections 2.13.2 through 2.13.5.

Since the baseline period for the air temperature and streamflow projections are centered on a period 25 years earlier (1950–2005) than the period for which we calibrated our temperature models (1990–2017), we proportionally reduced future scenarios by 23% to account for the changes that have already occurred since the 1950–2005 baseline period³⁹ (Table 2), following an approach similar to Isaak et al. (2017). The snowpack projections are relative to a 1971–2000 baseline period, but were not applied as changes from baseline but rather as absolute values, so it was not necessary to proportionally reduce the changes to account for the time elapsed between 1971–2000 and 1990–2017.

Climate change will also likely affect stream temperatures through additional mechanisms beyond those included in our spatial statistical models. Rising air temperatures are likely to increase wildfire activity and affect forest structure and composition. Increased severity and frequency of floods could cause geomorphic changes to stream channels, particularly if high-severity fire increases the susceptibility of hillslopes to landslides. It is not possible to incorporate such complex dynamics into our spatial statistical models of stream temperature.

³⁹ Midpoints of periods are 1978 for 1950–2005, 2003 for 1990–2017, and 2085 for 2070–2099. Total duration from 1978 to 2085 is 107 years. Since 2003 is 25 years after 1978, we reduced the future changes by $25/107 = 23\%$.

Table 2. Air temperatures and August streamflow selected for use in spatial statistical stream temperature model climate change scenarios.

Scenario Name	Time Period	Relative to 1950–2005 Baseline		Relative to 1971–2000 Baseline	Relative to 1990-2017 Baseline		
		August Air Temp.	August Streamflow	April 1 Snowpack	August Air Temp.	August Streamflow	April 1 Snowpack*
Moderate Emissions (RCP 4.5)	Late 21 st century (2070–2099)	+3.1 °C increase above historic	60% of historic (i.e., 40% decrease)	35% of historic (i.e., 65% decrease)	+2.4 °C increase above historic	69% of historic (i.e., 31% decrease)	37% of historic (i.e., 63% decrease)*
High Emissions (RCP 8.5)	Late 21 st century (2070–2099)	+5.7 °C increase above historic	40% of historic (i.e., 60% decrease)	16% of historic (i.e., 84% decrease)	+4.4 °C increase above historic	54% of historic (i.e., 46% decrease)	17% of historic (i.e., 83% decrease)*

*Note: For the sake of simplicity, the snowpack declines shown in this table are averaged across the whole Salmon River watershed, but for our stream temperature models we apply reach-specific values (see section 2.13.4).

2.13.2 REPRESENTATIVE CONCENTRATION PATHWAYS

The first step in making climate change predictions is to adopt assumptions about future concentrations of greenhouse gases. For our analysis, we primarily used two commonly used Representative Concentration Pathways (RCPs). RCP 8.5 is a high emissions scenario where greenhouse gas concentrations continue their current rapidly rising trajectory, with carbon dioxide (CO₂) concentrations reaching approximately 950 parts per million (ppm) by 2100. RCP 4.5 is a medium emissions scenario in which considerable greenhouse gas mitigation efforts stabilize CO₂ concentrations at approximately 540 ppm by the middle of the 21st century (van Vuuren 2011). As of February 2018, CO₂ concentrations are currently at 408 ppm⁴⁰.

2.13.3 AIR TEMPERATURE

Research teams around the world have developed general circulation models (GCMs) which simulate earth’s climate at a coarse spatial resolution. The Coupled Model Intercomparison Project (CMIP5) is an archive with results from many GCMs under several RCPs (Taylor et al. 2012). To make local predictions, it is necessary to spatially downscale the GCM results to higher resolution and correct biases (Pierce et al. 2016). *We used the Northwest Climate Toolbox to extract a time series for Forks of Salmon which shows that summer air temperatures are expected to be 3.1 °C and 5.7 °C higher under moderate (RCP 4.5) and high (RCP 8.5) emissions scenarios, respectively, by the end of the 21st century than during the historical 1950-2005 period* (Figure 8) (Hegewisch and Abatzoglou 2018). These predictions are based on an ensemble of 20 GCMs using version 2 of the Multivariate Adapted Constructed Analogs (MACA) methodology (Abatzoglou and 2012), trained using the University of Idaho gridMet dataset (Abatzoglou 2013).

⁴⁰ <https://climate.nasa.gov/vital-signs/carbon-dioxide/>

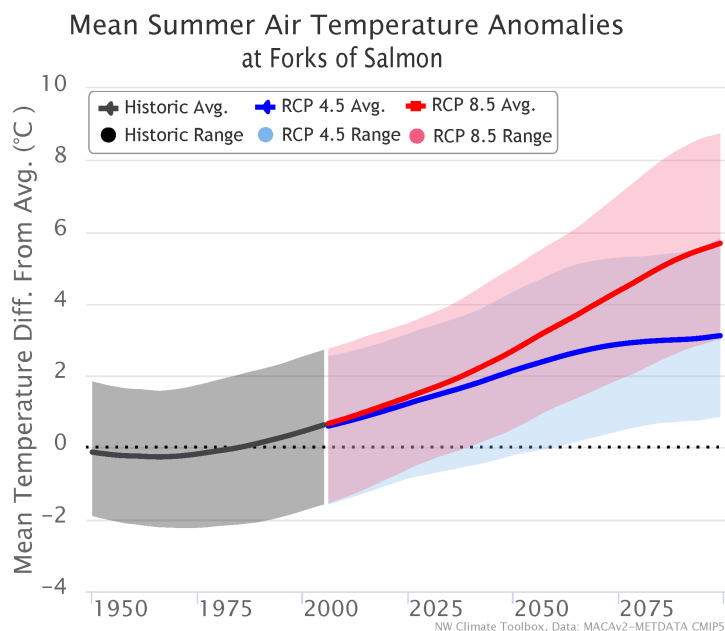


Figure 8. Modeled summer (June, July, and August) air temperature at Forks of Salmon for the historical period (1950-2005) and predictions for 2006 to 2099 under moderate (RCP 4.5) and high (RCP 8.5) greenhouse gas emissions scenarios from an ensemble of 20 general circulation models (GCMs). All temperature values are relative to the 1950-2005 mean and are smoothed to highlight long-term trends rather than short-term variability. Figure adapted from Hegewisch and Abatzoglou (2018).

2.13.4 APRIL 1 SNOWPACK

April 1 snowpack has declined dramatically across most of the Western U.S. in recent decades, and is expected to continue to decline (Mote et al. 2018). As noted above section 2.8.9, we used April 1 snowpack from the VIC hydrology model in our SSN stream temperature models for the modern climate. Mote et al. (2014) provides VIC hydrology predictions for 20 climate change scenarios (10 GCMs each for RCP4.5 and RCP8.5). For the historic period (1971-2000), the arrangement of individual years is essentially random because the Mote et al. (2014) VIC hydrology model uses climate inputs (e.g., precipitation, air temperature, etc.) simulated from GCMs rather than from observed data; therefore, the Mote et al. (2014) VIC hydrology outputs are intended to be used for comparing climate change effects across multi-decadal periods rather than any individual year. We downloaded⁴¹ GIS grids of multi-model 30-year means (average of the 10 GCMs) of April 1 snowpack for the 1971-2000 historical climate and 2070-2099 future climate for both RCP4.5 and RCP 8.5. For each 6-km pixel, we then calculated the ratio of the future snowpack (for both RCP4.5 and RCP8.5) to the historic snowpack.

The climate inputs to the Xiao et al. (2016) VIC hydrology model that we used to train our SSN stream temperature model are based on gridded versions of observed climate data, not simulated from GCMs. Thus, for each 6-km pixel we calculated 1971–2000 April 1 snowpack averages from the Xiao et al. (2016) VIC hydrology model outputs (Figure 9). We then multiplied these 1971–2000 averages by the ratios of the historic-to-future snowpack calculated from the Mote et al. (2014) VIC outputs (described at end of previous paragraph) to obtain predictions for average April 1 snowpack for each 6-km pixel for the period 2070–2099 under RCP4.5 and RCP8.5 (Figure 9). Finally, for each NHDplus reach, we then overlaid the delineated watershed polygon

⁴¹ https://climate.northwestknowledge.net/IntegratedScenarios/vis_summarymaps.php

(Section 2.7) on the 6-km pixels to calculate the average April 1 snowpack for 2070–2099 under RCP4.5 and RCP8.5.

Table 3 compares the predictions of the Salmon River watershed average April 1 snowpack for the datasets and methods described above (which we used in our stream temperature models) as well as an alternative set of predictions from Cal-Adapt. The Cal-Adapt tool⁴² provides VIC outputs for the 1990–2005 historical period as well as climate change projections using 10 GCMs selected by Pierce et al. (2016), downscaled using the Localized Constructed Analogs (LOCA) method (Pierce et al. 2014) and trained using the Livneh et al. (2015) climate dataset. Snowpack in Cal-Adapt is greater than in Xiao et al. (2016) and Mote et al. (2014), but relative declines from 1971-2000 to 2070-2099 are similar (~40% for RCP4.5 and ~80% for RCP 8.5).

Table 3. Comparison of modeled April 1 snowpack in the Salmon River watershed for historic and future climate periods, from multiple data sources.

Scenario and Time Period	Average April 1 snowpack in Salmon River watershed (mm snow water equivalent)			
	Xiao et al. 2016	Mote et al. 2014	Xiao et al. 2016 adjusted by Mote et al. 2014 predicted % declines	Cal-Adapt
Historic 1950–2006	284			498
Historic 1971–2000	270	285		467
Baseline 1990–2017	258			
Late 21 st century (2070–2099) Moderate Emissions (RCP 4.5)		118	95	193
Late 21 st century (2070–2099) High Emissions (RCP 8.5)		56	43	97

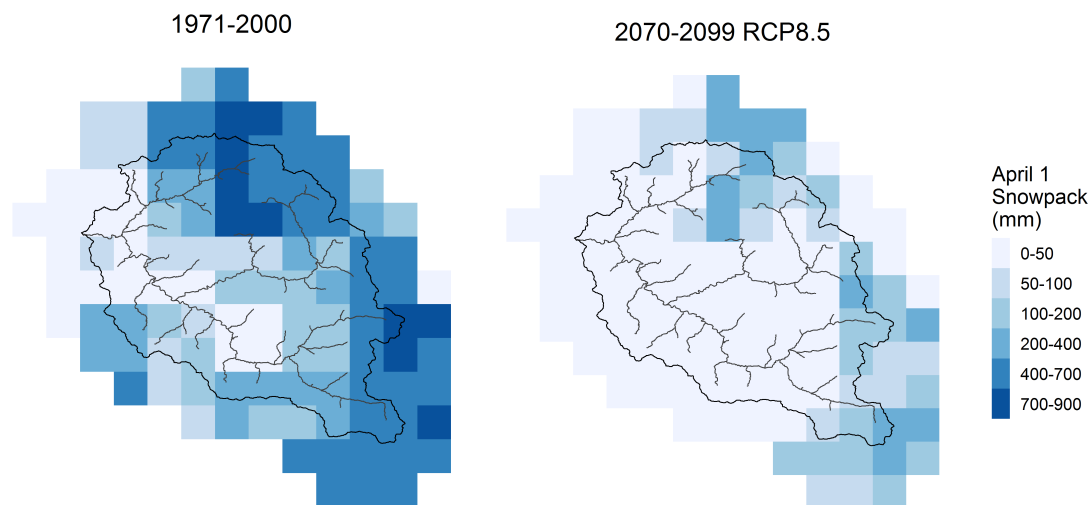


Figure 9. Modeled average April 1 snowpack for 1971–2000 (Xiao et al. 2016) and 2070–2099 under RCP8.5 (Xiao et al. 2016 adjusted by predicted percent declines from Mote et al. 2014)

⁴² <http://cal-adapt.org/>

2.13.5 STREAMFLOW

The magnitude of the streamflow response to climate change has more uncertainty than the predictions for air temperature and snowpack because it is dependent on watershed-specific factors such as geology (Safeeq et al. 2014). The best method to assess the streamflow response is to develop and calibrate a hydrologic model. Unfortunately, there are no existing publicly available and locally calibrated hydrologic models for the Salmon River, so we have to make assumptions based on models developed for other locations which have similar climate and elevation as the Salmon River. Two hydrologic models with climate change scenarios are available for the Sierra Nevada: Water Evaluation and Planning System (WEAP21) (Young et al. 2009, Null et al. 2010, Mehta et al. 2011) and Soil and Water Assessment Tool (SWAT) (Ficklin et al. 2012, Luo 2013, Ficklin et al. 2015). The Variable Infiltration Capacity (VIC) model (Liang et al. 1994) has also been implemented for the Western United States (Wenger et al. 2010, Mote et al. 2014), conterminous United States (Oubeidillah et al. 2014, Naz et al. 2016), and Klamath Basin (Gangopadhyay and Pruitt 2011). The US Bureau of Reclamation has also completed the technical portion of a Klamath Basin climate change study which includes a VIC model calibrated for the Salmon River watershed (Elsner and McGinnis 2014), but the report remains in management review and has not been publicly released.

With the exception of the unreleased Klamath Basin study, none of the VIC models were locally calibrated to the Salmon River, and monthly predictions for WEAP21 are not readily available. Thus, we based our Salmon River predictions on the SWAT predictions for three northern Sierra Nevada rivers from Ficklin et al. (2012) (Figure 10) and upper Trinity River and Upper Sacramento River VIC predictions from Mote et al. (2014) (Table 4), all of which have climate and mean elevation that are relatively similar to the Salmon River⁴³. The SWAT model predicts August streamflows will decrease to approximately 54-80% of historical levels by the 2080s (Figure 10). The Ficklin et al. (2012) SWAT model scenarios are based on GCMs from an older set of emissions trajectories (CMIP3) that have smaller air temperature increases (relative to the historic period, the end of century warming is 4.1 °C for A2 trajectory and 2.3 °C for B1 trajectory) than the RCP 4.5 and RCP 8.5 emissions trajectories from CMIP5, and therefore they likely underestimate streamflow changes (Ficklin et al. 2015). The VIC model for Trinity River predicts August flow will decrease to 32-53% by the 2080s (Table 4). *Based on these SWAT and VIC results, we decided to set the August streamflows in our SSN stream temperature climate scenarios at 60% of historic levels for RCP 4.5 and 40% for RCP 8.5.*

Statistical analysis of existing data is an alternative approach to hydrologic simulations, and has been previously applied to the Salmon River. Using a random forest model calibrated from long-term streamflow gages in coastal California, Grantham et al. (2018) predicted that August streamflows in the Salmon River will decline by 2.35% for each 1°C increase in air temperature from the 1975–1999 baseline; however, these predictions are likely an underestimate because 1) precipitation will shift from snow to rain, 2) the model does not explicitly include snow, 3) and the 58 calibration gages had much lower mean basin elevation (mean 740m) than the Salmon River (1298m). The Salmon River was included in 63 Western U.S. mountain streams analyzed by Dierauer et al. (2018), but results were not reported for individual sites. Warm winters resulted in significantly longer, more severe summer low flows (Dierauer et al. 2018).

Climate change is also likely to affect forest structure and composition which could affect hydrology, but it is not possible to incorporate such complex effects into our temperature models.

⁴³ Elevations from StreamCat (Hill et al. 2016): Salmon River at mouth (1298m), American River below Folsom Dam (1342m), Feather River at Oroville (1528m), Upper Sacramento River upstream of McCloud River (1124m), Trinity River below Trinity Lake (1435m), Yuba River below Engle bright Dam (1433m).

Table 4. Climate change projections for mean August flow at three sites (Trinity River, Feather River, American River) predicted by the Variable Infiltration Capacity (VIC) model using the mean of 10 general circulation models (GCMs) as meteorological inputs. Data from the Integrated Scenarios of Climate, Hydrology, and Vegetation for the Northwest project (Mote et al. 2014), accessed at https://climate.northwestknowledge.net/IntegratedScenarios/vis_streamflows.php.

Site	Time Period	RCP4.5 (cfs)	RCP8.5 (cfs)	RCP4.5 (as % of Historic Median)	RCP8.5 (as % of Historic Median)
a) Trinity Lake Inflow	Historical Climate (1950-2005)	257	257	100%	100%
	Early 21 st century (2010-2039)	146	215	57%	84%
	Mid-21 st century (2040-2069)	145	121	56%	47%
	late 21 st century (2070-2099)	137	83	53%	32%
b) Feather River at Oroville	Historical Climate (1950-2005)	2314	2314	100%	100%
	Early 21 st century (2010-2039)	1644	1908	71%	82%
	Mid-21 st century (2040-2069)	1633	1698	71%	73%
	late 21 st century (2070-2099)	1791	1453	77%	63%
c) Yuba River at Engelbright	Historical Climate (1950-2005)	1540	1540	100%	100%
	Early 21 st century (2010-2039)	1070	1135	69%	74%
	Mid-21 st century (2040-2069)	961	989	62%	64%
	late 21 st century (2070-2099)	1105	903	72%	59%
d) American River at Folsom	Historical Climate (1950-2005)	800	800	100%	100%
	Early 21 st century (2010-2039)	602	934	75%	117%
	Mid-21 st century (2040-2069)	553	581	69%	73%
	late 21 st century (2070-2099)	643	509	80%	64%

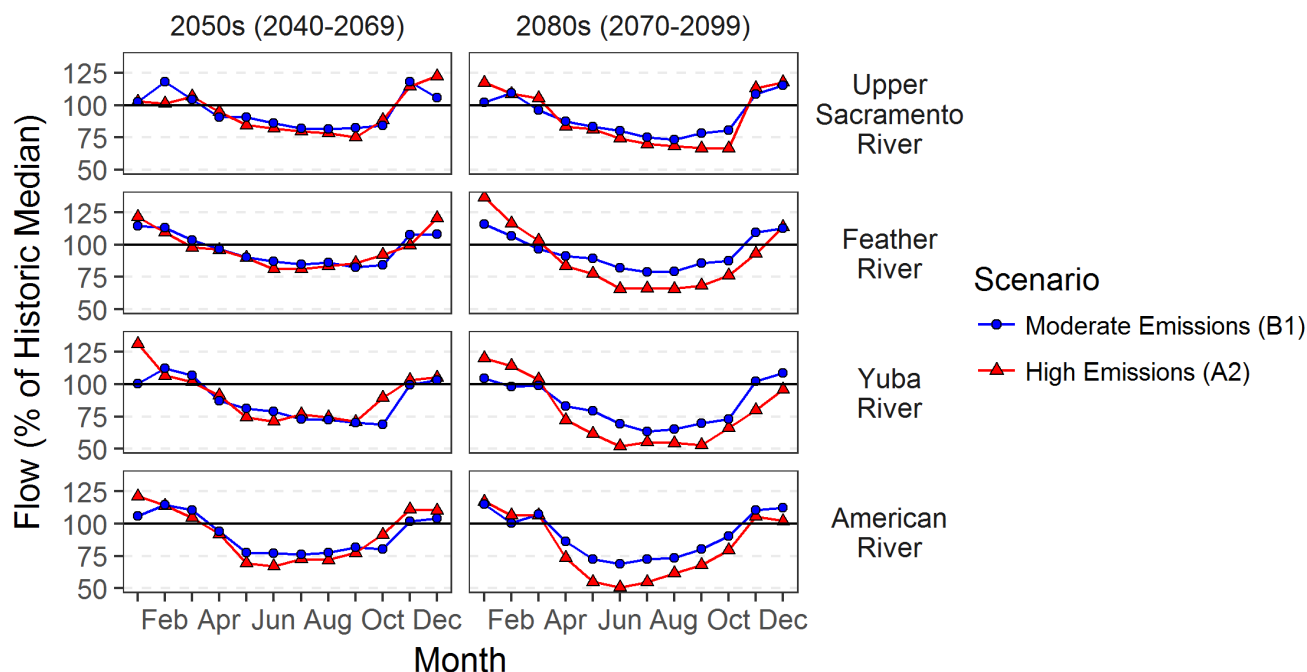


Figure 10. Monthly median streamflow for three Sierra Nevada rivers predicted by the Soil and Water Assessment Tool (SWAT) hydrologic model under moderate (B1) and high (A2) greenhouse gas emissions scenarios from 16 general circulation models (GCMs). Figure created using data from Ficklin et al. (2012). Flows are expressed as a percent of the median for the historic period (1960-2005).

3 RESULTS AND DISCUSSION

3.1 OVERALL SEASONAL PATTERNS IN STREAM TEMPERATURE AND RELATIONSHIPS BETWEEN TEMPERATURE METRICS

Stream temperatures in the Salmon River watershed typically peak in July or August (Figure 11). Averaged across all years and sites, the peak occurs around August 1 (Figure 11). On average, July is slightly warmer than August but much warmer than June (Figure 13). There is considerable year-to-year (and to a lesser extent, site-to-site) variation in the date that peak temperatures occur (Figure 12). MWMT temperatures occurred earlier in 2015 than in any other year (Figure 12).

Maximum weekly maximum temperature (MWMT), maximum weekly average temperature (MWAT), annual single maximum (MDMT), August mean (Aug_mean), and August mean (Aug_meanMx) temperatures for the entire Salmon River watershed dataset are all highly correlated (Figure 13). The strongest correlation is between MWMT and MDMT, with a Pearson Correlation Coefficient of 0.997 (Figure 14).

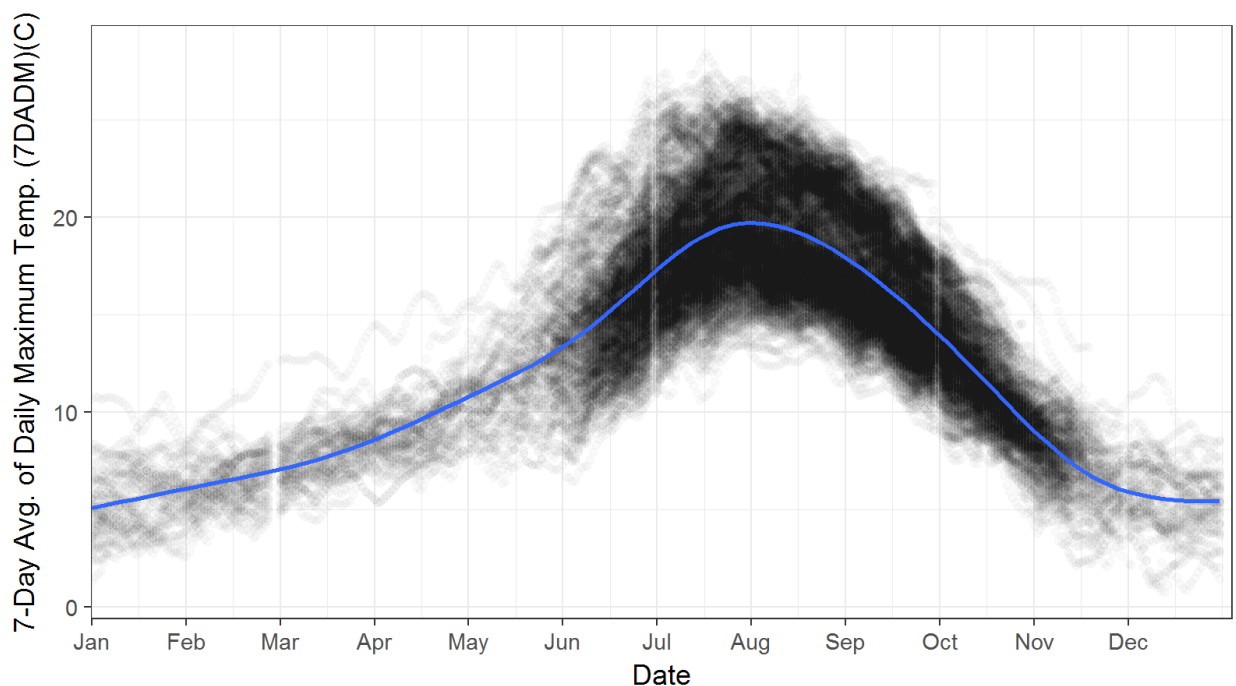


Figure 11. Seven-day moving averages of daily maximum temperature (7DADM) for every site and every year in the Salmon River watershed. Blue line is LOESS (LOcally Estimated Scatterplot Smoothing) smoother.

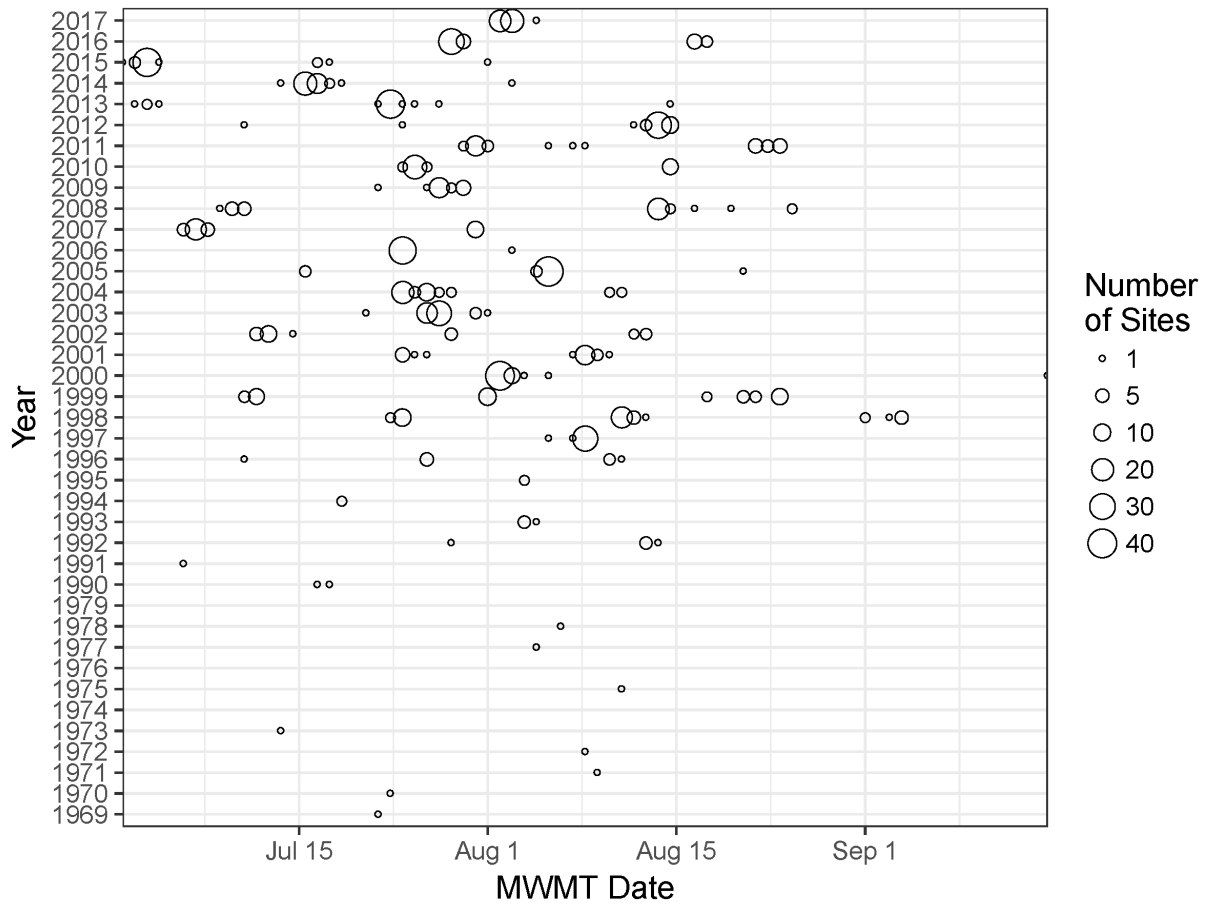


Figure 12. Date each year 1969–1979 and 1990–2017 upon which MWMT temperature occurred at sites in the Salmon River watershed. Size of circles corresponds to the number of sites.

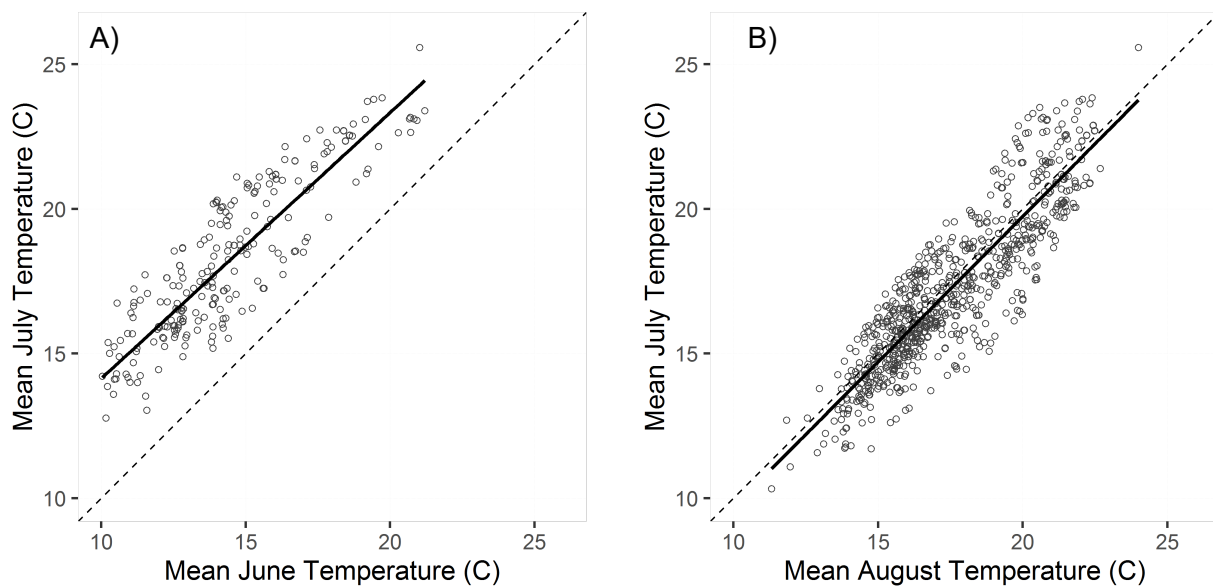


Figure 13. Comparison of mean July stream temperatures with (A) mean June stream temperatures, and (B) mean August stream temperatures, for each site-year in the 1990-2017 Salmon River watershed dataset. Each dot represents a single site and year. Due to a relative lack of site-years with complete June data (i.e., see Figure 16), there are many fewer points in A than B. Thick solid line is a linear regression and the thin dotted line is the 1:1 ($Y=X$) line.

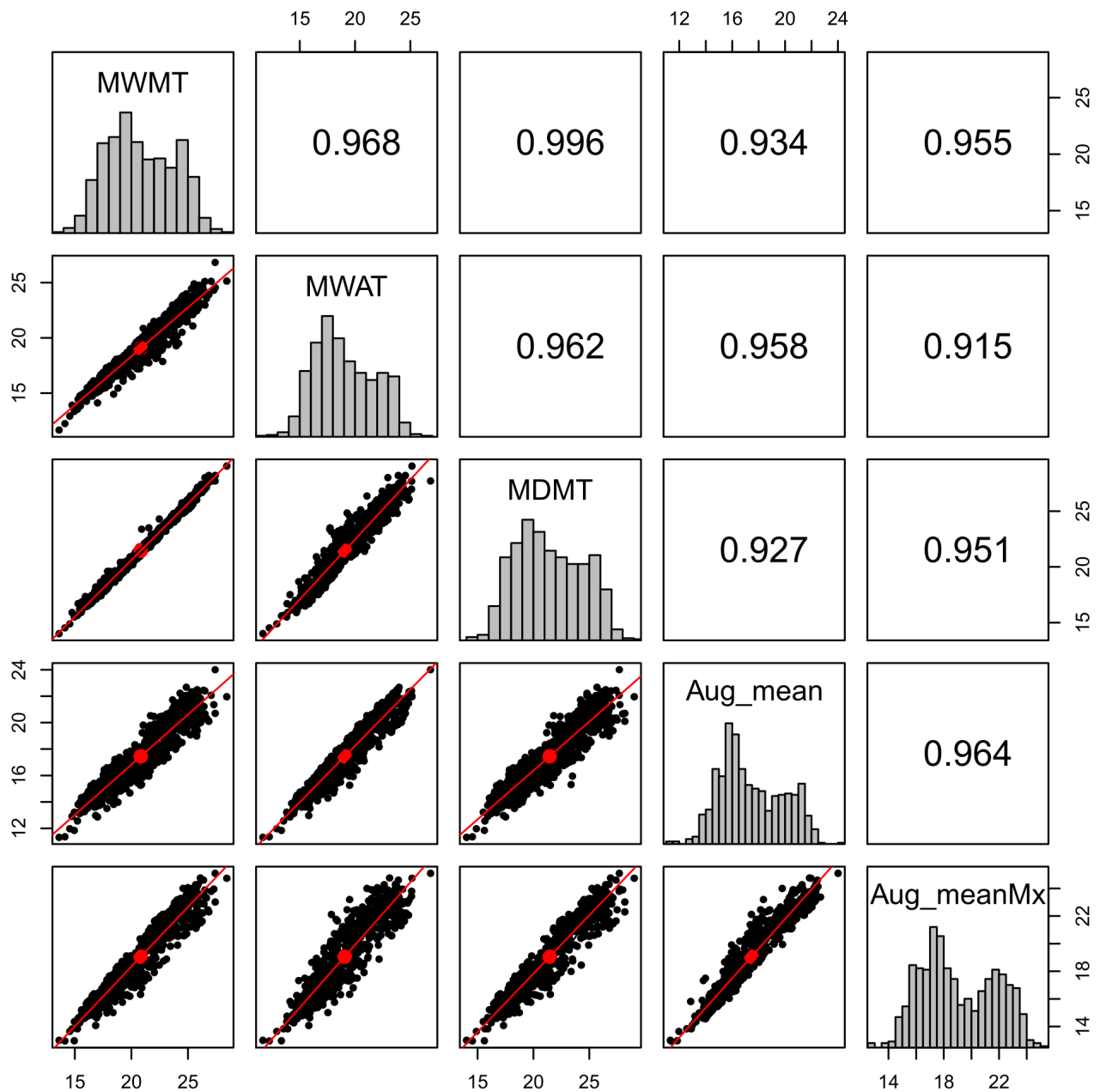


Figure 14. Correlation matrix comparing maximum weekly maximum temperature (MWMT), maximum weekly average temperature (MWAT), annual single maximum (MDMT), August mean (Aug_mean), and August mean temperatures (Aug_meanMx) for the entire Salmon River watershed dataset. The matrix includes a row and column for each variable, and the intersection of a row and column shows the correlation between a pair of variables. For example, the left column of the bottom row is a plot of MWMT vs. Aug_meanMx with linear trend line shown in red and each dot representing a single site and year, and the number (0.955) in the right column of the upper row is the Pearson Correlation Coefficient⁴⁴ between MWMT and Aug_mean. Grey bars along the symmetrical axis of the matrix are histograms showing the distribution of data for each variable.

⁴⁴ 1.000 would indicate a perfect positive correlation between the variables while zero would indicate a complete lack of relationship between the two variables

3.2 ANNUAL TIME SERIES OF BASINWIDE SUMMARIES OF STREAM TEMPERATURE, CLIMATE, AND WILDFIRE

Streamflow, air temperature (Isaak et al. 2017), and wildfires (David et al. 2018, Koontz et al. 2018) can affect water temperatures. Figure 15 shows annual time series for these variables for the entire Salmon River watershed for the period 1965–2017. Appendix F has similar graphs for each long-term monitoring site for the period 1977–2017. Major fires occurred in the Salmon River watershed in 1977, 1987, 2006, 2008, 2013, 2014, and 2017 (Figure 15a, Figure 18). In addition, fires in nearby watersheds transported large amounts of smoke into the Salmon River in 1999 and 2015 (Figure 15b). Volcanic eruptions in Mexico (El Chichón) and Philippines (Pinatubo) in 1982 and 1991, respectively, elevated sulfate aerosols and reduced solar radiation globally for several years (Randles 2017). Over the 1977–2017 time period, a substantially lower percent of South Fork Salmon River’s watershed burned compared to Wooley Creek, North Fork Salmon River, and the mainstem Salmon River (Figure 17, Figure 18). Post-fire erosion can occur over many years (Moody et al. 2013), so the full effects of recent fires may still be developing.

The number of sites where stream temperatures were monitored each year varied according to available resources, conditions, and changes to monitoring plans. This complicates watershed-wide comparisons of interannual variation in stream temperature, because calculating a simple average of all sites within a year could be biased due to different groups of sites being available in different years. Thus, to generate representative summaries that could be compared across years, we used linear mixed-effects models with random effects to calculate adjusted averages that account for the varying groups of sites monitored each year (Figure 15a,b). In 1966 through 1995, there were only 1 to 6 sites monitored per year (Figure 16c,d), so summaries are substantially less reliable in those years. Similarly, only a few sites per year were monitored during the month of May, so summaries for that month are also less reliable than other months.

Years with the warmest stream temperatures included 1977, 1992, 1994, 2001, 2009, and 2013–2015 (Figure 15f,g). These years generally coincided with sparse snowpack, low flows, high air temperatures (Figure 15d, e, f, g, h). Conversely, 1999 had among the lowest stream temperatures, with deep snowpack, high flows, and cool air temperatures, in addition to wildfire smoke following the start of the Megram fire on August 23, 1999. Other years with cool temperatures included 1993 (high flows and low air temperatures), 2008 (moderate flow and air temperatures, but widespread fires which started in late June), and 2010 (moderate snowpack and high flow) and 2011 (deep snowpack and high flow) (Figure 15a,b). Narrative categorizations of stream temperature, air temperature, smoke, snowpack, and streamflow in this paragraph refer to percentiles: low/cool/sparse = 0–33%, moderate = 34–66%, and high/deep = 67–100%.

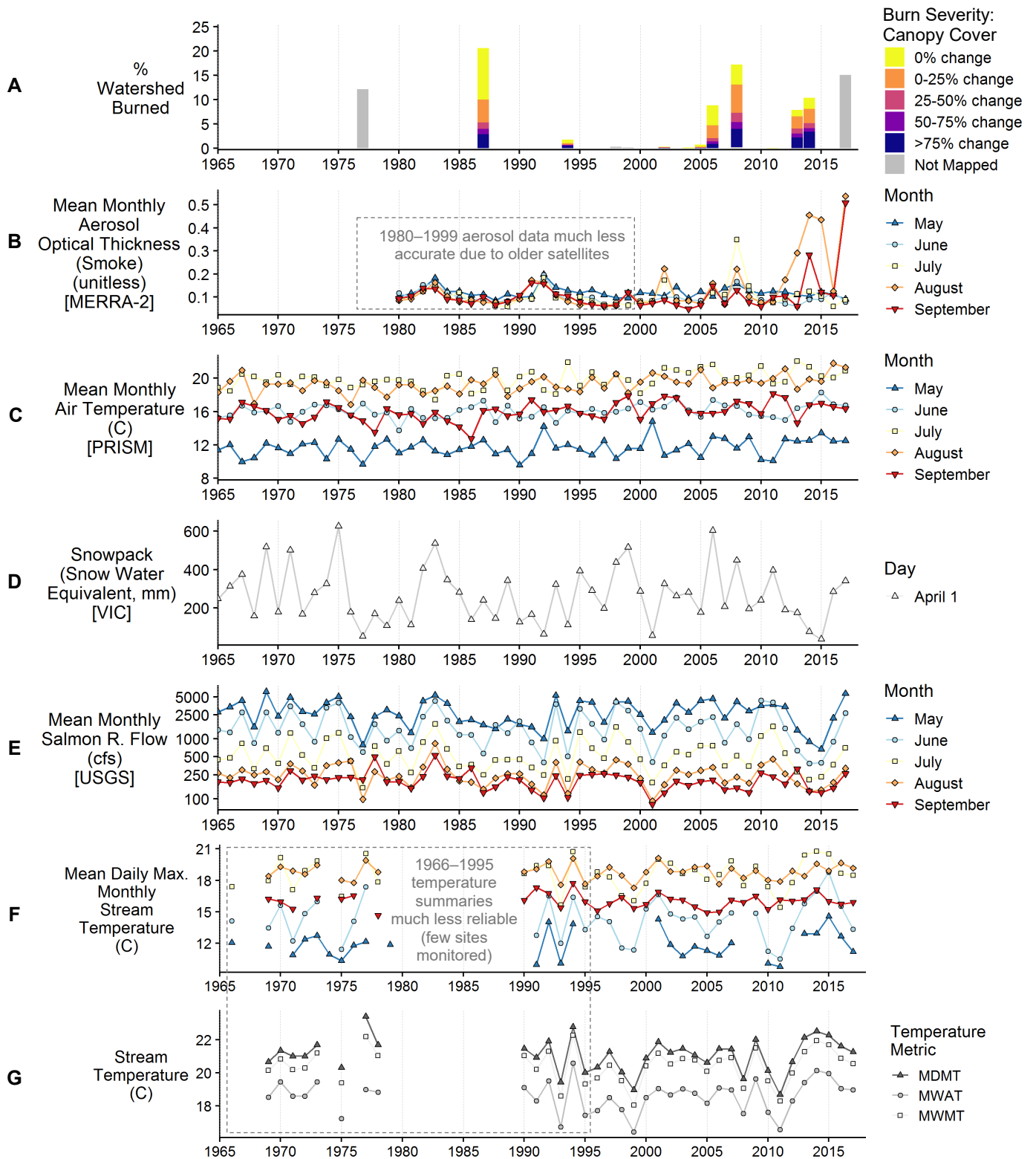


Figure 15. Annual time series 1965–2017 of: A) percent of Salmon River watershed burned, B) mean monthly aerosol optical thickness (a proxy for wildfire smoke) estimated from satellites, C) April 1 snowpack for Salmon River watershed from VIC hydrologic model, D) mean monthly air temperature for Salmon River watershed (from PRISM model), E) mean monthly flow measured at USGS gage, F) watershed summaries of mean daily maximum monthly stream temperature measured, and G) watershed summaries of seasonal stream temperature metrics (MDMT, MWMT, and MWAT). Values in F/G are not regular arithmetic averages but rather use a linear mixed-effects model to account for the varying group of sites monitored each year.

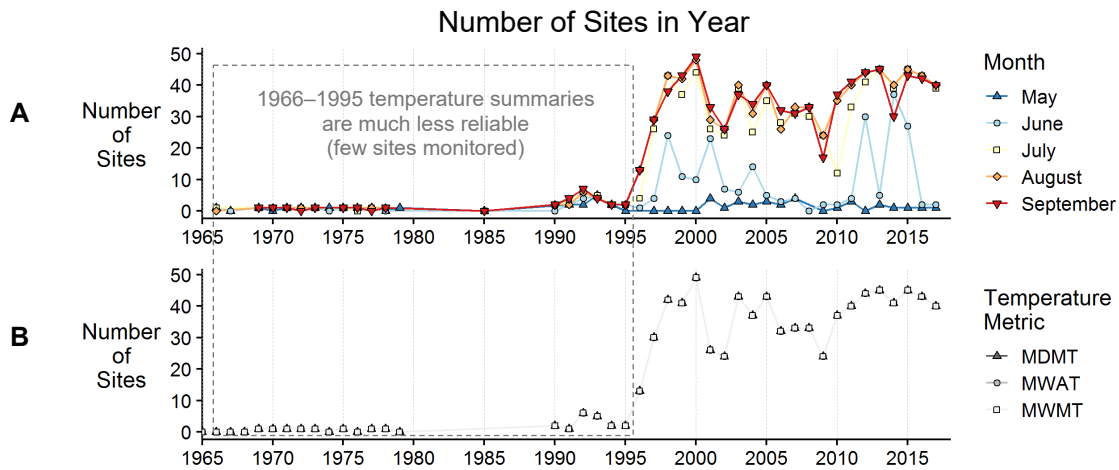


Figure 16. Number of sites per year 1966–2017 in the Salmon River watershed with data available for A) mean daily maximum monthly stream temperature, and B) seasonal stream temperature metrics (MDMT, MWMT, and MWAT), which were used to calculate the adjusted averages shown in Figure 15 A/B.

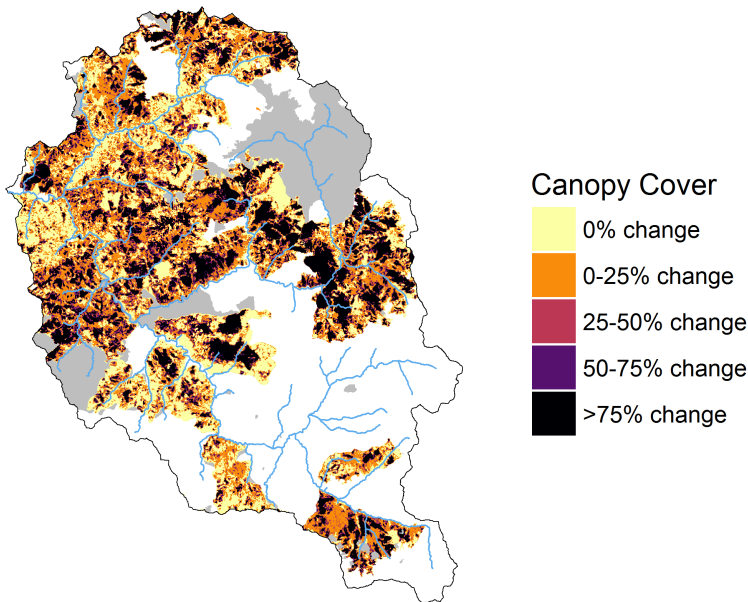


Figure 17. Map showing US Forest Service estimates of wildfire burn severity (percent canopy change) in the Salmon River watershed for years 1977–2017. Severity was not mapped in 1977 or 2017, so only perimeters (grey) are shown for those years.

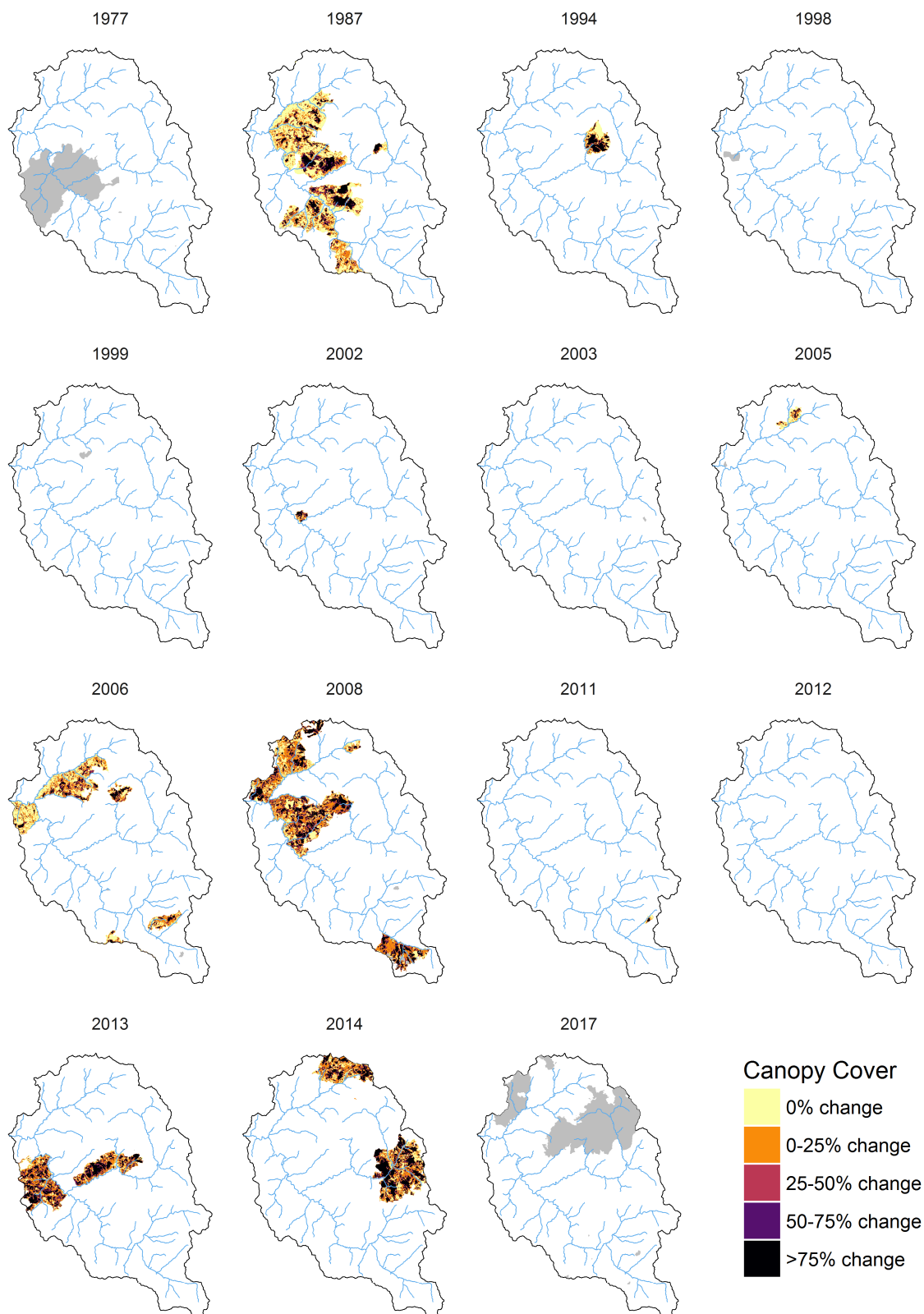


Figure 18. Maps showing US Forest Service estimates of wildfire burn severity (percent canopy change) in the Salmon River watershed for each year 1977–2017 in which at least 20 km² burned. Severity was not mapped in 1977 or 2017, so only perimeters are shown for those years.

3.3 LINEAR MIXED EFFECTS MODELS TO ACCOUNT FOR SITE-SPECIFIC VARIATION IN SENSITIVITY OF STREAM TEMPERATURE TO INTERANNUAL CLIMATE VARIABILITY

We used linear mixed-effects models to estimate the influence of climate (streamflow, air temperature, snowpack, and smoke) on August temperature metrics, and to assess site-specific variation in climate sensitivity. The models we tested are listed in Appendix D's Table 7 which includes AIC values. The final models included fixed effects for air temperature and snowpack, and random effects that allowed the streamflow and AOT (smoke) slopes/intercepts to vary by site. Air temperature sensitivity (i.e., expected change in stream temperature per unit change in air temperature) and snow sensitivity did not vary much between sites. In contrast, there was strong spatial variation in the sensitivity of stream temperatures to interannual variability in streamflow (Figure 19a). In particular, flow sensitivity (i.e., expected change in stream temperature per unit change in flow) appears to be lowest in small streams (blue lines in Figure 19a) and greatest at sites on the South Fork Salmon River (orange and red lines in Figure 19a). Smoke sensitivity was also lowest in small streams (blue lines in Figure 19b), but was greatest in the Salmon River and North Fork Salmon River (orange and red lines in Figure 19b). These spatial differences in smoke sensitivity may be partially due the coarse spatial resolution of the smoke data (as noted in section 2.8.11 above, all sites were assigned the same smoke value) and the fire locations (more area burned in the South Fork Salmon River, Figure 17).

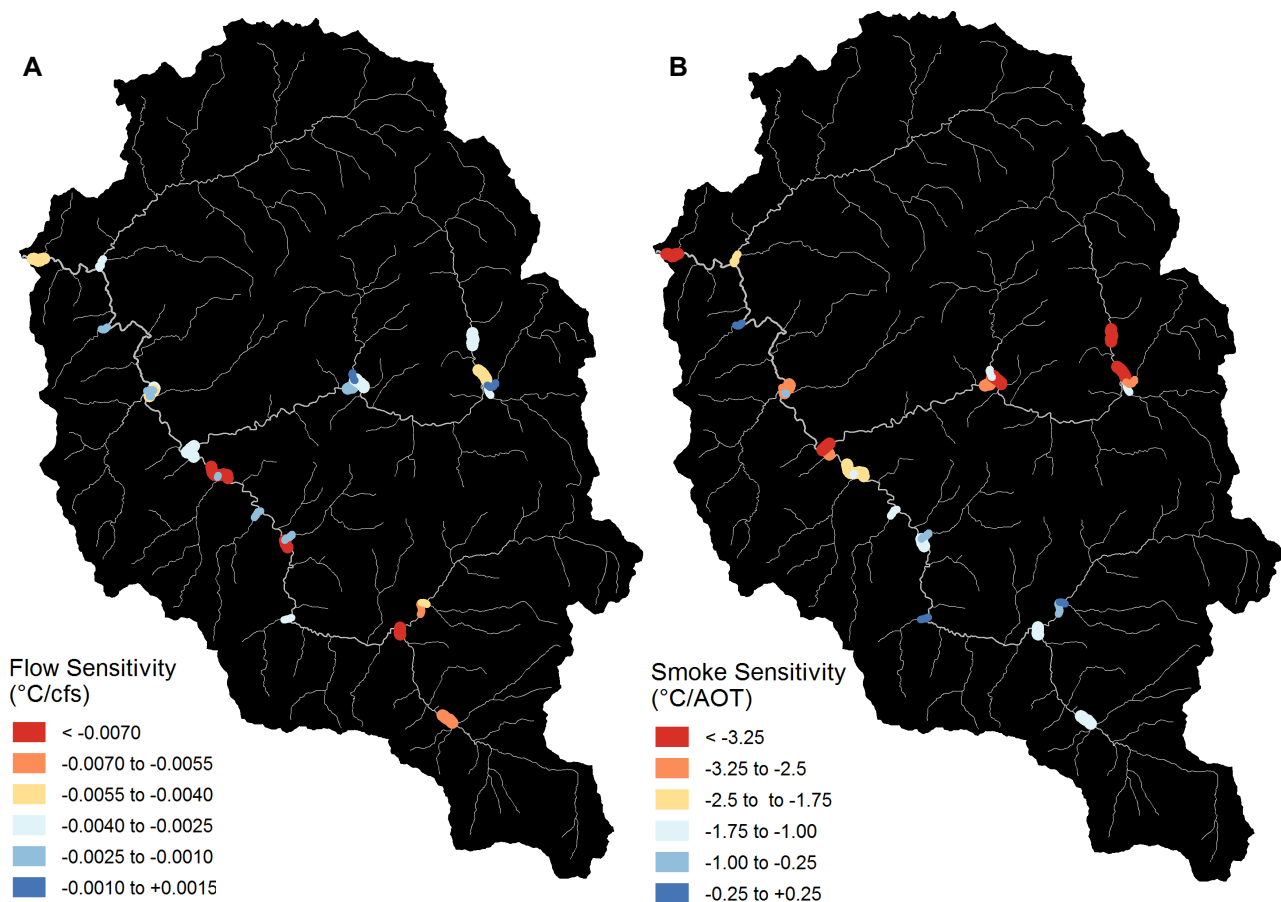


Figure 19. Maps showing sensitivity of mean daily maximum August stream temperature to gaged streamflow (i.e., expected change in stream temperature per unit change in flow) at 27 long-term monitoring sites in the Salmon River watershed. Sites are displayed as 1-km long reaches, with thick lines for sites on Salmon River, SF Salmon River, and NF Salmon River, and thinner lines for sites on other streams. Only streams with drainage area $\geq 3 \text{ km}^2$ are shown.

3.4 LONG-TERM TRENDS IN STREAM TEMPERATURE AND CLIMATE-ADJUSTED STREAM TEMPERATURE

To test for the presence of long-term trends in stream temperature, we calculated slopes for the period 1995-2017 and applied statistical tests (Figure 20, Figure 21, Figure 22). Linear mixed-effects models fit using all 27 long-term sites had slopes of 0.39 °C/decade (± 0.06 °C/decade standard error, $p < 0.001$) for mean August temperature and 0.21 (± 0.07 °C/decade standard error, $p < 0.003$) for mean daily maximum August temperature, which are similar to the median values of the individual sites' slopes (Figure 20a).

Increasing trends were much more common than decreasing trends (Figure 20a, Figure 21a, Figure 22a). Two sites had weak evidence of stream temperature decreases (North Russian Creek [$p = 0.025$] and NF Salmon River at Mule Bridge [$p = 0.045$]), and these were only for mean daily maximum August temperature. The sites with the largest magnitude of temperature increases (> 1.0 °C/decade) and strongest evidence ($p < 0.01$ for some metrics) were located on the SF Salmon River between the site upstream of East Fork SF (drainage area 204.2 km²) and the site downstream of Knownothing Creek (drainage area 742.6 km²). Other sites with evidence of temperature increases in at least one metric included Black Bear Creek, EF SF Salmon River, mainstem Salmon River downstream of Nordheimer, Knownothing Creek, Methodist Creek, Plummer Creek, and Taylor Creek (red/orange triangles in Figure 21a). Slopes were greater for annual temperature extreme metrics (MDMT, MWMT, and MWAT) than for August temperature metrics (Figure 20a, Figure 21a, Figure 22a).

We used linear mixed-effects models to account of the influence of climate (streamflow, air temperature, snowpack, and smoke) on August temperature metrics, yielding climate-adjusted stream temperature. The climate-adjusted temperature trends contrasted markedly to the temperature trends. A model fit using all 27 long-term sites had a slope of -0.09 °C/decade (standard error: 0.06 °C, $p < 0.001$) for mean August temperature while a model for mean daily maximum temperature had a slope of -0.14 °C/decade (standard error: 0.04 °C, $p < 0.001$). Seven sites had evidence of ($p < 0.05$) decreasing trends in climate-adjusted stream temperature (Figure 21b), meaning that in recent years temperatures at these sites have been cooler than would be expected based on climate conditions. These include two sites on the NF Salmon River as well as a single site each on North Russian Creek, South Russian Creek, Salmon River, Wooley Creek, and Nordheimer Creek (medium/dark blue triangles in Figure 21b and Figure 22b). The reasons for these decreases are unclear, but we speculate it may be due to recovery of riparian vegetation and channel conditions from past flood events (e.g., January 1, 1997). The SF Salmon River had no trends in climate-adjusted stream temperature (Figure 21b), suggesting that the steep increasing trends in stream temperatures during the 1995-2017 period (see Figure 21a, Figure 22a, and discussion in the preceding paragraph) are due to climate conditions (e.g., rising air temperatures, declining streamflow, and declining snowpack). Stream temperatures in the SF Salmon River are more sensitive to streamflow than other sites within the Salmon River watershed (Section 3.3 and Figure 19).

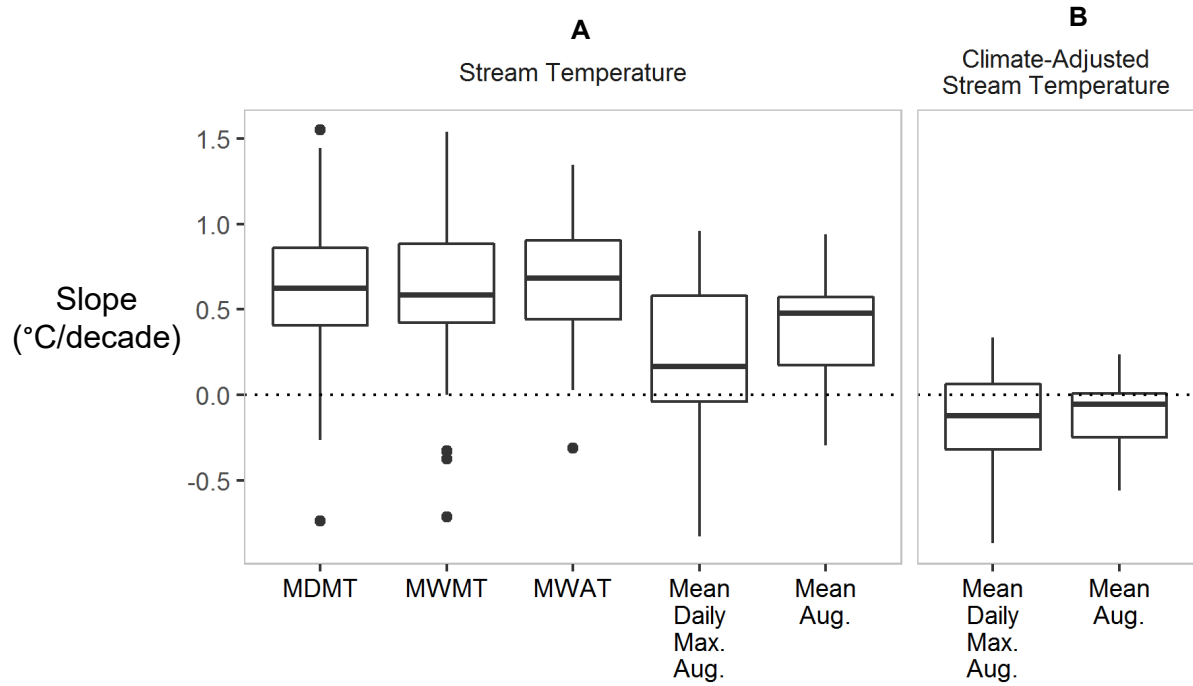


Figure 20. Boxplot of slopes (i.e., trend magnitudes) at 27 long-term sites in the Salmon River watershed for A) five stream temperature metrics [MDMT, MWMT, MWAT, mean daily maximum August temperature, and mean August temperature], and B) two climate-adjusted stream temperature metrics. The horizontal line inside the box is median, the upper and lower edges of the box are 25th and 75th percentiles, the upper whisker extends to the highest value that is within 1.5 times the interquartile range (75th minus 25th percentile) from the box's edge, and points plotted beyond the whiskers are outliers. Slopes for individual sites are presented in Figure 21 and Figure 22.

1995-2017 Trends by Site

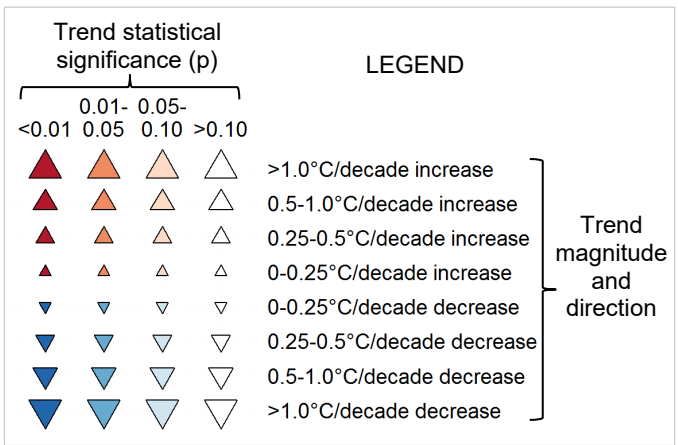
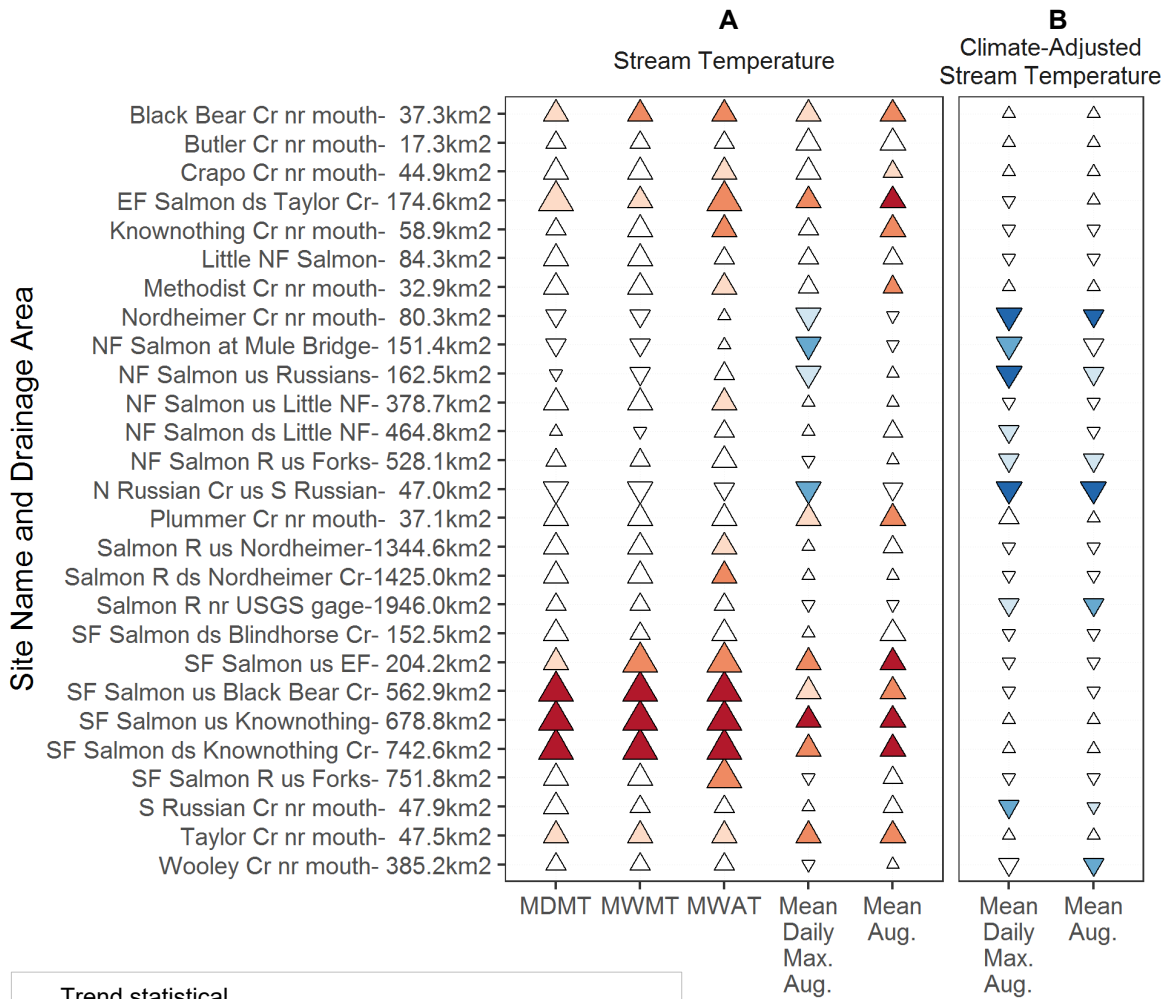


Figure 21. Site-specific results of statistical trend tests at 27 long-term sites in the Salmon River watershed for A) five stream temperature metrics [MDMT, MWMT, MWAT, mean daily maximum August temperature, and mean August temperature], and B) two climate-adjusted temperature metrics. Symbol shape shows direction (increasing/decreasing), size shows magnitude (°C/decade), and shading shows statistical significance (darker means more significant). Annual time series graphs are available in Appendix F. Key to abbreviations: Cr = Creek, R = River, nr = near, SF = South Fork, NF = North Fork, EF = East Fork, S = South, N = North, us = upstream, ds = downstream.

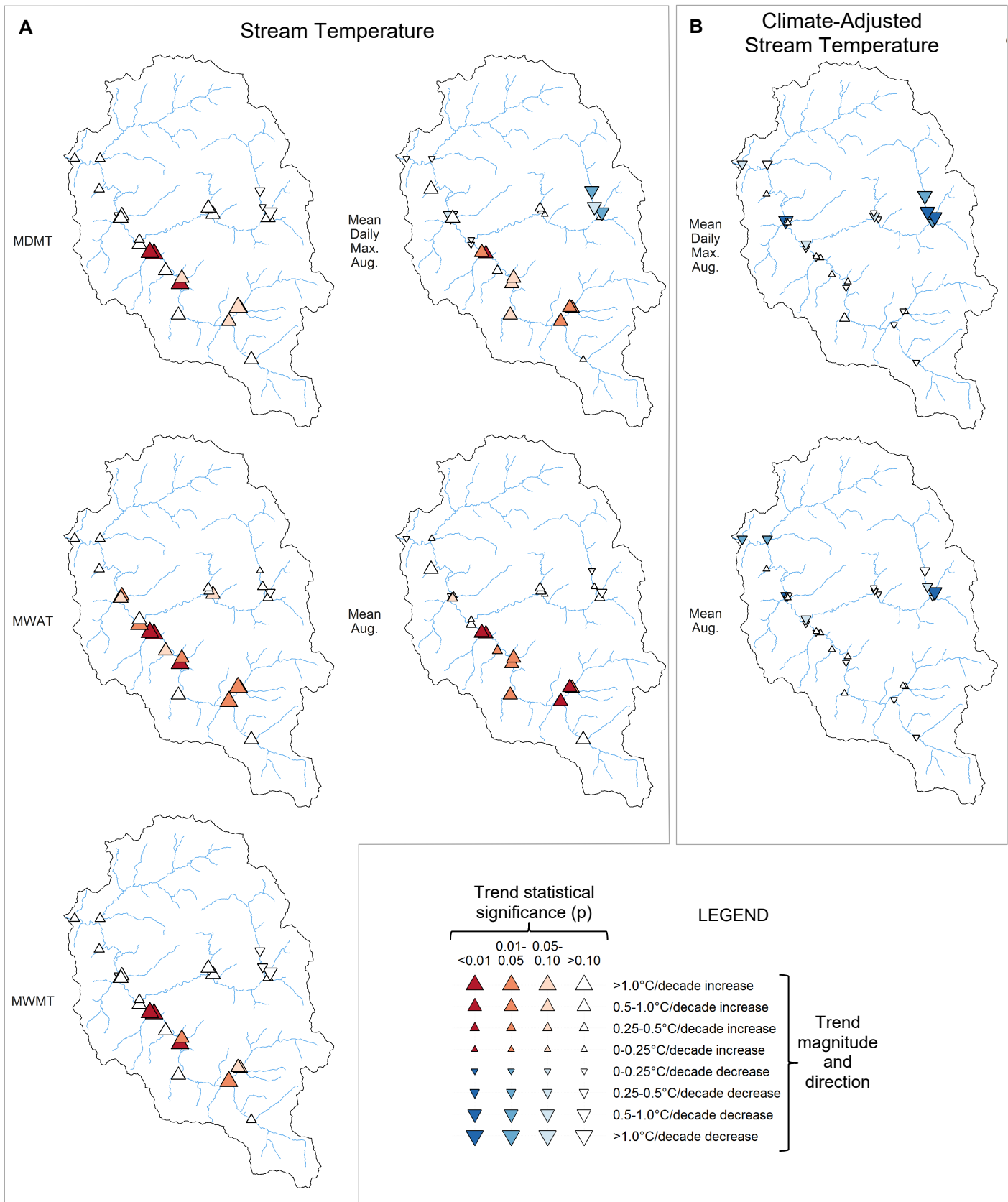


Figure 22. Map of site-specific results of statistical trend tests at 27 long-term sites in the Salmon River watershed for A) five stream temperature metrics [MDMT, MWMT, MWAT, mean daily maximum August temperature, and mean August temperature], and B) two climate-adjusted temperature metrics. Symbol shape shows direction (increasing/decreasing), size shows magnitude ($^{\circ}\text{C}/\text{decade}$), and shading shows statistical significance (darker means more significant).

3.5 SPATIAL STREAM-NETWORK MODEL CALIBRATION AND PERFORMANCE

We ran models using several different sets of predictor variables (Appendix E) to determine if alternative configurations would substantively affect the model outputs. All of these alternative models also performed well (Appendix E), indicating the models are relatively insensitive to the exact choice of predictor variables.

In the final spatial model for mean daily maximum August stream temperature, total root mean squared prediction error (RMSPE) was 0.62 °C while the RMSPE of the fixed effects (i.e., predictor variables excluding the random effects and spatial correlation) was 1.33 °C. Cross-validated r^2 was 0.95 (Figure 23). Model calibration utilized a total of 796 site-years from 102 unique sites.

Table 5 lists the variables included in the final spatial model for mean daily maximum August stream temperature. Large drainage areas and high air temperatures were associated with warm stream temperatures (i.e., model coefficients are positive) while high gaged flow, high elevation, high levels of smoke (AOT), deep snowpack, ample shade, and high average water yield were associated with cool stream temperatures (i.e., model coefficients are negative) (Table 5). Stream temperatures in the SF Salmon River have a high sensitivity to streamflow (i.e., when gaged flows are high, SF Salmon River temperatures are particularly cool) (Section 3.3, Figure 19). We experimented with adding additional variables (e.g., snowpack for summer months) to better represent the SF Salmon River's unique sensitivity to streamflow, but were only partly successful; thus, we also included a categorical variable SF Salmon (and associated interaction term) that allowed sites on the SF Salmon⁴⁵ to have a different relationship with flow than sites in the rest of the Salmon River watershed. The coarse spatial resolution of the snow data (see section 2.8.9) may be part of the reason we were not more successful in using quantitative variables to fully characterize the SF Salmon's sensitivity to flow. Exploratory data analyses showed that interannual differences in stream temperature were greater in small streams than large streams and rivers (Section 3.3), so we included a gage flow x drainage area interaction term to improve model fit.

Air temperature, gage flow, and drainage area were the most influential variables in the final spatial model (Table 5). There was also strong evidence for three interaction terms: gage flow x SF salmon (categorical), gage flow x drainage area, and drainage area x smoke (AOT). The air temperature coefficient is 0.44 (standard error: 0.064), meaning that stream temperature increased by 0.44 °C for each 1 °C increase in August air temperature. These responses to air temperature, flow, and snowpack can be used to infer the expected response to climate change (see section 3.5 below).

In the final spatial model, the predictor variables and spatial random effect accounted for the majority of the explained variance (35% and 42%, respectively), while the year and site random effects explained a relatively small fraction (3% and 8%, respectively) (Appendix E).

Figure 24 shows spatial model outputs for mean daily maximum August stream temperature for streams in the Salmon River watershed.

⁴⁵ Only includes the “mainstem” of the SF Salmon River, not its tributaries such as the East Fork of the South Fork Salmon River.

Table 5. Parameter estimates for the final spatial models used to predict mean August stream temperature in Salmon River watershed. Variables are listed in order of importance (i.e., absolute value of t statistic), except that interactions are listed at the bottom. b = coefficient (i.e., change in temperature per unit change in the variable) provided in the original units and standardized units; SE = standard error of coefficient (i.e., uncertainty in estimate of coefficient) provided in the original units and standardized units; p-value = probability that the coefficient is equal to zero (i.e., no effect), with lower p-values indicating greater degree of statistical significance; t = coefficient divided by standard error. The greater the absolute value (i.e., how far it is from zero in either a positive or negative direction) of the t statistic, the less uncertainty in the coefficient and the greater the influence of the variable on the predicted stream temperatures.

Variable Name	Variable Type	Standardized b (SE)	Original units b (SE)	p-value	t
Intercept		18.457 (0.298)		p <0.001	61.88
Air temperature (°C)	Temporal	0.83 (0.121)	0.44 (0.064)	p <0.001	6.83
Gage flow (cfs)	Temporal	-0.792 (0.128)	-0.00396 (0.00064)	p <0.001	-6.18
Drainage area (log, km ²)	Spatial	2.022 (0.473)	0.67 (0.157)	p <0.001	4.27
Elevation (m)	Spatial	-1.184 (0.314)	-0.00249 (0.00066)	p <0.001	-3.77
Aerosol optical thickness [AOT]	Temporal	-0.513 (0.137)	-1.79 (0.48)	p <0.001	-3.74
April 1 watershed snowpack (mm)	Spatio-temporal	-0.386 (0.112)	-0.00084 (0.000243)	p <0.001	-3.46
South Fork Salmon (Y/N)	Spatial	1.986 (0.538)		p <0.001	3.69
Average water yield	Spatial	-0.94 (0.364)	-4.96 (1.92)	p = 0.01	-2.58
Effective shade (%)	Spatial	-0.651 (0.265)	-1.79 (0.73)	p = 0.01	-2.46
Gage flow x South Fork Salmon	Interaction	-0.855 (0.119)		p <0.001	-7.18
AOT x Drainage area	Interaction	-0.628 (0.091)		p <0.001	-6.88
Gage flow x Drainage area	Interaction	-0.602 (0.092)		p <0.001	-6.57

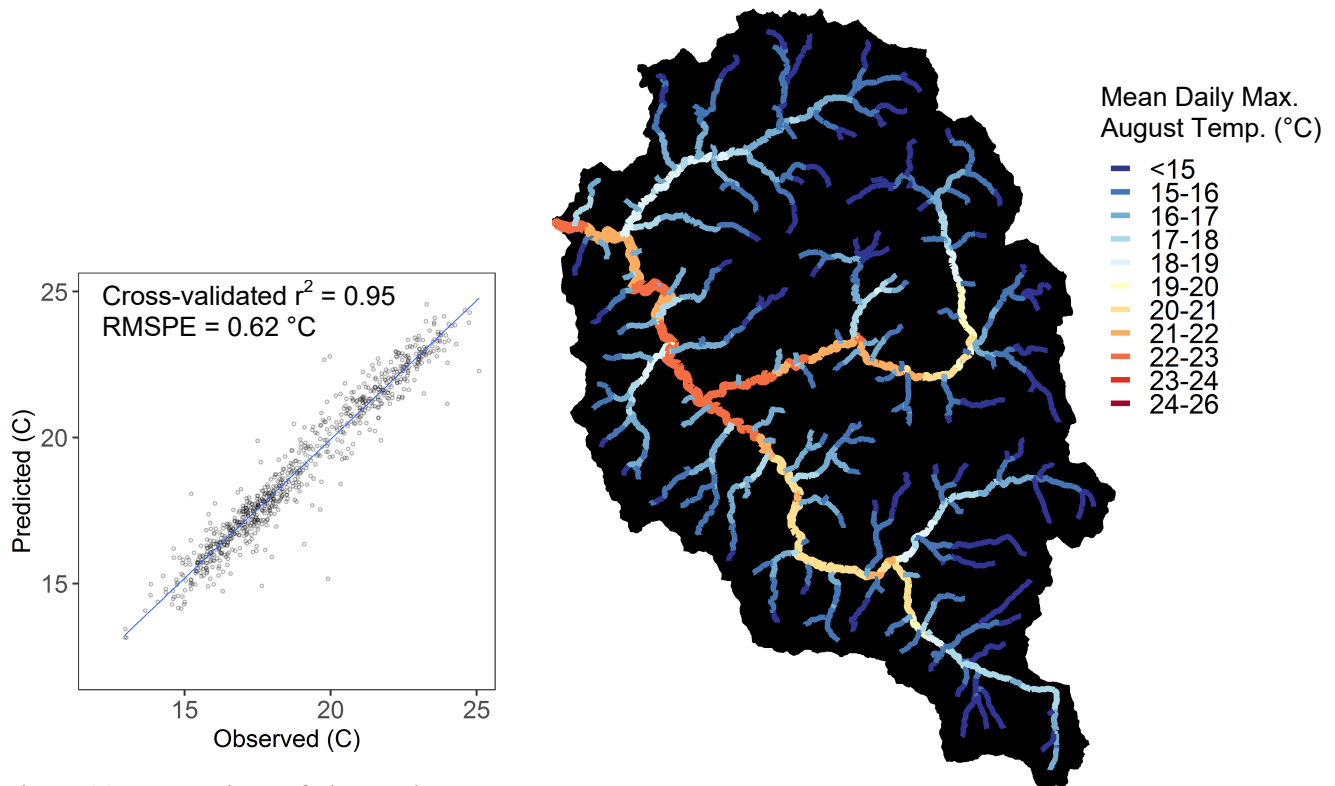


Figure 23. Comparison of observed mean daily maximum August stream temperature and predictions from the final spatial model for sites in the Salmon River watershed. RMSE = root mean squared prediction error.

Figure 24. Predicted mean daily maximum August temperature for streams in the Salmon River watershed for the period 1990-2017. Predictions are outputs from a spatial stream-network model which uses observed temperature data and GIS predictor variables as inputs. Only streams with drainage area ≥ 3 km² are shown.

3.6 CLIMATE CHANGE PREDICTIONS

Our spatial models predict that in the 2070–2099 period, mean daily maximum August stream temperatures will be warmer than the 1990–2017 baseline by 0.9–2.0°C under RCP4.5 or 1.7–3.3°C under RCP8.5, depending on the reach (Figure 25, Figure 26). Increases are predicted to be greatest in the South Fork Salmon River, with lesser increases in the North Fork and mainstem Salmon River. The smallest predicted increases occur in the upper reaches of small tributaries (Figure 26c,d).

Our predictions for increases in stream temperature are much larger than the 0.44–0.77 °C increase in mean August stream temperature predicted by NorWeST’s primary climate change scenario (S32) for the Northern California/Coastal Klamath unit which includes the Salmon River (Isaak et al. 2017). The small predicted increase in the NorWeST model is driven in large part by the low sensitivity to the 3.6°C increase in air temperature predicted by the global climate models (Isaak et al. 2017). As described above in section 3.3, air temperature sensitivity is the air temperature coefficient in the stream temperature model (i.e., change in stream temperature per unit change in air temperature). The air temperature sensitivity for the Northern California/Coastal Klamath NorWeST unit is 0.14 °C/°C, which is the second-lowest of the 23 NorWeST geographic units in the Western U.S. (Isaak et al. 2017). This low temperature sensitivity suggests that, relative to other geographic areas, stream temperatures in northwest California should be resilient to climate change. Alternatively, the NorWeST air temperature sensitivity might be skewed low due to complex spatial patterns of interannual air temperatures in northwest California that are not represented in the NorWeST model which uses a single air temperature within a year for all sites regardless of whether they are in the interior or coastal fog zone. The air temperature sensitivity in our spatial model was 0.44 °C/°C (Table 5). For comparison, air temperature sensitivities from previous studies in other areas include: 0.22 °C/°C for the lower Klamath River and adjacent coastal tributaries (Asarian et al. 2017), 0.47 °C/°C for 104 Pacific Northwest streams (Mayer et al. 2012), and 0.51 °C/°C for 246 Pacific Northwest streams (Luce et al. 2014).

A previous modeling effort predicted that the decadal mean (not specifically summer) mainstem Klamath River water temperatures would rise approximately 1–2.3°C over the 50-year period 2012-2061, depending on the global climate model (Perry et al. 2011).

The month-scale (i.e., August) thermal sensitivity approach used in this project for projecting stream temperature response to climate change may under-represent the magnitude because it does not account for climate change effects on groundwater temperatures which respond to air temperatures at longer time scales (Kurylyk et al. 2015, Burns et al. 2017, Leach and Moore 2019). At annual time scales, ground surface and shallow groundwater temperatures are approximately equal to annual average air temperatures, so groundwater temperatures should rise in tandem with air temperatures (Meisner et al. 1988), subject to a temporal lag that will vary by depth (Kurylyk et al. 2015). Groundwater influence on stream temperature can vary strongly with geology and watershed size (Briggs et al. 2017, Johnson et al. 2017). Relative to larger streams and rivers, temperatures in springs and small streams are likely to be more affected by changes in groundwater temperature, suggesting that the low sensitivity of these small streams to short-term (i.e., daily to monthly) fluctuations in air temperature likely under-represents their true response to a warming climate.

Stream temperatures may respond to climate warming in more complex ways than are included in our statistical models. For example, relative to a typical year, August temperature in Washington’s Snoqualmie River in a warm drought year (2015) warmed more in upland

tributaries than the mainstem, warming was spatially variable across upland tributaries, and lowland tributaries warmed less than other parts of the watershed (Steel et al. 2018).

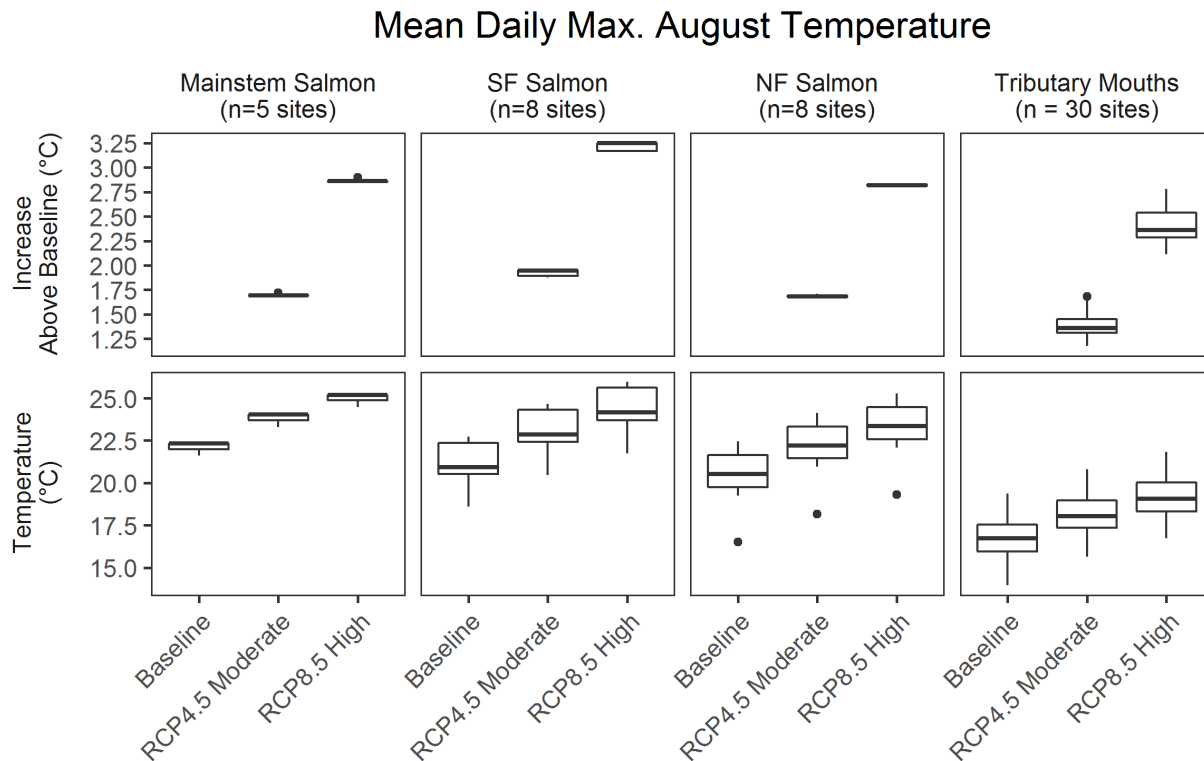


Figure 25. Comparisons of spatial stream-network model predictions for mean daily maximum stream temperatures, and increases above the 1990-2017 baseline, for streams in the Salmon River watershed predicted under moderate (RCP4.5) and high (RCP8.5) emissions future climate scenarios for 2070-2099. The tributaries included are the 30 largest tributaries⁴⁶ that are accessible to anadromous salmonids, excluding those that did not have long-term monitoring data. The horizontal line inside the box is median, the upper and lower edges of the box are 25th and 75th percentiles, the upper whisker extends to the highest value that is within 1.5 times the interquartile range (75th minus 25th percentile) from the box's edge, and points plotted beyond the whiskers are outliers.

⁴⁶ Black Bear Creek, Butler Creek, Cecil Creek, Crapo Creek, Crawford Creek, East Fork South Fork Salmon River, Eddy Gulch, Indian Creek, Knownothing Creek, Little North Fork Salmon River, Little South Fork Salmon River, Matthews Creek, Merrill Creek, Methodist Creek, Morehouse Creek, Nordheimer Creek, North Fork Wooley Creek, North Russian Creek, Plummer Creek, Right Hand North Fork Salmon River, Rush Creek, Sainte Claire Creek, Shadow Creek, Somes Creek, South Russian Creek, Specimen Creek, Taylor Creek, Uncles Creek, Whites Gulch, and Wooley Creek.

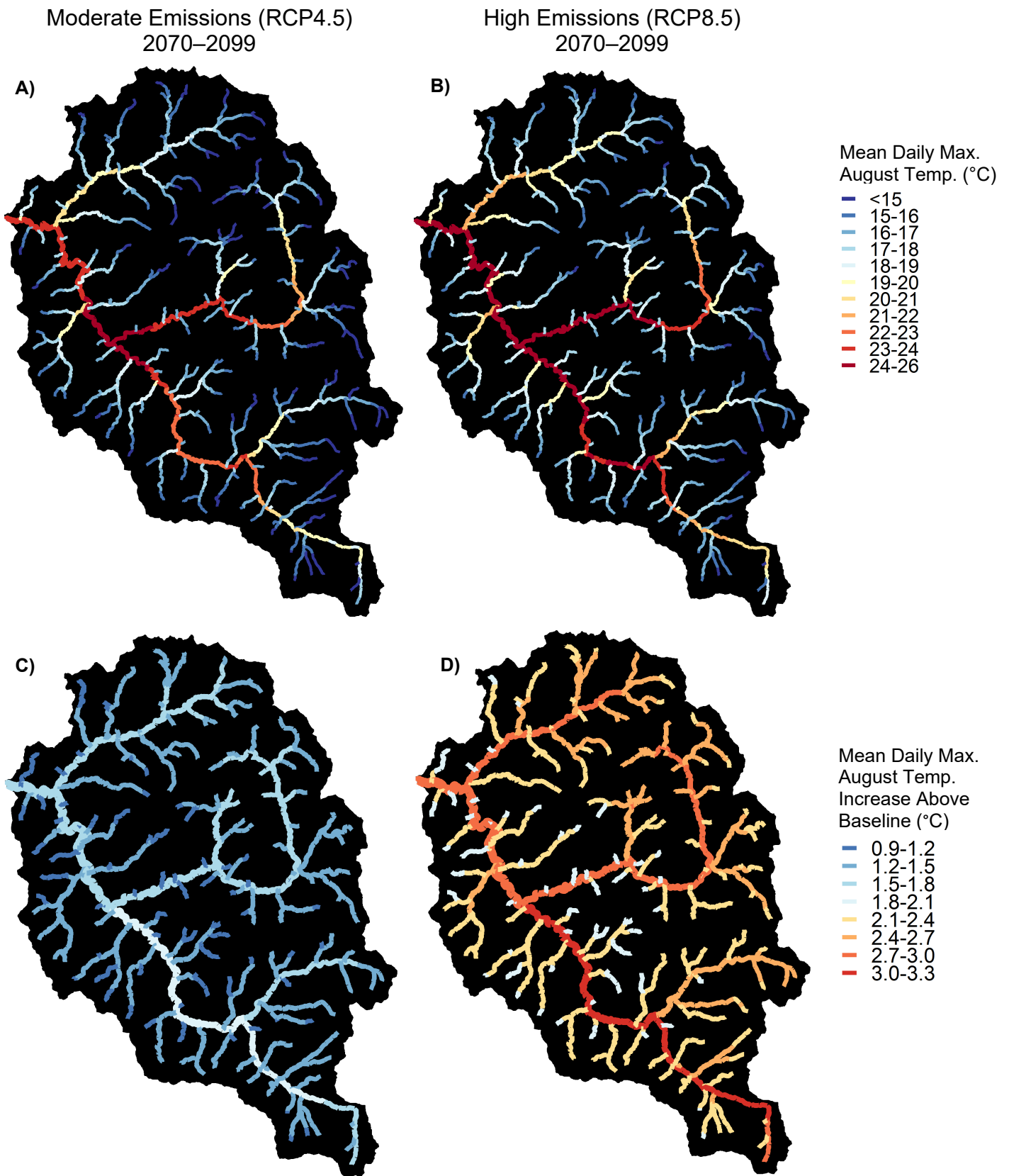


Figure 26. Map comparing spatial stream-network model predictions for mean daily maximum stream temperatures for streams in the Salmon River watershed predicted under (A) moderate RCP4.5 and (B) high RCP8.5 emissions future climate scenarios for 2070-2099, and (C, D) increases between the baseline and future scenarios. Only streams with drainage area $\geq 3 \text{ km}^2$ are shown.

3.7 MANAGEMENT IMPLICATIONS

Our results indicate that summer stream temperatures in the Salmon River watershed have increased over the study period in response to a warming climate. In addition, we predict that this warming trend will continue as global temperatures continue to rise. We provide reach-specific predictions for how stream temperatures will respond to climate change. These results corroborate previous research (Isaak et al. 2017, 2018) showing that small streams are anticipated to warm less than larger mainstem rivers. In addition, the South Fork Salmon River is expected to experience the greatest warming because while in the current climate it is remarkably cool (relative to its drainage area) during years with abundant snowpack and high late summer flow, as the climate continues to warm and snowpack diminishes, then years with high late summer flows will become increasingly rare and could eventually disappear. Temperature increases in Salmon River and its tributaries will increase the exposure of coldwater anadromous fish species to thermal stress and pose a threat to their populations, especially to spring-run Chinook salmon.

Our climate change predictions have important implications for efforts to restore fish and their habitat in the Salmon River watershed. At a global scale, reduced emissions of greenhouse gas would limit temperature increases and help maintain cool water temperatures. At a local scale, restoration actions should take into account the reach-specific anticipated responses to climate change:

- Given that creeks are cooler than rivers as well as anticipated to experience less future warming than rivers, creek mouths are likely to become increasingly important thermal refugia as peak summer river temperatures become increasingly inhospitable to coldwater species. Thus, these creek-mouth refugia deserve special attention for habitat restoration as well as watershed management to protect and enhance cold water sources. Tributary watershed management should focus on actions to promote riparian shade, increase the ability of the landscape to store and slowly release groundwater (e.g., meadow restoration and road removal), and appropriate upslope forest management to promote resiliency and reduce evapotranspiration (e.g., mechanical thinning, prescribed fire, and restoration of natural fire regimes). Fire suppression will become increasingly difficult. Allowing low intensity fires to reduce fuel loads would help protect mature riparian areas from damage in subsequent fires.
- The length of the Salmon River's South Fork and North Fork that are cool enough for spring-run Chinook salmon is predicted to contract upstream (Figure 26); therefore, habitat restoration actions that are intended to improve summer habitat, and rely on cool ambient river temperatures (as opposed to site-specific thermal refugia), should occur as far upstream as possible. In addition, along the mainstem of the Salmon River and warmer reaches (i.e. lower and middle) of the South Fork and North Fork, enhancement of thermal diversity through promotion of localized site-specific thermal refugia (i.e., side channels with hyporheic flow, etc.) would be beneficial.
- The future will require innovation in stream restoration techniques. Projects focused on cooling water will be necessary to counter balance warming trends. To keep up with climate change, restoration and regulators will need to find ways to reduce costs and accelerate implementation of complex projects like floodplain restoration.

4 ACKNOWLEDGMENTS

Countless people from many different entities have contributed to collection and compilation of the stream temperature data included in this report. The reports cited in the methods section list some of the persons who collected and organized data. Special thanks to Nicholas Cusick who did GIS analyses to calculate effective shade and assisted with compiling and cleaning of the SRNF temperature dataset. Grant Johnson (Karuk Tribe DNR) answered questions about data from the Karuk Tribe water quality program. Callie McConnell of the U.S. Forest Service (USFS) provided data from the USFS AqS database. Jay Stallman and Rafael Real de Asua (Stillwater Sciences) provided input on the climate change scenarios and information on Salmon River temperature dynamics derived from their analysis of thermal infrared data. Daniel Isaak, Sherry Wollrab, Gwynne Chandler, and David Nagel (USFS) and Seth Wenger (University of Georgia) provided information on the NorWeST model and tips on snapping the temperature sites to the GIS streams network. Erin Peterson and Jay Ver Hoef provided training on how to use STARS and SSN. Jill Beckman (formerly Karuk Tribe DNR) and Scott Harding (SRRC) provided advice on GIS datasets of meadows and geology for potential use in modeling tributary streamflows.

5 REFERENCES CITED

- Abatzoglou, J.T., 2013. Development of Gridded Surface Meteorological Data for Ecological Applications and Modelling. *International Journal of Climatology* 33:121–131.
- Abatzoglou, J.T. and T.J. Brown. 2012. A Comparison of Statistical Downscaling Methods Suited for Wildfire Applications. *International Journal of Climatology* 32:772–780. doi: 10.1002/joc.2312.
- Alexander, L. 1992. Upper South Fork of the Salmon River Riparian Study. Annual Report for Interagency Agreement 14-16-0001-91522. Klamath National Forest, Salmon River Ranger District. 35p. <http://www.fws.gov/yreka/Final-Reports/rmaap/1991-HP-07-KNF.pdf>.
- Asarian, J.E. 2016. Stream Temperatures in the South Fork Trinity River Watershed 1989-2015. Prepared by Riverbend Sciences for The Watershed Research and Training Center, Hayfork, CA.
- Asarian, J.E. and J.D. Walker, 2016. Long-Term Trends in Streamflow and Precipitation in Northwest California and Southwest Oregon, 1953-2012. *JAWRA Journal of the American Water Resources Association* 52:241–261. doi: 10.1111/1752-1688.12381.
- Asarian, J.E., P. Higgins, P. Trichilo. 2016. Stream Temperatures in the Eel River Basin 1980-2015, Phase 1: Compilation and Preliminary Analysis. Prepared by Riverbend Sciences and the Eel River Recovery Project for State Water Resources Control Board, Sacramento, CA. 73p. + appendices.
- Asarian, J.E. 2017. GIS Stream Temperature Modeling of Yurok Ancestral Territory. Prepared by Riverbend Sciences for the Yurok Tribe Environmental Program, Klamath, CA. 39 p. + appendices.
- Bair, E.H., K. Rittger, R.E. Davis, T.H. Painter, and J. Dozier, 2016. Validating Reconstruction of Snow Water Equivalent in California's Sierra Nevada Using Measurements from the NASA Airborne Snow Observatory. *Water Resources Research* 52:8437–8460. doi: 10.1002/2016WR018704.
- Bartholow, J.M., 2005. Recent Water Temperature Trends in the Lower Klamath River, California. *North American Journal of Fisheries Management* 25:152–162.

- Bates, D., M. Maechler, B. Bolker, S. Walker. 2015. Fitting Linear Mixed-Effects Models Using lme4. *Journal of Statistical Software*, 67(1), 1-48. doi:10.18637/jss.v067.i01.
- Belsley, D.A., E. Kuh, and R.E. Welsch, 1980. The Condition Number. *Regression Diagnostics: Identifying Influential Data and Sources of Collinearity* 100:104.
- Boyd M. and B. Kasper. 2003. Analytical methods for dynamic open channel heat and mass transfer: methodology for the Heat Source Model Version 7.0. <https://www.oregon.gov/deq/wq/tmdls/Pages/TMDLs-Tools.aspx>.
- Briggs, M.A., J.W. Lane, C.D. Snyder, E.A. White, Z.C. Johnson, D.L. Nelms, and N.P. Hitt, 2017. Shallow Bedrock Limits Groundwater Seepage-Based Headwater Climate Refugia. *Limnologia-Ecology and Management of Inland Waters*.
- Buchard, V., C.A. Randles, A.M. da Silva, A. Darnenov, P.R. Colarco, R. Govindaraju, R. Ferrare, J. Hair, A.J. Beyersdorf, L.D. Ziemba, and H. Yu. 2017. The MERRA-2 Aerosol Reanalysis, 1980 Onward. Part II: Evaluation and Case Studies. *Journal of Climate* 30:6851–6872. doi: 10.1175/JCLI-D-16-0613.1.
- Burns, E.R., Y. Zhu, H. Zhan, M. Manga, C.F. Williams, S.E. Ingebritsen, and J.B. Dunham, 2017. Thermal Effect of Climate Change on Groundwater-Fed Ecosystems. *Water Resources Research* 53:3341–3351. doi: 10.1002/2016WR020007.
- Chandler, G.L.; Wollrab, S.P.; Horan, D. L.; Nagel, D. E.; Parkes, S.L.; Isaak, D.J.; Wenger, S.J.; Peterson, E.E.; Ver Hoef, J.M.; Hostetler, S.W.; Luce, C.H.; Dunham, J.B.; Kershner, J.L.; Roper, B.B. 2016. NorWeST stream temperature data summaries for the western U.S. Fort Collins, CO: Forest Service Research Data Archive. <https://doi.org/10.2737/RDS-2016-0032>.
- Cressey, L. and K. Greenberg. 2008. Salmon River Riparian Assessment 2006-2008. Funded by Bella Vista Foundation and North Coast Regional Water Quality Control Board in cooperation with Klamath National Forest. Salmon River Restoration Council, Sawyers Bar, CA. <http://srrc.org/publications/programs/fisheries/SRRC%20Salmon%20River%20Riparian%20Assessment%20Report.pdf>
- Daly, C., M. Halbleib, J.I. Smith, W.P. Gibson, M.K. Doggett, G.H. Taylor, J. Curtis, and P.P. Pasteris, 2008. Physiographically Sensitive Mapping of Climatological Temperature and Precipitation across the Conterminous United States. *International Journal of Climatology* 28:2031–2064. doi: 10.1002/joc.1688.
- David, A.T., J.E. Asarian, and F.K. Lake. 2018. Wildfire Smoke Cools Summer River and Stream Water Temperatures. *Water Resources Research*. doi: 10.1029/2018WR022964.
- Detenbeck, N. 2017. Quality Assurance Project Plan, Project Title: Big Cold and Small Cold: Quantifying Thermal Regime Metrics for Policy Development, QAPP-AED-WDB-ND-2016-01-000. U.S. EPA – Atlantic Ecology Division.
- Dierauer, J.R., P.H. Whitfield, and D.M. Allen. 2018. Climate Controls on Runoff and Low Flows in Mountain Catchments of Western North America. *Water Resources Research* 54:7495–7510. doi: 10.1029/2018WR023087.
- Dunham, J., G. Chandler, B. Rieman, and D. Martin. 2005. Measuring Stream Temperature with Digital Data Loggers: A User's Guide. http://www.fs.fed.us/rm/pubs/rmrs_gtr150.pdf

- Elder, D, B. Olson, A. Olson, and J. Villeponteaux. 2002. Salmon River Sub-basin Restoration Strategy: Steps to Recovery and Conservation of Aquatic Resources: Report for The Klamath River Basin Fisheries Restoration Task Force, Interagency Agreement 14-16-0001-90532. USDA-Forest Service, Klamath National Forest, Yreka, Klamath National Forest and Salmon River Restoration Council, Sawyers Bar, CA. September 2002: 52 pp. https://www.fs.usda.gov/Internet/FSE_DOCUMENTS/stelprdb5110056.pdf
- Elsner, M. and S. McGinnis. 2014. Klamath River Basin Study Update. Presented to Klamath Basin Monitoring Program (KBMP) General Membership Meeting, November 6, 2014, Yreka, CA. http://www.kbmp.net/images/stories/pdf/Meeting_Materials/Meeting_15/17_Klamath_Basin_Study_Update_KBMP_Nov2014.pdf
- Ficklin, D.L., I.T. Stewart, and E.P. Maurer, 2012. Projections of 21st Century Sierra Nevada Local Hydrologic Flow Components Using an Ensemble of General Circulation Models1. *JAWRA Journal of the American Water Resources Association* 48:1104–1125. doi: 10.1111/j.1752-1688.2012.00675.x.
- Ficklin, D.L., S.L. Letsinger, I.T. Stewart, and E.P. Maurer, 2015. Assessing Differences in Snowmelt-Dependent Hydrologic Projections Using CMIP3 and CMIP5 Climate Forcing Data for the Western United States. *Hydrology Research*:nh2015101. doi: 10.2166/nh.2015.101.
- Flint, L.E. and A.L. Flint, 2008. A Basin-Scale Approach to Estimating Stream Temperatures of Tributaries to the Lower Klamath River, California. *Journal of Environment Quality* 37:57. doi: 10.2134/jeq2006.0341.
- Flint, L.E., and A.L. Flint. 2012. Estimation of stream temperature in support of fish production modeling under future climates in the Klamath River Basin: U.S. Geological Survey Scientific Investigations Report 2011–5171, 31 p.
- Flint, L.E., A.L. Flint, J.H. Thorne, and R. Boynton. 2013. Fine-Scale Hydrologic Modeling for Regional Landscape Applications: The California Basin Characterization Model Development and Performance. *Ecological Processes* 2:1–21. doi: 10.1186/2192-1709-2-25.
- Gangopadhyay, S. and T. Pruitt. 2011. West-Wide Climate Risk Assessments: Bias-Corrected and Spatially Downscaled Surface Water Projections. Technical Memorandum No. 86-68210-2011-01. US Department of the Interior, Bureau of Reclamation, Technical Service Center. https://wrrc.arizona.edu/sites/wrrc.arizona.edu/files/BOR_West-wide%20climate%20risk%20assessments.pdf.
- Grantham, T.E.W., D.M. Carlisle, G.J. McCabe, and J.K. Howard, 2018. Sensitivity of Streamflow to Climate Change in California. *Climatic Change* 149:427–441. doi: 10.1007/s10584-018-2244-9.
- Hart, Q.J., M. Brugnach, B. Temesgen, C. Rueda, S.L. Ustin, and K. Frame. 2009. Daily Reference Evapotranspiration for California Using Satellite Imagery and Weather Station Measurement Interpolation. *Civil Engineering and Environmental Systems* 26:19–33. doi: 10.1080/10286600802003500.
- Hedrick, A., H.-P. Marshall, A. Winstral, K. Elder, S. Yueh, and D. Cline. 2015. Independent Evaluation of the SNODAS Snow Depth Product Using Regional-Scale Lidar-Derived Measurements. *The Cryosphere* 9:13–23. doi: 10.5194/tc-9-13-2015.
- Hegewisch, K.C. and Abatzoglou, J.T. 2018. 'Future Time Series' web tool. NW Climate Toolbox (<https://climatetoolbox.org/>) accessed on 3/13/2018.

- Hill, R.A., M.H. Weber, S.G. Leibowitz, A.R. Olsen, and D.J. Thornbrugh. 2016. The Stream-Catchment (StreamCat) Dataset: A Database of Watershed Metrics for the Conterminous United States. *JAWRA Journal of the American Water Resources Association* 52:120–128. doi: 10.1111/1752-1688.12372.
- Homer, C.G., Dewitz, J.A., Yang, L., Jin, S., Danielson, P., Xian, G., Coulston, J., Herold, N.D., Wickham, J.D., and Megown, K. 2015. Completion of the 2011 National Land Cover Database for the conterminous United States-Representing a decade of land cover change information. *Photogrammetric Engineering and Remote Sensing*, v. 81, no. 5, p. 345-354
- Isaak, D.J., C.H. Luce, B.E. Rieman, D.E. Nagel, E.E. Peterson, D.L. Horan, S. Parkes, and G.L. Chandler. 2010. Effects of Climate Change and Wildfire on Stream Temperatures and Salmonid Thermal Habitat in a Mountain River Network. *Ecological Applications* 20:1350–1371. doi: 10.1890/09-0822.1.
- Isaak, D.J., E.E. Peterson, J.M. Ver Hoef, S.J. Wenger, J.A. Falke, C.E. Torgersen, C. Sowder, E.A. Steel, M.-J. Fortin, C.E. Jordan, A.S. Ruesch, N. Som, and P. Monestiez, 2014. Applications of Spatial Statistical Network Models to Stream Data. *Wiley Interdisciplinary Reviews: Water* 1:277–294. doi: 10.1002/wat2.1023.
- Isaak, D.J., S.J. Wenger, E.E. Peterson,; J.M. Ver Hoef, S.W. Hostetler, C.H. Luce, J.B. Dunham, J.L. Kershner, B.B. Roper, D.E. Nagel, G.L. Chandler, S.P. Wollrab, S.L. Parkes, D.L. Horan. 2016. NorWeST modeled summer stream temperature scenarios for the western U.S. Fort Collins, CO: Forest Service Research Data Archive. <https://doi.org/10.2737/RDS-2016-0033>.
- Isaak, D., S. Wenger, E. Peterson, J. Ver Hoef, N. David, C. H Luce, S. Hostetler, J. Dunham, B. B Roper, S. P Wollrab, G. L Chandler, D. L Horan, and S. Parkes-Payne. 2017. The NorWeST Summer Stream Temperature Model and Scenarios for the Western U.S.: A Crowd-Sourced Database and New Geospatial Tools Foster a User-Community and Predict Broad Climate Warming of Rivers and Streams. *Water Resources Research*. doi: 10.1002/2017WR020969. doi:10.1002/2017WR020969.
- Isaak, D.J., C.H. Luce, D.L. Horan, G.L. Chandler, S.P. Wollrab, and D.E. Nagel. 2018. Global Warming of Salmon and Trout Rivers in the Northwestern U.S.: Road to Ruin or Path Through Purgatory? *Transactions of the American Fisheries Society*. doi: 10.1002/tafs.10059. doi:10.1002/tafs.10059.
- Johnson, Z.C., C.D. Snyder, and N.P. Hitt, 2017. Landform Features and Seasonal Precipitation Predict Shallow Groundwater Influence on Temperature in Headwater Streams: SPATIOTEMPORAL PREDICTORS OF GW DYNAMICS. *Water Resources Research* 53:5788–5812. doi: 10.1002/2017WR020455.
- Kier Associates. 1991. Long Range Plan for the Klamath River Basin Conservation Area Fishery Restoration Program. U.S. Fish and Wildlife Service, Klamath River Fishery Resource Office. Yreka, CA. 403 pp. http://www.krisweb.com/biblio/gen_usfws_kierassoc_1991_lrp.pdf
- Klamath National Forest. 1994a. Bear Country Landscape Analysis and Design Final. USDA-Klamath National Forest, Salmon River Ranger District. https://www.fs.usda.gov/Internet/FSE_DOCUMENTS/stelprdb5403320.pdf.
- Klamath National Forest. 1994b. Upper South Fork of the Salmon River Ecosystem Analysis. USDA-Klamath National Forest, Salmon River & Scott River Ranger Districts. https://www.fs.usda.gov/Internet/FSE_DOCUMENTS/stelprdb5403530.pdf
- Klamath National Forest, 1995a. Little North Fork/Crapo Late Successional Reserve Assessment. USDA-Klamath National Forest. https://www.fs.usda.gov/Internet/FSE_DOCUMENTS/stelprdb5403322.pdf.

- Klamath National Forest, 1995b. Main Salmon River Ecosystem Analysis. USDA-Klamath National Forest. https://www.fs.usda.gov/Internet/FSE_DOCUMENTS/stelprdb5403333.pdf.
- Klamath National Forest, 1995c. North Fork Watershed Analysis. USDA-Klamath National Forest. https://www.fs.usda.gov/Internet/FSE_DOCUMENTS/stelprdb5403336.pdf.
- Klamath National Forest, 1996. Taylor/Carter Meadows Late Successional Reserve Assessment. USDA-Klamath National Forest. https://www.fs.usda.gov/Internet/FSE_DOCUMENTS/stelprdb5403728.pdf.
- Klamath National Forest. 1997. Lower South Fork Salmon River Ecosystem Analysis. USDA-Klamath National Forest. https://www.fs.usda.gov/Internet/FSE_DOCUMENTS/stelprdb5403327.pdf.
- Klamath National Forest, 1999. Klamath National Forest Late Successional Reserves, Forest Wide LSR Assessment. USDA-Klamath National Forest. https://www.fs.usda.gov/Internet/FSE_DOCUMENTS/stelprdb5403298.pdf.
- Koontz, E.D., E.A. Steel, and J.D. Olden. 2018. Stream Thermal Responses to Wildfire in the Pacific Northwest. *Freshwater Science* 37:731–746. doi: 10.1086/700403.
- Kuznetsova, A, PB Brockhoff, RHB Christensen. 2017. lmerTest Package: Tests in Linear Mixed Effects Models. *Journal of Statistical Software* 82(13): 1-26. doi: 10.18637/jss.v082.i13.
- Kurylyk, B.L., K.T. MacQuarrie, D. Caissie, and J.M. McKenzie, 2015. Shallow Groundwater Thermal Sensitivity to Climate Change and Land Cover Disturbances: Derivation of Analytical Expressions and Implications for Stream Temperature Modeling. *Hydrology and Earth System Sciences* 19:2469–2489.
- Laurie, G., 2012. Stream Temperature Monitoring on the Klamath National Forest, 2010 to 2011. Klamath National Forest. http://www.fs.usda.gov/Internet/FSE_DOCUMENTS/stelprdb5369224.pdf. Accessed 14 Aug 2015.
- Laurie, G. and M. Reichert, 2011. Stream Shade Monitoring on the Klamath National Forest, 2010. Klamath National Forest. http://www.fs.usda.gov/Internet/FSE_DOCUMENTS/stelprdb5312674.pdf.
- Leach, J.A. and R.D. Moore. 2019. Empirical Stream Thermal Sensitivities May Underestimate Stream Temperature Response to Climate Warming. *Water Resources Research* 55:5453–5467. doi: 10.1029/2018WR024236.
- Lewis, T.E., D.R. Lamphear, D.R. McCanne, A.S. Webb, J.P. Krieter, and W.D. Conroy. 2000. Regional Assessment of Stream Temperatures across Northern California and Their Relationship to Various Landscape-Level and Site-Specific Attributes. Humboldt State University Foundation Arcata, California, USA. http://wvvvv.krisweb.com/biblio/ncc_hsu_lewisetal_2000_fspegass.pdf
- Liang, X., D.P. Lettenmaier, E.F. Wood, and S.J. Burges, 1994. A Simple Hydrologically Based Model of Land Surface Water and Energy Fluxes for General Circulation Models. *Journal of Geophysical Research: Atmospheres* 99:14415–14428. doi: 10.1029/94JD00483.
- Livneh, B., E. A. Rosenberg, C. Lin, B. Nijssen, V. Mishra, K. M. Andreadis, E. P. Maurer, and D. P. Lettenmaier. 2013. A long-term hydrologically based dataset of land surface fluxes and states for the conterminous United States: Update and extensions. *J. Climate*, 26, 9384–9392, doi:10.1175/JCLI-D-12-00508.1.

- Livneh, B., T.J. Bohn, D.W. Pierce, F. Munoz-Arriola, B. Nijssen, R. Vose, D.R. Cayan, and L. Brekke. 2015. A Spatially Comprehensive, Hydrometeorological Data Set for Mexico, the U.S., and Southern Canada 1950–2013. *Scientific Data* 2:sdata201542. doi: 10.1038/sdata.2015.42.
- Luce, C., B. Staab, M. Kramer, S. Wenger, D. Isaak, and C. McConnell, 2014. Sensitivity of Summer Stream Temperatures to Climate Variability in the Pacific Northwest. *Water Resources Research* 50:3428–3443. doi: 10.1002/2013WR014329.
- Mayer, T.D. 2012. Controls of Summer Stream Temperature in the Pacific Northwest. *Journal of Hydrology* 475:323–335. doi: 10.1016/j.jhydrol.2012.10.012.
- Mayer, T.D. and S.W. Naman. 2011. Streamflow Response to Climate as Influenced by Geology and Elevation. *Journal of the American Water Resources Association (JAWRA)* 47:724–738. doi: 10.1111/j.1752-1688.2011.00537.x.
- McCullough, D.A. 2010. Are Coldwater Fish Populations of the United States Actually Being Protected by Temperature Standards? *Freshwater Reviews* 3:147–199. doi: 10.1608/FRJ-3.2.4.
- Mehta, V.K., D.E. Rheinheimer, D. Yates, D.R. Purkey, J.H. Viers, C.A. Young, and J.F. Mount. 2011. Potential Impacts on Hydrology and Hydropower Production under Climate Warming of the Sierra Nevada. *Journal of Water and Climate Change* 2:29–43. doi: 10.2166/wcc.2011.054.
- Meisner, J.D., J.S. Rosenfeld, and H.A. Regier, 1988. The Role of Groundwater in the Impact of Climate Warming on Stream Salmonines. *Fisheries* 13:2–8. doi: 10.1577/1548-8446(1988)013<0002:TROGIT>2.0.CO;2.
- Miller, J.D., E.E. Knapp, C.H. Key, C.N. Skinner, C.J. Isbell, R.M. Creasy, and J.W. Sherlock. 2009. Calibration and Validation of the Relative Differenced Normalized Burn Ratio (RdNBR) to Three Measures of Fire Severity in the Sierra Nevada and Klamath Mountains, California, USA. *Remote Sensing of Environment* 113:645–656.
- Miller, J.D. and B. Quayle. 2015. Calibration and Validation of Immediate Post-Fire Satellite-Derived Data to Three Severity Metrics. *Fire Ecology* 11.
- Miller, J.D., H.D. Safford, and K.R. Welch, 2016. Using One Year Post-Fire Fire Severity Assessments to Estimate Longer-Term Effects of Fire in Conifer Forests of Northern and Eastern California, USA. *Forest Ecology and Management* 382:168–183.
- Miller, J.D. and A.E. Thode. 2007. Quantifying Burn Severity in a Heterogeneous Landscape with a Relative Version of the Delta Normalized Burn Ratio (DNBR). *Remote Sensing of Environment* 109:66–80.
- Moody, J.A., R.A. Shakesby, P.R. Robichaud, S.H. Cannon, and D.A. Martin. 2013. Current Research Issues Related to Post-Wildfire Runoff and Erosion Processes. *Earth-Science Reviews* 122:10–37. doi: 10.1016/j.earscirev.2013.03.004.
- Mote, P., D. Turner, D.P. Lettenmaier, D. Bachelet, and J. Abatzoglou. 2014. Integrated Scenarios of Climate, Hydrology, and Vegetation for the Northwest, Final Report. <https://climate.northwestknowledge.net/IntegratedScenarios/pages/publicationsreports/IntegrateScenariosFinalReport2014-10-07.pdf>.
- Mote, P.W., S. Li, D.P. Lettenmaier, M. Xiao, and R. Engel. 2018. Dramatic Declines in Snowpack in the Western US. *Npj Climate and Atmospheric Science* 1. doi: 10.1038/s41612-018-0012-1.
- Nagel, D., E. Peterson, D. Isaak, J. Ver Hoef, and D. Horan. 2017. National Stream Internet Protocol and User Guide, version 3-22-2017. U.S. Forest Service, Rocky Mountain Research Station, Boise, Idaho. <https://www.fs.fed.us/rm/boise/AWAE/projects/NationalStreamInternet/downloads/NationalStreamInternetProtocolandUserGuide.pdf>

- National Research Council (NRC). 2004. Endangered and Threatened Fishes in the Klamath River Basin: Causes of Decline and Strategies for Recovery. Washington, DC: The National Academies Press. <https://doi.org/10.17226/10838>.
- National Marine Fisheries Service (NMFS). 2014. Final Recovery Plan for the Southern Oregon/Northern California Coast Evolutionarily Significant Unit of Coho Salmon (*Oncorhynchus kisutch*). National Marine Fisheries Service. Arcata, CA. http://www.nmfs.noaa.gov/pr/recovery/plans/cohosalmon_soncc.pdf
- National Operational Hydrologic Remote Sensing Center (NOHRSC). 2004. Snow Data Assimilation System (SNODAS) Data Products at NSIDC, Version 1. Boulder, Colorado USA. NSIDC: National Snow and Ice Data Center. doi: <https://doi.org/10.7265/N5TB14TC>.
- Naz, B.S., S.-C. Kao, M. Ashfaq, D. Rastogi, R. Mei, and L.C. Bowling, 2016. Regional Hydrologic Response to Climate Change in the Conterminous United States Using High-Resolution Hydroclimate Simulations. *Global and Planetary Change* 143:100–117.
- North Coast Regional Water Quality Control Board (NCRWQCB). 2005. Salmon River, Siskiyou County, California Total Maximum Daily Load for Temperature and Implementation Plan Adopted June 22, 2005, NCRWQCB Resolution No. R1-2005-0058. Prepared by North Coast Regional Water Quality Control Board, Santa Rosa, California.
- North Coast Regional Water Quality Control Board (NCRWQCB). 2010. Final Staff Report for the Klamath River Total Maximum Daily Loads (TMDLs) Addressing Temperature, Dissolved Oxygen, Nutrient and Microcystin Impairments in California, the Proposed Site Specific Dissolved Oxygen Objectives for the Klamath River and California, and the Klamath River and Lost River Implementation Plans. NCRWQCB, Santa Rosa, CA. http://www.waterboards.ca.gov/northcoast/water_issues/programs/tmdls/klamath_river/
- Null, S.E., J.H. Viers, and J.F. Mount, 2010. Hydrologic Response and Watershed Sensitivity to Climate Warming in California's Sierra Nevada. *PLOS ONE* 5:e9932. doi: 10.1371/journal.pone.0009932.
- Ohmann, J.L. and M.J. Gregory. 2002. Predictive Mapping of Forest Composition and Structure with Direct Gradient Analysis and Nearest-Neighbor Imputation in Coastal Oregon, U.S.A. *Canadian Journal of Forest Research* 32:725–741. doi: 10.1139/x02-011.
- Ohmann, J.L., M.J. Gregory, and H.M. Roberts. 2014. Scale Considerations for Integrating Forest Inventory Plot Data and Satellite Image Data for Regional Forest Mapping. *Remote Sensing of Environment* 151:3–15. doi: 10.1016/j.rse.2013.08.048.
- Oubeidillah, A.A., S.-C. Kao, M. Ashfaq, B.S. Naz, and G. Tootle. 2014. A Large-Scale, High-Resolution Hydrological Model Parameter Data Set for Climate Change Impact Assessment for the Conterminous US. *Hydrol. Earth Syst. Sci.* 18:67–84. doi: 10.5194/hess-18-67-2014.
- Perry, R.W., Risley, J.C., Brewer, S.J., Jones, E.C., and Rondorf, D.W. 2011. Simulating Daily Water Temperatures of the Klamath River under Dam Removal and Climate Change Scenarios. U.S. Geological Survey Open-File Report 2011-1243:78pp.
- Peterson E.E. and J.M. Ver Hoef. 2014. STARS: An ArcGIS toolset used to calculate the spatial information needed to fit spatial statistical models to stream network data. *Journal of Statistical Software*, 56(2).
- Pierce, D.W., D.R. Cayan, and L. Dehann. 2016. Creating Climate Projections to Support the 4th California Climate Assessment. http://docketpublic.energy.ca.gov/PublicDocuments/16-IEPR-04/TN211805_20160614T101821_Creating_Climate_projections_to_support_the_4th_California_Clim.pdf.

- Pierce, D.W., D.R. Cayan, and B.L. Thrasher. 2014. Statistical Downscaling Using Localized Constructed Analogs (LOCA). *Journal of Hydrometeorology* 15:2558–2585. doi: 10.1175/JHM-D-14-0082.1.
- Randles, C.A., A.M. da Silva, V. Buchard, P.R. Colarco, A. Darmenov, R. Govindaraju, A. Smirnov, B. Holben, R. Ferrare, J. Hair, Y. Shinozuka, and C.J. Flynn. 2017. The MERRA-2 Aerosol Reanalysis, 1980 Onward. Part I: System Description and Data Assimilation Evaluation. *Journal of Climate* 30:6823–6850. doi: 10.1175/JCLI-D-16-0609.1.
- R Core Team. 2018. R: A language and environment for statistical computing. R Foundation for Statistical Computing, Vienna, Austria. URL <https://www.R-project.org/>.
- Safeeq, M., G.E. Grant, S.L. Lewis, M.G. Kramer, and B. Staab. 2014. A Hydrogeologic Framework for Characterizing Summer Streamflow Sensitivity to Climate Warming in the Pacific Northwest, USA. doi: 10.5194/hess-18-3693-2014. doi:10.5194/hess-18-3693-2014.
- Sengupta, M., Y. Xie, A. Lopez, A. Habte, G. Maclaurin, and J. Shelby. 2018. The National Solar Radiation Data Base (NSRDB). *Renewable and Sustainable Energy Reviews* 89:51–60. doi: 10.1016/j.rser.2018.03.003.
- Sowder, C. and E.A. Steel. 2012. A Note on the Collection and Cleaning of Water Temperature Data. *Water* 4:597–606. doi: 10.3390/w4030597. <http://www.mdpi.com/2073-4441/4/3/597/pdf>
- Steel, E.A., A. Marsha, A.H. Fullerton, J.D. Olden, N.K. Larkin, S.-Y. Lee, and A. Ferguson. 2018. Thermal Landscapes in a Changing Climate: Biological Implications of Water Temperature Patterns in an Extreme Year. *Canadian Journal of Fisheries and Aquatic Sciences*. doi: 10.1139/cjfas-2018-0244.
- Stillwater Sciences. 2018. Salmon River Floodplain Habitat Enhancement and Mine Tailing Remediation Project. Phase 1: Technical Analysis of Opportunities and Constraints. Prepared by Stillwater Sciences, Arcata, California for Salmon River Restoration Council, Sawyers Bar, California. https://srrc.org/publications/programs/habitatrestoration/Salmon%20River%20Floodplain%20Enhancement%20Tech%20Memo_Final%202018.pdf
- Strange, J.S., 2010. Upper Thermal Limits to Migration in Adult Chinook Salmon: Evidence from the Klamath River Basin. *Transactions of the American Fisheries Society* 139:1091–1108. doi: 10.1577/T09-171.1.
- Strange, J. 2011. Salmonid Use of Thermal Refuges in the Klamath River: 2010 Annual Monitoring Study. Yurok Tribal Fisheries Program, Hoopa, CA. Available online at: http://www.yuroktribe.org/departments/fisheries/documents/thermal_refugia_report_FINAL_2010_YTFP_000.pdf
- Taylor, K. E., R. J. Stouffer, and G. A. Meehl, 2012: An Overview of CMIP5 and the experiment design. *Bull. Am. Met. Soc.*, 93, 485-498, doi:10.1175/BAMS-D-1111-00094.00091.
- Tetra Tech, Inc. 2004. Description of the Klamath and Lost Rivers Water Quality Databases. Draft July 16, 2004. Prepared for U.S. Environmental Protection Agency Region 10, U.S. Environmental Protection Agency Region 9, Oregon Department of Environmental Quality, and the North Coast Regional Water Quality Control Board. Tetra Tech, Inc.
- U.S. Environmental Protection Agency (EPA). (2014) Best Practices for Continuous Monitoring of Temperature and Flow in Wadeable Streams. Global Change Research Program, National Center for Environmental Assessment, Washington, DC; EPA/600/R-13/170F. Available from the National Technical Information Service, Springfield, VA. <http://www.epa.gov/ncea>.

- van Vuuren, D.P., J. Edmonds, M. Kainuma, K. Riahi, A. Thomson, K. Hibbard, G.C. Hurtt, T. Kram, V. Krey, J.-F. Lamarque, T. Masui, M. Meinshausen, N. Nakicenovic, S.J. Smith, and S.K. Rose. 2011. The Representative Concentration Pathways: An Overview. *Climatic Change* 109:5. doi: 10.1007/s10584-011-0148-z.
- Ver Hoef J.M., Peterson E.E., Clifford D., and Shah R. 2014. SSN: An R package for spatial statistical modeling on stream networks. *Journal of Statistical Software*, 56(3).
- Watershed Sciences, Inc. 2010. Airborne Thermal Infrared Remote Sensing Salmon River Basin, California. Submitted to the Salmon River Restoration Council by Watershed Sciences, Inc., Corvallis, OR.
http://www.srrc.org/publications/programs/monitoring/SRRC%20Salmon_River_TIR_Report%202009.pdf
- Watercourse Engineering, Inc. 2003. Klamath River Water Quality 2000 Monitoring Program - Project Report. Sponsored by U.S. Bureau of Reclamation Klamath Falls Area Office with support from PacifiCorp. Watercourse Engineering, Inc. Napa, CA. 92p.
- Welsh Jr, H.H., G.R. Hodgson, B.C. Harvey, and M.F. Roche, 2001. Distribution of Juvenile Coho Salmon in Relation to Water Temperatures in Tributaries of the Mattole River, California. *North American Journal of Fisheries Management* 21:464–470.
- Wenger, S.J., C.H. Luce, A.F. Hamlet, D.J. Isaak, and H.M. Neville, 2010. Macroscale Hydrologic Modeling of Ecologically Relevant Flow Metrics. *Water Resources Research* 46:W09513. doi: 10.1029/2009WR008839.
- Xiao, M., B. Nijssen, and D.P. Lettenmaier. 2016. Drought in the Pacific Northwest, 1920–2013. *Journal of Hydrometeorology* 17:2391–2404. doi: 10.1175/JHM-D-15-0142.1.
- Young, C.A., M.I. Escobar-Arias, M. Fernandes, B. Joyce, M. Kiparsky, J.F. Mount, V.K. Mehta, D. Purkey, J.H. Viers, and D. Yates, 2009. Modeling the Hydrology of Climate Change in California’s Sierra Nevada for Subwatershed Scale Adaptation1. *JAWRA Journal of the American Water Resources Association* 45:1409–1423. doi: 10.1111/j.1752-1688.2009.00375.x.

APPENDIX A: TABLE OF TRIBUTARY STREAMFLOW

Table A6. Mean August streamflow estimated at 23 sites where streamflow was measured on at least 4 dates. Site flows estimated from the linear mixed-effects model were input into a spatial model to estimate flows throughout the entire stream network (Figure 5). Linear regression formulas (right column) were not used in this report, but are provided here for future use, and are within a few percent of the linear mixed-effects model results.

Long-Term Streamflow Site	Water-shed Area (mi ²)	Estimated Mean August Streamflow at Site		Linear Regression Formula for Individual Sites
		Spatial Model (cfs)	Mixed-Effects Model (cfs)	
Black Bear	14.3	2.1	1.7	$\log_{10}(\text{site flow}) = 0.592 \cdot \log_{10}(\text{USGS flow}) - 1.194$
Butler	6.6	2.9	3.2	$\log_{10}(\text{site flow}) = 0.520 \cdot \log_{10}(\text{USGS flow}) - 0.742$
Crapo	17.3	9.7	11.0	$\log_{10}(\text{site flow}) = 0.748 \cdot \log_{10}(\text{USGS flow}) - 0.759$
Duncan	1.6	0.4	0.4	$\log_{10}(\text{site flow}) = 0.727 \cdot \log_{10}(\text{USGS flow}) - 2.198$
EF SF Salmon R.	67.0	16.6	15.8	$\log_{10}(\text{site flow}) = 1.198 \cdot \log_{10}(\text{USGS flow}) - 1.688$
Knownothing	22.7	8.6	8.7	$\log_{10}(\text{site flow}) = 0.799 \cdot \log_{10}(\text{USGS flow}) - 0.983$
Little NF Salmon R	32.5	17.5	19.8	$\log_{10}(\text{site flow}) = 0.715 \cdot \log_{10}(\text{USGS flow}) - 0.429$
Merrill	4.7	1.1	1.1	$\log_{10}(\text{site flow}) = 0.644 \cdot \log_{10}(\text{USGS flow}) - 1.521$
Methodist	12.4	2.0	1.7	$\log_{10}(\text{site flow}) = 1.115 \cdot \log_{10}(\text{USGS flow}) - 2.443$
NF Salmon > Forks	203.7	62.7	60.1	$\log_{10}(\text{site flow}) = 1.008 \cdot \log_{10}(\text{USGS flow}) - 0.646$
NF Salmon in Sawyers	135.0	34.3	32.9	$\log_{10}(\text{site flow}) = 1.089 \cdot \log_{10}(\text{USGS flow}) - 1.107$
Nordheimer	30.9	11.5	11.9	$\log_{10}(\text{site flow}) = 0.778 \cdot \log_{10}(\text{USGS flow}) - 0.796$
North Russian > S Russian	17.9	4.7	4.6	$\log_{10}(\text{site flow}) = 1.481 \cdot \log_{10}(\text{USGS flow}) - 2.902$
Plummer	14.2	3.5	3.3	$\log_{10}(\text{site flow}) = 0.608 \cdot \log_{10}(\text{USGS flow}) - 0.954$
Salmon R @ Oak Bottom	750.7	268.9	250.0	$\log_{10}(\text{site flow}) = 1.012 \cdot \log_{10}(\text{USGS flow}) - 0.037$
Salmon R below Forks	496.8	129.6	134.7	$\log_{10}(\text{site flow}) = 1.173 \cdot \log_{10}(\text{USGS flow}) - 0.683$
SF Salmon above Forks	290.2	74.6	79.1	$\log_{10}(\text{site flow}) = 1.116 \cdot \log_{10}(\text{USGS flow}) - 0.784$
SF Salmon below Cecilville < St Clair	181.0	50.4	40.8	$\log_{10}(\text{site flow}) = 1.000 \cdot \log_{10}(\text{USGS flow}) - 0.795$
SF Salmon below Cecilville > St Clair	170.1	49.8	59.3	$\log_{10}(\text{site flow}) = 1.165 \cdot \log_{10}(\text{USGS flow}) - 1.022$
Somes	4.5	2.7	3.1	$\log_{10}(\text{site flow}) = 0.702 \cdot \log_{10}(\text{USGS flow}) - 1.203$
South Russian	18.4	6.4	6.7	$\log_{10}(\text{site flow}) = 1.256 \cdot \log_{10}(\text{USGS flow}) - 2.200$
Taylor	18.3	4.4	4.2	$\log_{10}(\text{site flow}) = 1.336 \cdot \log_{10}(\text{USGS flow}) - 2.584$
Wooley	148.6	78.1	88.1	$\log_{10}(\text{site flow}) = 0.729 \cdot \log_{10}(\text{USGS flow}) + 0.181$

APPENDIX B: EFFECTIVE SHADE MODEL

The Washington Department of Ecology's Shade spreadsheet tool⁴⁷ was used to calculate effective topographic and riparian shade for each 1-km stream reach. The Shade tool had been used in many TMDLs, often to create inputs for the Heat Source model (Boyd and Kasper 2003). GIS analyst Nicholas Cusick did the data pre-processing and ran the Shade tool, advised by Eli Asarian. Our methods are similar to those applied by Peter Leinenbach and colleagues (Detenbeck 2017).

Wetted width and bankfull width data

Wetted width and bankfull width were estimated by regressing watershed area (from NHDplus/NSI) with field measurements collected during the Salmon River TMDL (NCRWQCB 2005). Width units are meters and drainage area units are square kilometers. Formulas are:

$$\text{Wetted width} = 1.7548 * (\text{drainage area})^{0.3268}$$

$$\text{Bankfull width} = 2.8785 * (\text{drainage area})^{0.3604}$$

Canopy cover and canopy height data

Canopy cover and canopy height data were obtained from the LEMMA (Landscape Ecology, Modeling, Mapping, and Analysis) Gradient Nearest Neighbor (GNN)⁴⁸ 30-meter resolution dataset (Ohmann and Gregory 2002, Ohmann et al. 2014):

CANCOV: Canopy cover of all live trees

STNDHGT: Stand height, computed as average of heights of all dominant and codominant trees

LEMMA GNN uses Landsat remote sensing to impute (assign) each 30-meter pixel to the forestry field plot that most closely matches its Landsat spectral signatures and landscape characteristics such as climate, topography, elevation, and location. The LEMMA GNN dataset was developed primarily to map late-seral forests but includes a wide variety of forest types. An alternative canopy height/cover dataset that we could have used instead of LEMMA GNN is LandFire⁴⁹.

GIS data processing

tTools ArcGIS Python add-in⁵⁰ was used to calculate the elevation, aspect, and topographic angles for each 1-km reach. Buffer tool and Multiple Ring Buffer tools in ArcGIS/Python were used to produce three buffers (0–30m, 30–90m, and 90–210 m) on each side of each 1-km reach. Zonal statistics were used to calculate average elevation, STNDHGT, and CANCOV for each buffer for each 1-km reach.

Options in the Shade spreadsheet

Channel incision: 1 meter	Vegetation overhang: 0 meters
Number of days: 1	Date: August 1, 2017
Latitude: 41.38°	Longitude: -123.45°
Method: Chen ⁵¹	

⁴⁷ 10-Feb-2015 version downloaded from: <https://ecology.wa.gov/Research-Data/Data-resources/Models-spreadsheets/Modeling-the-environment/Models-tools-for-TMDLs>

⁴⁸ <https://lemma.forestry.oregonstate.edu/data/structure-maps>

⁴⁹ <https://www.landfire.gov/>

⁵⁰ 10-Nov-2015 version downloaded from: <https://ecology.wa.gov/Research-Data/Data-resources/Models-spreadsheets/Modeling-the-environment/Models-tools-for-TMDLs>

⁵¹ Chen method accounts for vegetative and topographic shade in contrast to the ODEQ method which only accounts for vegetative shade

APPENDIX C: COMPARISON OF SNOW DATASETS

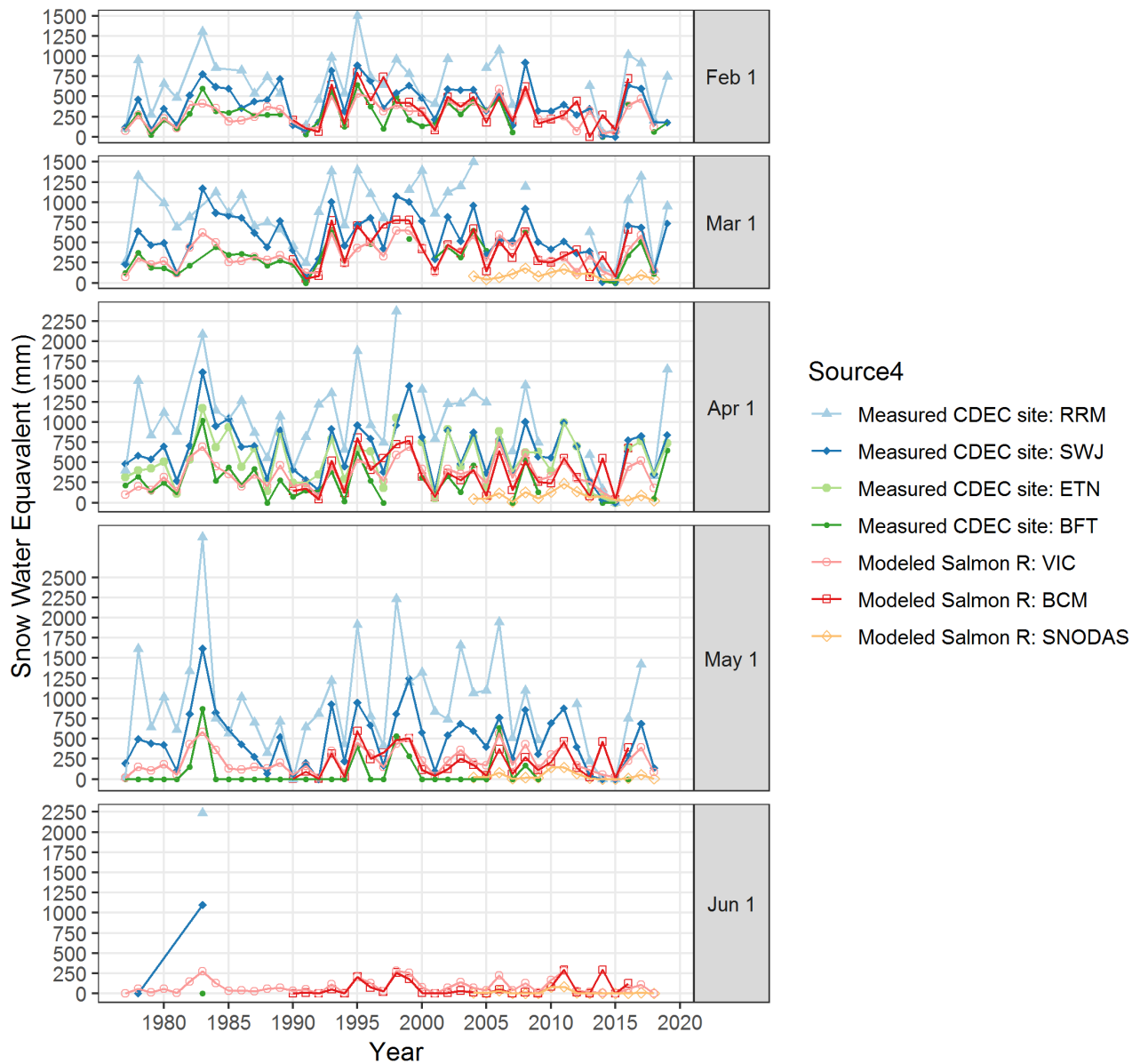


Figure C27. Comparison of annual time series of snow water equivalent at specific measured Snow Course sites (BFT, ETN, RRM, SWJ) and model predictions summarized across the whole Salmon River watershed (BCM and SNODAS), by month for 1977–2018. ETN = Etna Mountain (elev. 5900 ft), SWJ = Swampy John (elev. 5500 ft), BFT = Big Flat (elev. 5100 ft), RRM = Red Rock Mountain (elev. 6700 ft). See section 2.8.9 for information on data sources.

APPENDIX D: ADDITIONAL DETAILS ON LINEAR-MIXED EFFECTS MODELS

Table D7. Comparison of linear mixed-effects models to predict mean August stream temperature and mean daily maximum August stream temperature for streams in the Salmon River watershed and surrounding areas. AIC = Akaike information criterion. Lower AIC values generally indicate better models. Key to abbreviations: airtemp_DA = August watershed air temperature, flow = August flow at Salmon River USGS gage, vicsnowyr4 = April 1 snowpack, aotmerra8 = August aerosol optical thickness, aotsolar8 = August solar radiation, (1 | site) = random slope and intercept, (0 + variable | site) = random slope.

Temperature Metric	Model Name	Predictor Variables in Model	Random Effects	AIC
Mean daily max. August	Final (Air, flow with random slopes, snow, AOT with random slopes)	airtemp_DA + flow + vicsnowyr4 + aotmerra8	(1 site) + (0 + flow site) + (0 + aotmerra8 site)	949.4
	Air, flow with random slopes, snow with random slopes, AOT with random slopes	airtemp_DA + flow + vicsnowyr4 + aotmerra8	(1 site) + (0 + flow site) + (0 + aotmerra8 site) + (0 + vicsnowyr4 site)	951.4
	Air, flow with random slopes, snow, AOT	airtemp_DA + flow + vicsnowyr4 + aotmerra8	(1 site) + (0 + flow site)	975.7
	Air, flow with random slopes, snow, solar	airtemp_DA + flow + vicsnowyr4 + solmerra8	(1 site) + (0 + flow site)	1020.1
	Air, flow with random slopes, snow	airtemp_DA + flow + vicsnowyr4	(1 site) + (0 + flow site)	1048.8
	Air, flow with random slopes	airtemp_DA + flow	(1 site) + (0 + flow site)	1078.3
	Air with random slopes, flow with random slopes	airtemp_DA + flow	(1 site) + (0 + flow site) + (0 + airtemp_DA site)	1080.3
	Air, flow	airtemp_DA + flow	(1 site)	1115.0
Mean August	Final (Air, flow with random slopes, snow, AOT with random slopes)	airtemp_DA + flow + vicsnowyr4 + aotmerra8	(1 site) + (0 + flow site) + (0 + aotmerra8 site)	709.6
	Air, flow with random slopes, snow with random slopes, AOT with random slopes	airtemp_DA + flow + vicsnowyr4 + aotmerra8	(1 site) + (0 + flow site) + (0 + aotmerra8 site) + (0 + vicsnowyr4 site)	711.6
	Air, flow with random slopes, snow, AOT	airtemp_DA + flow + vicsnowyr4 + aotmerra8	(1 site) + (0 + flow site)	722.4
	Air, flow with random slopes, snow	airtemp_DA + flow + vicsnowyr4	(1 site) + (0 + flow site)	739.6
	Air, flow with random slopes, snow, solar	airtemp_DA + flow + vicsnowyr4 + solmerra8	(1 site) + (0 + flow site)	741.1
	Air, flow with random slopes	airtemp_DA + flow	(1 site) + (0 + flow site)	786.8
	Air with random slopes, flow with random slopes	airtemp_DA + flow	(1 site) + (0 + flow site) + (0 + airtemp_DA site)	788.8
	Air, flow	airtemp_DA + flow	(1 site)	826.1

APPENDIX E: ADDITIONAL DETAILS ON SPATIAL STREAM-NETWORK MODELS

Table E8. Proportion of total variance explained by the covariates (predictor variables), spatial autocovariance, and random effects in the final spatial stream-network model for mean daily maximum August temperature.

Model Component	Purpose/Description	Proportion of Variance Explained
Covariates	Predictor variables (drainage area, canopy, etc.)	0.35
Exponential tailup	Upstream-facing spatial autocovariance of flow-connected sites. Spatial weighting at tributary confluences is apportioned according to watershed area. Distance is measured along the channel length and its influence declines exponentially.	0.42
Site	Random effect for site. Data collected at the same site in multiple years are nested together. Each unique site is assigned a random intercept (i.e., add or subtract a set number of degrees) to account for intrinsic differences between sites not explained by other factors already included in the model.	0.08
Year	Random effect for year. Data collected in the same year are nested together. Each year is assigned a random intercept (i.e., add or subtract a set number of degrees) to account for intrinsic differences between years not explained by other factors already included in the model.	0.03
Nugget	Residual error (i.e., not explained by covariates or spatial autocovariance, or random effects).	0.12

Table E9. Comparison of summary statistics for alternative spatial stream-network models to predict mean daily maximum August stream temperature for streams in the Salmon River watershed and surrounding areas. RMSPE = root mean squared prediction error, AIC = Akaike information criterion. Lower RMSPE and AIC generally indicate better models. elev = Elevation, shadechen = effective shade, airtemp_DA = August watershed air temperature, flow = August flow at Salmon River USGS gage, baseflow = average water yield, cumdrainag = log of drainage area, SFcat = SF Salmon (Y/N categorical variable), vicsnowyr4 = April 1 snowpack, vicsnowyr5 = May 1 snowpack, vicsnowyr6 = June 1 snowpack, aotmerra8 = August aerosol optical thickness, vicsnowyr4:flow = interaction of flow and vicsnowyr4, SFcat:flow = interaction of flow and SFcat, cumdrainag:flow = interaction of cumdrainag and flow.

Model Name	Predictor Variables in Model	AIC	RMSPE (°C)
Final (with August baseflow and drainage area)	elev + shadechen + airtemp_DA + baseflow + flow + vicsnowyr4 + aotmerra8 + cumdrainag + SFcat + aotmerra8:cumdrainag + cumdrainag:flow + SFcat:flow	1636.7	0.618
April 1 snow, distance from headwaters	elev + shadechen + airtemp_DA + flow + vicsnowyr4 + aotmerra8 + mainlenkm + SFcat + aotmerra8:mainlenkm + mainlenkm:flow + SFcat:flow	1639.2	0.615
May 1 snow, distance from headwaters	elev + shadechen + airtemp_DA + flow + vicsnowyr5 + aotmerra8 + mainlenkm + SFcat + aotmerra8:mainlenkm + mainlenkm:flow + SFcat:flow	1639.6	0.616
April 1 snow x flow interaction, distance from headwaters	elev + shadechen + airtemp_DA + flow + vicsnowyr4 + aotmerra8 + mainlenkm + SFcat + aotmerra8:mainlenkm + vicsnowyr4:flow + mainlenkm:flow + SFcat:flow	1640.2	0.615
April 1 snow, drainage area	elev + shadechen + airtemp_DA + flow + vicsnowyr4 + aotmerra8 + cumdrainag + SFcat + aotmerra8:cumdrainag + cumdrainag:flow + SFcat:flow	1640.7	0.620
April 1 snow, drainage area, additive function = drainage area	elev + shadechen + airtemp_DA + flow + vicsnowyr4 + aotmerra8 + cumdrainag + SFcat + aotmerra8:cumdrainag + cumdrainag:flow + SFcat:flow	1640.8	0.620
June 1 snow, distance from headwaters	elev + shadechen + airtemp_DA + flow + vicsnowyr6 + aotmerra8 + mainlenkm + SFcat + aotmerra8:mainlenkm + mainlenkm:flow + SFcat:flow	1645.3	0.617
April 1 snow, distance from headwaters, no AOT:flow interaction	elev + shadechen + airtemp_DA + flow + vicsnowyr4 + aotmerra8 + mainlenkm + SFcat + mainlenkm:flow + SFcat:flow	1674.9	0.629
April 1 snow, log distance from headwaters, no AOT:flow interaction	elev + shadechen + airtemp_DA + flow + vicsnowyr4 + aotmerra8 + mainlnkml + SFcat + mainlnkml:flow + SFcat:flow	1679.3	0.638
April 1 snow, distance from headwaters, August baseflow, no AOT:flow interaction	elev + shadechen + baseflow + airtemp_DA + flow + vicsnowyr4 + mainlenkm + SFcat + mainlenkm:flow + SFcat:flow	1682.4	0.630
April 1 snow, log distance from headwaters, no AOT	elev + shadechen + airtemp_DA + flow + vicsnowyr4 + mainlenkm + SFcat + mainlenkm:flow + SFcat:flow	1682.8	0.630
April 1 snow, drainage area, no AOT:flow interaction	elev + shadechen + airtemp_DA + flow + vicsnowyr4 + aotmerra8 + cumdrainag + SFcat + cumdrainag:flow + SFcat:flow	1684.7	0.637
April 1 snow, distance from headwaters, no AOT:flow interaction, so SF cat	elev + shadechen + airtemp_DA + flow + vicsnowyr4 + aotmerra8 + mainlenkm + mainlenkm:flow	1726.8	0.648
Same variables as final but no interactions	elev + shadechen + airtemp_DA + baseflow + flow + vicsnowyr4 + aotmerra8 + cumdrainag + Sfcats	1768.1	0.673

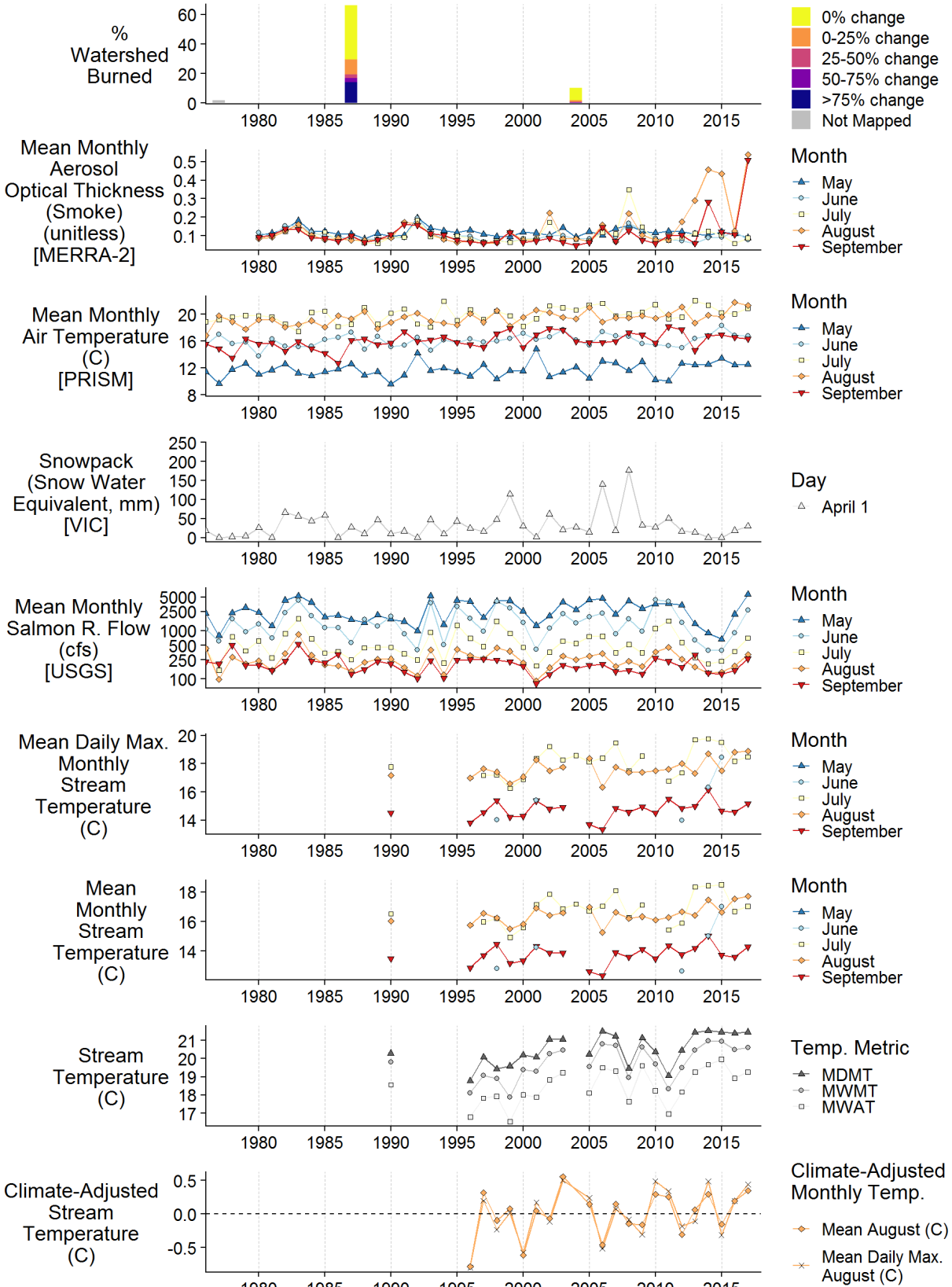
APPENDIX F: Annual Time Series of Climate, Fire, and Stream Temperature at Long-Term Monitoring Sites

This appendix is a series of graphs. There is one page for each site long-term temperature monitoring site (stream temperatures monitored for at least eight years). Graphs are titled by a combination of site name, drainage area, and 1-km reach ID code.

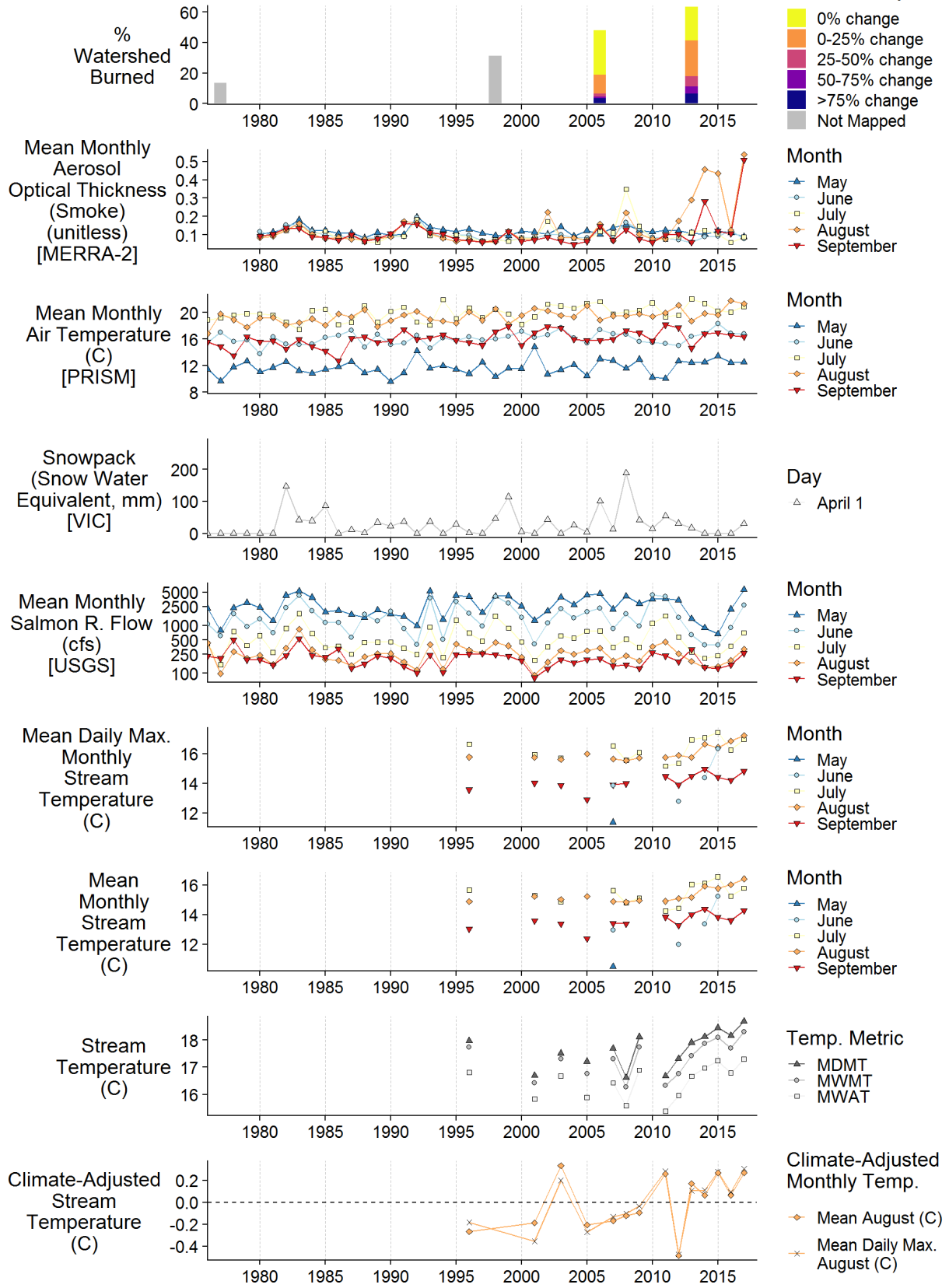
Caption for all graphs:

In top to bottom order, the graph panels show: A) percent of site's watershed area burned, B) mean monthly aerosol optical thickness (a proxy for wildfire smoke) at center of Salmon River watershed estimated from satellites, C) mean monthly air temperature for entire Salmon River watershed from PRISM model, D) April 1 snowpack for site's watershed from VIC hydrologic model, E) mean monthly flow measured at Salmon River USGS gage, F) mean daily maximum monthly stream temperature measured at site, and G) mean monthly stream temperature measured at site, H) seasonal stream temperature metrics (MDMT, MWMT, and MWAT) measured at site, and I) climate-adjusted August stream temperature at site. Climate-adjusted temperatures are only shown for sites with at least 14 years of complete August stream temperature data.

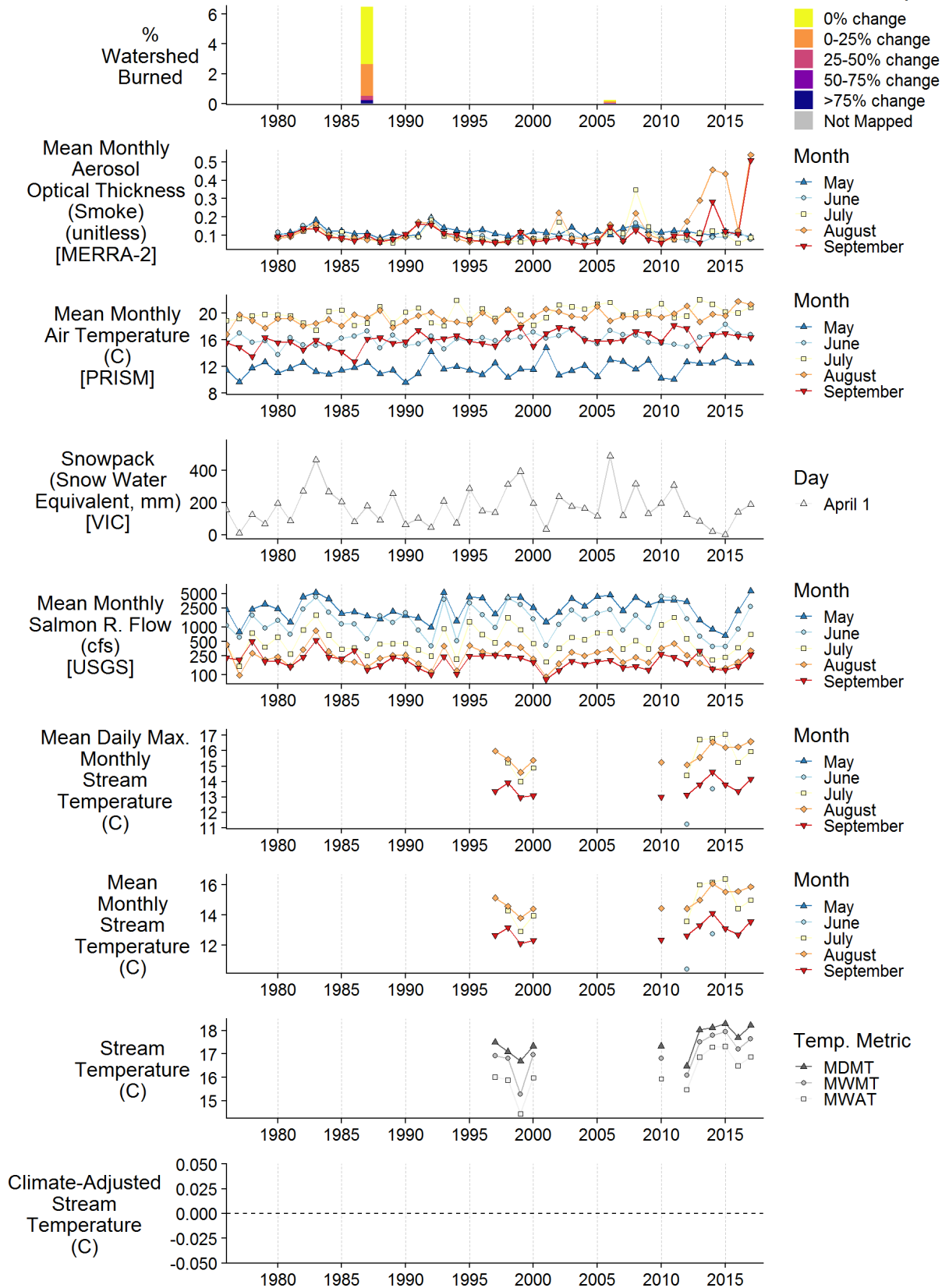
Black Bear Cr nr mouth- 37.3km2-129300



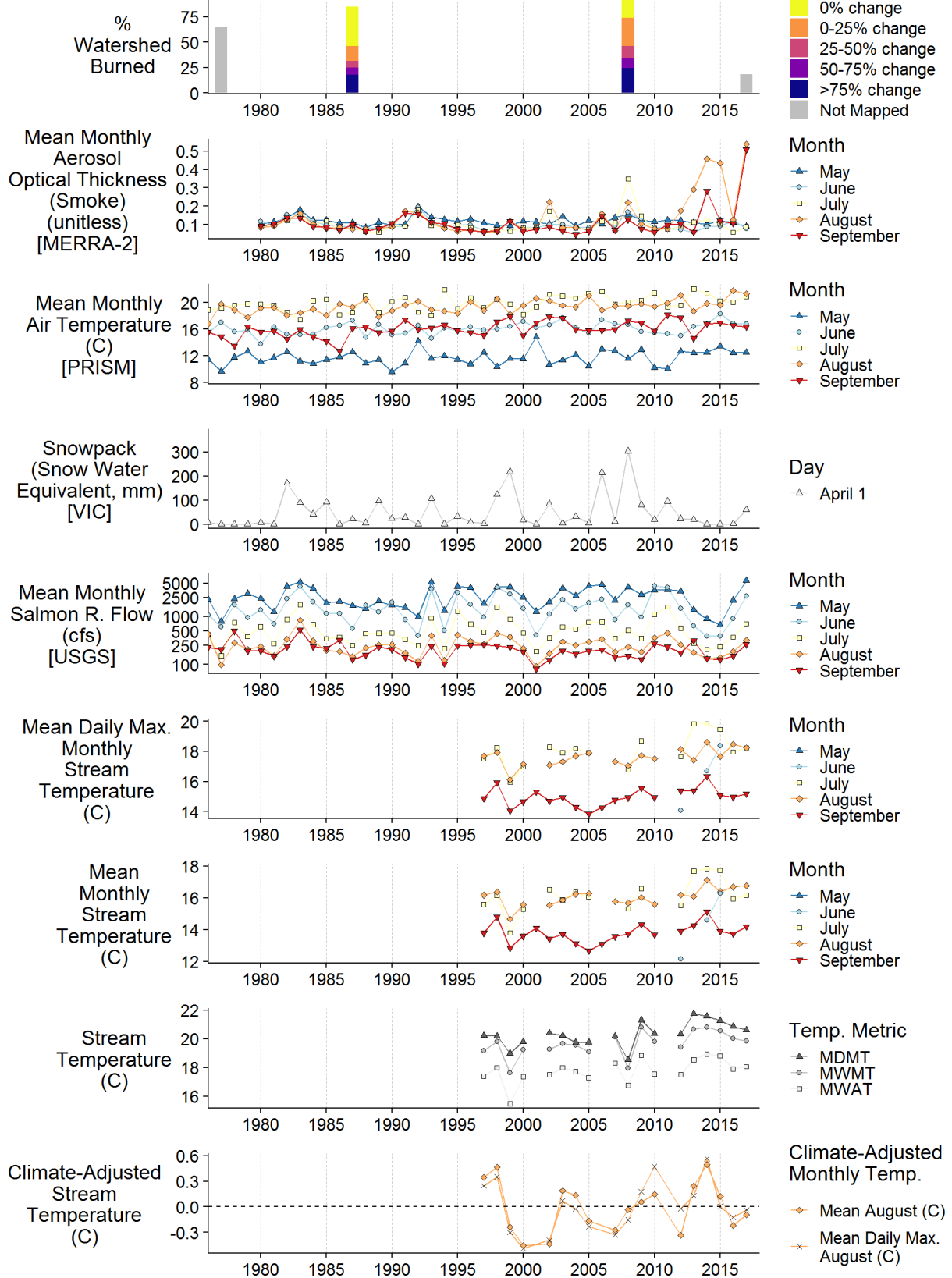
Butler Cr nr mouth- 17.3km2-131098



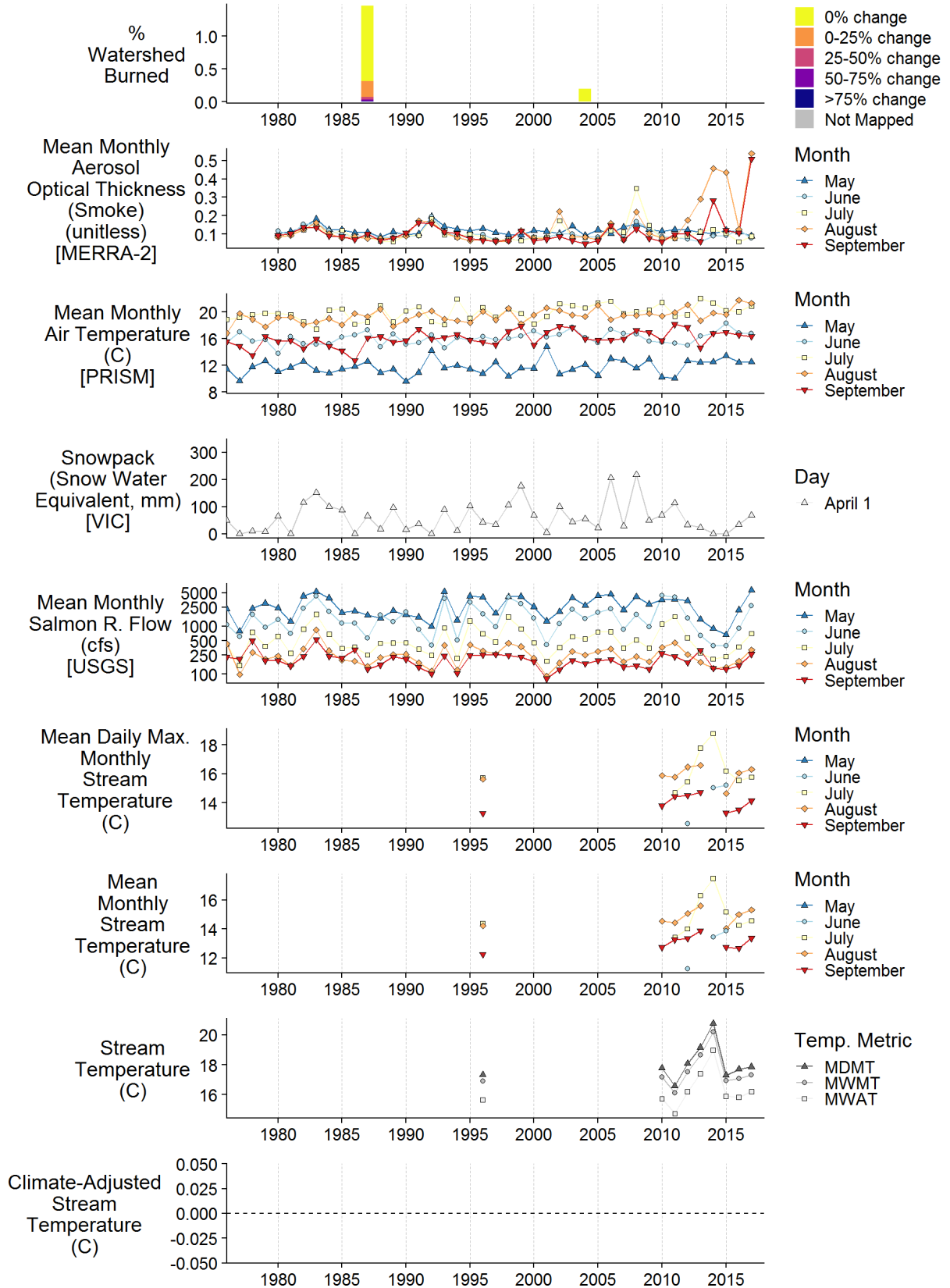
Cecil Cr nr mouth- 14.8km2-128203



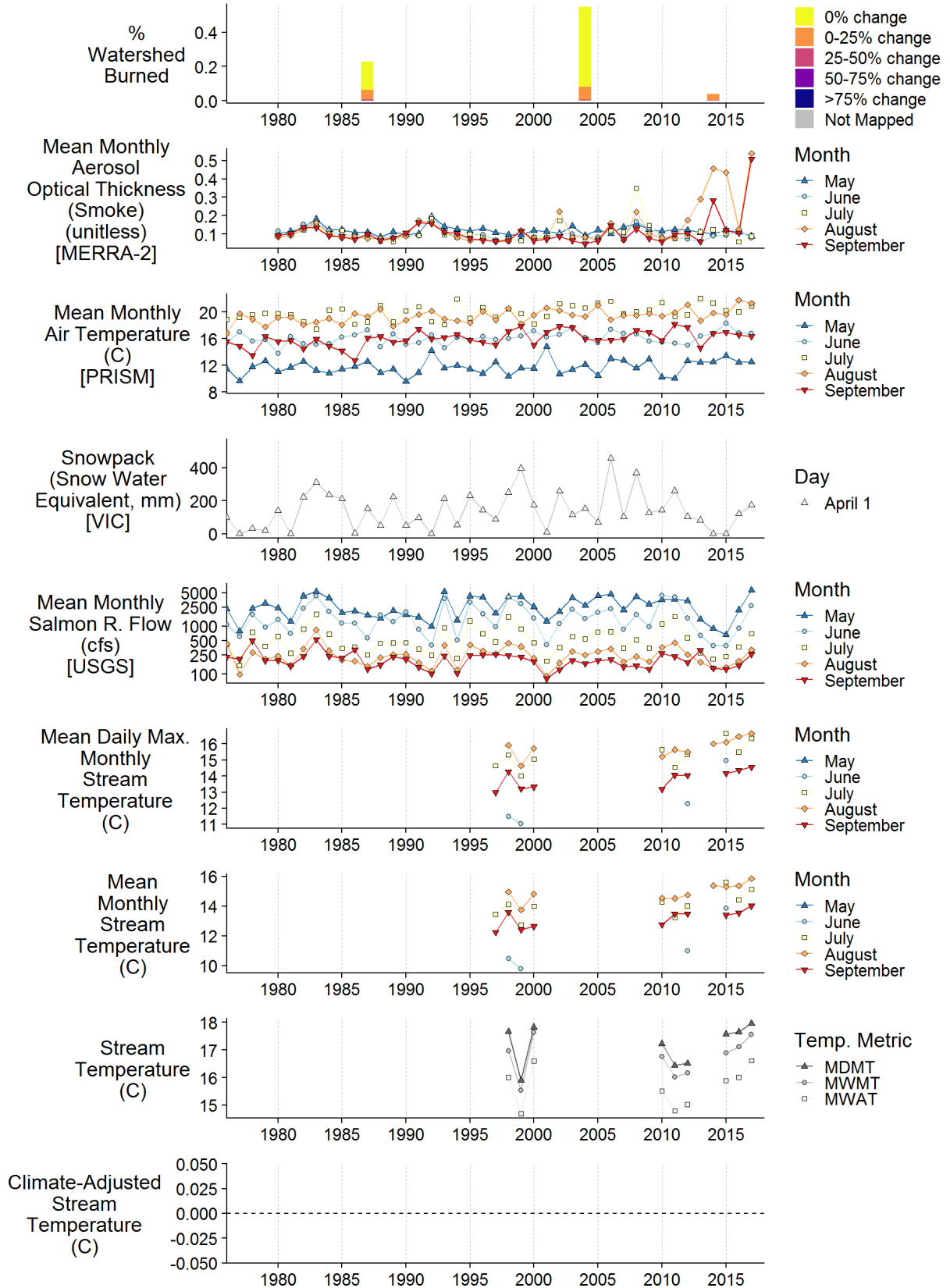
Crapo Cr nr mouth- 44.9km2-130525



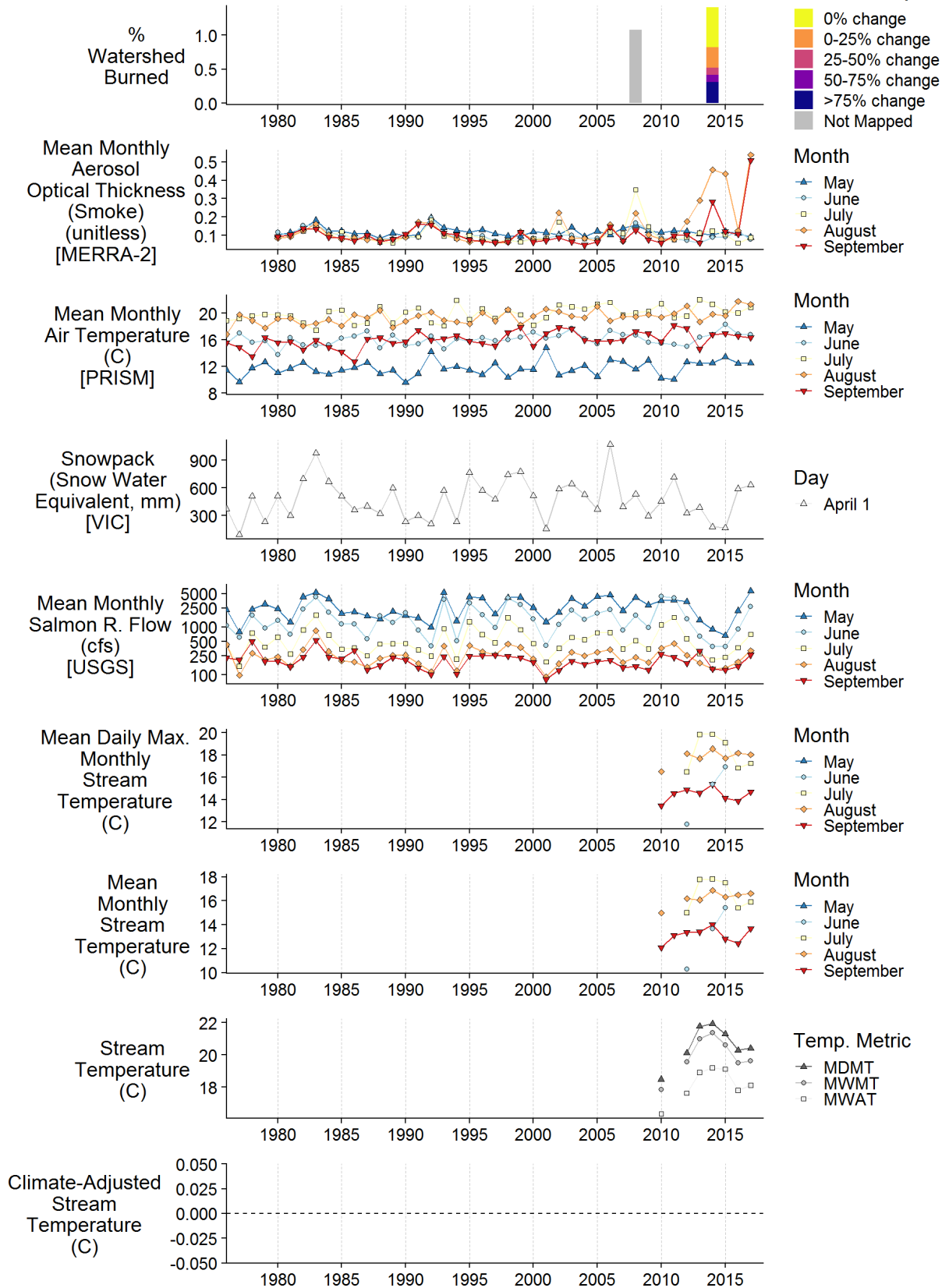
Crawford Cr (Salmon) nr mouth- 34.0km2-128718



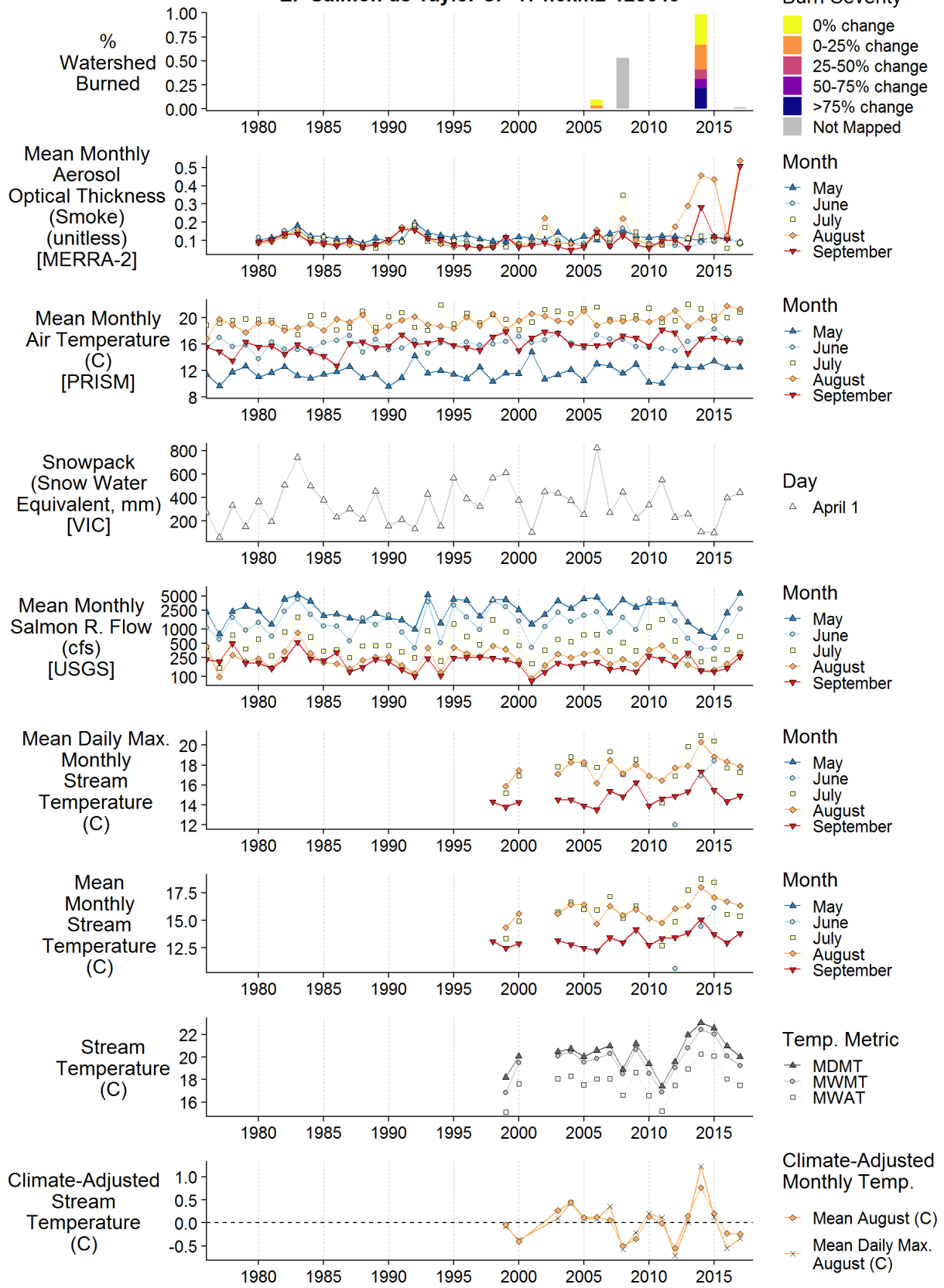
Eddy Gulch nr mouth- 18.0km2-129951



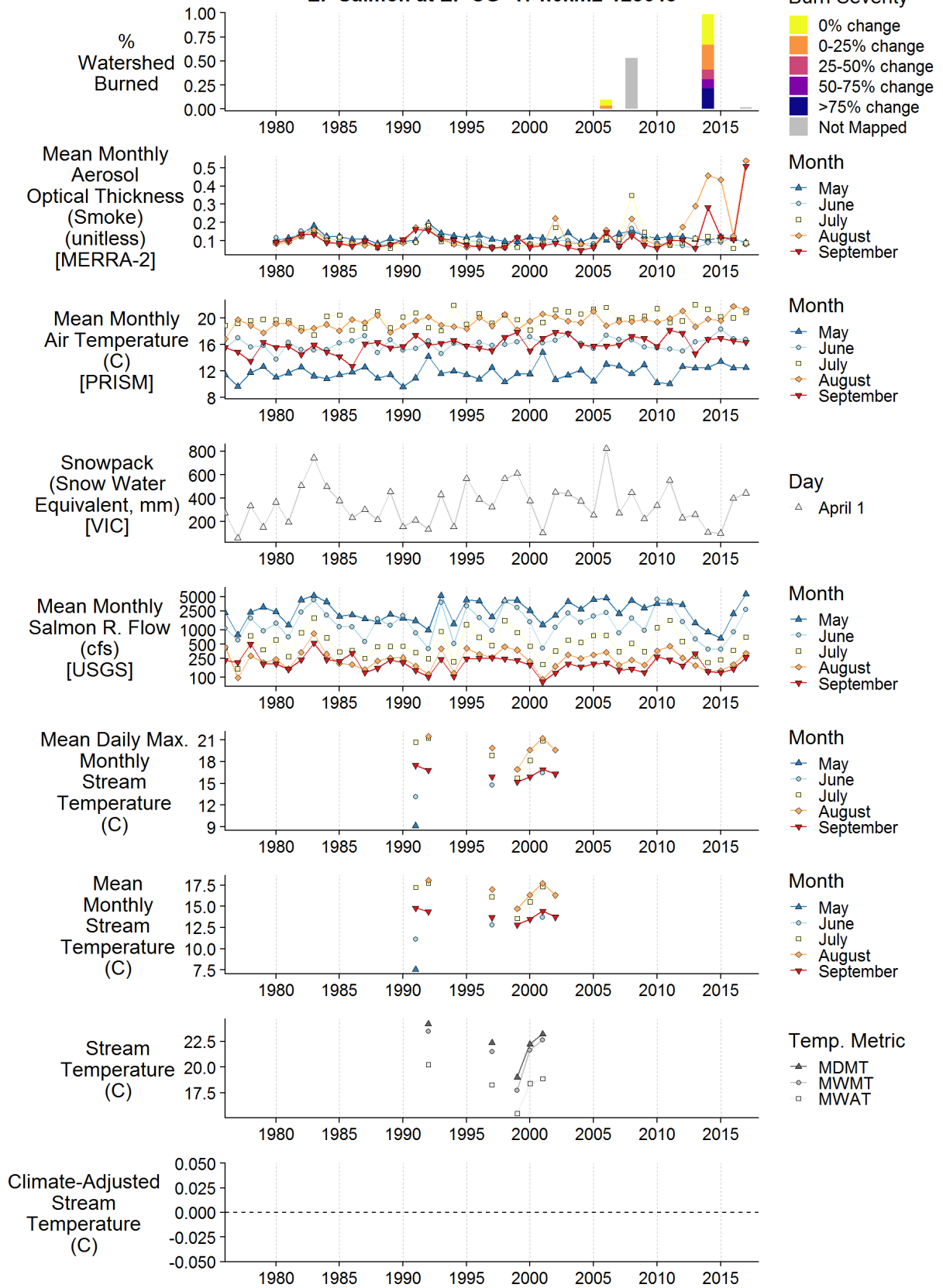
EF Salmon us Shadow Cr- 86.3km2-129031



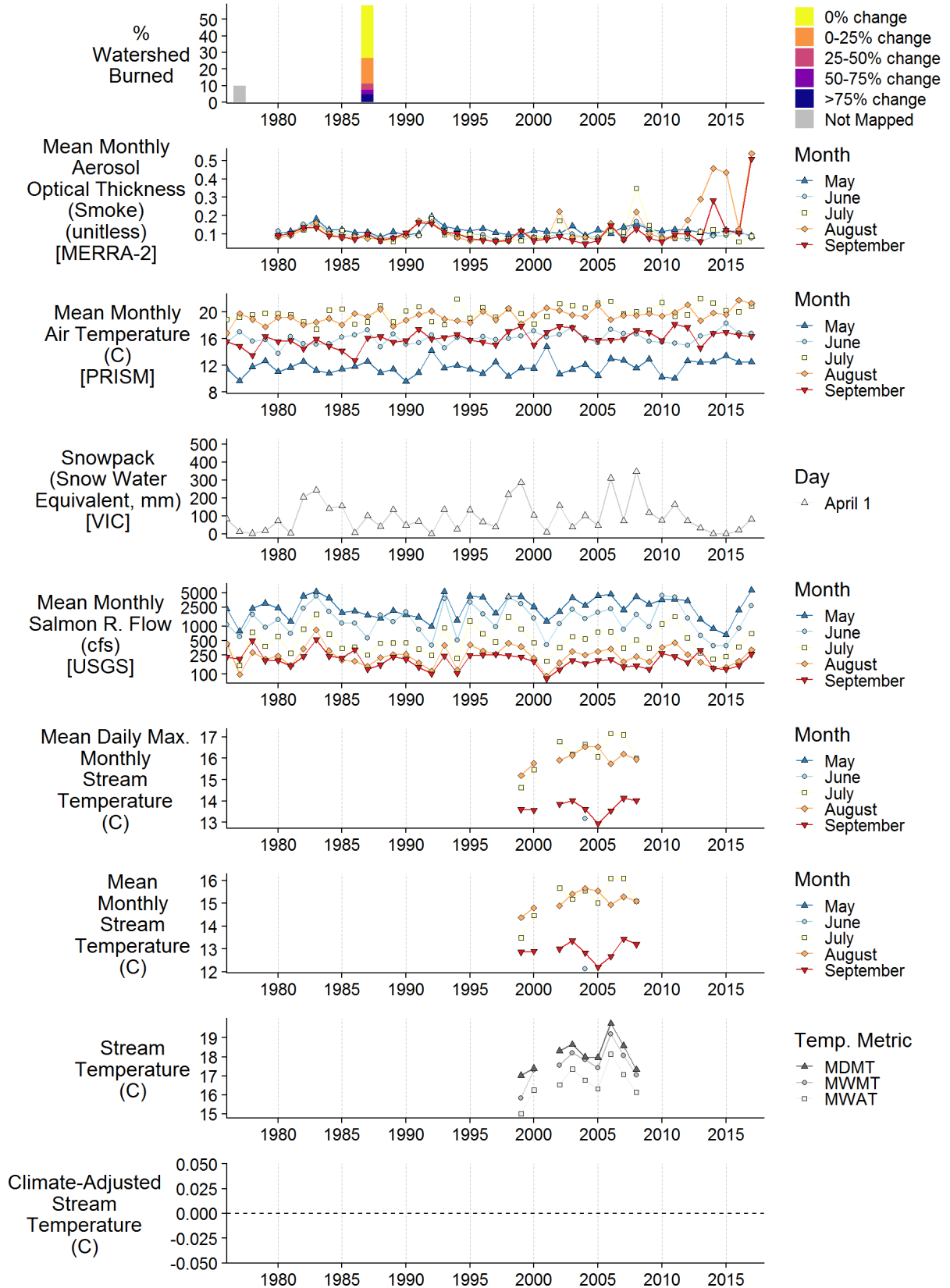
EF Salmon ds Taylor Cr- 174.6km2-128643



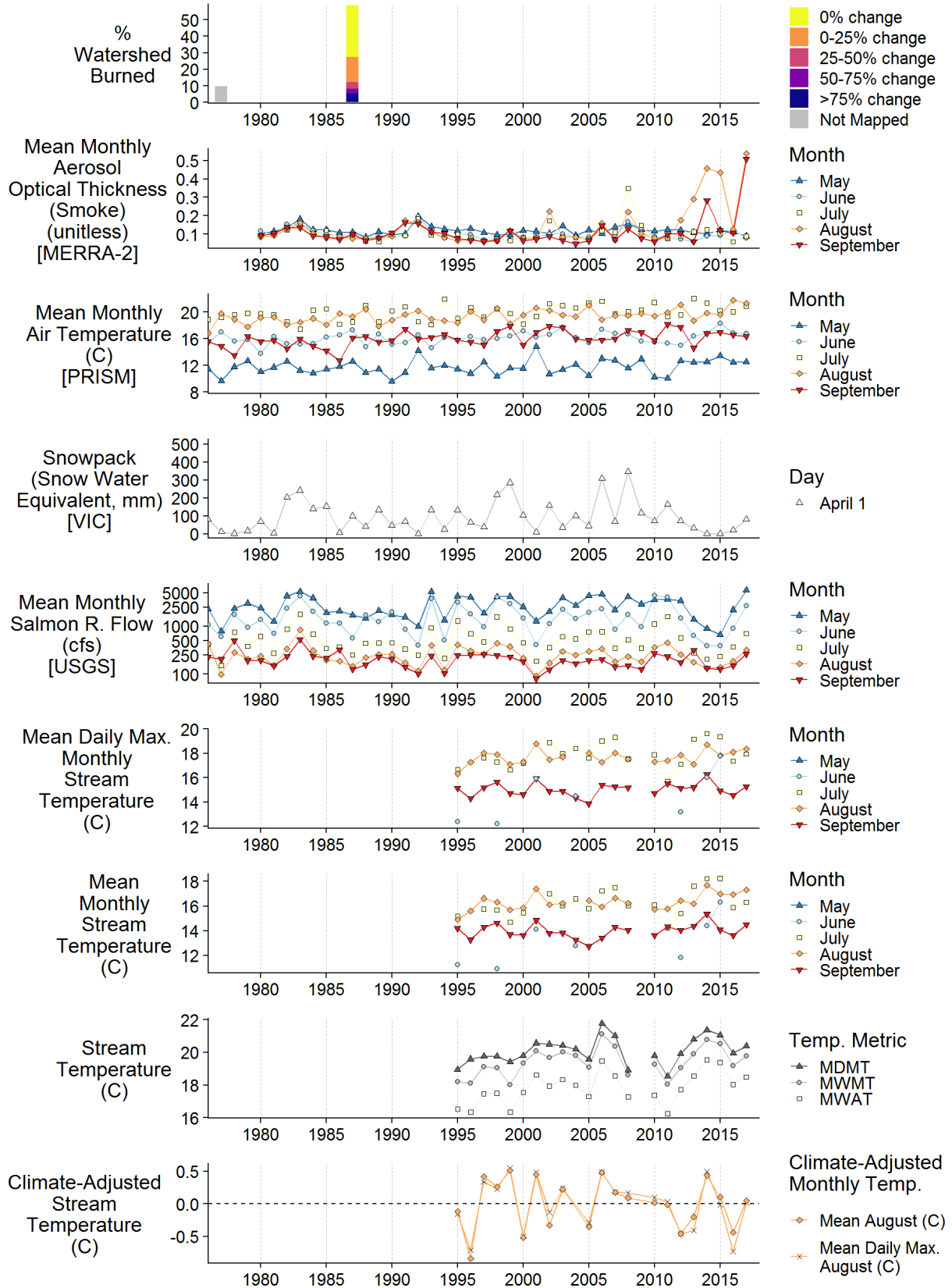
EF Salmon at EF CG- 174.6km2-128645



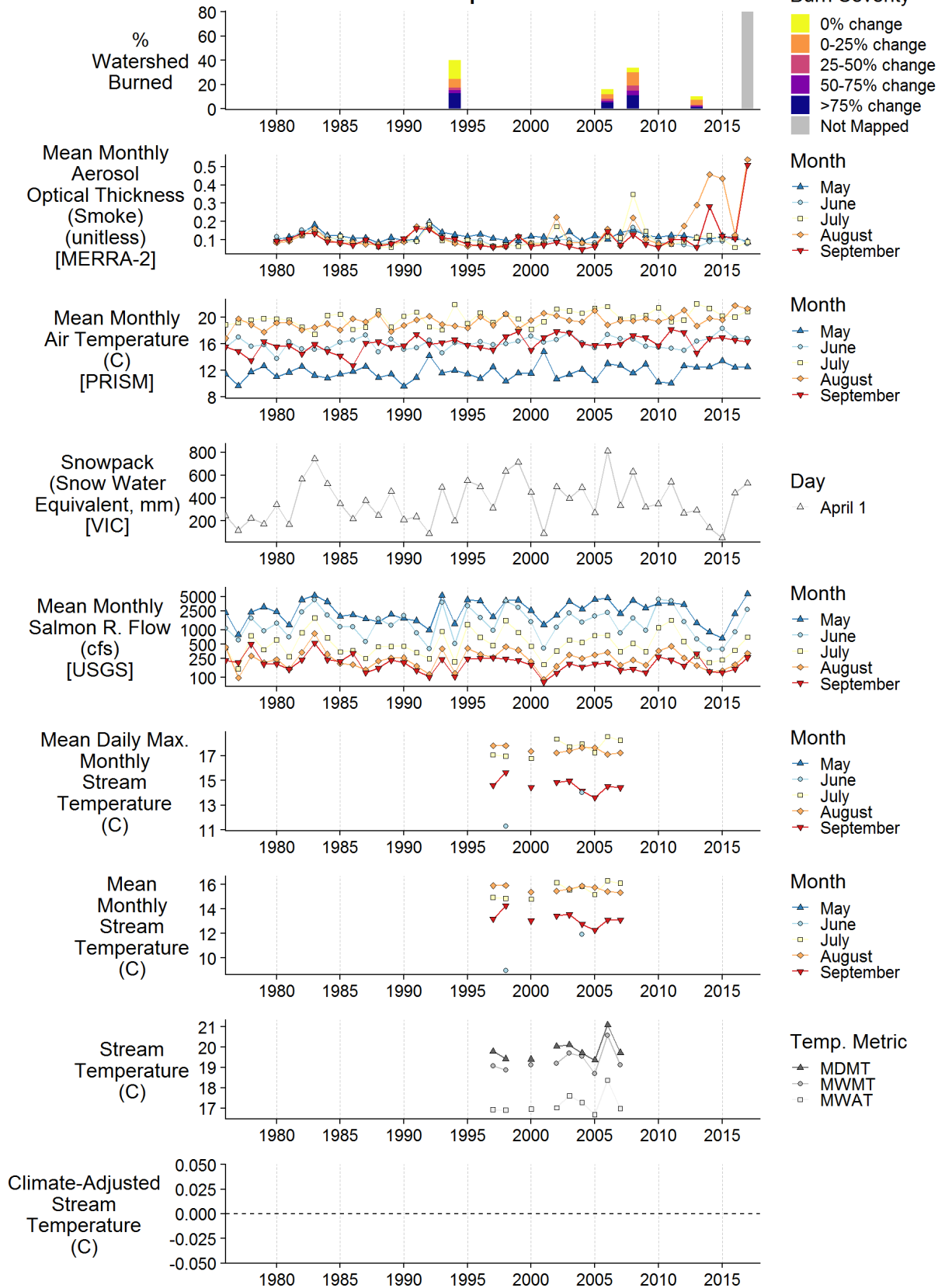
Knownothing ds Forks- 57.2km2-129426



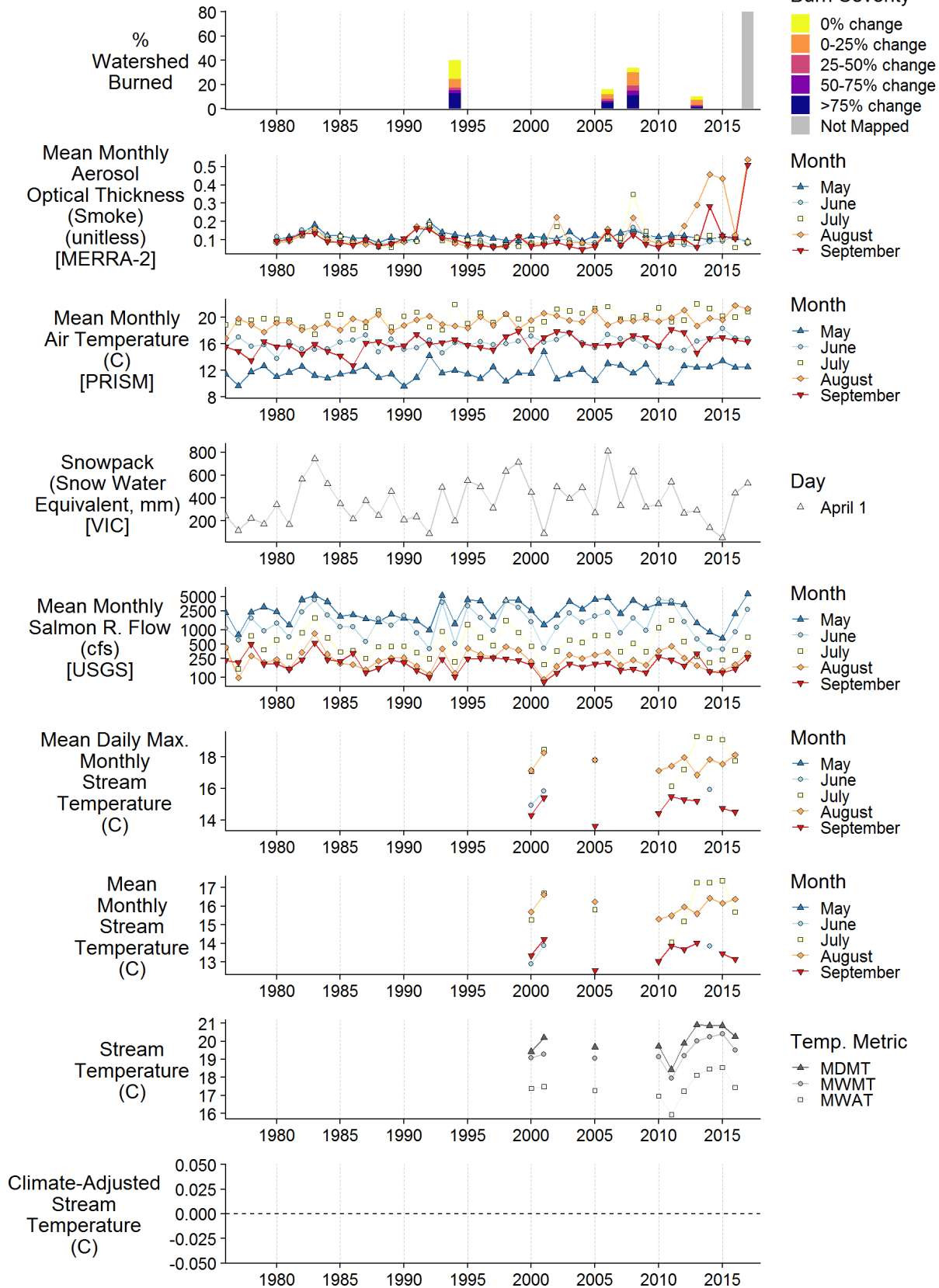
Knownothing Cr nr mouth- 58.9km2-129664



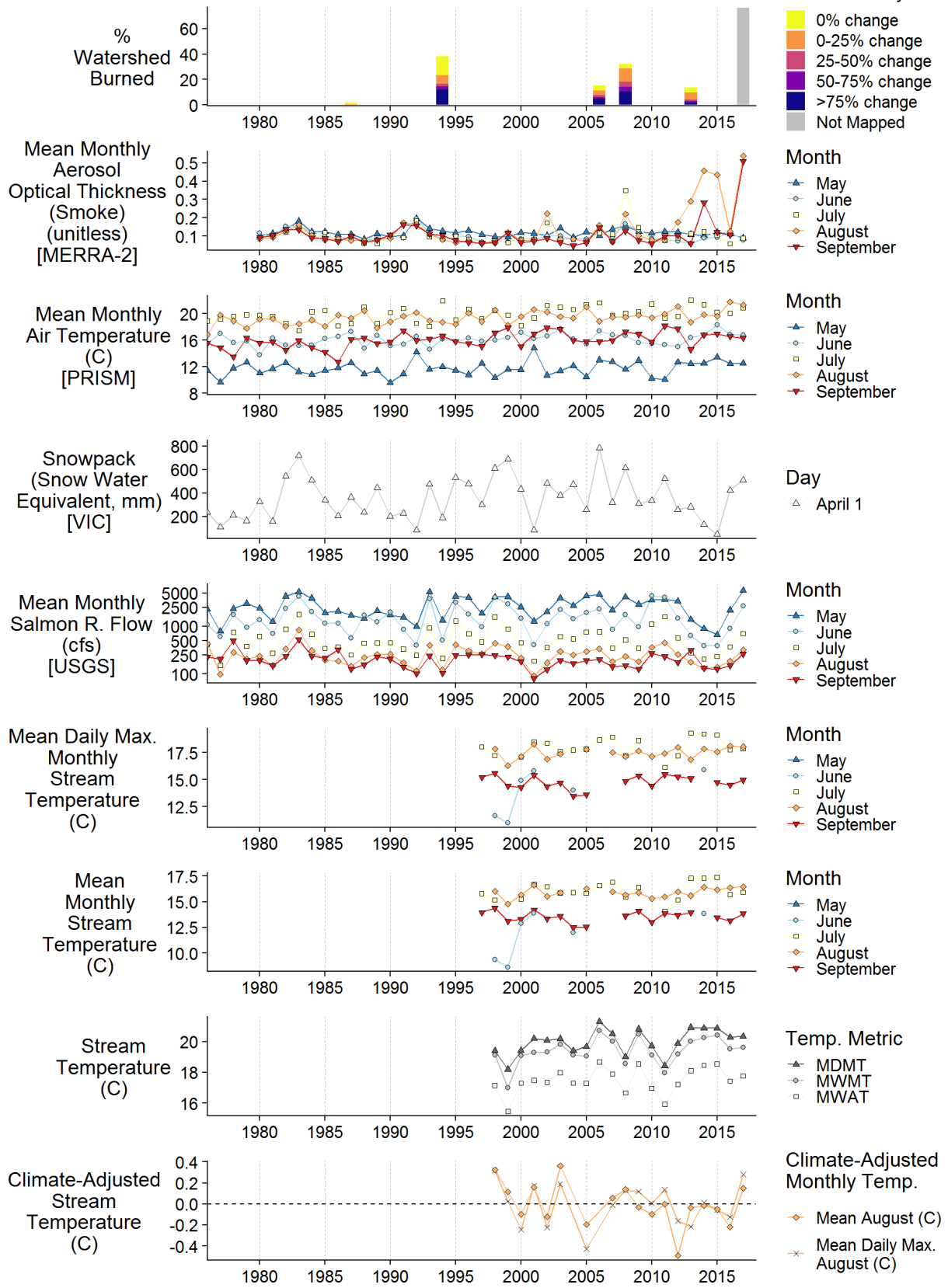
Little NF Salmon ds Specimen- 80.4km2-130935



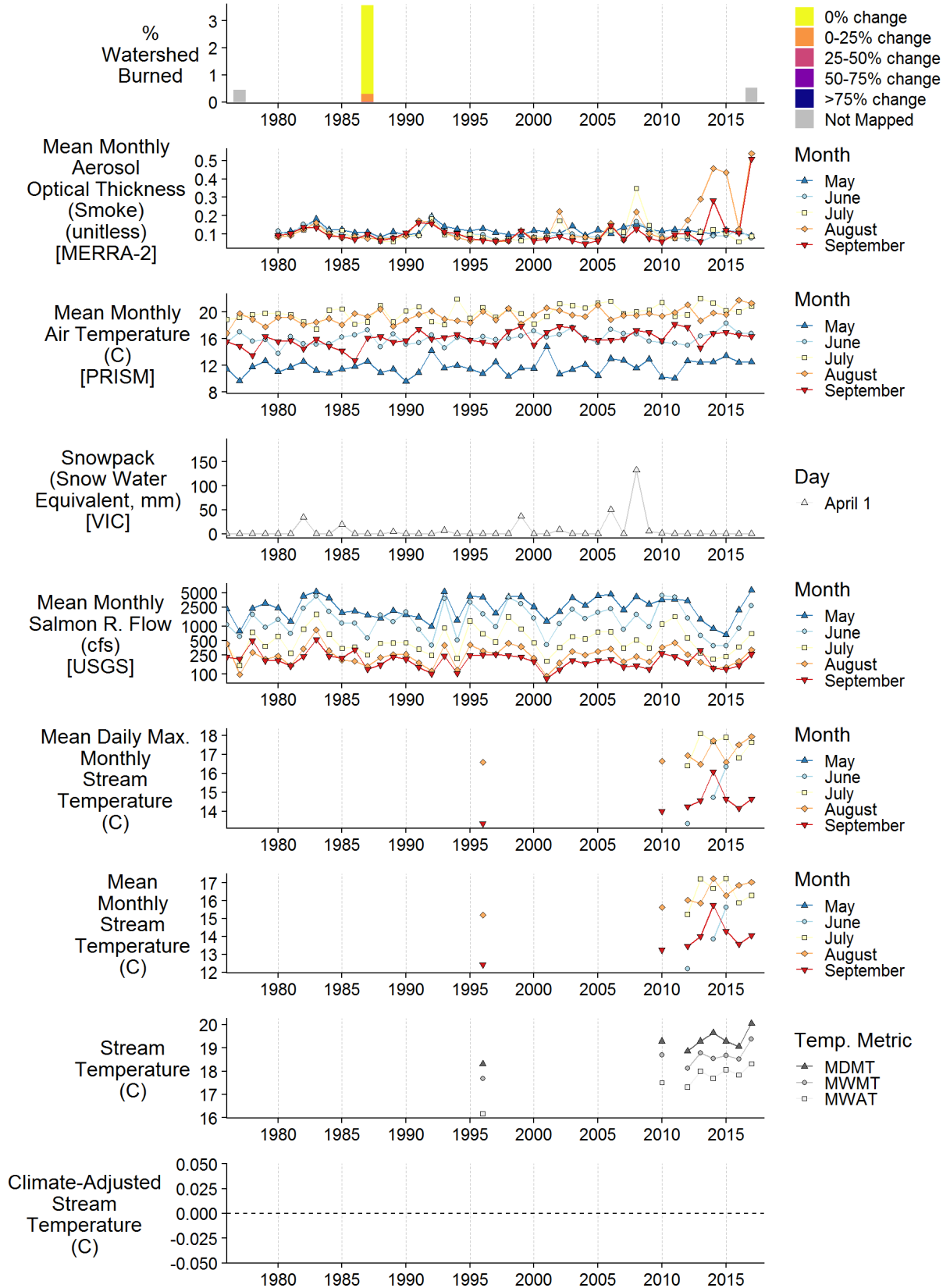
Little NF Salmon us Garden Gulch- 80.4km2-130937



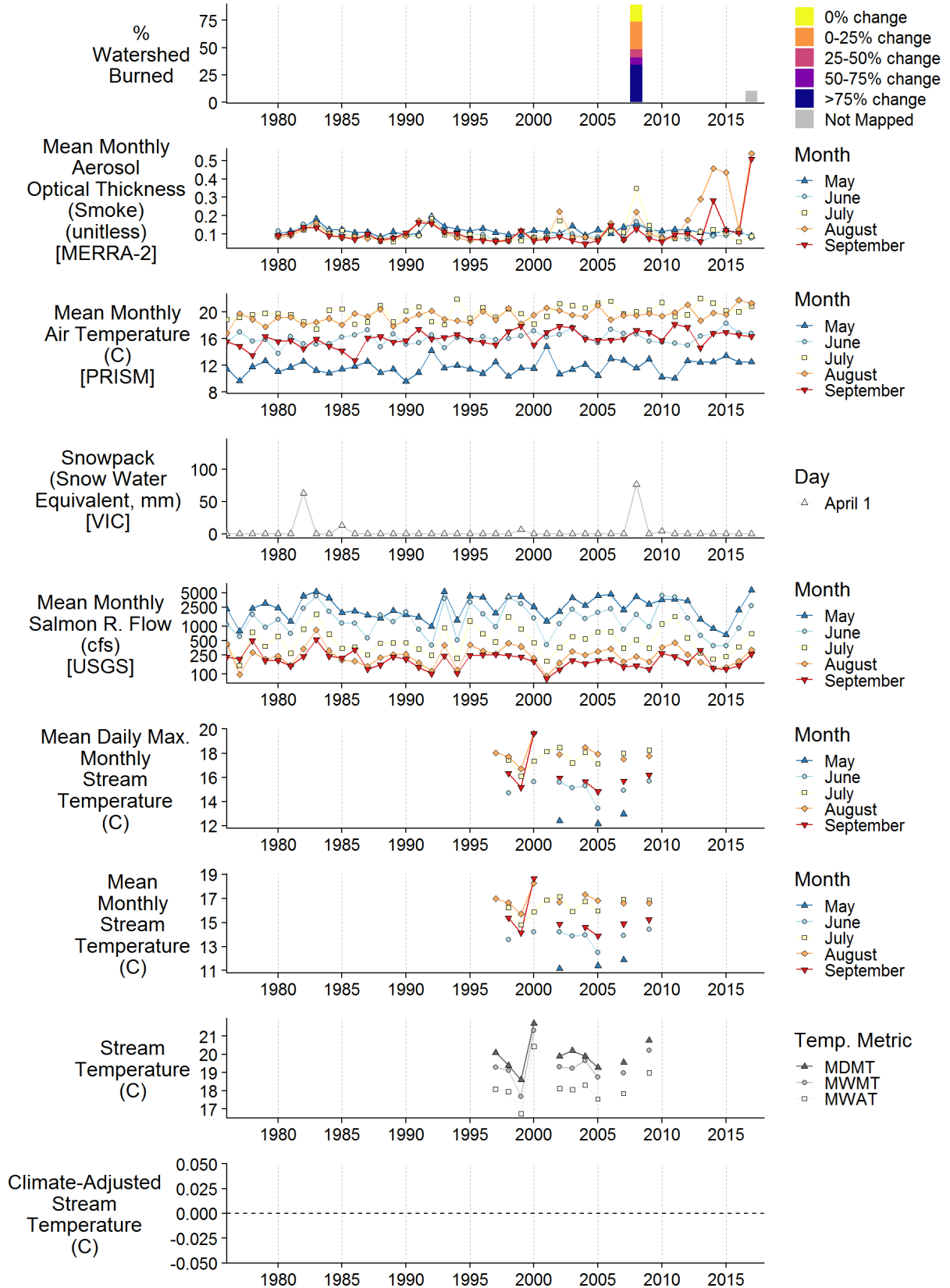
Little NF Salmon- 84.3km2-130694



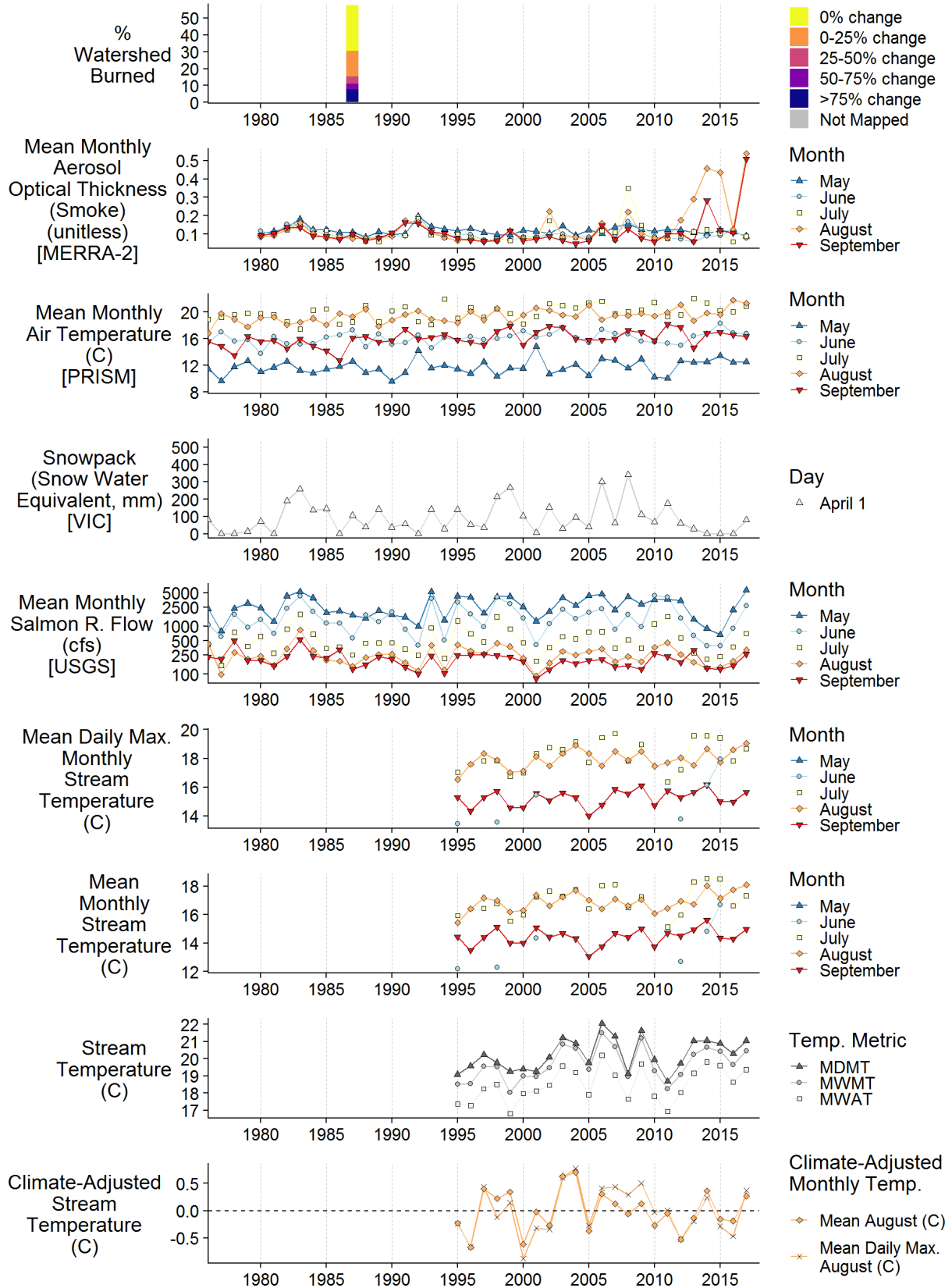
Matthews Cr nr mouth- 18.7km2-129018



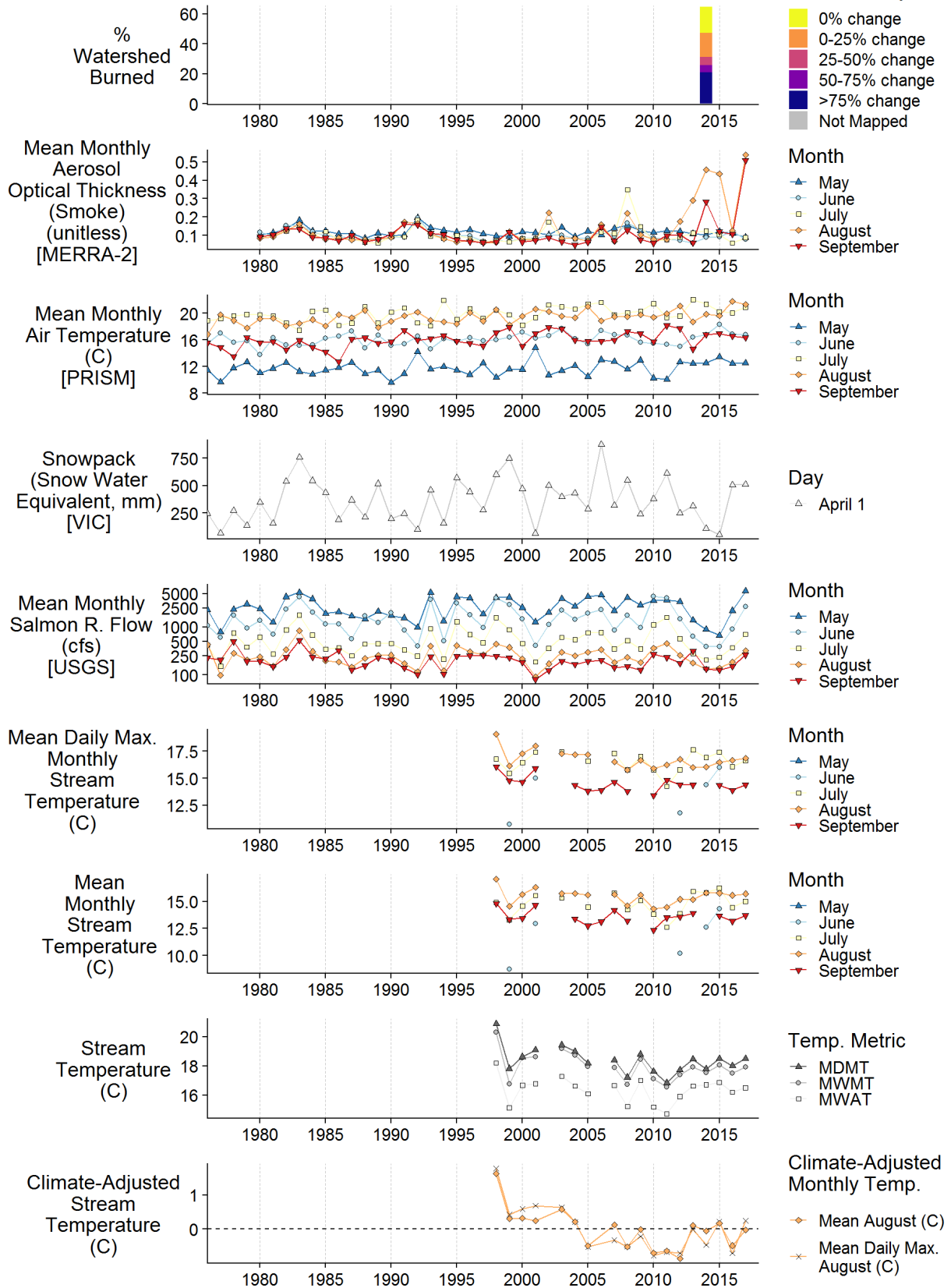
Merrill Cr nr mouth- 12.5km2-132565



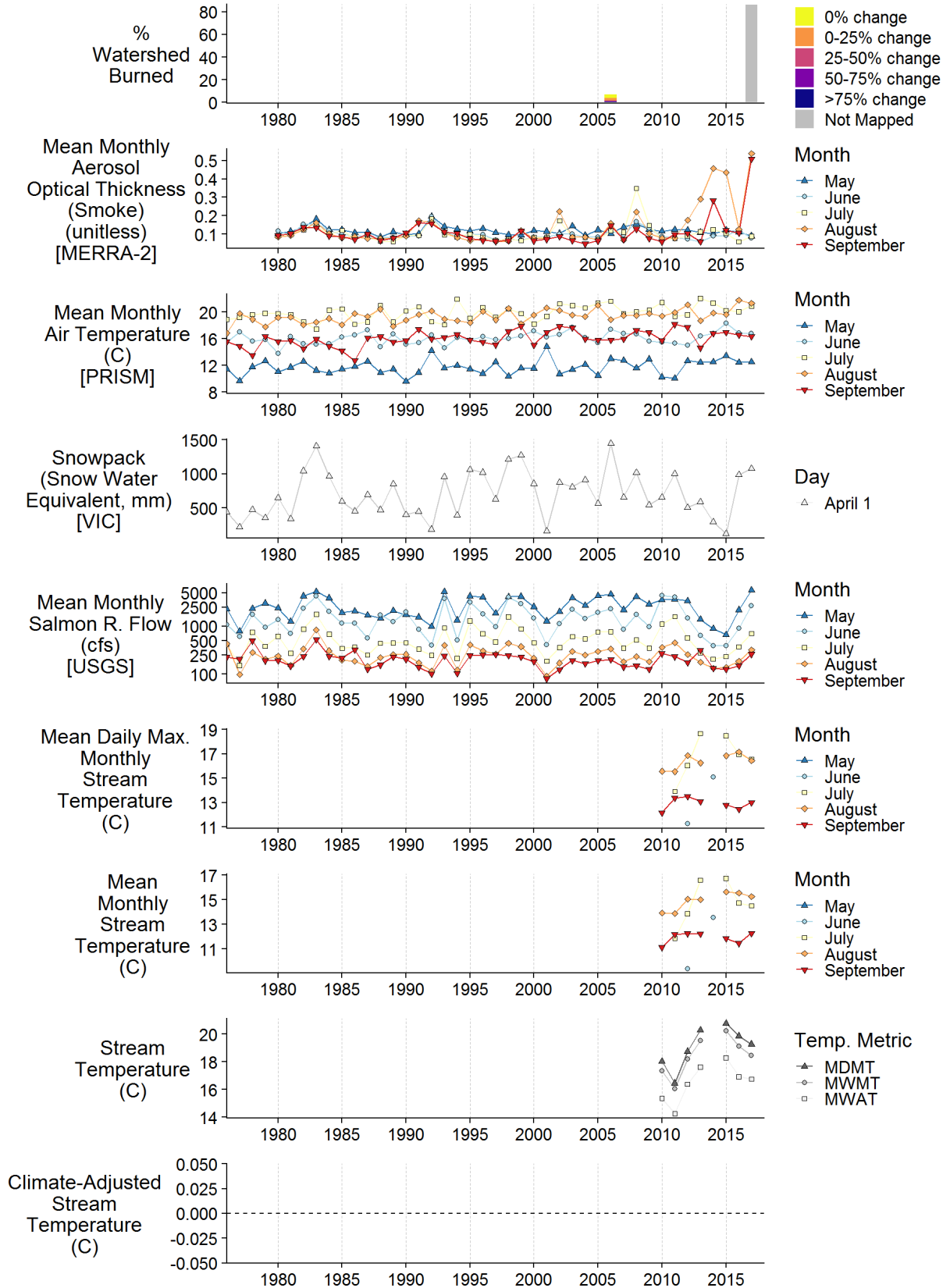
Methodist Cr nr mouth- 32.9km2-129186



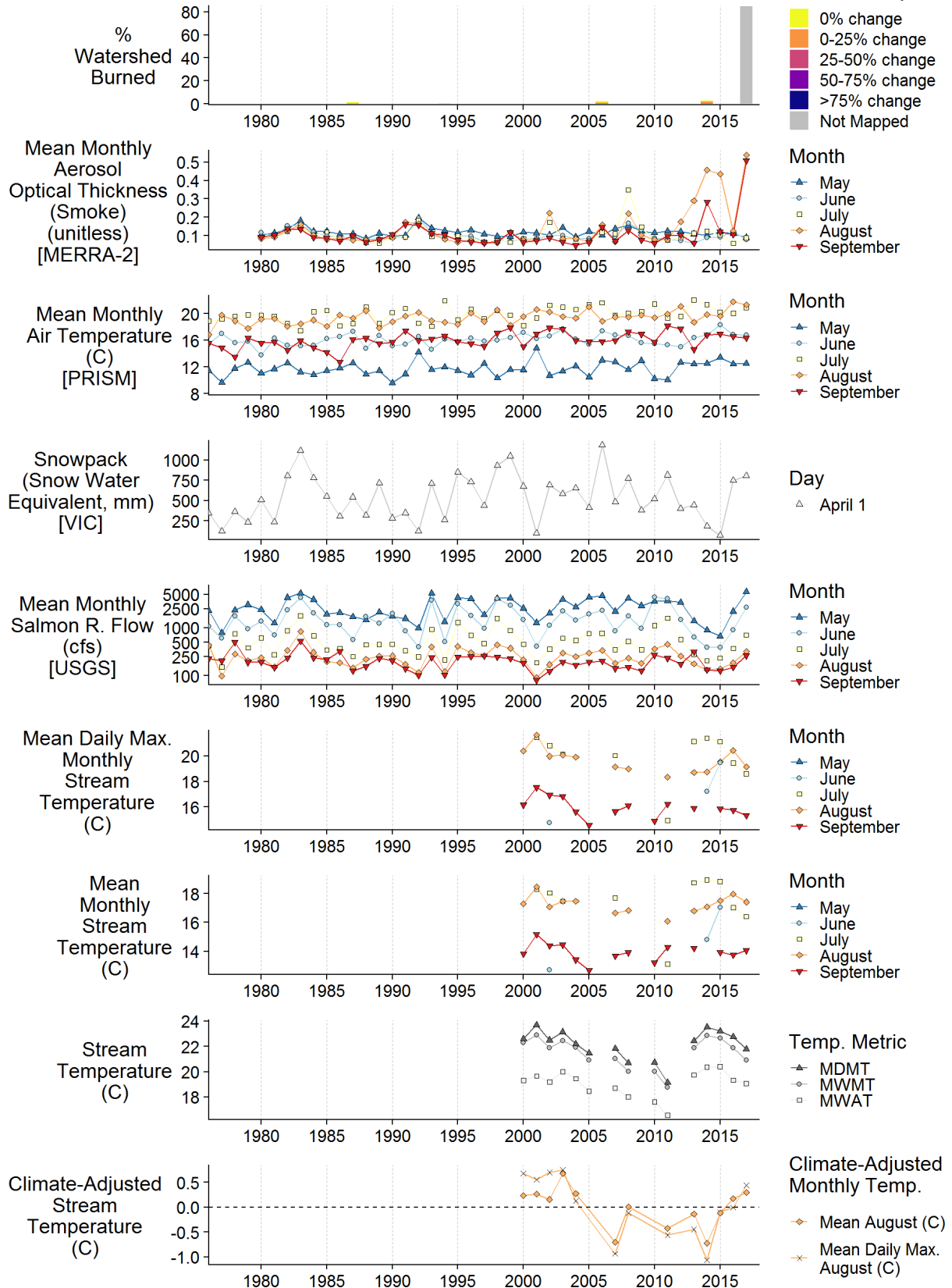
N Russian Cr us S Russian- 47.0km2-130777



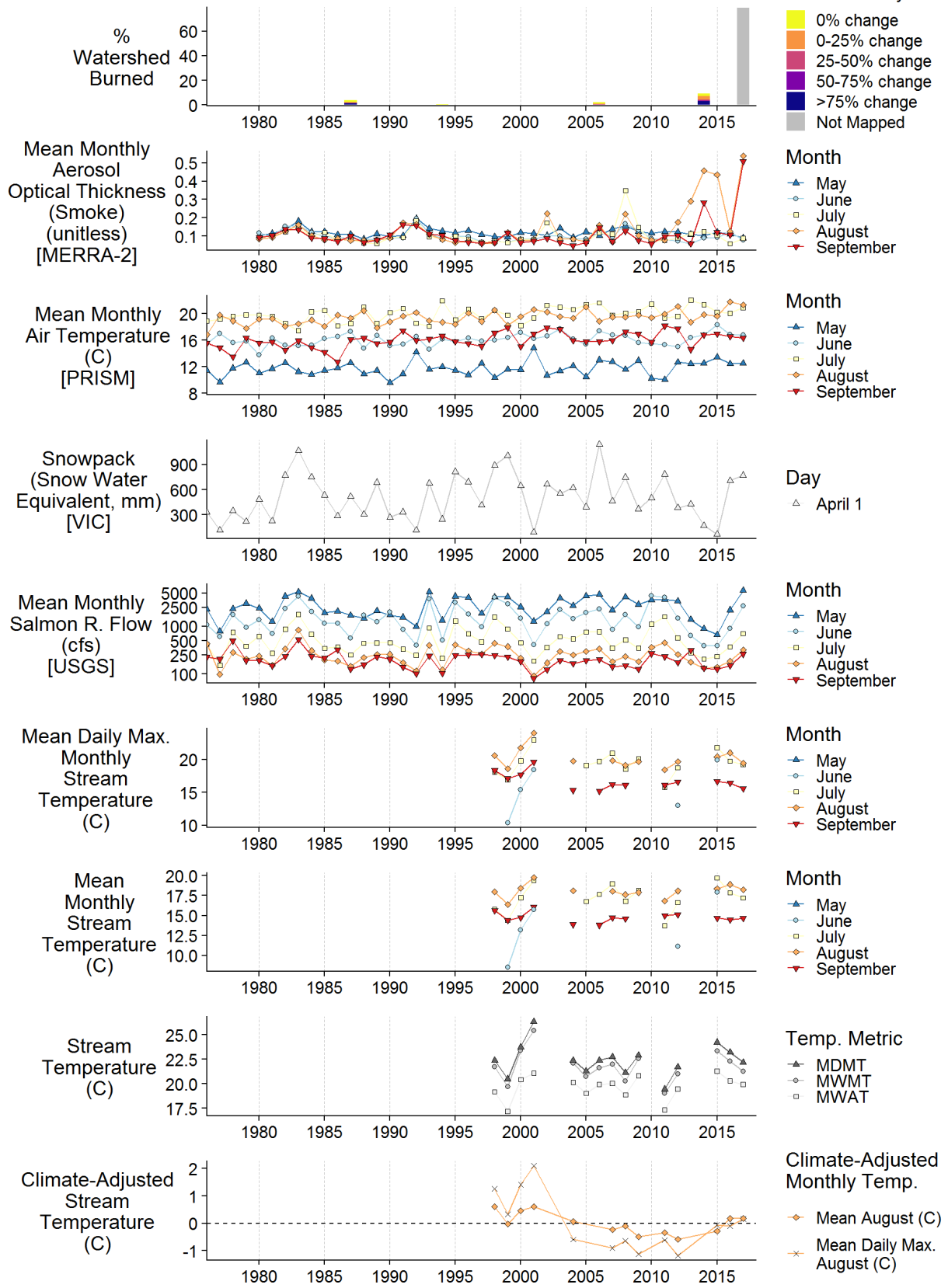
NF Salmon us Right Hand Fk- 47.5km2-132172



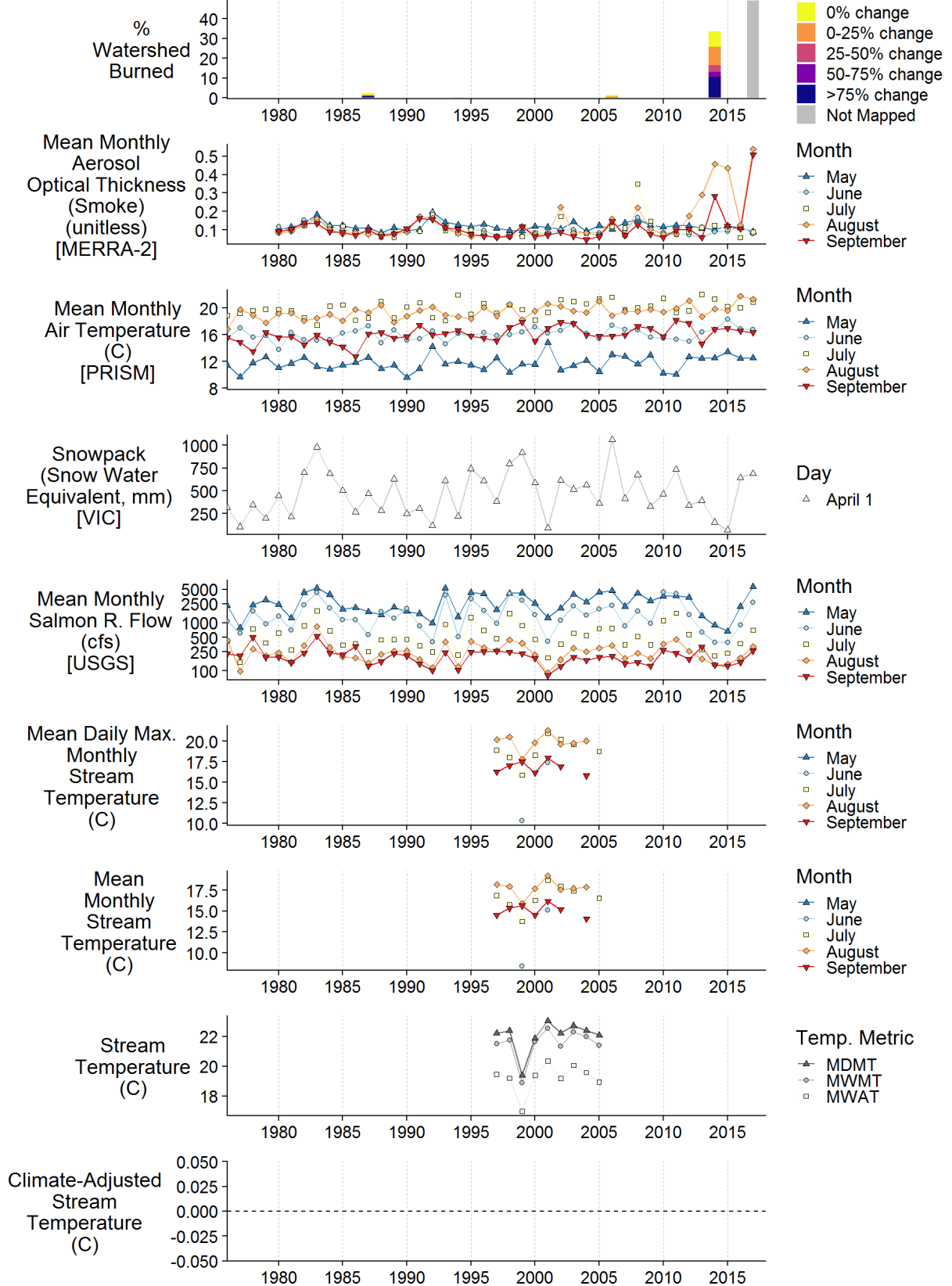
NF Salmon at Mule Bridge- 151.4km2-131191



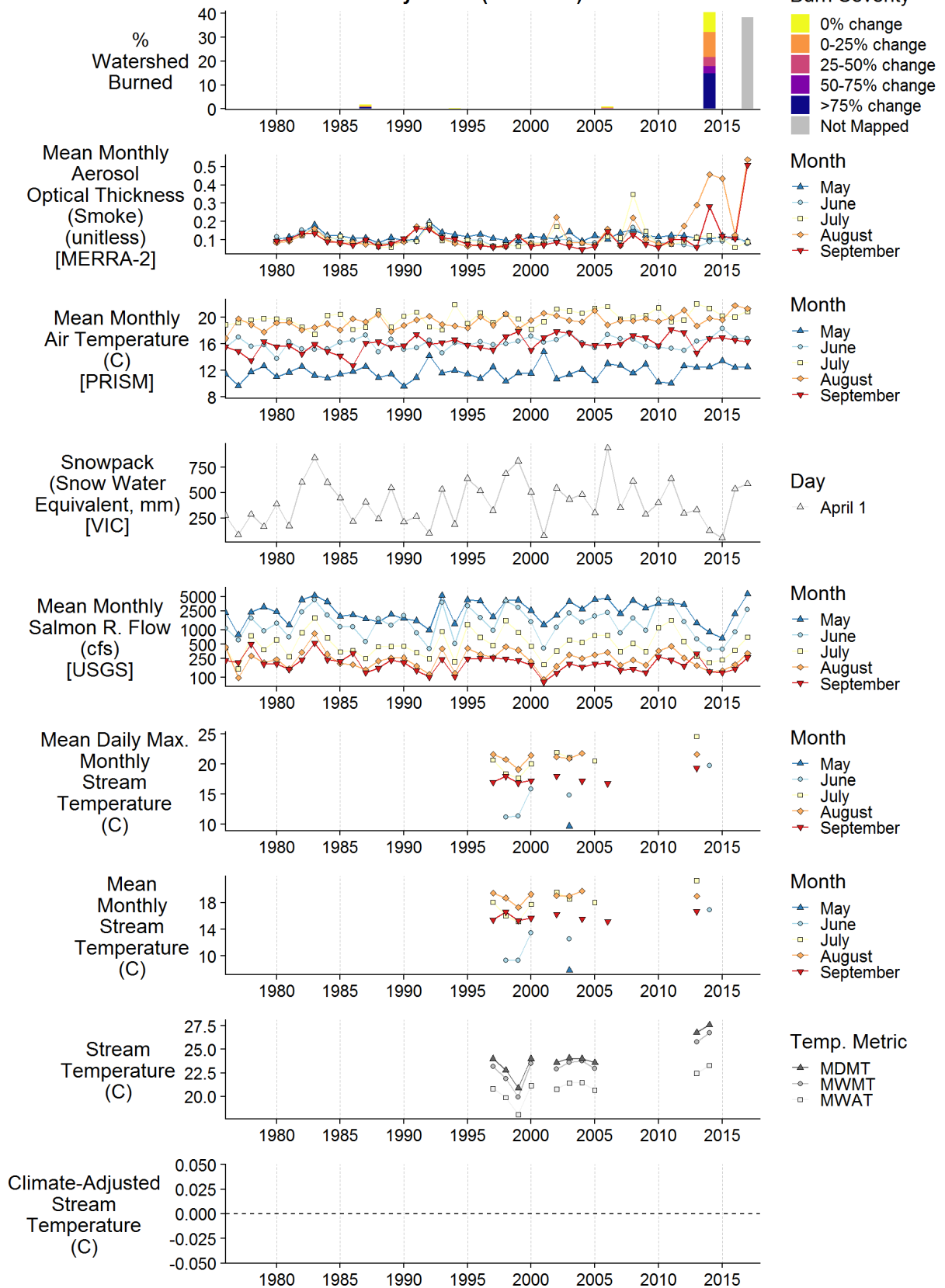
NF Salmon us Russians- 162.5km2-130783



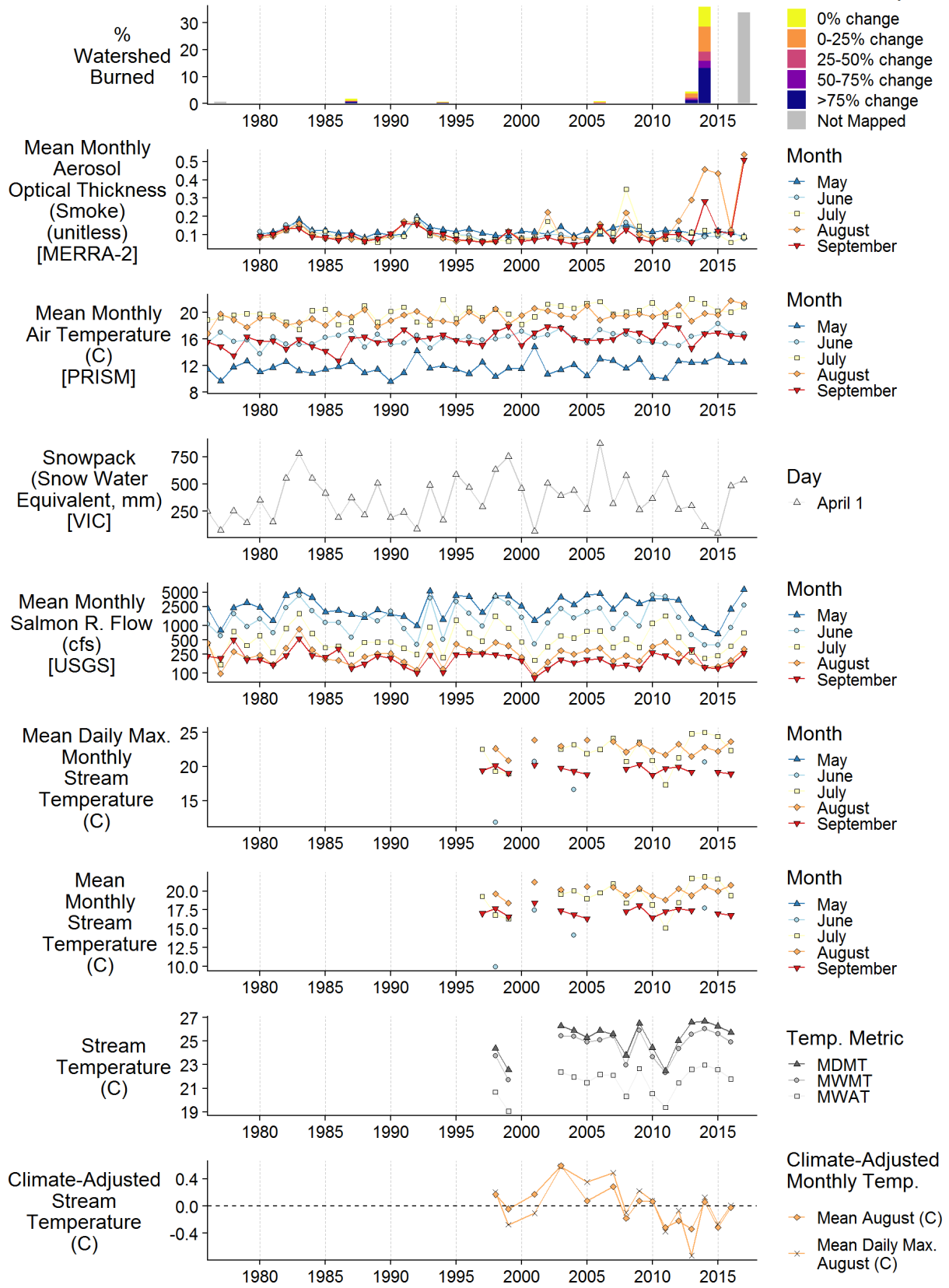
NF Salmon ds Russians- 260.4km2-130540



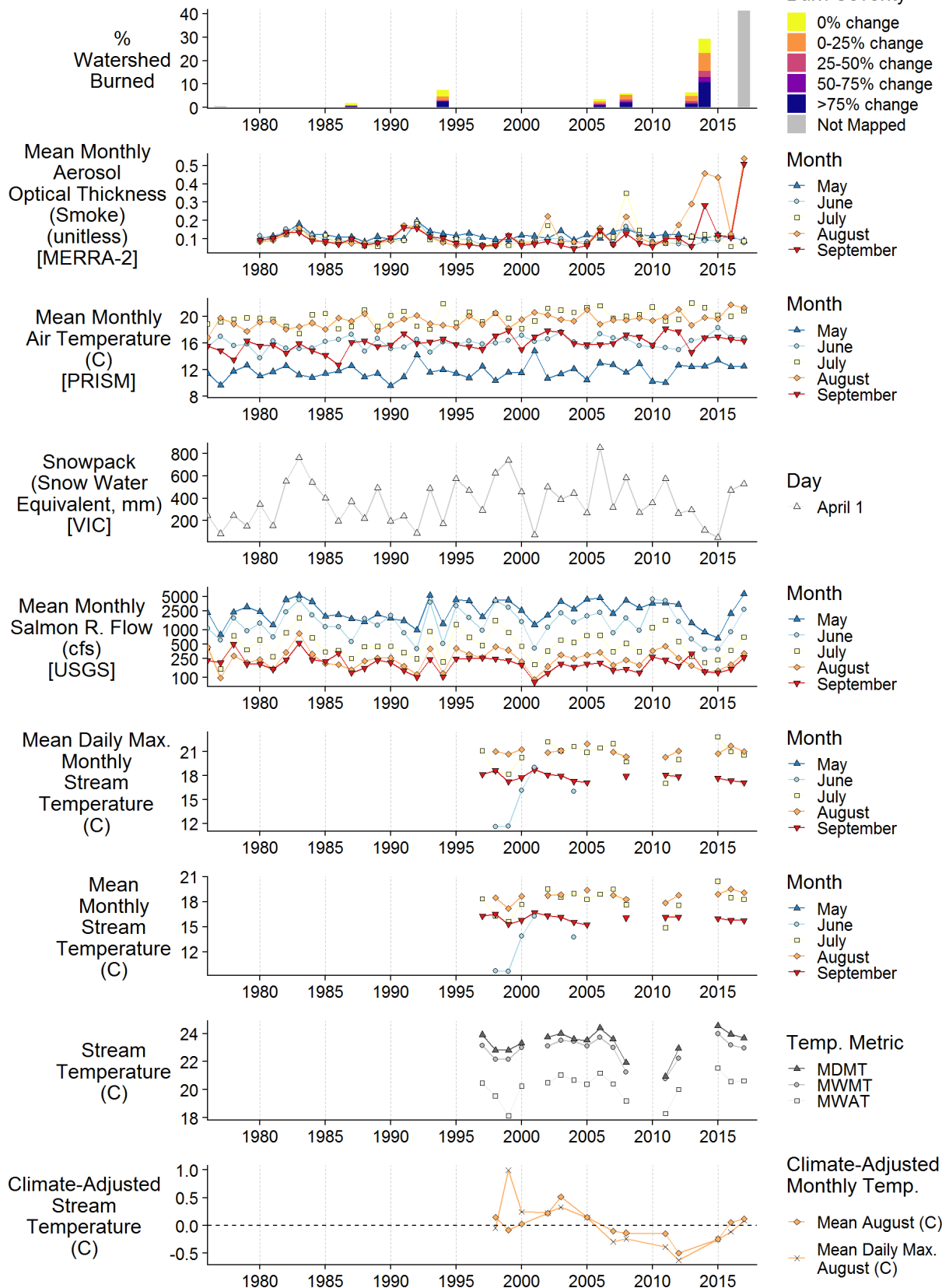
NF Salmon ds Eddy Gulch (Holzem's)- 334.9km2-130267



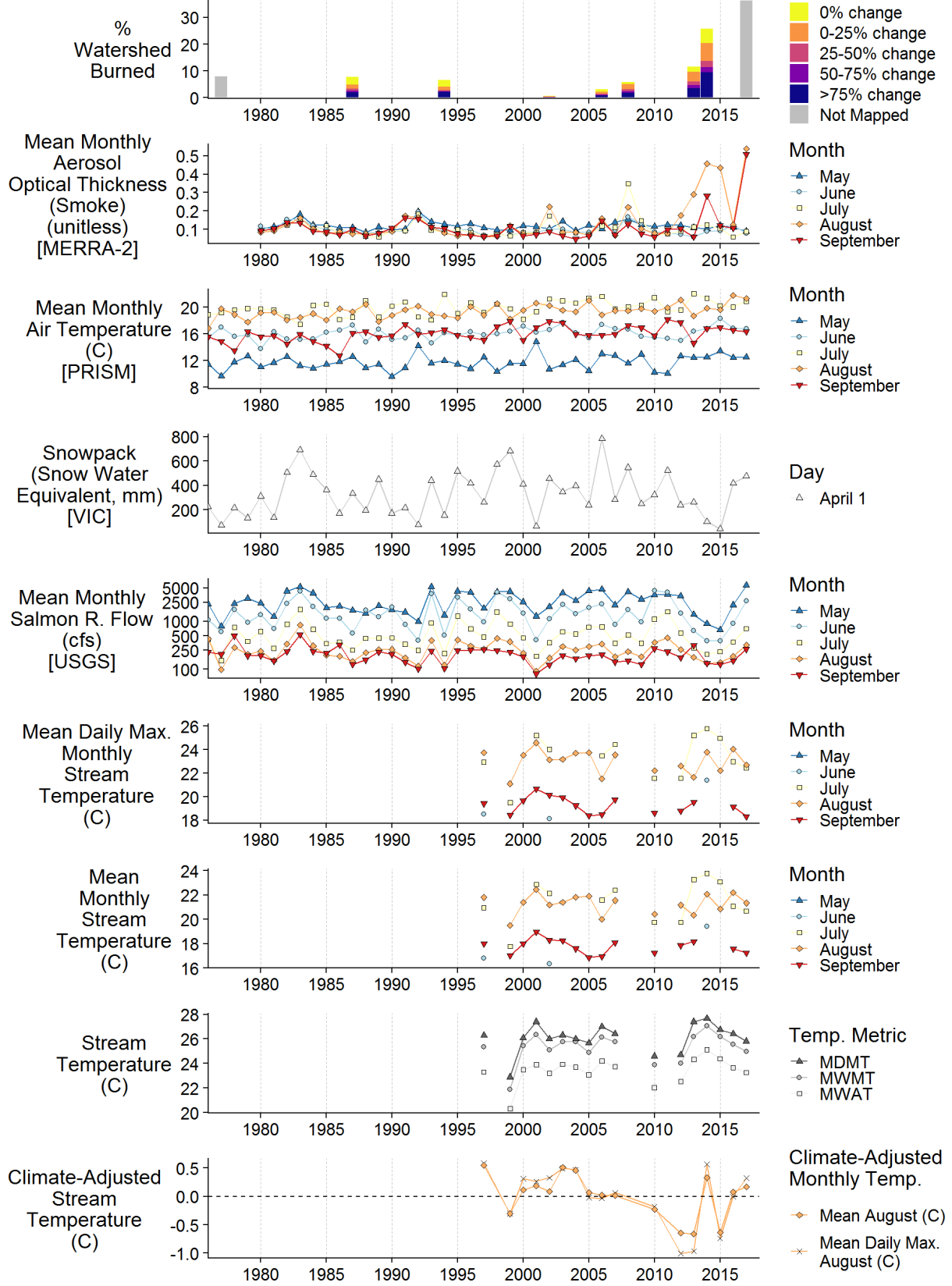
NF Salmon us Little NF- 378.7km2-130561



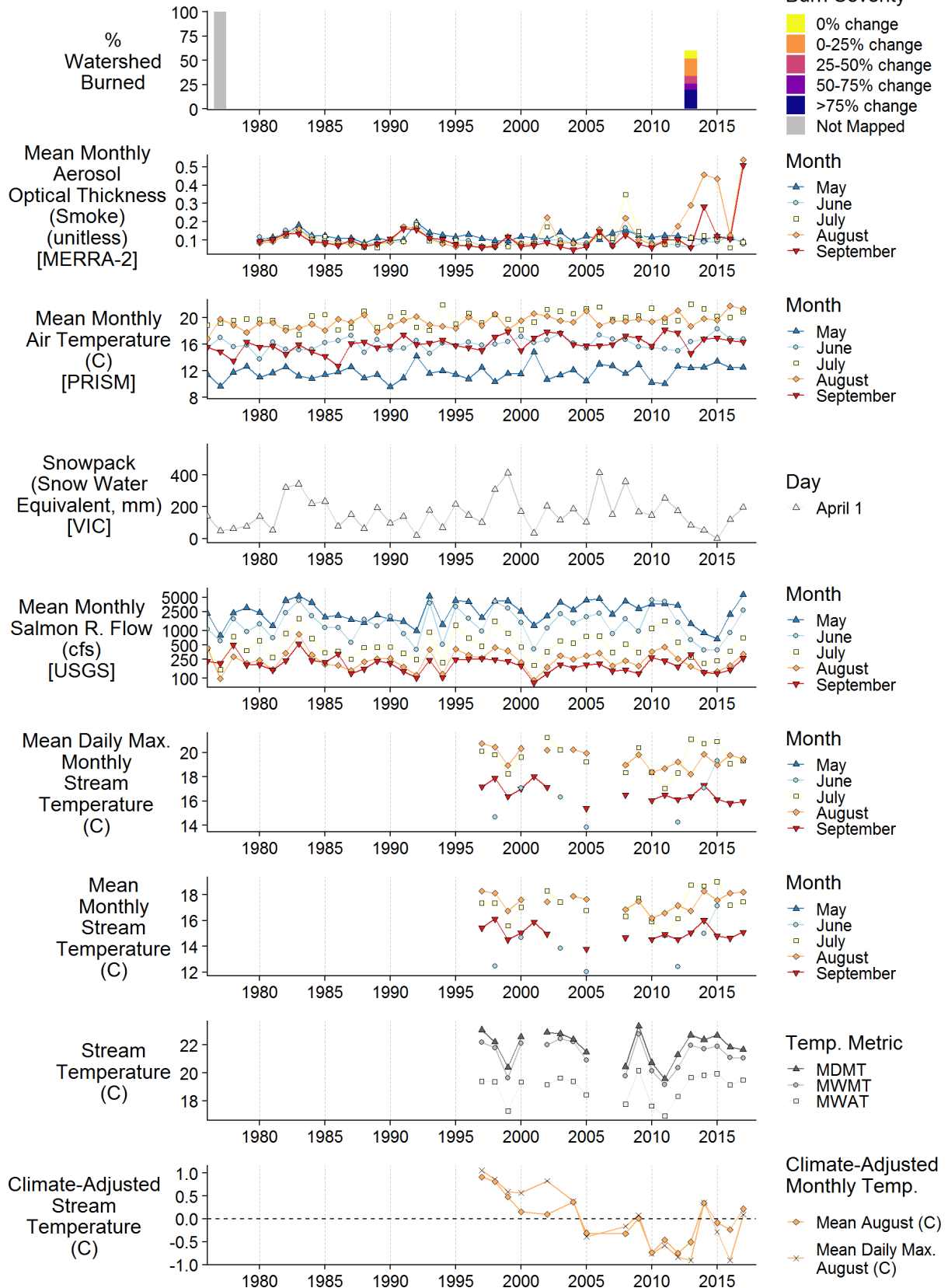
NF Salmon ds Little NF- 464.8km2-130639



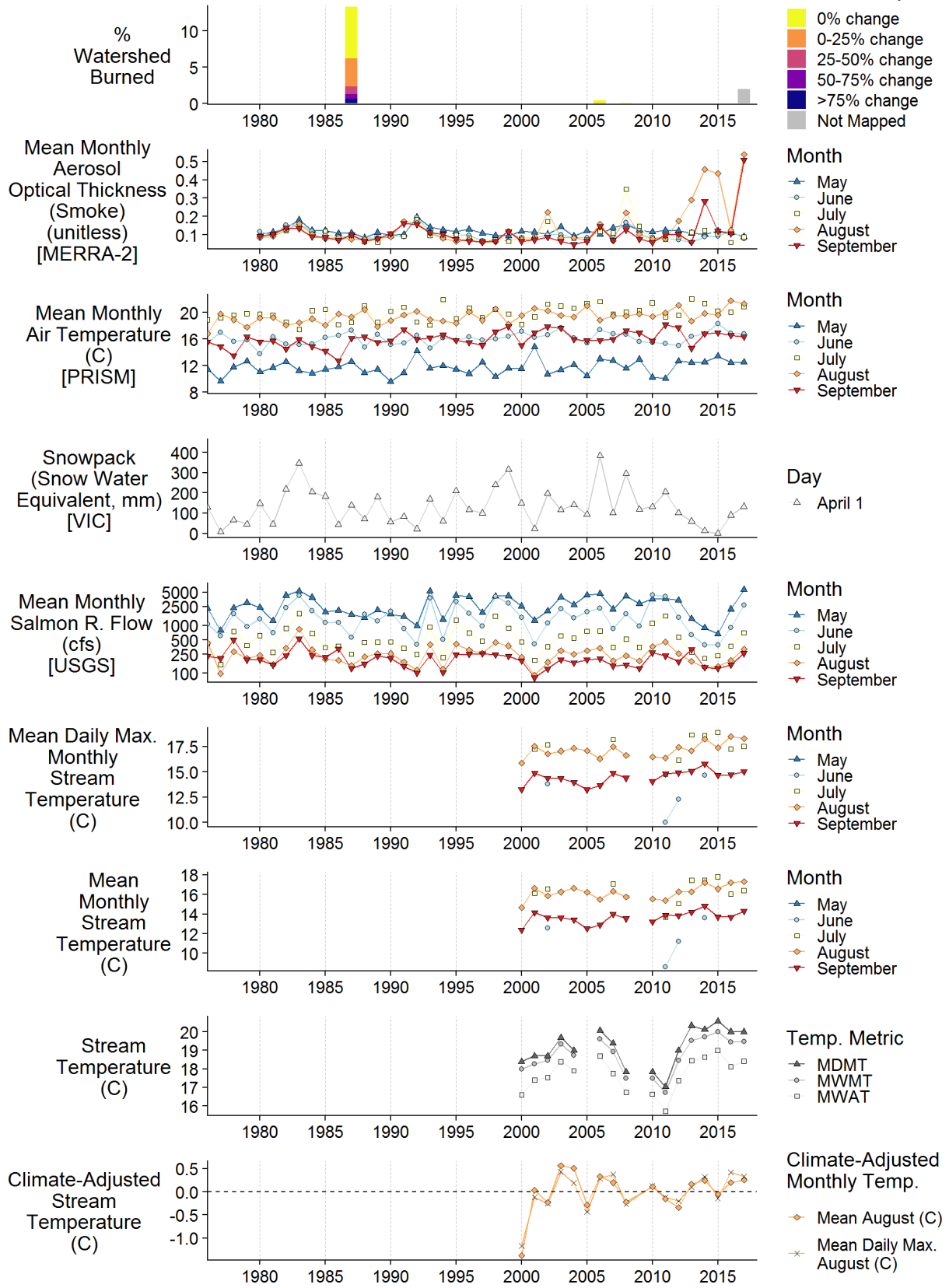
NF Salmon R us Forks- 528.1km2-130116



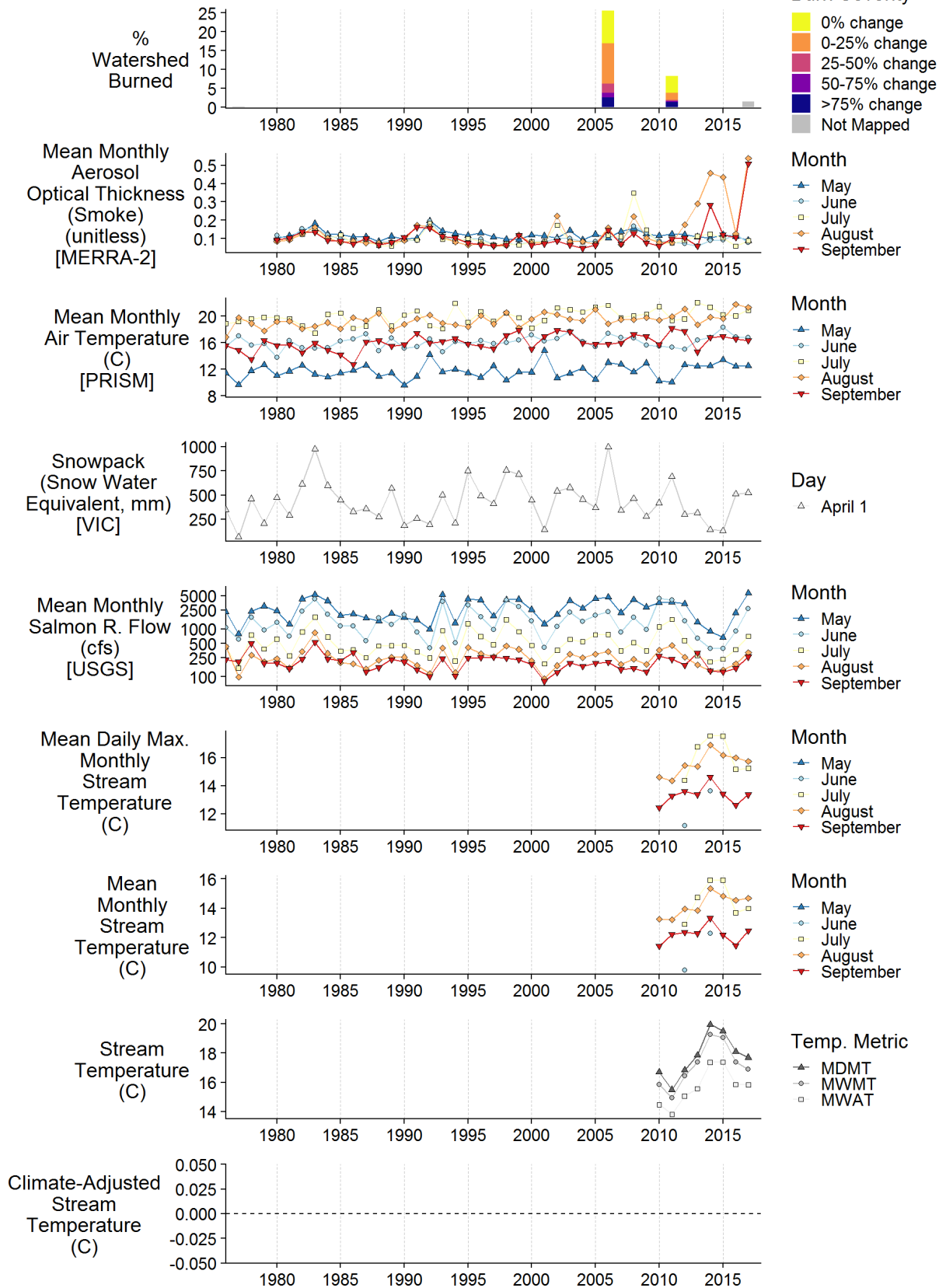
Nordheimer Cr nr mouth- 80.3km2-130389



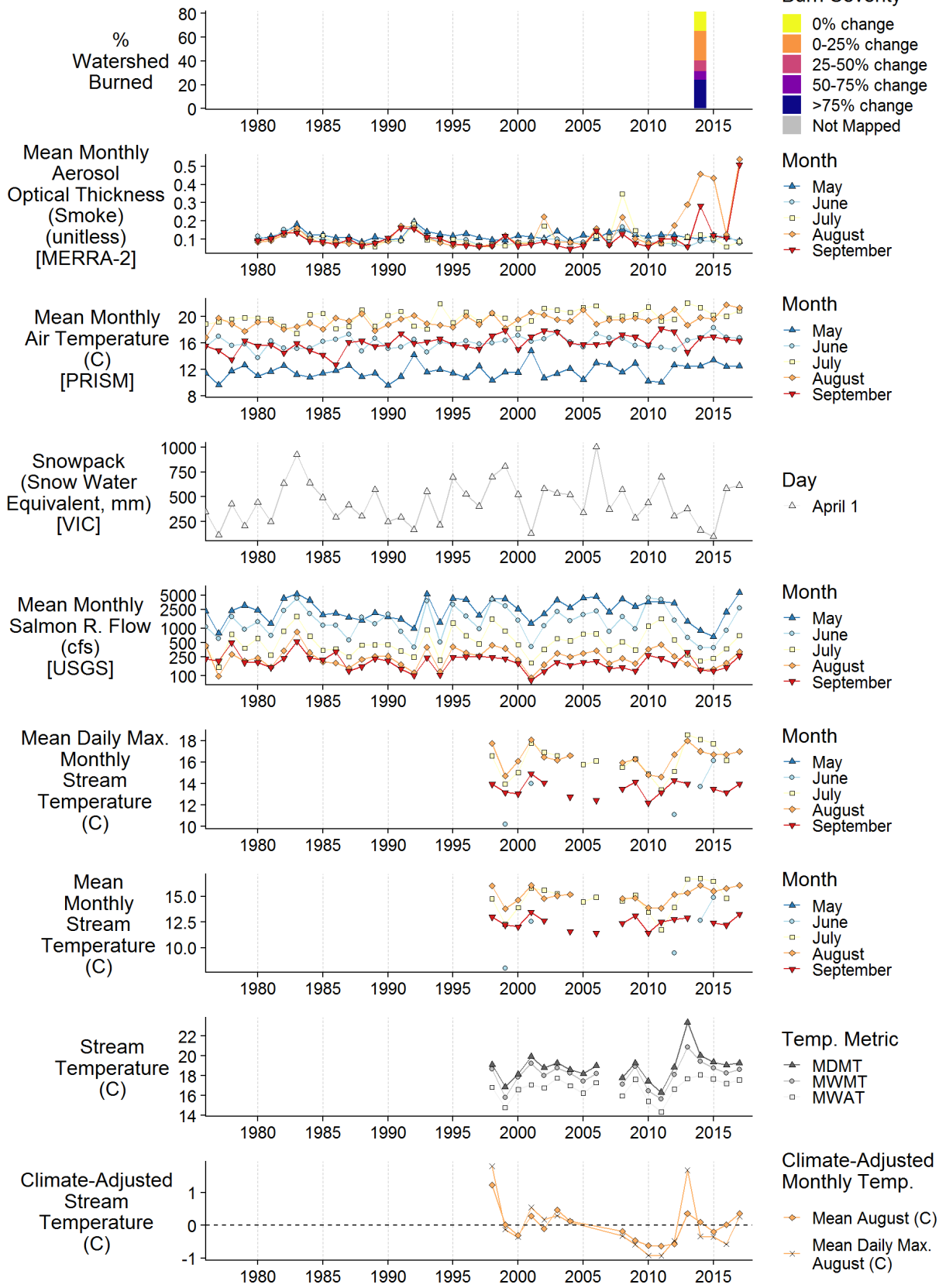
Plummer Cr nr mouth- 37.1km2-128455



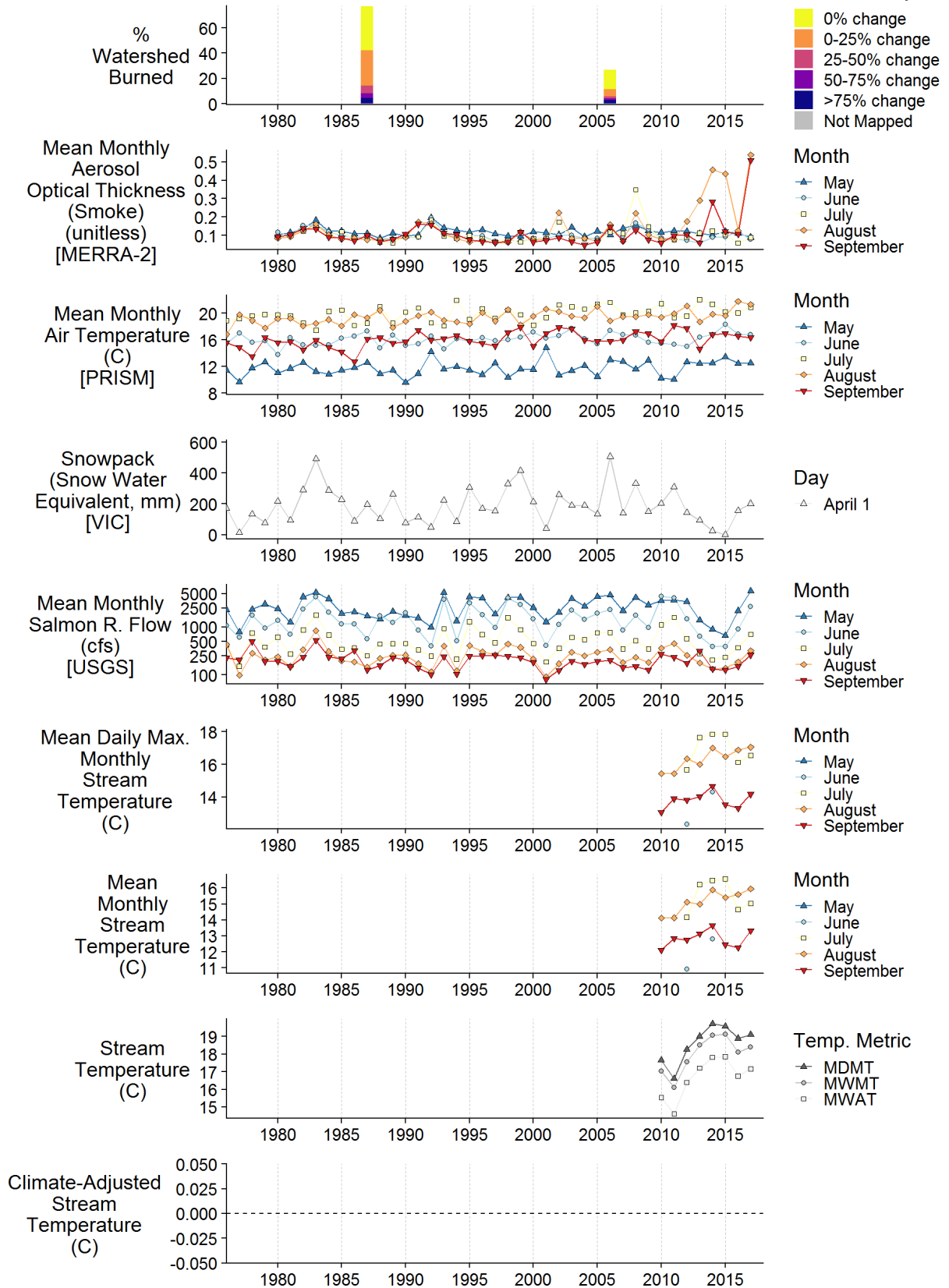
Rush Cr nr mouth- 29.1km2-127796



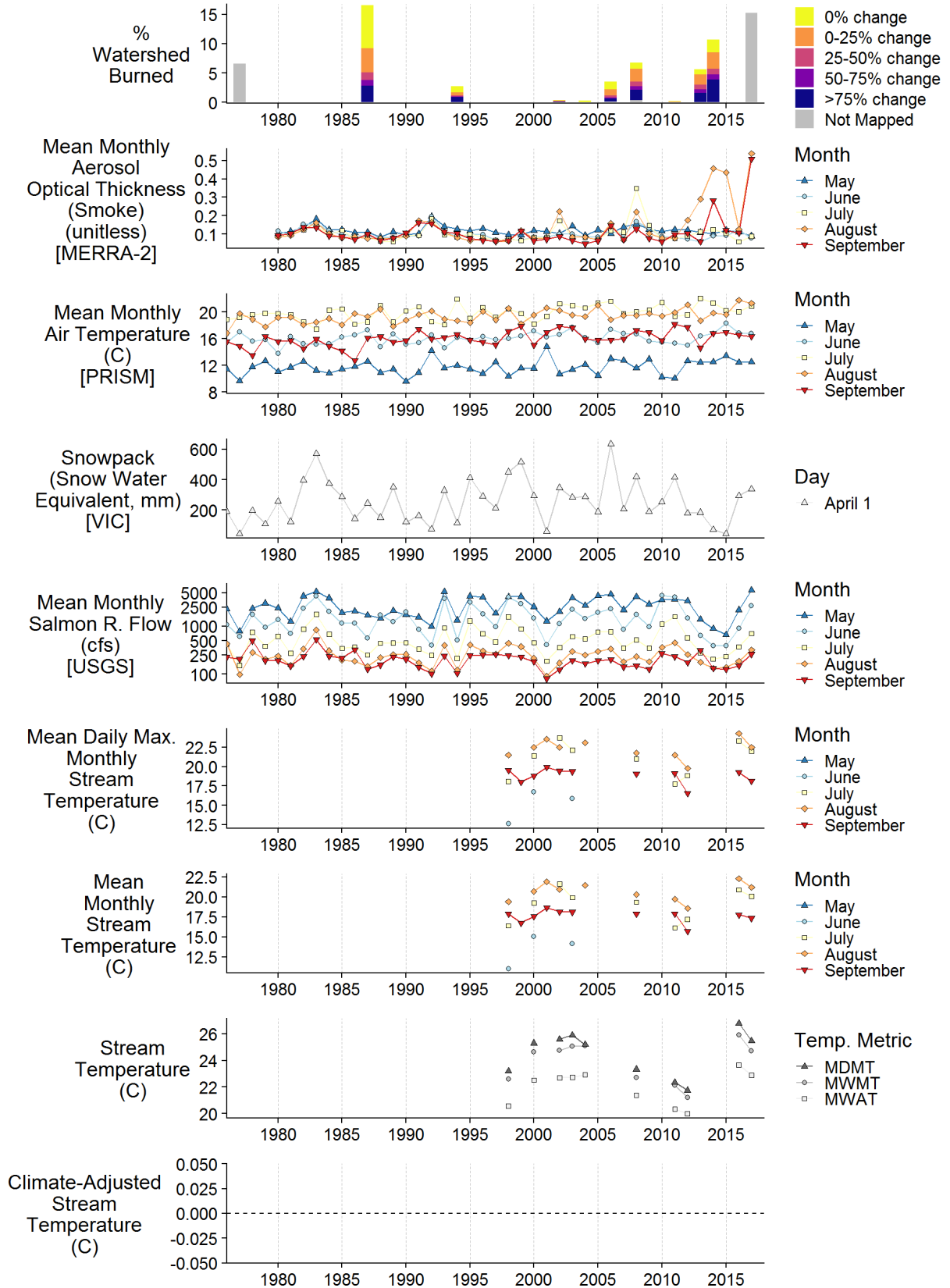
S Russian Cr nr mouth- 47.9km2-130442



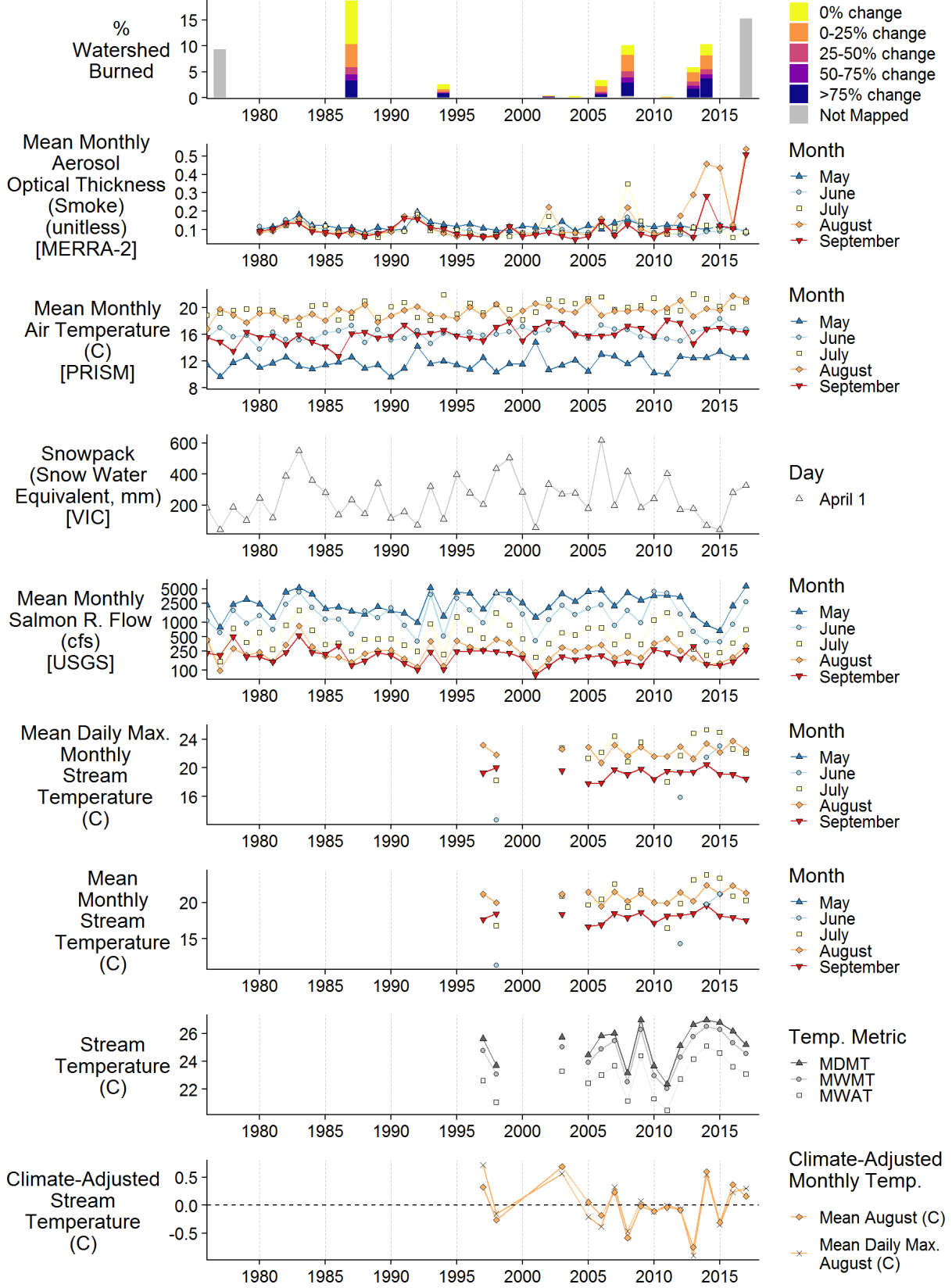
Sainte Claire Cr nr mouth- 27.5km2-128082



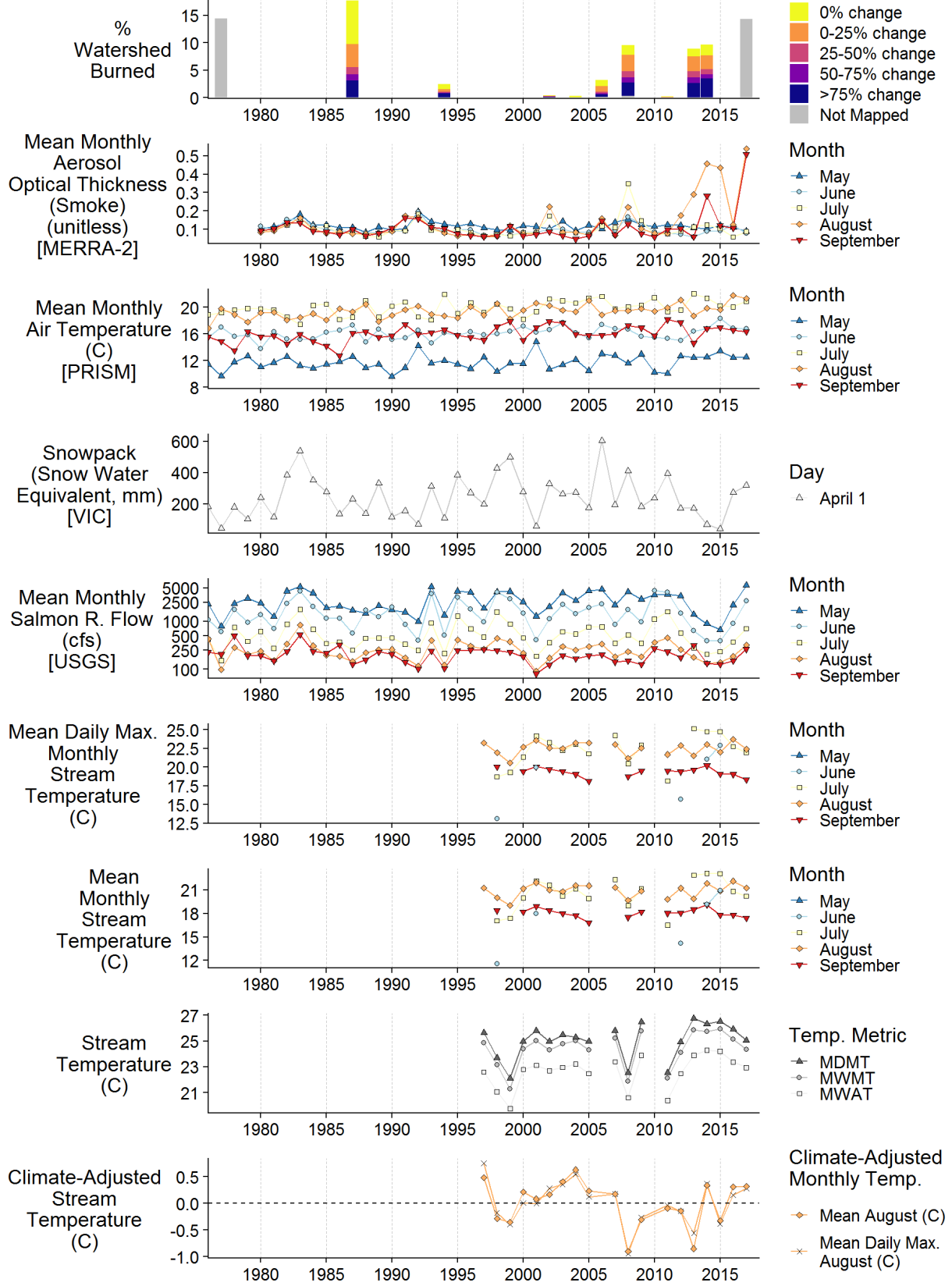
Salmon R ds Forks-1288.6km2-130028



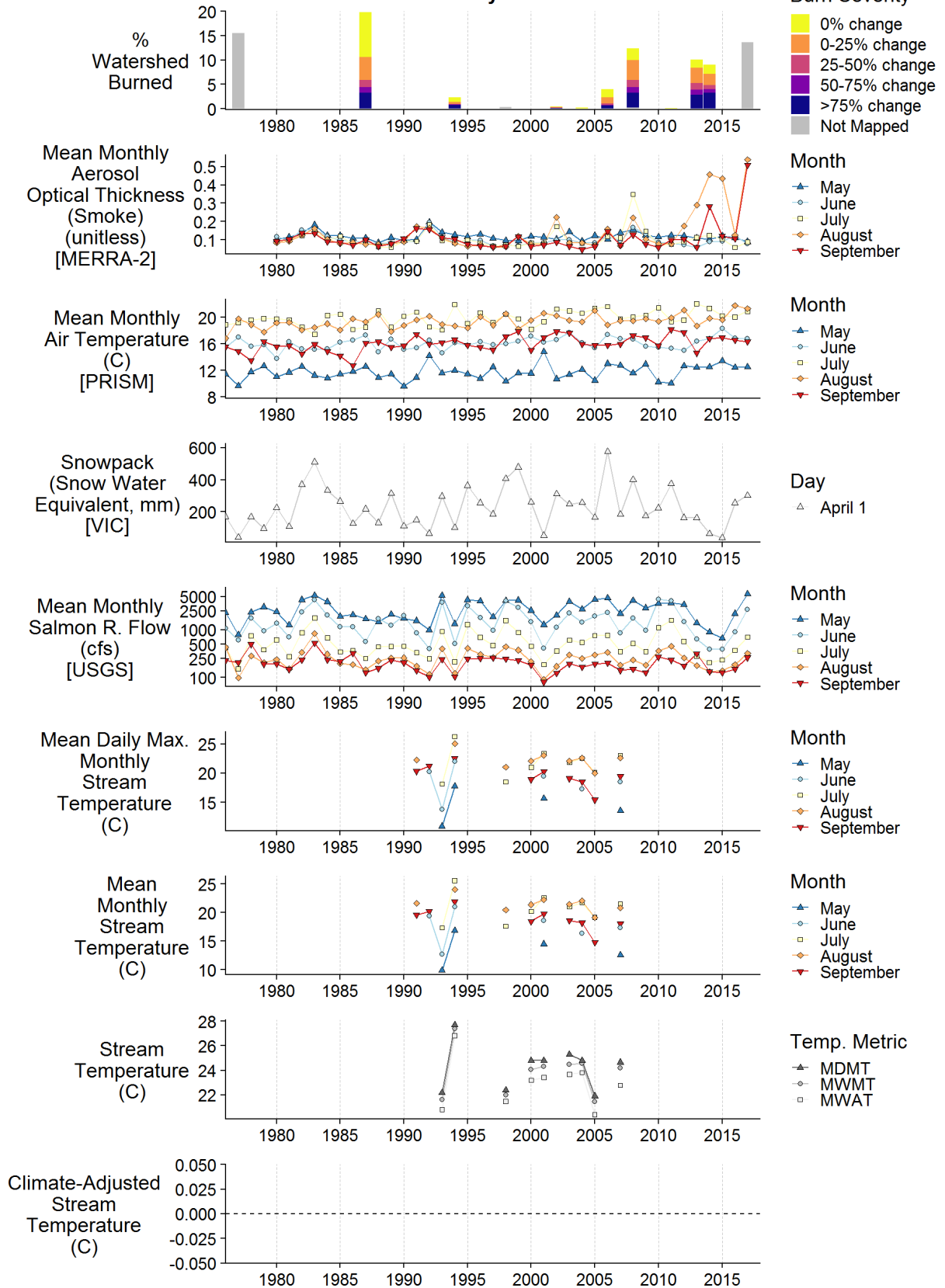
Salmon R us Nordheimer-1344.6km2-130480



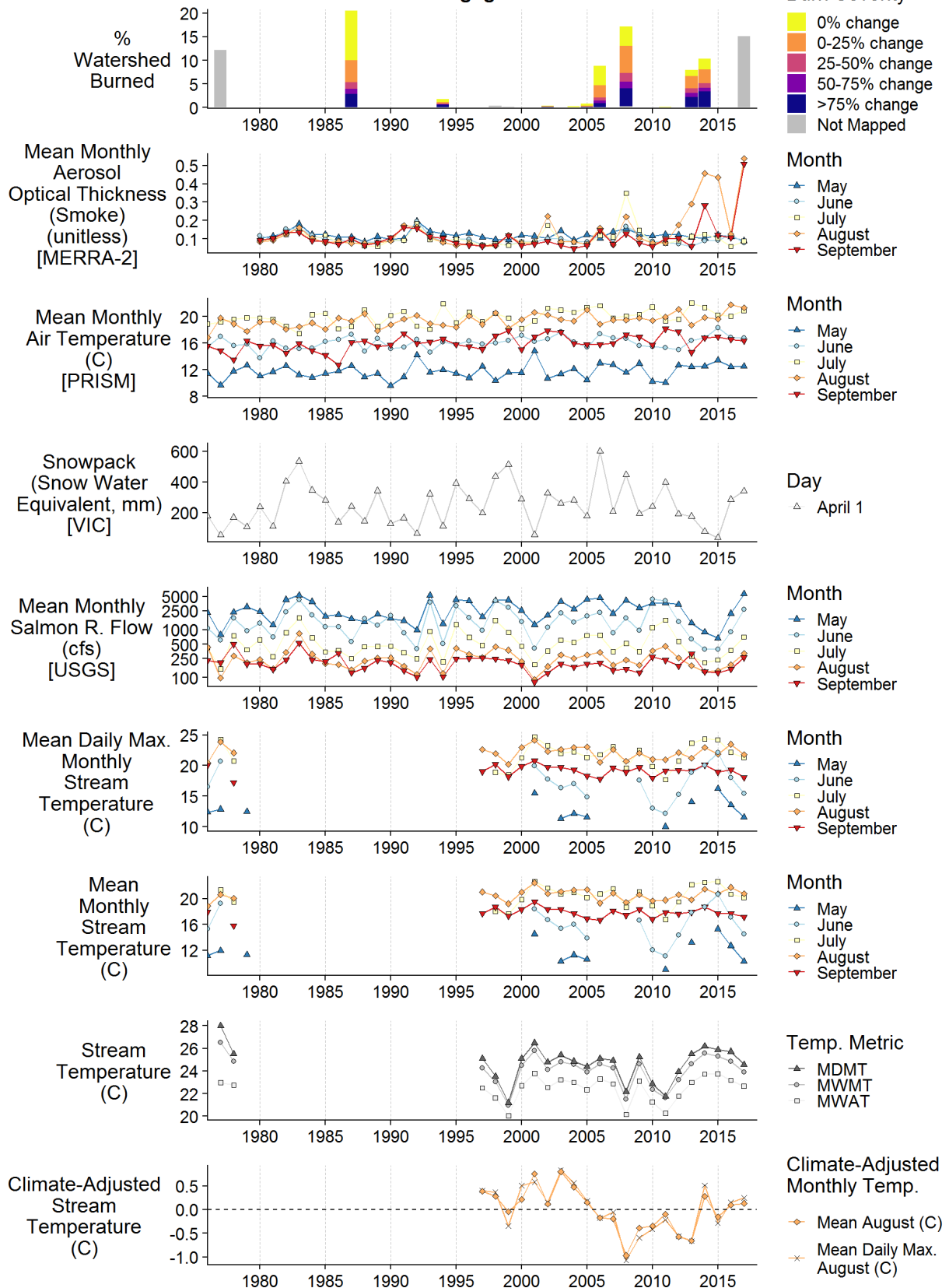
Salmon R ds Nordheimer Cr-1425.0km2-130521



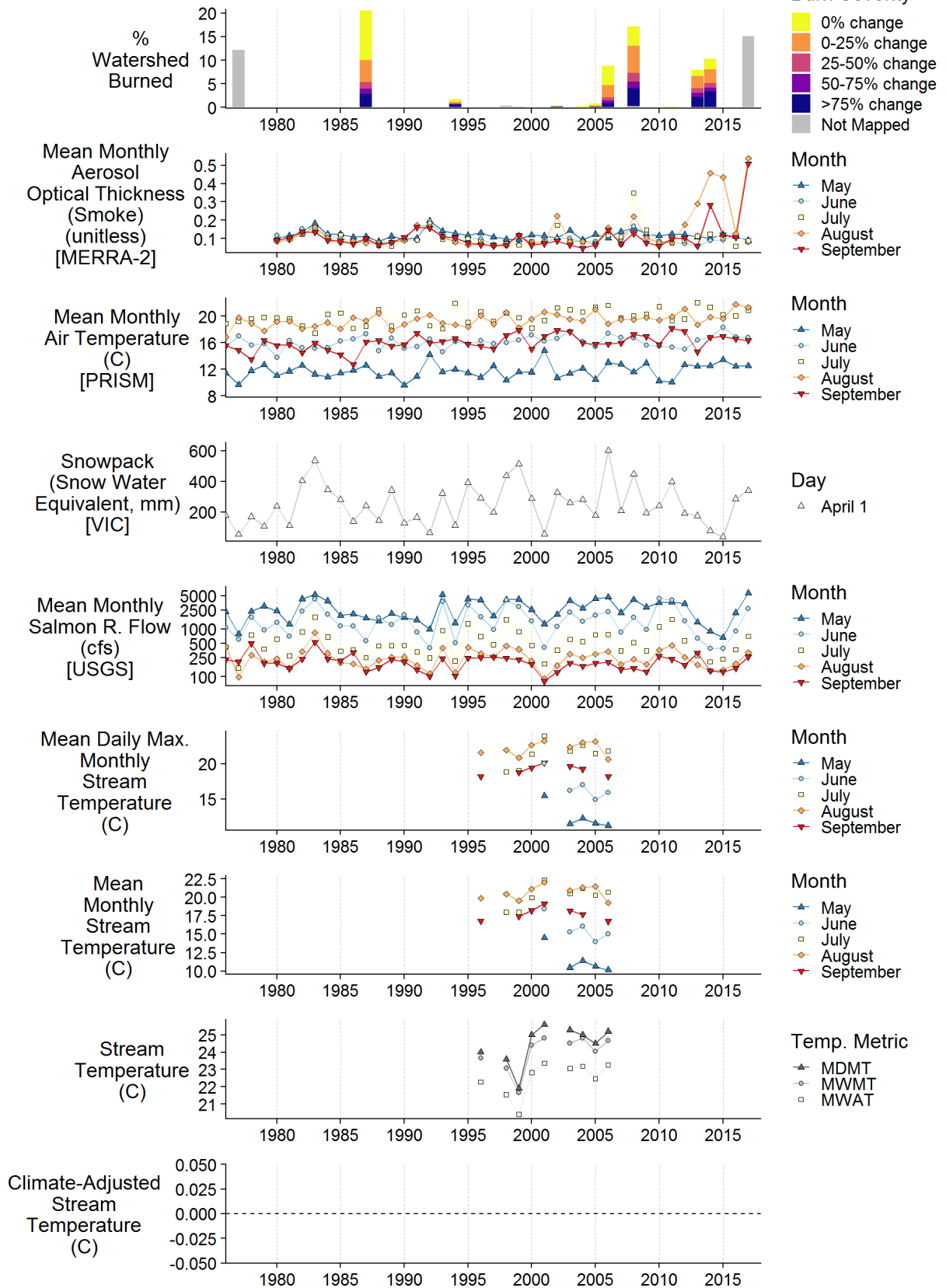
Salmon R us of Wooley Cr-1519.6km2-131557



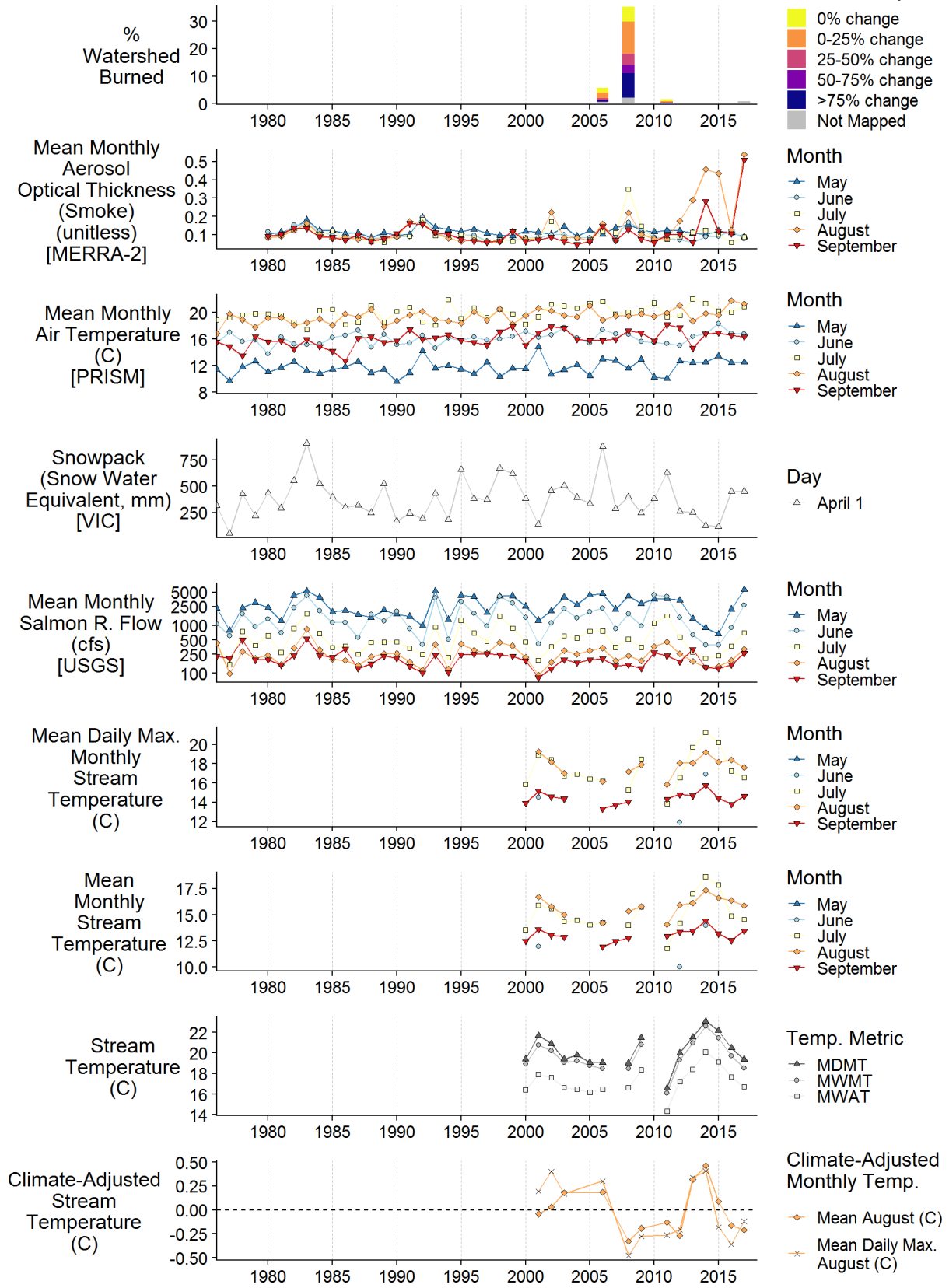
Salmon R nr USGS gage-1946.0km2-131830



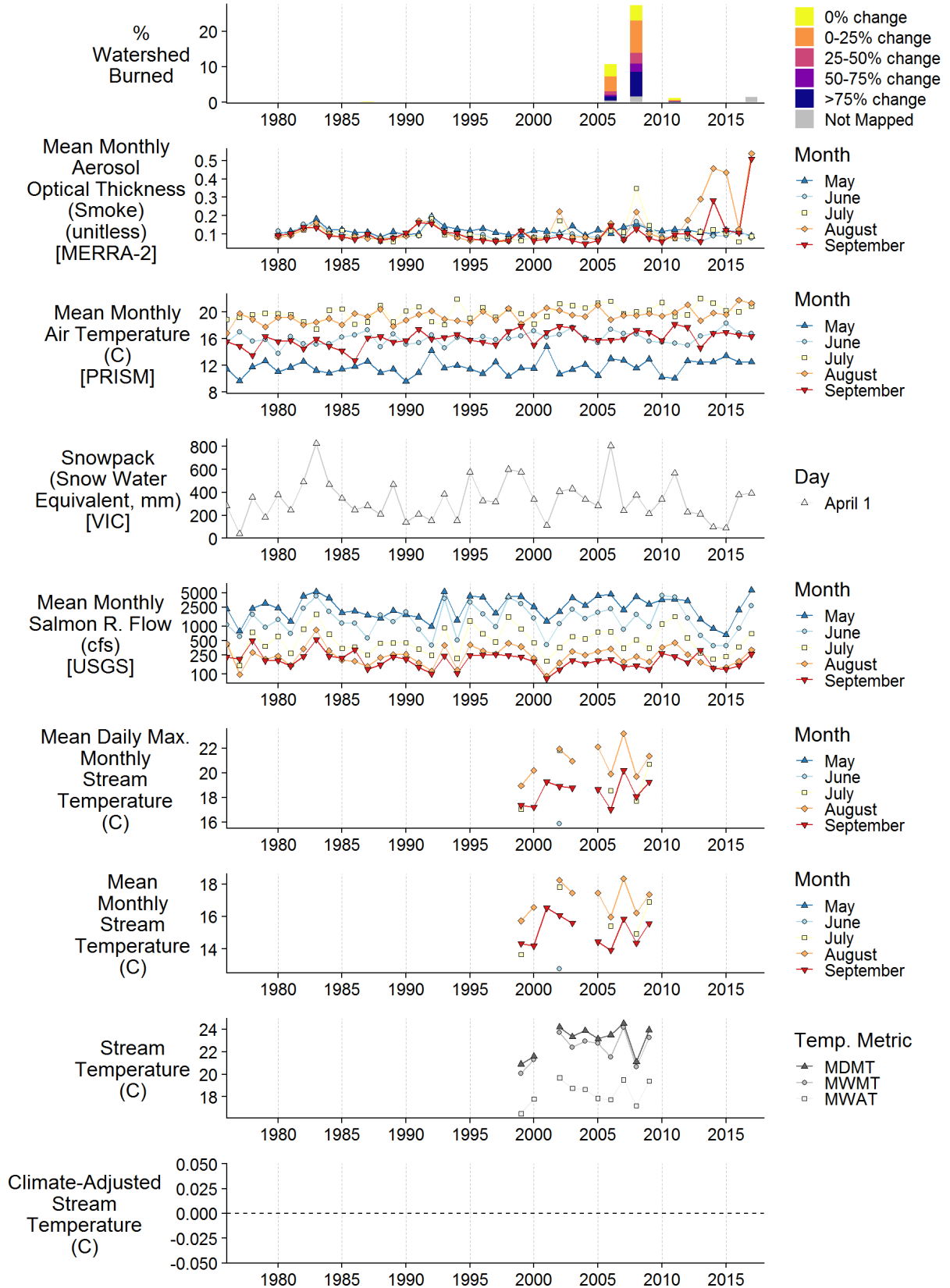
Salmon R nr mouth-1946.0km2-131831



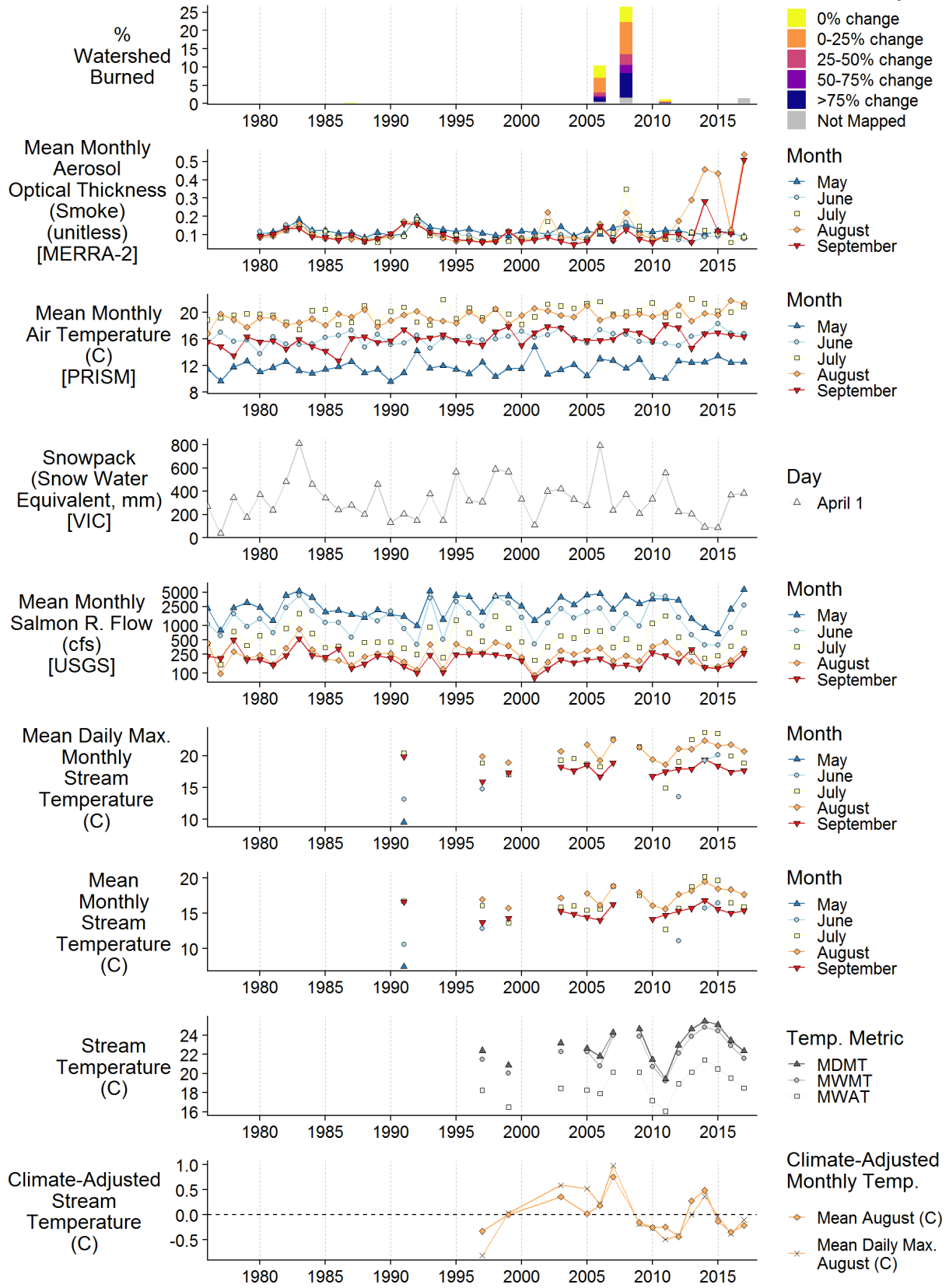
SF Salmon ds Blindhorse Cr- 152.5km2-127606



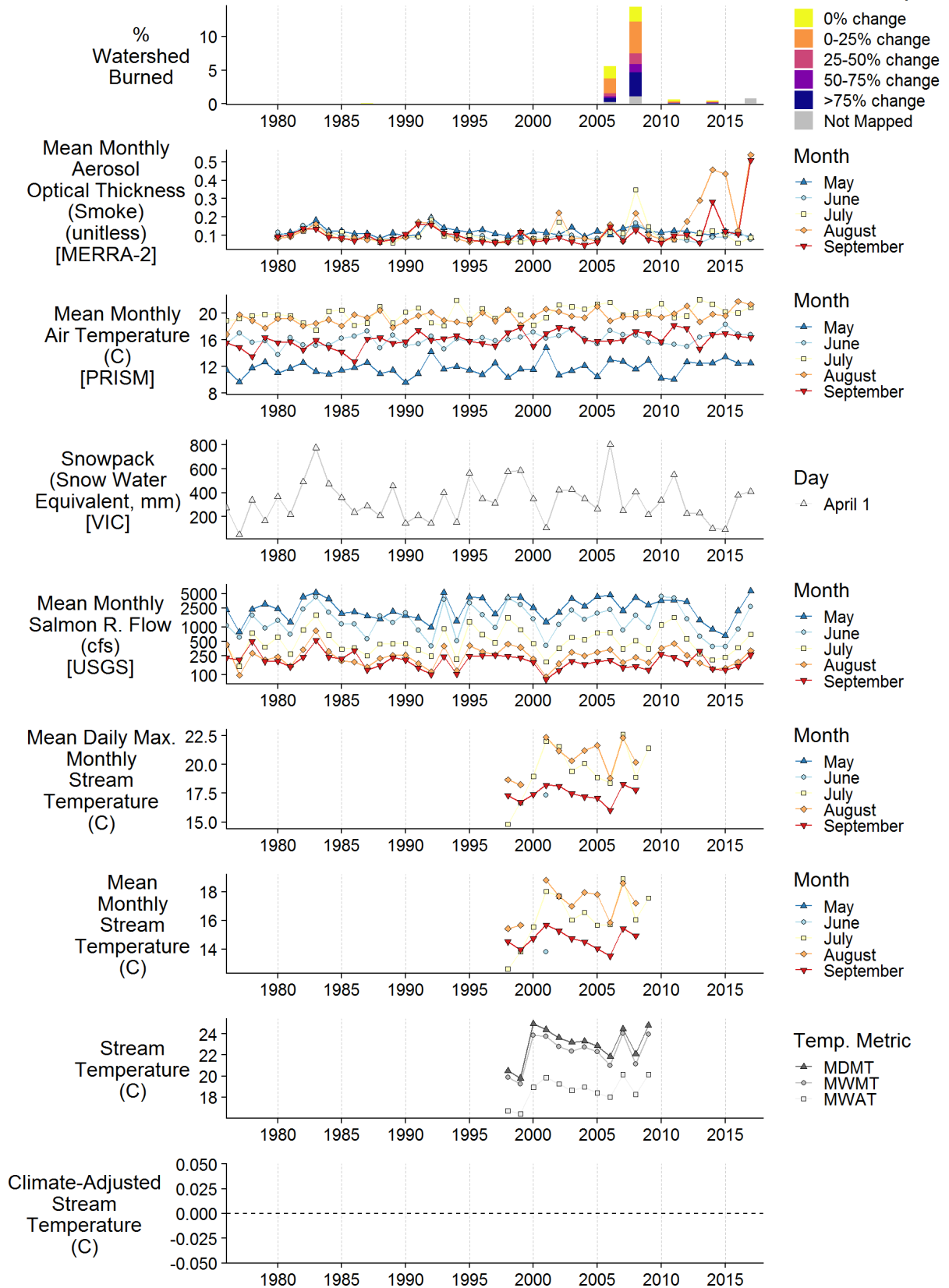
SF Salmon at Petersburg- 198.2km2-127904



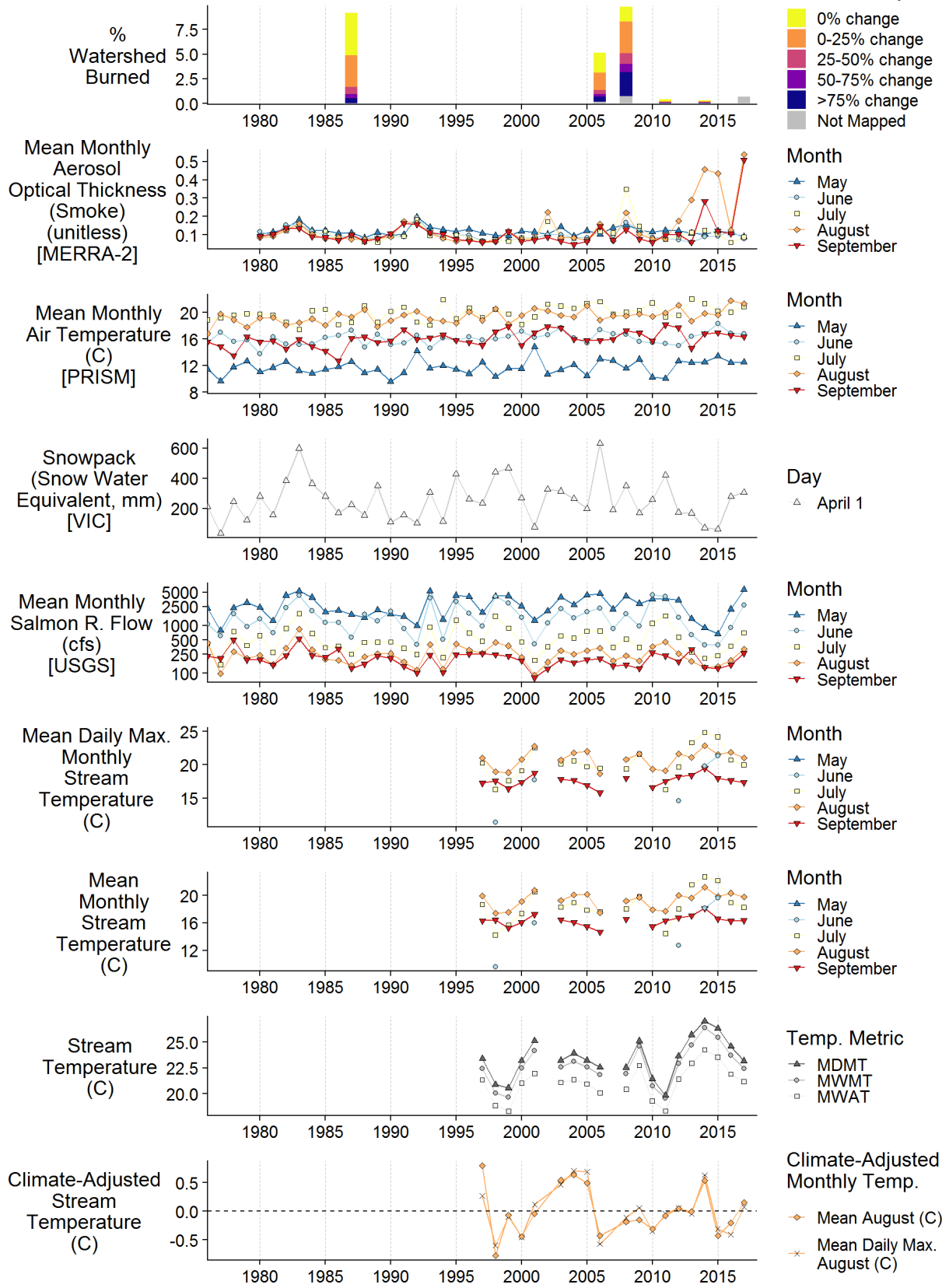
SF Salmon us EF- 204.2km2-128297



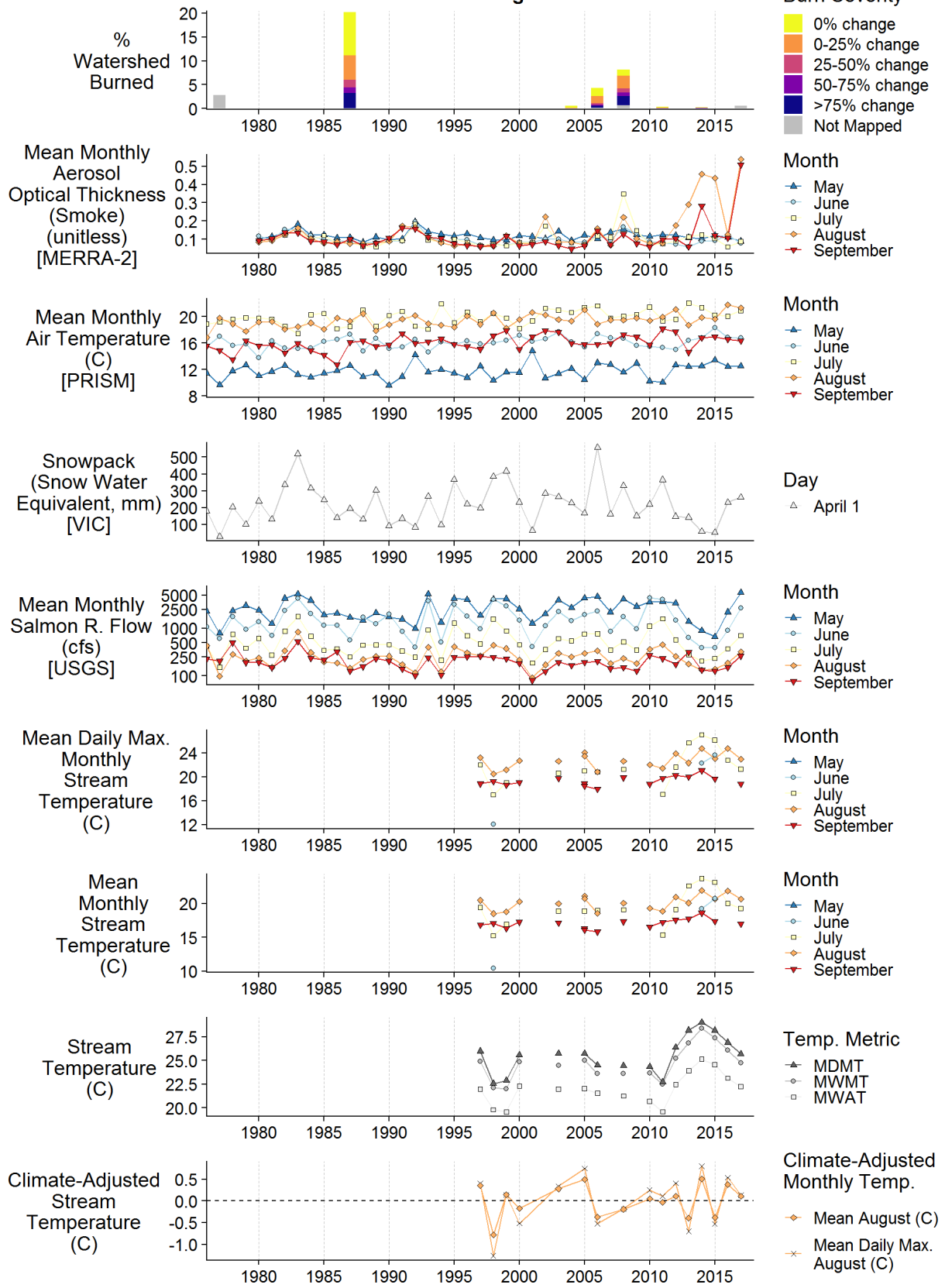
SF Salmon ds EF- 382.0km2-128408



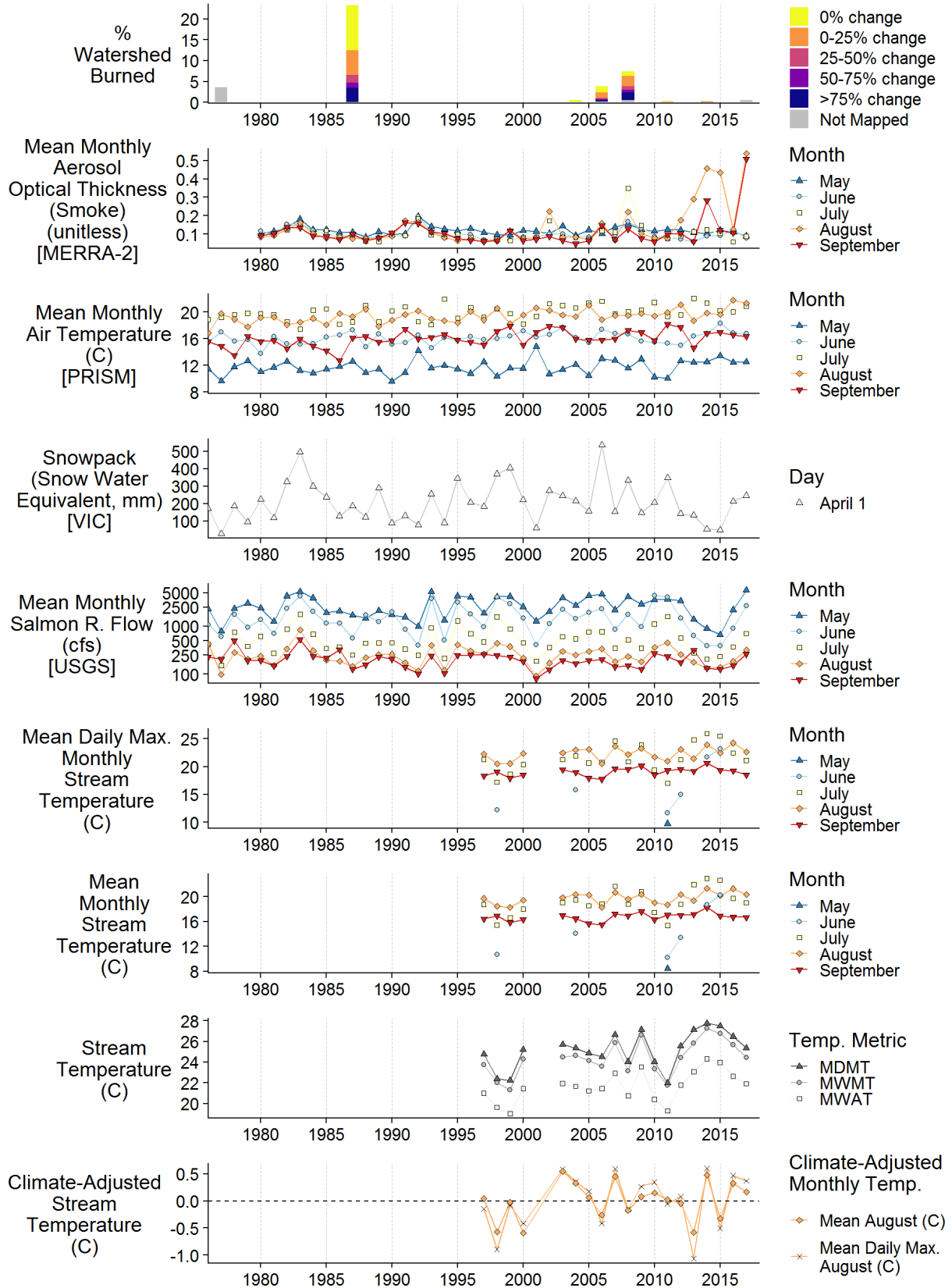
SF Salmon us Black Bear Cr- 562.9km2-129134



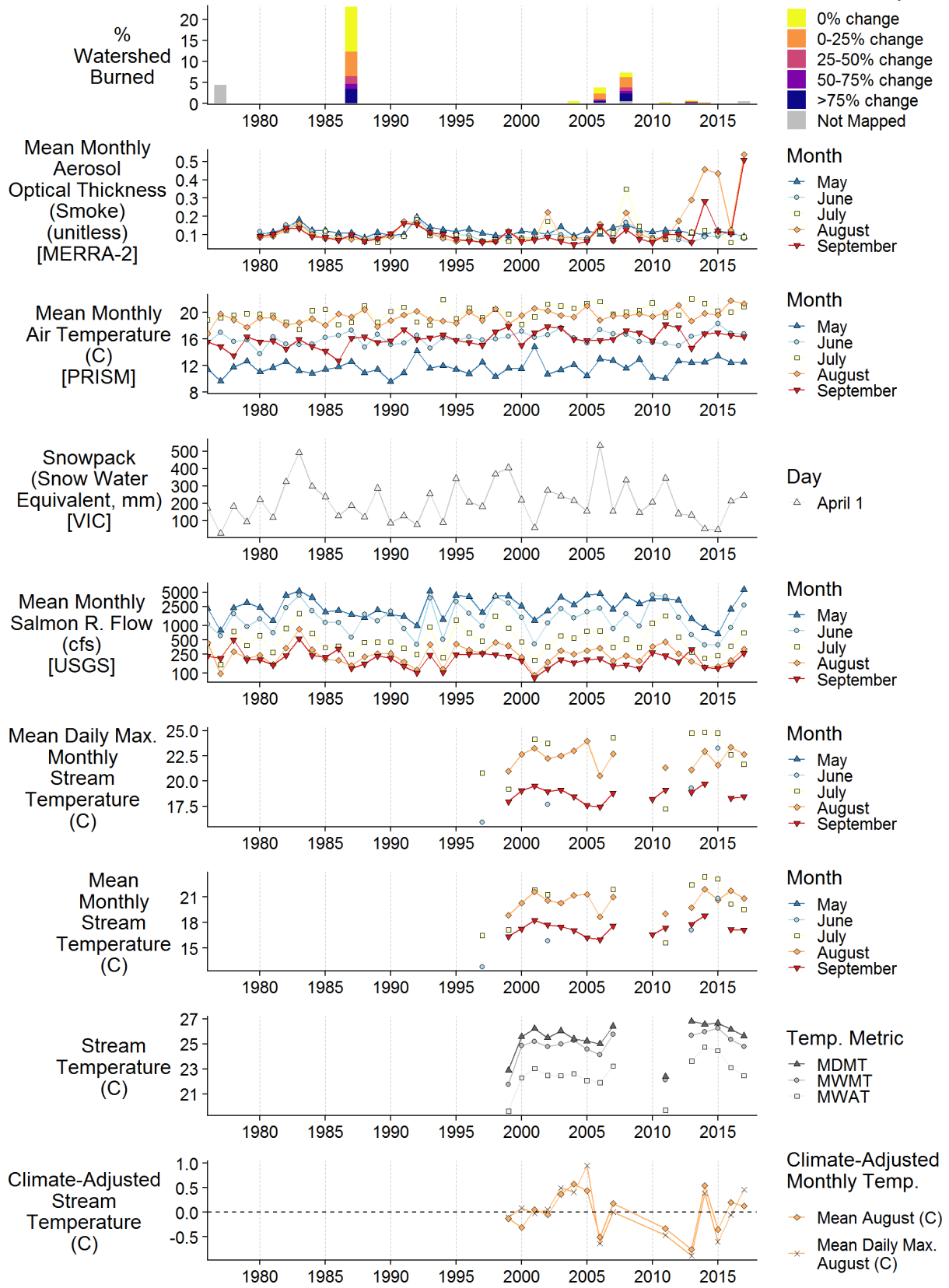
SF Salmon us Knownothing- 678.8km2-129761



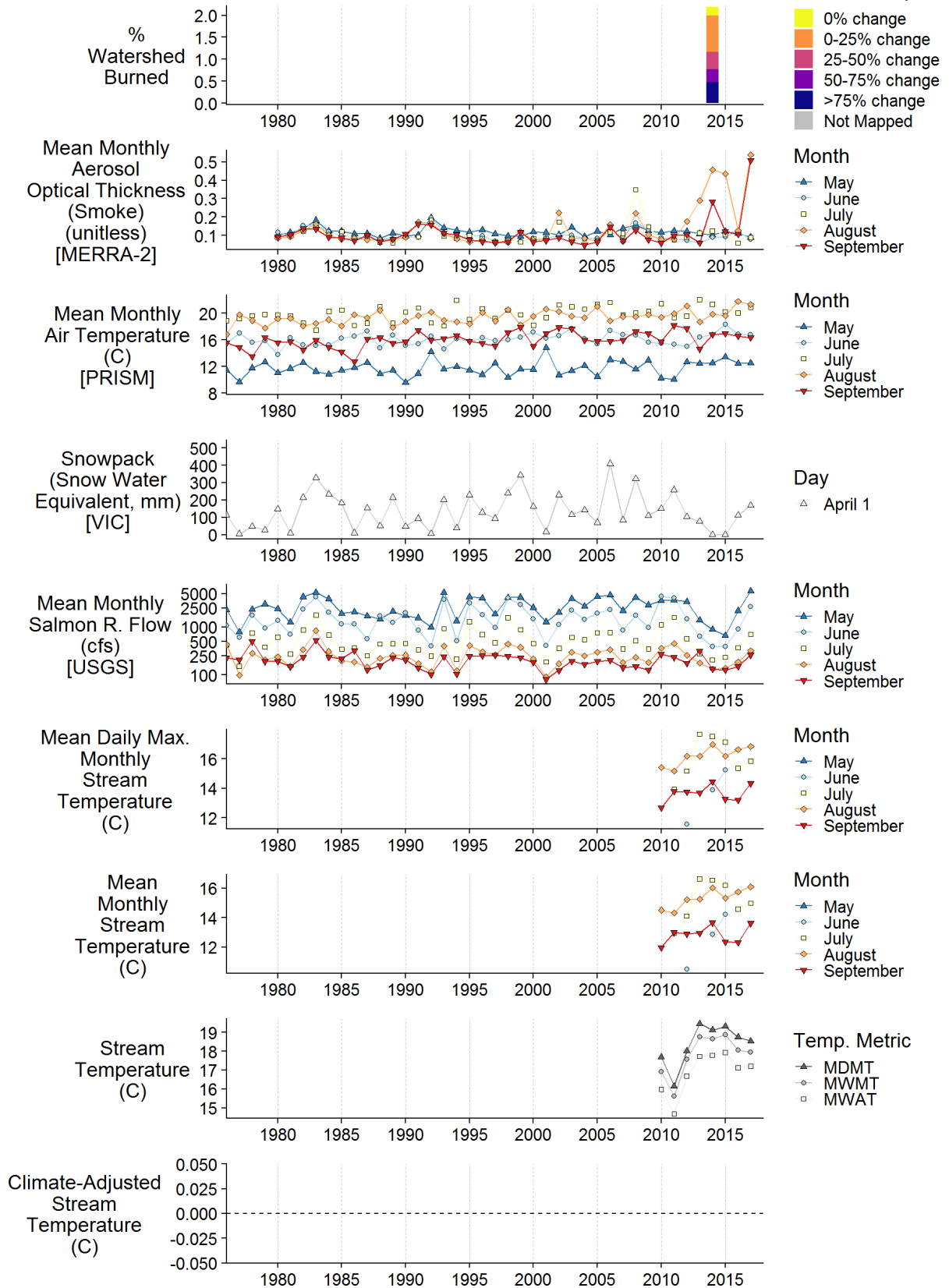
SF Salmon ds Knownothing Cr- 742.6km2-129788



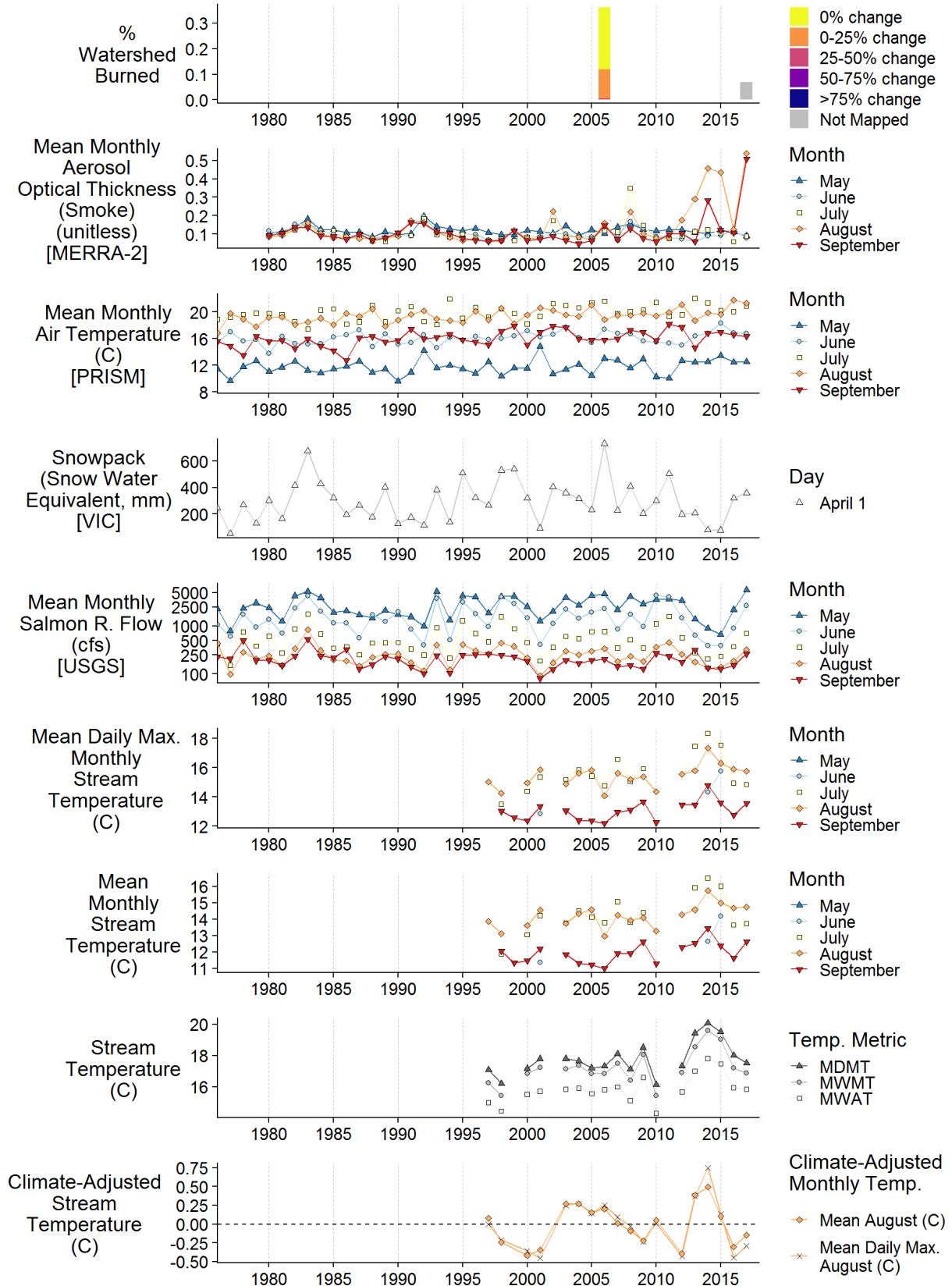
SF Salmon R us Forks- 751.8km2-129936



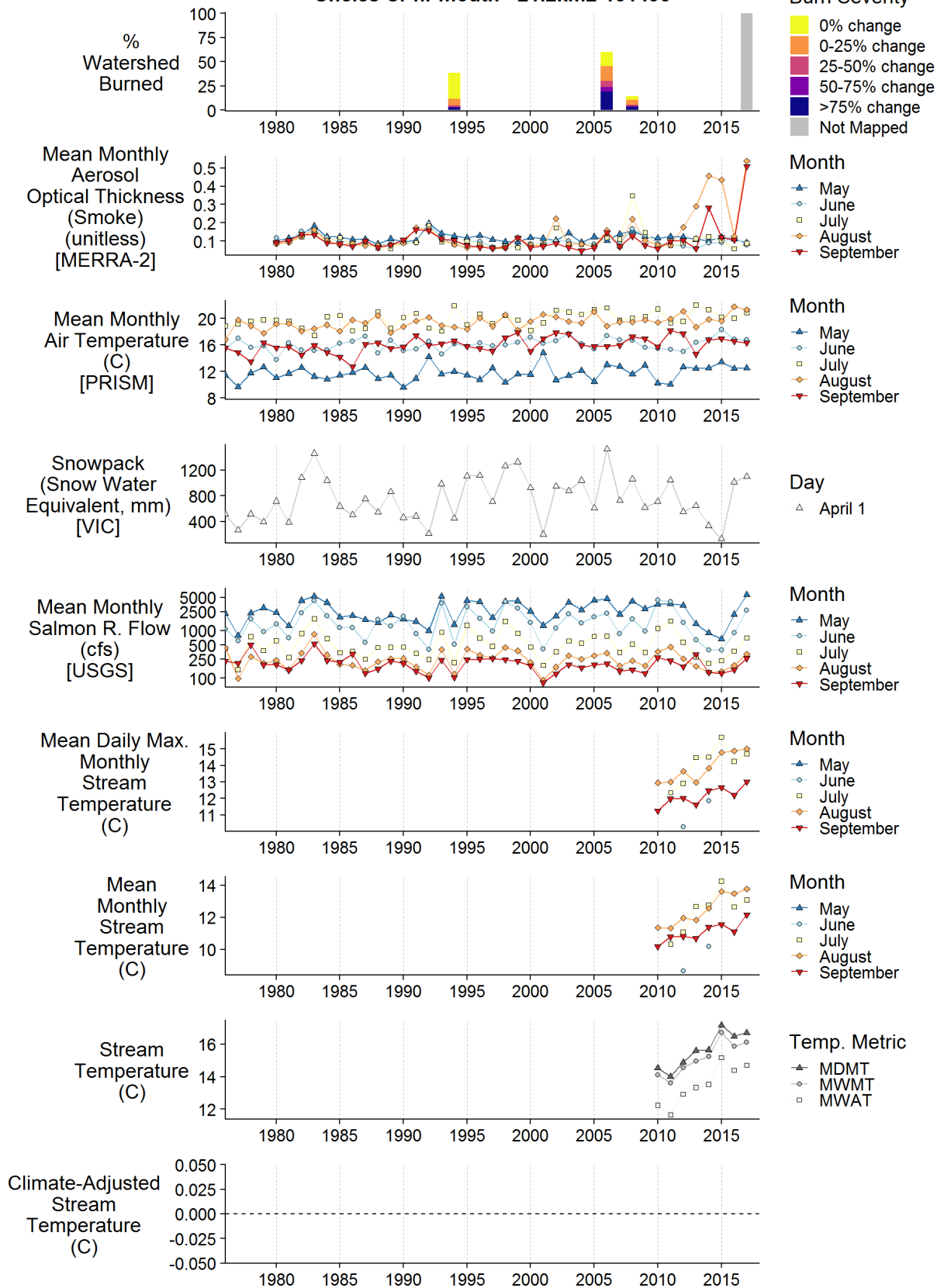
Shadow Cr nr mouth- 23.1km2-129119



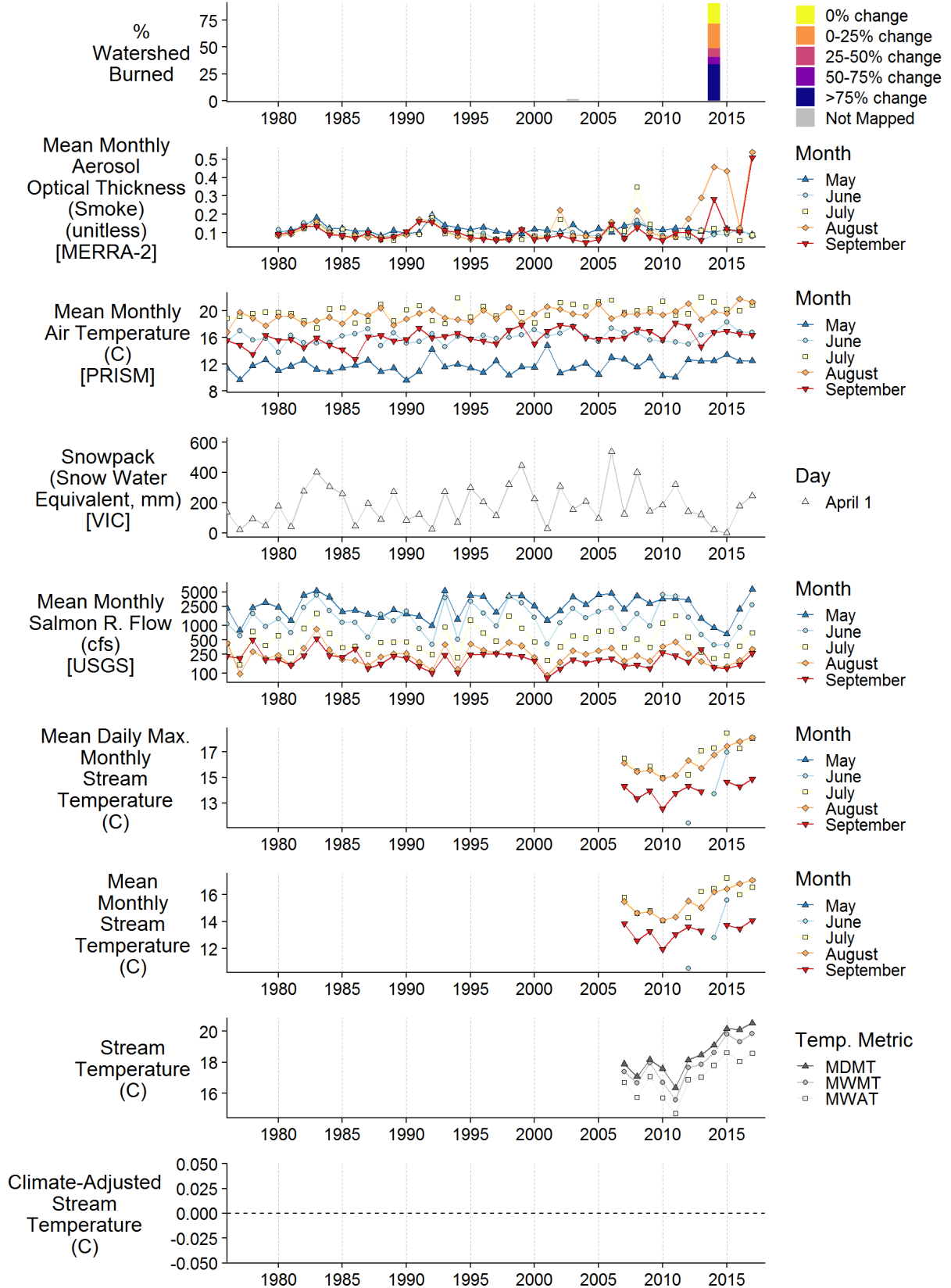
Taylor Cr nr mouth- 47.5km2-128562



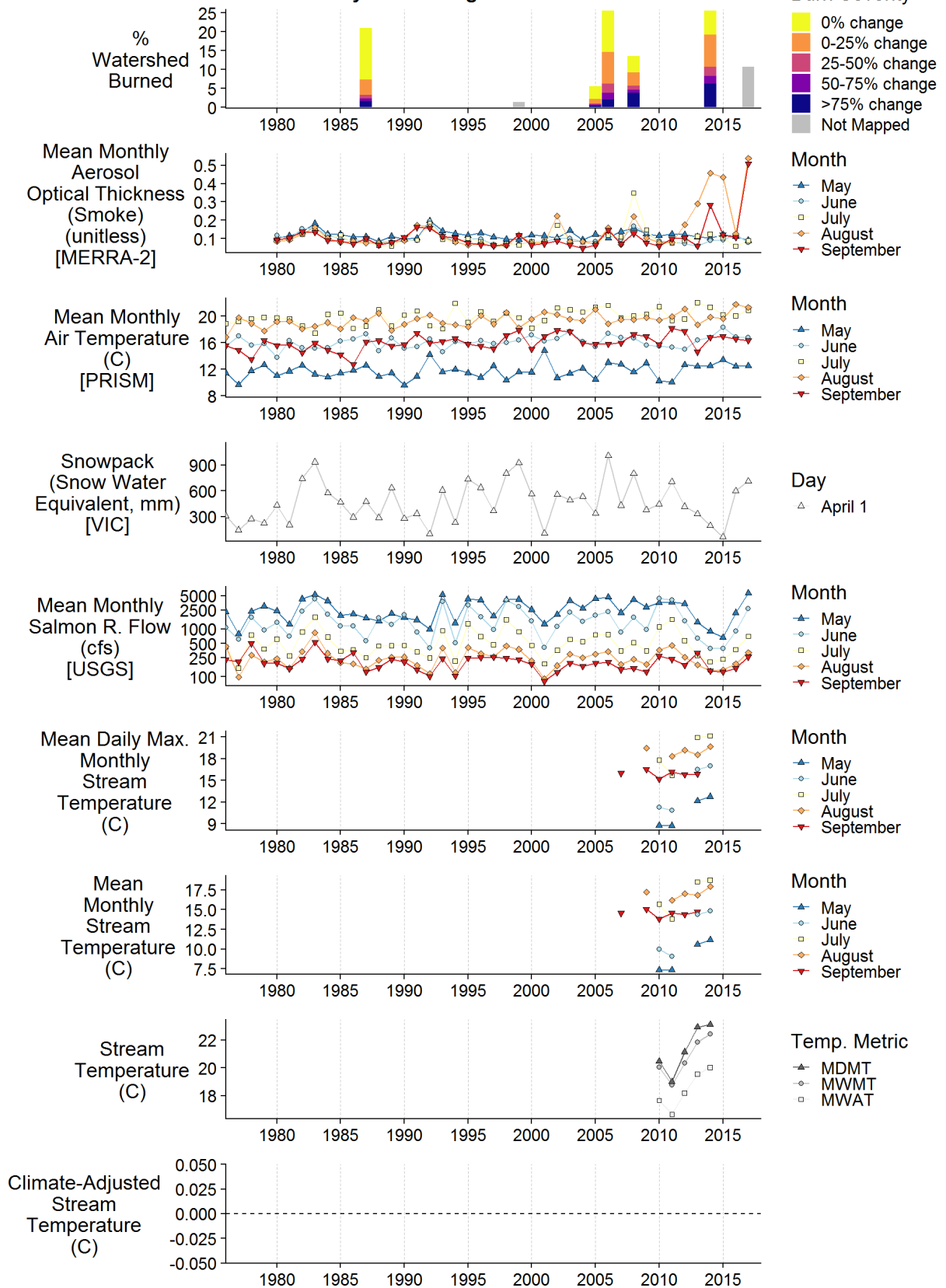
Uncles Cr nr mouth- 21.2km2-131493



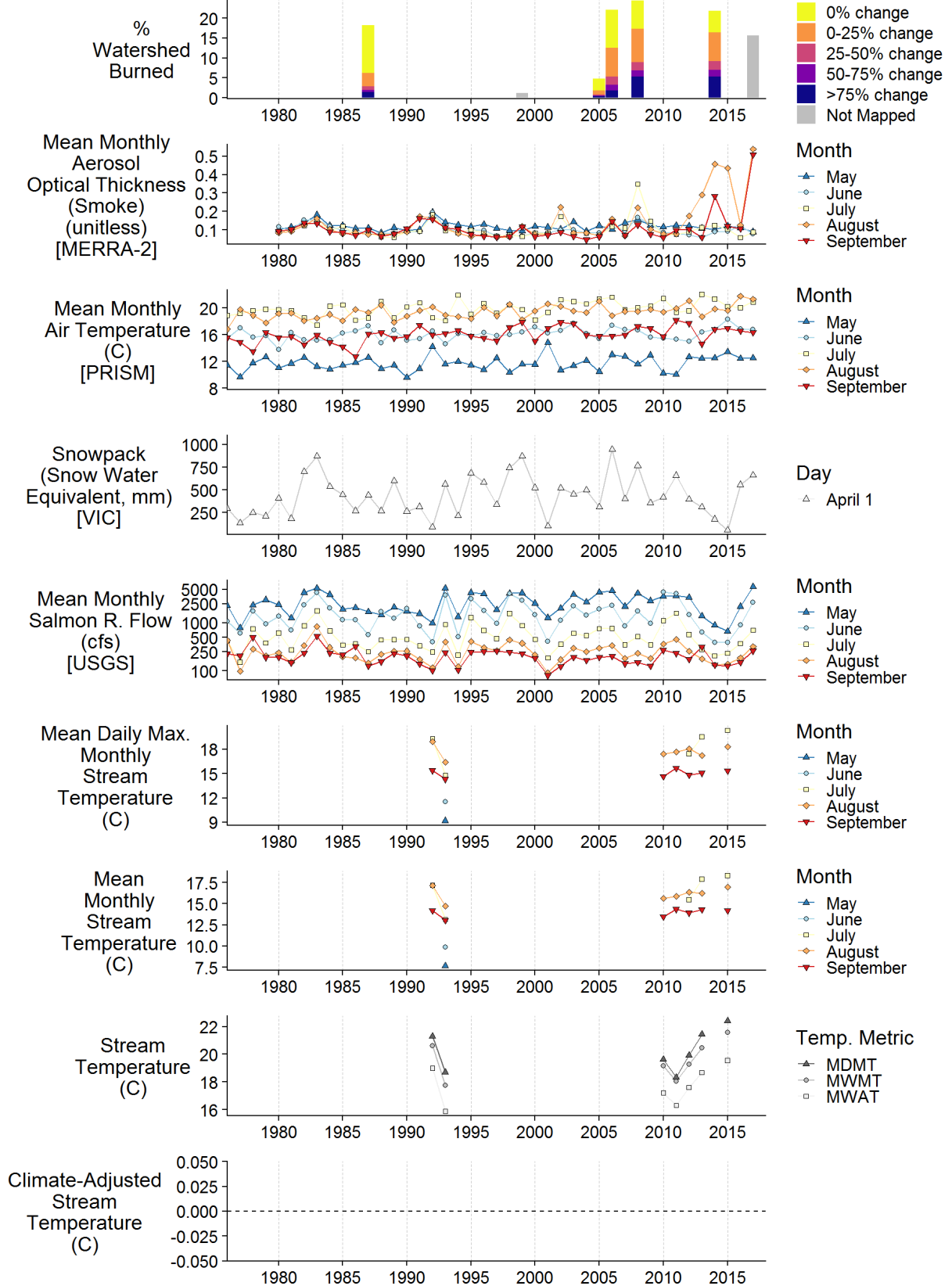
Whites Gulch nr mouth- 34.8km2-130155



Wooley Cr us Bridge Cr- 250.2km2-132652



Wooley Cr ds from Bridge Cr- 292.4km2-132640



Wooley Cr nr mouth- 385.2km2-131826

